



Understanding the settlement of
Balanus amphitrite
through the molecular and structural
characterisation of the
settlement-inducing protein complex

Helen Elizabeth Pagett

A thesis submitted to Newcastle University in candidature for the
Degree of Doctor of Philosophy

School of Marine Science and Technology

June 2011

Abstract

Many barnacle species are gregarious and their cypris larvae display a remarkable ability to explore surfaces before committing to permanent attachment. The cuticular tissue of adult barnacles contains an α_2 -macroglobulin-like glycoprotein contact cue referred to as the settlement-inducing protein complex (SIPC) which increases the attractiveness of surfaces and signals cyprids to settle. Despite decades of research into marine fouling and the development of anti-fouling systems, detailed knowledge of the biochemical and structural composition of marine pheromone cues is poor. This cue is key to barnacle gregarious settlement and represents an attractive target for custom synthesis of antagonistic surfaces.

Using the tropical acorn barnacle *Balanus amphitrite*, this project endeavoured to characterise the structure and glycan moiety of the SIPC. The SIPC active fraction was purified by ion exchange chromatography and gel filtration and detected through SDS-PAGE gel antibody immunoblotting. The carbohydrate structure was characterised using a combination of hydrophilic interaction liquid chromatography with fluorescence detection (HILIC-fluorescence) and exoglycosidase digestions. This provided evidence of predominantly oligomannose glycans with the occurrence of monofucosylated oligomannose glycans in lower proportions. The characterisation of high mannose glycosylation is supported by observations on the effect of mannose in solution increasing settlement in *B. amphitrite* cypris larvae.

Protocols to create surface bound carbohydrate-functionalised polymers were successfully developed and confirmed using X-ray photoelectron spectroscopy, ellipsometry and contact angle measurements. These surfaces were shown to act as SIPC mimics, cueing settlement on contact. The SIPC is known to contain seven potential *N*-glycosylation sites. Additional work using transmission electron microscopy and atomic force microscopy has further enhanced understanding of the glycoprotein structure. Obtaining complete structural characterisation of the SIPC remains a goal that has the potential to inspire solutions to the age-old problem of barnacle fouling.

Acknowledgements

As a marine biologist, I have many people to acknowledge for their help during my foray into the dark arts of glycobiology and synthetic chemistry. To name a few...

I would like to thank colleagues and friends in the Invertebrate Reproduction and Development Laboratory at Newcastle University, namely Dr Nick Aldred, Sheelagh Conlan and my supervisors Professor Tony Clare and Dr Gary Caldwell for advice and support throughout my research.

Many thanks to Professor Pauline Rudd and everyone in the Rudd Group at the National Institute for Bioprocessing Research and Training, Dublin. Special thanks to Jodie Abrahams, Dr Jonathan Bones, Dr Matthew Campbell and Dr Niaobh O'Donoghue for their instruction and assistance during glycan analysis.

I would like to thank Prof Neil Cameron and everyone in the NRC Group at Durham University especially Richard Brogdon, Lauren Cowie, Louise Bateson, Dr Alison Parry and Dr David Johnson for their advice and patience with structural chemistry.

For assistance with structural biology of the SIPC protein, special thanks should go to Professor Rick Lewis, Professor J Robin Harris and Dr Jon Marles-Wright at the Institute for Cell and Molecular Biosciences Newcastle University. I am very grateful to Dr Lidija Šiller and Ross Little at CEAM, Newcastle University for running XPS analysis and assistance with interpreting results. To Dr InYee Phang at the University of Twente, Netherlands for his time spent on AFM analysis.

To COIPM and the organisers of the International Congress on Marine Fouling and Corrosion for the opportunity to showcase my research and for useful discussions. Thanks also to the organisers and attendees of the annual meeting of GlycoScience Ireland for insight into the many applications of glycan research.

This research would not have been possible without the financial assistance from the NERC Blue Skies studentship (NER/S/A/2007/14628).

Finally I owe a great deal to David, Mum and Dad for their long-suffering support and endless encouragement!

Contents

Abstract	i
Acknowledgements.....	ii
Contents	iii
List of Figures.....	vi
List of Tables	xi
Chapter 1. Introduction	1
1.1 The barnacle	1
1.1.1 Barnacle Nomenclature - the Cirripedia.....	1
1.1.2 <i>Balanus amphitrite</i>	1
1.1.3 Barnacle Biology and Morphology	3
1.1.4 Barnacle Reproduction	4
1.1.5 Settlement.....	9
1.1.6 Factors affecting settlement	12
1.1.7 Gregarious behaviour	14
1.1.8 Marine glycobiology and glycoproteins.....	16
1.1.9 The settlement-inducing protein complex.....	17
1.1.10 Cyprid Temporary Adhesive	20
1.1.11 Waterborne cue	21
1.1.12 Taxonomic Affinity	22
1.1.13 Inhibition of settlement	24
1.1.14 Biofouling.....	24
1.1.15 Antifouling Approaches	26
1.1.16 Modern Antifouling Approaches	28
1.1.17 Stationary Structures	30
1.2 Project Rationale.....	32
Chapter 2. Settlement Bioassay Development	34
2.1 Introduction	34
2.1.1 24-well plate assays.....	34
2.1.2 Video Tracking.....	35
2.1.3 Post tracking settlement assay.....	36
2.1.4 Nitrocellulose Membrane Spot Assay	37
2.1.5 Drop Assay	37
2.1.6 Aims and Objectives	38
2.2 Materials and Methods	38
2.2.1 Barnacle husbandry	38
2.2.2 Laboratory maintenance of <i>B. amphitrite</i> adults.....	38
2.2.3 Petri dish rearing of barnacles	39
2.2.4 Resin barnacle mimics	39
2.2.5 24-well plate assays.....	39
2.2.6 Video Tracking.....	40
2.2.7 Post tracking settlement assay	41
2.2.8 Nitrocellulose Membrane Spot Assay	41
2.3 Results	42
2.3.1 Video Tracking Assay	42

2.3.2	Settlement Assay	45
2.3.3	Nitrocellulose Membrane Spot Assay	47
2.4	Discussion	48
Chapter 3. Purification and characterisation of glycan moiety of the settlement-inducing protein complex (SIPC) of <i>Balanus amphitrite</i>		50
3.1	Introduction	50
3.1.1	Aims and Objectives	52
3.2	Materials and Methods	53
3.2.1	Purification of a 'Crude Extract' of Adult Barnacles	53
3.2.2	Total protein assay	54
3.2.3	Ion Exchange Chromatography	54
3.2.4	Protein precipitation	55
3.2.5	SDS-PAGE gel electrophoresis	55
3.2.6	Western blots	56
3.2.7	Immunostaining	56
3.2.8	Ultrafiltration	57
3.2.9	Gel filtration chromatography	57
3.2.10	Sodium periodate glycan removal	58
3.2.11	Confirmation of glycan presence	59
3.2.12	Preparation of samples for release of N-glycans	59
3.2.13	Release of N-glycans from gels	60
3.2.14	Labelling of N-glycans	61
3.2.15	HILIC-fluorescence glycan profiling	61
3.2.16	Exoglycosidase digestions	62
3.2.17	Sugars in solution	62
3.3	Results	63
3.3.1	Protein purification	63
3.3.2	Confirmation of glycan presence	67
3.3.3	HILIC-fluorescence	68
3.3.4	Sugars in solution	75
3.4	Discussion	78
3.4.1	SIPC purification	78
3.4.2	SIPC glycan characterisation	78
3.4.3	Sugars in solution	79
3.4.4	Conclusion	81
Chapter 4. Functionalised glycopolymers		82
4.1	Introduction	82
4.1.1	Aims and objectives	87
4.2	Materials and Methods	87
4.2.1	Carbohydrate functionalised polymers - method development 1	88
4.2.2	Carbohydrate functionalised polymers - method development 2	100
4.2.3	Carbohydrate functionalised polymers - method development 3	102
4.2.4	Contact Angle	105
4.2.5	Ellipsometry	105
4.2.6	XPS	105
4.2.7	Drop Assay	109
4.3	Results	109
4.3.1	Carbohydrate functionalised polymers	109

4.3.2	Contact Angle.....	109
4.3.3	Ellipsometry	110
4.3.4	XPS.....	111
4.3.5	Drop Assay.....	123
4.4	Discussion.....	124
Chapter 5. Physical characteristics of the settlement-inducing protein complex		130
5.1	Introduction	130
5.1.1	Aims and Objectives	132
5.2	Materials and methods.....	133
5.2.1	Atomic force microscopy	133
5.2.2	Transmission electron microscopy (TEM).....	133
5.2.3	Protein Structure Analysis.....	134
5.2.4	Mass Spectrometry of proteins and <i>N</i> -glycans.....	136
5.3	Results	137
5.3.1	Atomic force microscopy	137
5.3.2	Transmission electron microscopy	139
5.3.3	Protein Structure Analysis.....	143
5.3.4	Mass spectrometry of proteins and <i>N</i> -glycans	151
5.4	Discussion.....	151
Chapter 6. Discussion		155
6.1	Introduction	155
6.2	New findings in context.....	155
6.3	Future research	159
6.4	Final Thoughts.....	164
References		166
Appendix A		190
Appendix B		191
Appendix C		195
Appendix D		198
Appendix E		200
Appendix F.....		212

List of Figures

Figure 1 - A sessile adult <i>Balanus</i> barnacle (a) Dorsal view showing the layout of the shell exterior (b) Lateral section showing internal structures (both author's own).....	3
Figure 2 - A <i>Balanus</i> barnacle (a) The <i>Balanus</i> barnacle life cycle (b) A ventral view of a <i>Balanus amphitrite</i> nauplius larvae (both author's own).....	6
Figure 3 - A <i>Balanus amphitrite</i> cyprid (a) A light micrograph of a whole <i>B. amphitrite</i> cyprid larva with extended antennules and thoracopods (b) A <i>B. amphitrite</i> cyprid larva showing internal structures (both author's own).....	8
Figure 4 - The antennular attachment organ of <i>Balanus amphitrite</i> (a) A light micrograph of cyprid antennules (author's own) (b) A SEM image of the cyprid antennule. Labelled features are the second, third and fourth antennular segments (2nd a.s., 3rd a.s. and 4th a.s. respectively), the cuticular velum (v) encircling the attachment disc (a.d.), the hair-like cuticular villi (c.v.) and the axial sense organ (a.s.o.) in the centre of the attachment disc. Sensory setae (s.s.) are present on all three antennular segments, but are especially prevalent on the 4th a.s. The cyprid body is labelled c.b. (from Aldred and Clare, 2008)	8
Figure 5 - Glass microscope slide showing the gregarious nature of <i>Balanus amphitrite</i> spat (courtesy of Dr Nick Aldred).....	15
Figure 6 - Lateral section of an adult <i>Balanus</i> barnacle showing the successive cuticular slips exposing new SIPC (Bourget, 1987).	17
Figure 7 – The proteinaceous cyprid footprints of <i>Balanus amphitrite</i> stained on nitrocellulose membrane (from Phang et al., 2007).	20
Figure 8 - Behavioural parameters measured for <i>Balanus amphitrite</i> cyprids when tracked for 5 minutes with EthoVision 3.1. (a) mean velocity (cm/s), (b) mean distance (cm), (c) mean total turn angle (°), (d) mean angular velocity (°/s) and (e) mean meander (°/cm). The letters indicate which treatments are significantly different from each other (i.e. treatment with A is significantly different to the other treatment with A). Error bars are ± standard error.	44
Figure 9 - Settlement of <i>Balanus amphitrite</i> cyprids in the presence of adult barnacles, resin mimics of barnacles and no adult (a) Mean percentage settlement of cyprids after 24 hours in dishes with four treatments. (b) Mean percentage settlement of cyprids after 48 hours in dishes with four treatments. (c) Proximity of cyprid settlement to an adult barnacle in the centre of a petri dish. The letters indicate which treatments are significantly different from each other (i.e. treatment with A is significantly different to the other treatment with A). Error bars are ± standard error.	46
Figure 10 - Mean number of <i>Balanus amphitrite</i> cyprids settled in a nitrocellulose membrane spot assay treated with the SIPC, Tris and BSA. Error bars are ± standard error.	48
Figure 12 - SDS-PAGE gel of <i>Balanus amphitrite</i> SIPC (A) molecular standard showing the 78kDa band, (B) native denatured SIPC showing the 76, 88 and 98 kDa subunits (arrowheads) and (C) sodium periodate treated SIPC	59
Figure 13 - Total protein assay of <i>Balanus amphitrite</i> SIPC protein fractions using a 98-well plate and every 5 th fraction from the ion exchange column. The standards are on the left and fraction samples on the right. Fractions showing protein present are blue.	63

Figure 14 - Total protein from the crude extract of <i>Balanus amphitrite</i> proteins after charge separation by ion exchange chromatography.....	64
Figure 15 - Stained PVDF membrane Western blot of ion exchange chromatography separated fractions of <i>Balanus amphitrite</i> crude protein extract. The numbers refer to the time of elution in minutes.	64
Figure 16 - Total protein from the crude extract of <i>Balanus amphitrite</i> after charge separation by ion exchange chromatography with the fractions containing SIPC indicated.....	65
Figure 17 - SIPC active fractions (from antibody immunoblotting) of <i>Balanus amphitrite</i> after size separation by gel filtration chromatography, with the fractions containing protein indicated.	65
Figure 18 - Stained PVDF membrane Western blot of gel filtration chromatography separated fractions of <i>Balanus amphitrite</i> proteins, active fractions indicate SIPC. The numbers refer to the time of elution in minutes.	66
Figure 19 - SIPC active fraction of <i>Balanus amphitrite</i> after size separation by gel filtration chromatography with the fractions containing SIPC indicated.	66
Figure 20 - SDS-PAGE gel of denatured <i>Balanus amphitrite</i> SIPC showing a band of higher mass (A), the three major subunits (B, C and D) and two fainter bands (E and F).	67
Figure 21 - Pro-Q Emerald stained gel showing glycans present in <i>Balanus amphitrite</i> SIPC as well as the 75 and 25 kDa bands from the protein standard on the left.	68
Figure 22 - HPLC chromatograms of <i>Balanus amphitrite</i> SIPC including the gel blank. The grey area shows peaks that are artefacts from the gel blank to be discarded. Bands A to F are subunits of the Native SIPC, as shown in the adjacent SDS-PAGE gel (see Figure 20 for the full gel).....	69
Figure 23 - HPLC chromatogram of total <i>N</i> -glycans released from native <i>Balanus amphitrite</i> SIPC	69
Figure 24 - HPLC chromatograms of total <i>N</i> -glycans released from the native <i>Balanus amphitrite</i> SIPC and gel fractions A-F with Dextran ladder assigned GU values. These GU values are displayed here as vertical values in thousands (e.g. 96069). GU value is rounded to the nearest thousand as shown on the GU scale below the x-axis. For further analysis the GU values are similarly displayed (e.g. 9.61). ✕ indicates absence of a peak.....	70
Figure 25 - HILIC chromatogram showing the glycans released from the native <i>Balanus amphitrite</i> SIPC from the in-gel block showing the oligomannose series M2-9 along with a dextran ladder to find the GU values. Molecular representations of the sugars are included. The individual monosaccharides are represented as follows: open circle, mannose; dotted diamond, fucose, dotted line, α linkage; solid line, β linkage.....	72
Figure 26 - Key to carbohydrates, linkages and structures as used in this research as used in Harvey et al. (2009)	72
Figure 28 - Effect of exogenous sugars on the settlement of 1-day-old <i>Balanus amphitrite</i> cyprids when compared to artificial seawater (ASW). (a) mannose and galactose at 24 hours (b) SIPC at 24 hours (c) IBMX at 24 hours. Note the different scales on the x axes.	77
Figure 29 - Synthesis pathways for maleic anhydride polymers (a) Reaction scheme for the production of poly(styrene-co-maleic acid) glycopolymers from Donati et al. (2002) (b) Synthesis and assembling of 'hairy' glycol-nanoparticles from poly{styrene-co-[(maleic anhydride)- <i>alt</i> -styrene]} from Su et al.(2009) (c) Polymer structures formed by carbohydrate-polymer attachment via 1) the anomeric hydroxyl, 2) C2 hydroxyl, 3) C3 hydroxyl, 4) C4 hydroxyl and 5) C6 hydroxyl, in the reaction of glucose with poly(styrene maleic anhydride) from Galgali et al. (2007)	85

Figure 30 - The structure of a glycosylation site using the $NX_{\neq p}S/T$ rule; where Asn-Xaa (\neq Pro)-Ser or Asn-Xaa (\neq Pro)-Thr (where Xaa is any amino acid except Pro, as it renders the Asn inaccessible).	87
Figure 31 - Three steps of Method 1 for the synthesis of <i>Balanus amphitrite</i> SIPC mimic (a) The desired product of the first step; 1-O-(6'-Fmoc-aminohexyl)-2,3,4,6-tetra-O-acetyl- β -D-galactopyranoside (b) Step two; deprotection of the carbohydrate and removal of Fmoc (c) Step three; addition of Gantrez [®] polymer. ...	88
Figure 32 - A thin layer chromatograph of the product of the 1-O-(6'-Fmoc-aminohexyl)-2,3,4,6-tetra-O-acetyl- β -D-galactopyranoside reaction, clearly showing residual Fmoc and unwanted products. Rf values for each are quoted.	90
Figure 33 - Auto-column trace of the 1-O-(6'-Fmoc-aminohexyl)-2,3,4,6-tetra-O-acetyl- β -D-galactopyranoside reaction, clearly showing unwanted peaks along with the desired product (Peak 2).....	91
Figure 34 - TLC plate showing (top plate) the three auto-column peaks from Figure 33 (1-O-(6'-Fmoc-aminohexyl)-2,3,4,6-tetra-O-acetyl- β -D-galactopyranoside reaction). (bottom plate) TLC plate suggesting that there is no contamination between peaks.	91
Figure 35 - Proton ¹ H NMR spectrum for 1-O-(6'-Fmoc-aminohexyl)-2,3,4,6-tetra-O-acetyl- β -D-galactopyranoside showing unreacted galactose pentaacetate, Fmoc and unwanted peaks.....	92
Figure 36 - Resonance structure resulting from the delocalisation of a nitrogen lone pair. The rotation about the C-N bond becomes fixed thus resulting in a different chemical environment for the NH and other local protons.	93
Figure 37 - Low Resolution Mass Spectrometry trace of 1-O-(6'-Fmoc-aminohexyl)-2,3,4,6-tetra-O-acetyl- β -D-galactopyranoside.....	94
Figure 38 - TLC plate showing the product (peak 2 from Figure 33 the 1-O-(6'-Fmoc-aminohexyl)-2,3,4,6-tetra-O-acetyl- β -D-galactopyranoside reaction) and impurity as separated using 9:1 chloroform:methanol solvent mix.	95
Figure 39 - Auto-column trace of the product peak 1-O-(6'-Fmoc-aminohexyl)-2,3,4,6-tetra-O-acetyl- β -D-galactopyranoside, clearly showing unwanted products with the desired product	95
Figure 40 - TLC plate showing the six fractions of the peak in Figure 39, the unwanted product and the desired 1-O-(6'-Fmoc-aminohexyl)-2,3,4,6-tetra-O-acetyl- β -D-galactopyranoside.	95
Figure 41 - Proton ¹ H NMR spectrum on the uncontaminated product peak (1-O-(6'-Fmoc-aminohexyl)-2,3,4,6-tetra-O-acetyl- β -D-galactopyranoside) still showing unwanted products	96
Figure 42 - Auto-column trace of the contaminated product peak 1-O-(6'-Fmoc-aminohexyl)-2,3,4,6-tetra-O-acetyl- β -D-galactopyranoside, showing only one peak despite the previous TLC showing impurities	97
Figure 43 - TLC plate showing the four fractions of the peak in Figure 42, the contaminated 1-O-(6'-Fmoc-aminohexyl)-2,3,4,6-tetra-O-acetyl- β -D-galactopyranoside.	97
Figure 44 - Proton ¹ H NMR spectrum of the product peak (1-O-(6'-Fmoc-aminohexyl)-2,3,4,6-tetra-O-acetyl- β -D-galactopyranoside) still showing unwanted peaks.....	98
Figure 45 - COSY NMR showing the same product as Figure 44, (1-O-(6'-Fmoc-aminohexyl)-2,3,4,6-tetra-O-acetyl- β -D-galactopyranoside) and unwanted peaks.....	99
Figure 46 - Proton ¹ H NMR spectrum of the Gantrez [®] -aminohexanol product. Only solvents are visible as the product was insoluble in dimethyl sulphoxide.	101

Figure 47 - The undesired insoluble interchain network formed by heating the Gantrez [®] and reactants.....	101
Figure 48 - The undesired ring-opened Gantrez [®] as a consequence of dialysis with water	102
Figure 49 - Hydroxyl binds to the oxygen to again form the undesired interchain network	102
Figure 50 - Immobilisation of the reactant layers (glass, APTES, Gantrez [®] , aminoethanol, galactose pentaacetate) and final product creating the carbohydrate functionalised polymers to mimic <i>Balanus amphitrite</i> SIPC.....	103
Figure 51 - Structure of the carbohydrate functionalised polymer surface modification to mimic <i>Balanus amphitrite</i> SIPC, showing the progress from silicon wafer (striped box), aminated (green), polymer (purple), linker (blue) and carbohydrate (orange). This figure shows galactose as the terminal carbohydrate.....	106
Figure 52 - Sample set up inside XPS chamber to reduce charging using an electron gun and gold	108
Figure 53 - Contact angle results, mean angle or θ ($^{\circ}$) \pm SE for each of the carbohydrate functionalised polymer surface modifications to mimic <i>Balanus amphitrite</i> SIPC. Error bars are \pm standard error	110
Figure 54 - Ellipsometry results for each of the carbohydrate functionalised polymer surface modifications to mimic <i>Balanus amphitrite</i> SIPC indicating the change in depth of surface layers. Error bars are \pm standard error.	110
Figure 55 - Wide scan survey spectra for all elements for all samples of the carbohydrate functionalised polymer surface modification to mimic <i>Balanus amphitrite</i> SIPC; (a) aminated, (b) Gantrez [®] , (c) aminoethanol, (d) glucose, (e) mannose and (f) galactose. * indicates an unidentifiable peak not found in the elemental database.....	112
Figure 56 - High resolution spectra for carbon(1s) for all samples of the carbohydrate functionalised polymer surface modification to mimic <i>Balanus amphitrite</i> SIPC; (a) aminated, (b) Gantrez [®] , (c) aminoethanol, (d) glucose, (e) mannose and (f) galactose.	113
Figure 57 - High resolution spectra for nitrogen(1s) for all samples of the carbohydrate functionalised polymer surface modification to mimic <i>Balanus amphitrite</i> SIPC; (a) aminated, (b) Gantrez [®] , (c) aminoethanol, (d) glucose, (e) mannose and (f) galactose.	114
Figure 58 - High resolution spectra for oxygen(1s) for all samples of the carbohydrate functionalised polymer surface modification to mimic <i>Balanus amphitrite</i> SIPC; (a) aminated, (b) Gantrez [®] , (c) aminoethanol, (d) glucose, (e) mannose and (f) galactose.	115
Figure 59 - High resolution spectra for silicon(2p) for all samples of the carbohydrate functionalised polymer surface modification to mimic <i>Balanus amphitrite</i> SIPC; (a) aminated, (b) Gantrez [®] , (c) aminoethanol, (d) glucose, (e) mannose and (f) galactose.	116
Figure 60 - Mean cyprid settlement on the carbohydrate functionalised polymer surface modification to mimic <i>Balanus amphitrite</i> SIPC at 24 and 48 hours. Error bars are \pm standard error.....	123
Figure 61 - Mean cyprid settlement on the carbohydrate functionalised polymer surface modification to mimic <i>Balanus amphitrite</i> SIPC at 48 hours. Error bars are \pm standard error.	124
Figure 62 - Examples of characterised protein structures from other aquatic organisms; (a) haemoglobin from the annelid worm <i>Nereis virens</i> showing hexameric molecules (from Harris et al., 2006) (b) haemocyanin from the European spiny lobster, <i>Palinurus elephas</i> showing three subunits (from Meissner et al., 2003) (c) haemocyanin from the Californian keyhole limpet, <i>Megathura crenulata</i> showing cylindrical structures	

consisting of ten globular masses (from Dube et al. 1995) (d) haemocyanin from the chiton <i>Acanthochiton fascicularis</i> showing the ‘man-in-the-boat’ structure (from Harris et al. 2004)	132
Figure 63 - Representative AFM micrographs of <i>Balanus amphitrite</i> SIPC (a) 1:500 dilution on methyl-terminated glass, (b) 1:500 dilution on highly ordered pyrolytic graphite, (c) 1:500 dilution on amine-terminated glass and (d) 1:500 dilution on Mica 1:1000.....	138
Figure 64 - High resolution three-dimensional TEM micrograph of <i>Semibalanus balanoides</i> protein adhesive showing properties similar to Figure 63(a) (from Phang et al., 2009).....	138
Figure 65 - A representative TEM micrograph of <i>Balanus amphitrite</i> SIPC (a) deglycosylated (100% solution) showing distortion, (b) native (glycosylated) (100% solution) showing clustering, (c) deglycosylated (100% solution) (d) deglycosylated (10% solution) and (e) deglycosylated precipitated pellet (100% solution). All scale bars indicate 100nm. < indicates an individual particle.	141
Figure 66 - Nine 2D class averages of TEM images of deglycosylated <i>Balanus amphitrite</i> SIPC from 266 particles. Each class average contains approximately 15 particles.	142
Figure 67 - A hypothetical model of <i>Balanus amphitrite</i> SIPC on a surface, showing a membrane anchor, protein backbone and exposed sugars. Components not shown to scale.	142
Figure 68 - ESPrpt alignment output of <i>Balanus amphitrite</i> SIPC and <i>Anopheles gambiae</i> TEP1r (Baxter et al., 2007). Black shading denotes identical amino acids when comparing the two sequences giving the 26% homology. The ▲▲▲ indicates the NX _p S/T sequence for glycosylation and ★ represents the ‘GCGEQ’ sequence indicative of a thioester bond.....	144
Figure 69 - PyMOL representation of <i>Anopheles gambiae</i> TEP1r (Baxter et al., 2007) showing disulphide bonds as red spheres	145
Figure 70 – TEM image of <i>Balanus amphitrite</i> SIPC (white shadow) and <i>Anopheles gambiae</i> TEP1r (colour) (Baxter et al., 2007) overlaid show the structural and folding similarities	145
Figure 71 - FASTA amino acid sequence of <i>Balanus amphitrite</i> SIPC from Dreanno (2006c) showing the possible glycosylation sites. NX _p S/T sequons are shown in blue with asparagines predicted to be N-glycosylated shown in red. In addition, possible disulphide bond sites (cysteines) are shown in green.	146
Figure 72 - The DomPred prediction of sequence discontinuities (Marsden et al., 2002) in the <i>Balanus amphitrite</i> SIPC amino acid sequence, indicating where domains occur. The x-axis represents the amino acid sequence.	147
Figure 73 - Pro-Q Emerald stained SDS-PAGE gel of native, denatured and deglycosylated <i>Balanus amphitrite</i> SIPC, showing some fluorescence but no band detail.....	148
Figure 75 - Graphical output of the potential O-glycosylation sites on <i>Balanus amphitrite</i> SIPC from NetOGlyc 3.1 (Julenius et al., 2005). The blue line indicates the potential for the site and the red line shows the potential above which glycosylation is considered likely. The amino acid (T or S), position in the sequence and score (>0.5 is predicted to be glycosylated)	150
Figure 76 - Tabular output of the potential C-glycosylation sites on <i>Balanus amphitrite</i> SIPC from NetCGlyc 1.0 (Julenius, 2007). Scores above 0.5 are predicted to be glycosylated.	151

List of Tables

Table 1 - Structure details of the glycans of <i>Balanus amphitrite</i> SIPC with glucose unit (GU) and percentage area from the HILIC-fluorescence data. ^a Allocated peak numbers, see Figure 23. ^b Glucose Unit. ^c The amount of glycan present as a percentage of the total glycans measured by HPLC.	73
Table 2 - Structural assignment with relative percentage areas of peaks present in native <i>Balanus amphitrite</i> SIPC and gel fractions A-F. ✕ indicates absence of a peak.	73
Table 3 - Predicted bonds at each stage of the carbohydrate functionalised polymer surface modification to mimic <i>Balanus amphitrite</i> SIPC, as indicated by Figure 51 showing aminated (green), polymer (purple), linker (blue) and carbohydrate (orange) terminated surfaces.	107
Table 4 - High-resolution spectrum component positions for carbon (1s), nitrogen (1s), oxygen (1s) and silicon (2p) signals on the aminated surface of the functionalised polymer surface modification to mimic <i>Balanus amphitrite</i> SIPC.	117
Table 5 - High-resolution spectrum component positions for carbon (1s), nitrogen (1s), oxygen (1s) and silicon (2p) signals on Gantrez [®] surface of the functionalised polymer surface modification to mimic <i>Balanus amphitrite</i> SIPC.	118
Table 6 - High-resolution spectrum component positions for carbon (1s), nitrogen (1s), oxygen (1s) and silicon (2p) signals on aminoethanol surface of the functionalised polymer surface modification to mimic <i>Balanus amphitrite</i> SIPC.	119
Table 7 - High-resolution spectrum component positions for carbon (1s), nitrogen (1s), oxygen (1s) and silicon (2p) signals on glucose surface of the carbohydrate functionalised polymer surface modification to mimic <i>Balanus amphitrite</i> SIPC.	120
Table 8 - High-resolution spectrum component positions for carbon (1s), nitrogen (1s), oxygen (1s) and silicon (2p) signals on mannose surface of the carbohydrate functionalised polymer surface modification to mimic <i>Balanus amphitrite</i> SIPC.	121
Table 9 - High-resolution spectrum component positions for carbon (1s), nitrogen (1s), oxygen (1s) and silicon (2p) signals on galactose surface of the carbohydrate functionalised polymer surface modification to mimic <i>Balanus amphitrite</i> SIPC.	122

Chapter 1. Introduction

1.1 The barnacle

In the 19th century, Harvard biologist Louis Agassiz described the barnacle as "nothing more than a little shrimp-like animal standing on its head in a limestone house and kicking food into its mouth" and though a little simplistic, it is essentially true. However the consequence of the barnacle and the 'limestone house' is of great economic and environmental importance. As an introduction to this research, this chapter provides an overview of the relevant literature associated with the project to bring the study into context.

1.1.1 Barnacle Nomenclature - the Cirripedia

All barnacles are classified in the subphylum Crustacea and infraclass Cirripedia. There are four orders within Cirripedia, of which the order Thoracica and family Balanidae will be the focus of this review. The Balanidae are currently divided into three sub-families; Balanidae, Concavinae and Megabalanidae. There is a proposed fourth sub-family - the Amphibalanidae. Due to the lack of formal definitions for the Balanidae, Pitombo (2004) endeavoured to use new morphological characteristics to review the classification of this family. Following this, there was debate over the naming of *Balanus amphitrite* as Pitombo (2004) revised the classification of *B. amphitrite*, including it in the new genus *Amphibalanus*. This led to the reclassification of *B. amphitrite* as *Amphibalanus amphitrite*; a change that was opposed by Clare and Høeg (2008). Overall there has been little adherence to this change in classification and for the purposes of this research, the barnacle studied will be referred to as *Balanus amphitrite*.

1.1.2 *Balanus amphitrite*

The striped acorn barnacle, *B. amphitrite*, was first described by Darwin in 1854. *B. amphitrite* is a circumtropical barnacle with a distribution that also extends into temperate waters from the Mediterranean to as far south as New Zealand. As one of the most widely distributed barnacles, it has a wide tolerance range for salinity and temperature (Bishop, 1950). Consequently, this euryhaline species can successfully inhabit both marine and brackish water (Fernando, 1999). Having previously been found in the Suez Canal in 1924 and on a cross-channel vessel in 1917, *B. amphitrite* was found on buoys in Shoreham

Harbour Canal, Sussex in 1937 (Bishop, 1950). It is considered that southern Britain is the northern-most limit of this barnacle species due to the low sea temperatures elsewhere. It is thought that warm water discharges such as thermal effluent from power stations eased the introduction of tropical species onto temperate coastlines (Bishop, 1950). There are three possible methods of introduction for *B. amphitrite*; firstly, the transport of the adult barnacle on the hulls of ships niche areas (e.g. sea chests) as fouling organisms, secondly, the transfer of pelagic barnacle larvae in the ballast water of ships and finally, transport on the shells of shellfish. However, the specific origin of this barnacle in the UK has not been confirmed due to its varied worldwide distribution (Eno and Clark, 1997).

The sturdy construction of the outer plates and large attachment surface of the sessile barnacle means that they are suitably adapted for life in the intertidal zone where current and wave action are strong (Ruppert and Barnes, 1994). However, this zone introduces further stresses such as large temperature ranges (from low during immersion to high after several hours out of water), small windows of feeding time (when immersed) and changes in salinity (saline submersion to terrestrial freshwater run-off). Some barnacles are better adapted to temperature and salinity changes and these dominate the high shore species. *B. amphitrite* is both euryhaline and eurythermal (Desai and Anil, 2005) and thus is a strong invading species once introduced (Foster, 1987). *B. amphitrite* has been observed surviving inland on the shores of tide-less saline lakes such as Salton Sea, California (Foster, 1987).

As a tropical barnacle, the development of *B. amphitrite* from hatching to adult is fairly rapid and is counted on a scale of several days rather than weeks, as is the case of more temperate barnacles such as *Semibalanus balanoides* (Clare and Matsumura, 2000). In tropical waters, where temperatures are relatively stable, breeding is continuous throughout the year with a slight dip in seasons with low salinities and reduced food supply. In temperate waters, *B. amphitrite* breeds seasonally with a peak in the summer as temperatures between 17 and 32°C appear best for breeding (Fernando, 1999).

The most important factor in the ability of barnacle species to survive is the time taken to reach maturity. *B. amphitrite* grows quickly and in comparison with other species has a relatively small adult size along with a less discriminatory choice of substrata. This allows the barnacles to make use of the available spaces that appear within the populated area before other species have the opportunity to become established (Foster, 1987).

1.1.3 Barnacle Biology and Morphology

Figure 1(a) shows the smooth calcareous wall plates of the barnacle shell, in which the barnacle develops with the carapace opening upward to allow the cirri to extend, as shown in Figure 1(b) (Ruppert and Barnes, 1994, Pitombo, 2004). These plates are for protection against predators and to reduce desiccation when immersed at low tide as they are impermeable when the aperture is closed. The underside of the barnacle is the basis, which is either calcareous or membranous. It is in this region that the cement glands are contained for adhesion to the substratum (Ruppert and Barnes, 1994).

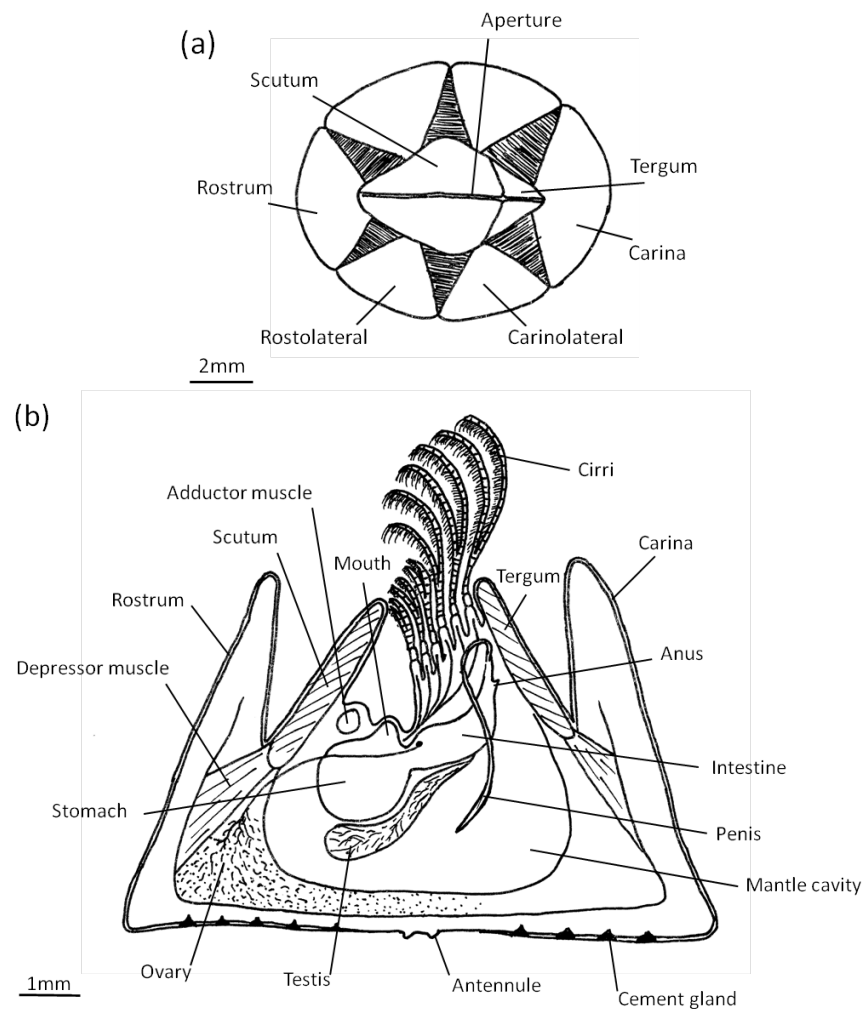


Figure 1 - A sessile adult *Balanus* barnacle (a) Dorsal view showing the layout of the shell exterior (b) Lateral section showing internal structures (both author's own)

Within the wall of plates, the organism itself is covered by an operculum formed by the scutum and tergum, see Figure 1(b). Both of these paired plates are moveable but can also be locked together using internal muscles or interlocking teeth. The body of the barnacle is orientated so that the appendages are directed toward the mantle aperture. These appendages consist of six pairs of biramous cirri that are used for feeding. Each of the cirri has setae to assist in the capture of planktonic food.

For feeding to occur, the scutum and tergum open and the cirri extend into the water column. Both sides sweep in and down acting like a net to catch food. To move the food toward the mouth, one pair of cirri scrape food off the other two pairs and transfer them down (Anderson, 1994). The mandibles and maxillae in the foregut then grind the food against a thickened cuticle plate. The ground food is then passed to the midgut, which contains seven digestive ceca and two pancreatic glands. These secrete enzymes which begin extracellular digestion. The digested food is then passed on to the hindgut where faecal pellets are formed (Ruppert and Barnes, 1994).

Blood is circulated through the mantle walls of the barnacle by a blood pump between the adductor muscle and oesophagus. Barnacles do not have gills and it appears that the cirri and mantle are the sites for gas exchange (Ruppert and Barnes, 1994).

1.1.4 Barnacle Reproduction

Barnacles as opportunists, produce large numbers of larvae of which only a few are likely to survive and settle appropriately (Crisp, 1976b). Barnacles produce many more larvae than are needed, thus upon settling there is a much greater concentration of larvae than is needed for survival (Crisp, 1960). Settling frequently and in high densities allows some of the population to be removed by predators whilst still allowing the population to survive (Foster, 1987). Barnacle nauplii are pelagic and thus distribution into the water column is dependent on currents and tides, which allows an increase in the range of dispersal leading to a more even population density and the opportunity for widening the gene flow (Crisp, 1976a).

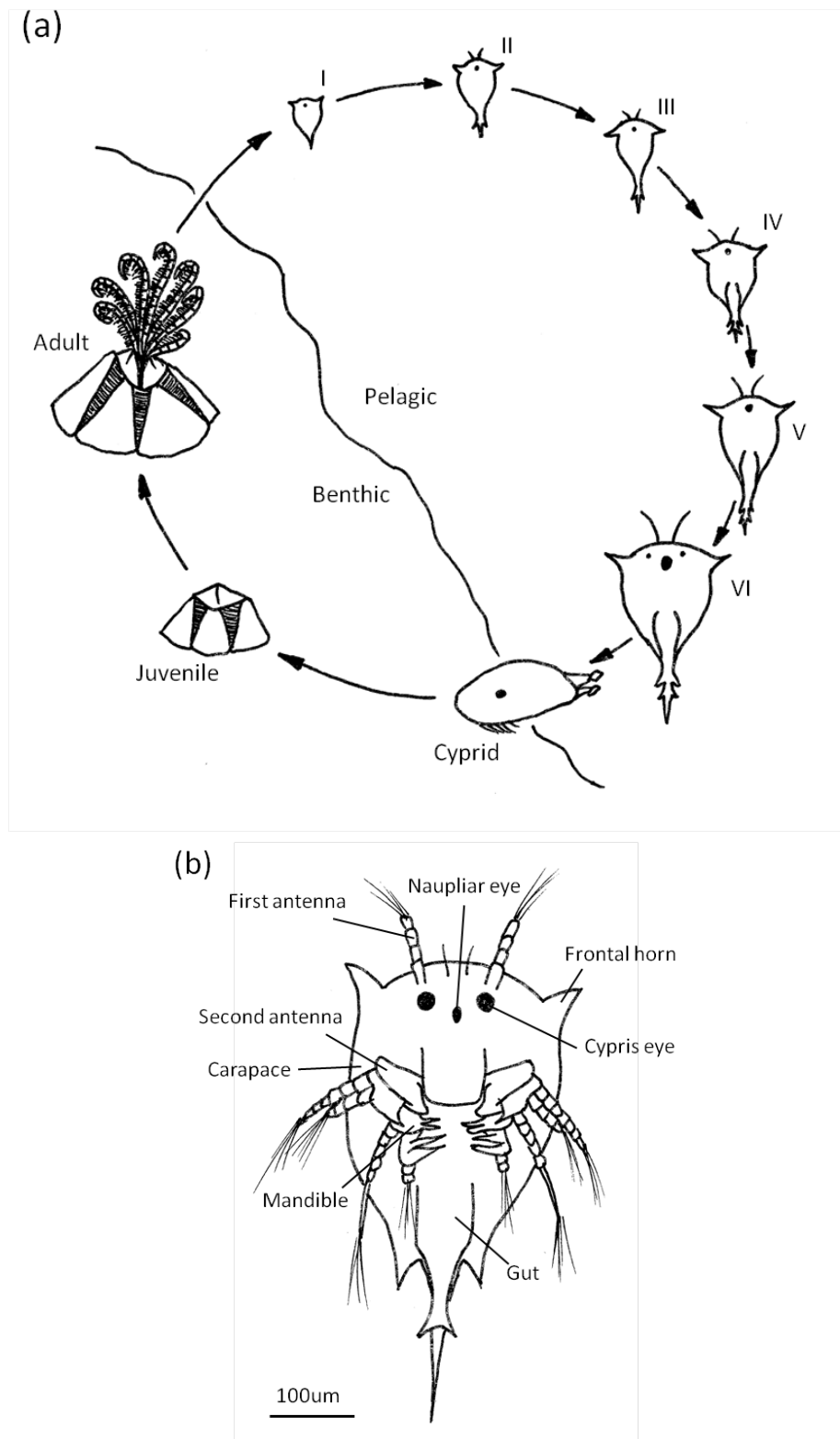
Barnacles are hermaphroditic and the majority are obligatory cross-fertilisers thus require adults to settle close to one another (Crisp, 1979). As a sessile invertebrate, the maintenance of the adult population relies on the ability of the larvae to recognise and settle in the adult

habitat (Finelli and Wethey, 1999). This gregarious behaviour must occur at settlement as only limited movement is possible afterwards. This not only allows easier cross-fertilisation but also monopolises the area for a single species, thus excluding competitors (Crisp, 1979).

Unfertilised eggs are stored initially in the ovaries, which are found in the mantle walls. Paired oviducts at the base of the cirri run to the oviducal gland, which creates an ovisac to keep the eggs together once deposited in the mantle cavity. The cephalic region houses the testes and sperm ducts which lead to the penis. This penis is extendable and for successful fertilisation to occur sperm must be deposited into the mantle cavity of another barnacle (Barnes et al., 2001). As barnacles are quasi internally fertilised, the sperm, deposited as a single mass near the cirri, must penetrate the ovisac to reach the eggs (Ruppert and Barnes, 1994).

Once fertilised, the eggs are brooded in the mantle cavity until hatching is induced by pheromonal eicosanoids (Ruppert and Barnes, 1994). This is normally triggered by the secretion of the eicosanoids and planktonic events, as coincidence with a bloom in the plankton population provides sufficient food for the planktonic larvae (Walker et al., 1987). The seasonal recruitment of barnacles is exemplified in areas that experience a monsoon season. During monsoon months recruitment is low, although reproduction does not stop entirely. However if there is little nutrition available for the adults during the monsoon season this has a negative effect on the quality of the larvae produced after the season is over (Desai and Anil, 2005).

After release, the non-feeding first stage nauplii, rapidly moult into the second stage, which is planktotrophic, see Figure 2(a). Dependant on the species, it can take from four days to several weeks for the naupliar stages to reach the sixth and final stage of moulting and growth (Walker et al., 1987). This final stage, see Figure 2(b) has a shield-shaped carapace with a pair of characteristic horns at the anterior end. These horns are connected to paired glands that secrete a proteinaceous discharge, which makes the limbs of the nauplius sticky. It is conjectured that this increases drag and decreases sinking rate when the nauplius is not actively swimming.



Next to these horns, ventrally, there are uniramous antennules (first antennae) followed by biramous second antennae and biramous mandibles posteriorly. The antennae are the structures used for locomotion whereas the antennules seem to be used only to counterbalance the ventral thoracic process during swimming. The labrum, which lies between the antennae, covers the mouth. There are four phases to the feeding mechanism used by nauplii. These are particle capture (or filtration), transfer of particles onto the ventral surface, transport forward towards the mouth and finally, ingestion. Above the mouth, close to the antennules, are the frontal filaments, which are unsegmented and filiform. The thorax of the nauplius tapers to the ventral thoracic process and the carapace tapers to the caudal spine above this. There is also a single median nauplius eye present in stages I to IV, and paired compound eyes in stages V and VI (Walker et al., 1987).

The final (VI) stage nauplius metamorphoses into the non-feeding cypris larva, termed an atypical lecithotroph, as it utilises the energy accumulated as triglyceride and cyprid major protein (CMP) during its preceding pelagic form rather than from a yolk provided by the adult barnacle (Shimizu et al., 1996). This means that adult barnacles can produce smaller and more numerous eggs. Non-lecithotrophic larvae are however at an increased risk of predation, starvation and excessive dispersal (Crisp, 1976a).

The cyprid, see Figure 3 (a) and (b), has a bivalved carapace that consists of three distinct layers; an inner lamellate endocuticle, an exocuticle with pore canals and a thin outer epicuticle. This carapace can be opened or closed. When open, six pairs of biramous thoracic appendages extend from the posterior and a single pair of antennules protrudes from the anterior (Figure 4a). These antennules form the articulated walking appendages and adhesive organs, as although the frontal horns are no longer present their associated glands remain.

These antennules have four segments. The second segment has a modified cuticle along with additional muscle groups allowing higher degrees of manoeuvrability (Lagersson and Høeg, 2002). The third segment is a bell shaped attachment organ (Nott and Foster, 1969) (See Figure 4b) and is covered with villi, setae and gland pores as well as cement ducts (Walker et al., 1987).

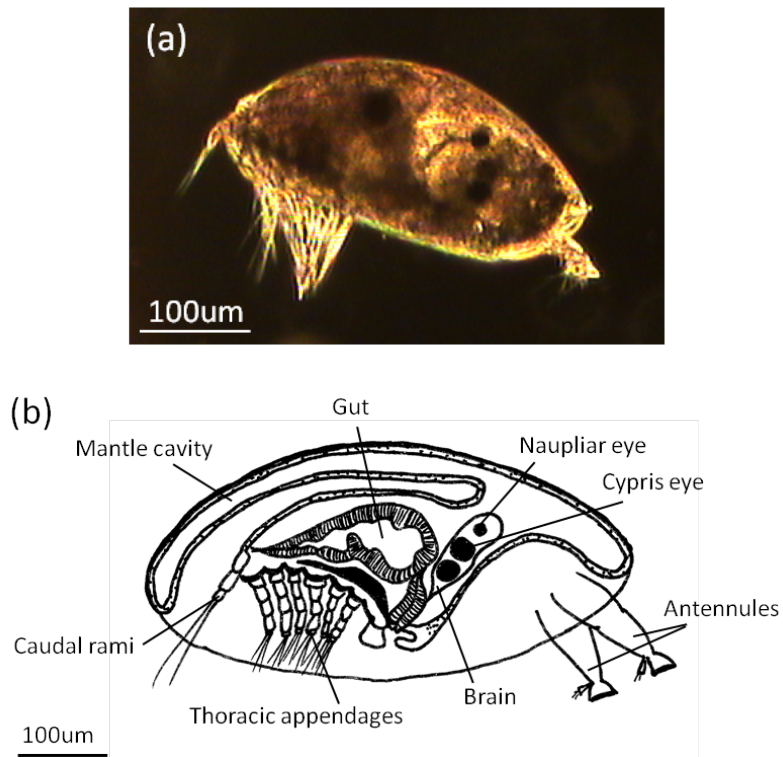


Figure 3 - A *Balanus amphitrite* cyprid (a) A light micrograph of a whole *B. amphitrite* cyprid larva with extended antennules and thoracopods (b) A *B. amphitrite* cyprid larva showing internal structures (both author's own)

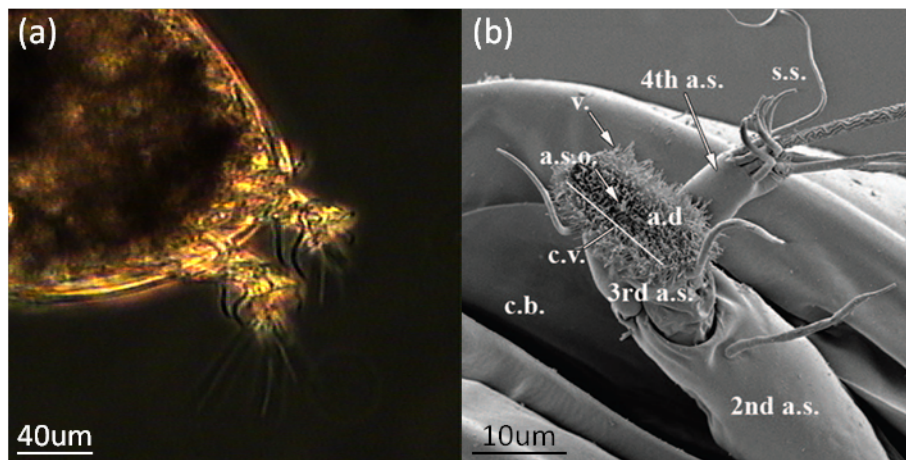


Figure 4 - The antennular attachment organ of *Balanus amphitrite* (a) A light micrograph of cyprid antennules (author's own) (b) A SEM image of the cyprid antennule. Labelled features are the second, third and fourth antennular segments (2nd a.s., 3rd a.s. and 4th a.s. respectively), the cuticular velum (v) encircling the attachment disc (a.d.), the hair-like cuticular villi (c.v.) and the axial sense organ (a.s.o.) in the centre of the attachment disc. Sensory setae (s.s.) are present on all three antennular segments, but are especially prevalent on the 4th a.s. The cyprid body is labelled c.b. (from Aldred and Clare, 2008)

It was first thought that the attachment disc functioned as a sucker but due to the large number of villi, increasing the surface area for contact with uneven surfaces, its suitability as an adhesive pad became clear (Nott, 1969). It is flexible and can be peeled from the surface it is attached to (Yule and Walker, 1987). The fourth segment is attached to the side of the third and is covered in sensory setae (Walker et al., 1987). The antennules of cirripede larvae are highly adapted to the exploratory phase and this is only possible because of the unique joint and muscle groups found in the antennule (Lagersson and Høeg, 2002).

Once the nauplius has metamorphosed into the cyprid, it can begin the settlement process. This normally occurs within 14 days of metamorphosis as the cyprids can only remain active as long as they have sufficient reserves of triglyceride and cyprid major protein contained in oil cells (Walker et al., 1987, Crisp, 1976b). The cyprid adapts its behaviour to increase the chance of contact with the substratum by controlling its vertical position in the water column, although this is species dependant (Finelli and Wethey, 1999). The cyprid responds to physical factors such as light, pressure, contour, gravity and current as well as chemical and biological stimuli in its search for an appropriate area to settle (Crisp, 1965, Crisp, 1976b). It was observed that the larvae of sublittoral species swim downwards, away from light before settlement whereas the larvae of intertidal species continue to swim upwards, as this appears to be the most effective mechanism for the larvae to be carried towards favourable habitats (Crisp, 1976b, Hui and Moyse, 1987). This behaviour also ensures larvae are retained in or distributed from an estuary depending on the habitat required (Dineen and Hines, 1994).

1.1.5 Settlement

Cyprids can delay metamorphosis and postpone settling until conditions are suitable and an appropriate surface is found (Knight-Jones, 1953, Knight-Jones and Stephenson, 1950). Once a suitable area has been identified, the settlement process begins. This has three distinct stages; attachment, exploration and fixation. The cyprid first uses a temporary adhesive from the antennules to adhere to the substratum momentarily while exploring for a suitable substratum. It appears that a cyprid can assess the biochemical properties of a surface (Yule and Walker, 1987), in what Crisp and Meadows (1963) referred to as 'tactile chemical sense'.

During exploration under static laboratory conditions, several search patterns are observed. First, 'wide searching' (within one or two centimetres of the contact point) where the cyprid walks steadily with little change in direction which allows a rapid assessment of the substratum (Finelli and Wethey, 1999). Each step can take five or six seconds, allowing full assessment of the substratum (Crisp, 1976b). This is followed by 'close searching' when a suitable substratum is located, where direction changes are often and sharp, sometimes simply twisting round on the antennule. The joints of the antennule are such that cyprids can move rapidly, at around two body lengths per second (Aldred and Clare, 2008). During walking, the cyprid demonstrates independent control over the attachment of each antennule (Nott and Foster, 1969) allowing close examination of the area through pivoting on one antennule whilst testing the substratum with the other (Knight-Jones and Crisp, 1953). Only small distances are covered to allow a thorough investigation of the substratum in that small area. The cyprids have been observed flicking the fourth antennular segment whilst exploring a substratum (Clare et al., 1994) and stepping from one antennule to the other on a single point and swinging their body in arcs. This appears to ensure there are no objects nearby and guarantees the cyprid an area the length of its body free from competition all around (Crisp, 1976b). This 'territoriality' means that cyprids settle from adults at a distance large enough to allow a little growth initially without leaving enough substratum free for other species to colonise (Hui and Moyse, 1987). If the cyprid comes into contact with an unexpected stimulus such as an air bubble, silt particle or algal filament it may leave the surface altogether in order to find a more suitable area (Nott and Foster, 1969, Crisp, 1976b). However, rejecting the substratum is risky as it may be some time before the cyprid comes into contact with a new surface. Thus the age of the cyprid will have some bearing on whether it chooses to reject a substratum or not (Hui and Moyse, 1987). By using this strategy, cyprids are able to find the most suitable position in relation to other barnacles and reduce intraspecific spatial competition without reducing interspecific competitiveness (Hui and Moyse, 1987).

It has been noted that settlement rates change with cyprid age. Settlement is low when cyprids are young and steadily increases as aging occurs (Rittschof et al., 1984). Older cyprids also appear to be less discriminatory in regard to picking an ideal surface (Kirby, 2006). Older cyprids also begin to lose their ability to discriminate between substrata (Clare et al., 1994). This is thought to be more connected to the physiological condition of the

non-feeding cyprid rather than age (Miron et al., 2000). Interestingly, the age of a cyprid also changes the settlement response in the presence of a biofilm. In the case of 0-day-old cyprids, settlement was inhibited but in 5-day-old cyprids, it was induced (Harder et al., 2001). Once a suitable area has been identified, the settling cyprid will rotate and flick the posterior cirri to 'sweep' the substratum before turning to face the incident light (Knight-Jones and Crisp, 1953). Following this, permanent fixation occurs using proteinaceous secretion from the cement glands, which release a volume large enough to embed the attachment organs and fourth segments as well as the cyprid ventral surface (Crisp et al., 1985). As it is fluid, the cyprid cement flows into and around structures on the surface, providing a stable mechanical key once cured (Yule and Walker, 1987). As cyprid cement is not a homogenous mass but a loose reticulum where the outer layers are in contact with the seawater, there is a curing time of around 1-3 hours. The cyprid then begins to metamorphose once more to take on the calcareous shelled adult form (Walker et al., 1987). Around 3 hours after permanent fixation, the cement has an increased tenacity of $9 \times 10^5 \text{Nm}^{-2}$. Phang et al. (2006) demonstrated a rapid curing of the cement to prevent dislodging. However, within 24 hours there is the production of 'juvenile cement' which has a tenacity of only $1.7 \times 10^5 \text{Nm}^{-2}$. After 40 days, the adult cement apparatus produces cement with a tensile strength of $9.3 \times 10^5 \text{Nm}^{-2}$ (Yule and Walker, 1987).

The shell growth is now continuous and the growth of the mantle and cirri is facilitated by the periodic shedding of the cuticle. A newly settled barnacle is around 3mm diameter at the end of the first months growth in the field (Ruppert and Barnes, 1994). Barnacles have adopted the 'droplet secretion pattern' of adhesion (Yamamoto, 1999), to maintain the shell growth, the barnacle secretes more droplets of cement. This forms growth rings reminiscent of tree-rings that can be viewed in cross-section when appropriately stained (Yamamoto, 1999). The barnacle shell plates are held in place by fixation fibres which are in turn connected to the base plate (or membrane). It is this base plate that is cemented to the substratum (Yule and Walker, 1987). The adult proteinaceous cement produced is comparable to a two part adhesive as two separate glands secrete a base and curing agent to allow permanent adhesion (Lunn, 1974). In the event of detachment, an adult barnacle of some species can also secrete a secondary cement to reattach and repair minor cracks in the shell base (Yamamoto, 1999).

Depending of the geographical location of the release, there can be larger quantities of cyprids attempting to settle than there is available space. In this case, it is normal for a large number of juveniles to die during the initial stages of settlement. It is due to the lack of suitable natural substratum that artificial structures in the marine environment are so readily fouled (Giúdice, 1999). Crowding occurs as there is commonly contact between individuals leading to mortality as individuals may be crushed, undercut or smothered by others. However, there have been adaptations to crowding. When the edges of two barnacles meet, there is a reduction of growth along that edge in both individuals (Hui and Moyse, 1987). Membranous-based barnacles, such as *Semibalanus balanoides*, have the ability to re-adjust their position and slide after settling and morphing into the adult stage. This ability to remain semi-mobile as well as strongly adhering to the substratum allows the barnacles to grow on the growing shells of other organisms and also move into adjacent empty areas if under continuous pressure from neighbouring barnacles (Crisp, 1960).

1.1.6 Factors affecting settlement

Several factors affect the settlement of cyprids; these include salinity, water flow and the characteristics of the settlement surface (Prendergast et al., 2009). The most effective of these is the settlement-inducing protein complex (SIPC) produced by the barnacles themselves (see Chapter 1.1.9). Although salinity is an important factor in the settlement of barnacles it appears to be less important than chemical cues. The SIPC in association with certain salinities (dependent upon species), stimulates settlement (Dineen and Hines, 1992). Without the SIPC or a crude version referred to as ‘adult extract’, few larvae will settle, regardless of salinity. This assures that the larvae will settle in an area that has previously supported adult growth (Dineen and Hines, 1994). It was noted that sessile organisms appear to distribute themselves along salinity gradients. This could be due to two reasons: firstly, settlement of the larvae at a salinity suitable for the adult reduces the stress of extreme salinities in adulthood and secondly, larvae settled in inappropriate salinities after indiscriminate settlement can lead to the death of those juveniles (Dineen and Hines, 1992). It was also noted that older cyprids will settle at higher salinities than younger ones and may show the urgency to settle indiscriminately to avoid being flushed from the estuarine system (Dineen and Hines, 1992). As euryhaline species barnacles can survive with this large variation in estuarine salinities.

Cyprids are initially negatively rheotactic, swimming with the current, before reaching a solid surface where they exhibit rheotaxy at the surface and settle. Because of this, maximum attachment occurs where water flow is just fast enough for the cyprid to maintain its position by swimming along the surface against the current (Crisp, 1955). Some species' cyprids appear to prefer sites where there is a strong and steady current of water, and it has been noted that barnacles in these areas are individually larger and are part of larger populations (Crisp, 1955). However, it is thought that the flow of water appears to only bring cyprids in contact with surfaces and does not have a direct influence at the time of settlement (Crisp and Meadows, 1963).

Barnacle cyprids are discriminatory when selecting suitable surfaces and are affected by texture, contour and surface films (Gabbott and Larman, 1987). If the surface is not desirable, the cyprid will detach and swim off in search of a more suitable one, such as bare rock (Knight-Jones, 1953).

Prendergast et al. (2008) found that texture affected several aspects of cyprid exploratory behaviour including exploratory distance, velocity, speed and time spent in contact with a surface. Cyprids preferentially settle on rough rather than smooth surfaces, possibly due to the 'lock and key' adhesion required by the adult barnacle (Aldred and Clare, 2009). Cyprids are rugophilic and thus tend to settle in depressions in the substratum, preferring small pits over larger ones (Barnett and Crisp, 1979). This research has recently been further developed by Schumacher et al. (2007) who studied changing the rugosity of surface features in polydimethylsiloxane elastomer (PDMS_e) to identify the critical spacing and width of feature for reduction of settlement; 2µm for *Ulva linza* spores and 20µm for *B. amphitrite* cyprids. It is thought that these provide a refuge from strong water flow, debris scouring and browsing by predators (Finelli and Wetthey, 1999, Crisp, 1976b). In addition, rough concave surfaces are preferred to smooth convex surfaces (Crisp et al., 1985).

Neal and Yule (1994) discovered that *Elminius modestus* and *Balanus perforatus* showed increased tenacity on surfaces covered in relatively thin, dense biofilms associated with high shear. It is thought that these biofilms provide the cyprid with an instant indication of the suitability of the surface as they are more sensitive to change than long established adult barnacles. In some organisms, such as the spirorbid polychaete *Janua (Dexiospira) brasiliensis*, the species of biofilm and associated flora is important for settlement. In this

case, a film of the diatom *Nitzschia corona* reduced settlement but the green macroalga *Ulva lobata* induced it (Kirchman et al., 1982). The authors have found that the presence of a mature, natural biofilm does appear to promote settlement. However published literature on the subject of natural biofilm is uncommon as results are rarely reproducible and the exact makeup of films is difficult to characterise. The above papers focus on monoculture films and even so results can appear arbitrary as settlement can be induced or inhibited based on the species of algae, age of film or stage of colony growth. However, *B. amphitrite* is unusual among barnacles in that cyprids will also settle on pristine surfaces.

Cyprid settlement is also affected by background colour as researched by Yule and Walker (1984). Dark coloured backgrounds (red and black) had more cyprids exploring the surface than lighter coloured (blue, yellow and white), and in addition the force required to remove a cyprid from a dark background was greater. This may simply display the cyprids willingness to release from a lighter surface as it considers it less desirable for settlement.

1.1.7 Gregarious behaviour

Above all other stimuli, it appears that the presence of other conspecifics induces thorough investigation of, and settlement on a surface. Most barnacles must exhibit gregarious behaviour in order to reproduce effectively and it is this requirement that forms the focus for this research. Under certain circumstances, larvae die before settling in areas free from conspecifics (Toonen and Pawlik, 1994). This may be because, for the non-feeding cyprid stage, the longer it remains in the plankton, the risk of not finding a suitable surface before lipid supplies run low, increases. This is known as the ‘desperate larva hypothesis’ (Elkin and Marshall, 2007). The gregarious nature of barnacle larvae also ensures that they settle in conditions favourable to the adult population (Nott and Foster, 1969). This also means that in areas where there were very few of each species, settlement occurs in small groups meaning that breeding could still occur (Knight-Jones and Stephenson, 1950). However, there is a compromise to be made. Crisp (1979) discovered a trade-off between proximity and fitness as barnacles less than one centimetre apart had lower tissue growth due to competition for food, leading to lower egg production and poorer overall fitness.

The obvious monospecies patches that occur naturally on the shore are a product of the gregarious nature of cirripedes but each zone is related to habitat preference among the initial settlers (Barnett and Crisp, 1979). Aggregations of organisms occur over time and in

several stages. Firstly there are the solitary larvae that initially colonise a previously uninhabited area then followed by newer gregarious larvae which settle in that are due to the presence of the initial colonizers (Toonen and Pawlik, 1994). Initially *Elminius modestus* cyprids settle in groups when first colonising surfaces and later arriving cyprids move slightly away from the group, spacing out evenly (Knight-Jones and Stephenson, 1950). The gregarious nature and group settlement pattern is shown in Figure 5.

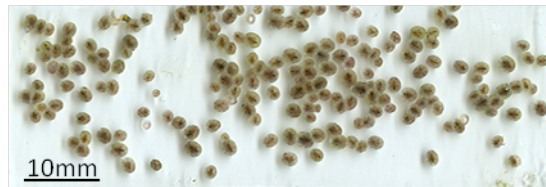


Figure 5 - Glass microscope slide showing the gregarious nature of *Balanus amphitrite* spat (courtesy of Dr Nick Aldred)

The cyprid larva responds to chemical and physical characteristics of the substratum as well as biogenic cues from conspecifics. This leads to the characteristic gregarious settlement patterns observed in barnacles (Dreanno et al., 2006a). Under laboratory conditions, adults may be the initial point of focus for cyprids, forming the ‘super-stimulus’ for exploration but the settlement of new cyprids does not require contact with an adult or even newly metamorphosed cyprids as the exploratory footprints of other cyprids provide enough of a stimulus (Yule and Walker, 1985).

Vogan et al. (2003) experimented with the eicosanoids hepoxilin and trioxilin, and found that they are inducers of larval egg hatching in barnacles. It was thought that further development in these areas may find other eicosanoids that could affect settlement leading to greater understanding of the role of pheromone cues. Snell et al. (1993) found that a glycoprotein found in the corona of female rotifer *Brachionus plicatilis* was used by males for mate recognition and copulating behaviour. Similarly, female copepods produce a trail of pheromones to increase the probability of mate encounter (Yen and Lasley, 2010). This is particularly important for organisms such as copepods that only mate once, to ensure that the mating event is successful through mate recognition (Lonsdale et al., 1998). The gregarious behaviour in barnacles works in a similar way through the glycoprotein settlement factor.

1.1.8 Marine glycobiology and glycoproteins

Glycobiology is the study of the structure, chemistry, biosynthesis, and biological functions of glycans or carbohydrate containing molecules (Caldwell and Pagett, 2010). In short, glycobiology demonstrates how protein and lipid-linked sugars affect biological processes (Taylor and Drickamer, 2003). The term ‘glycan’ refers to the carbohydrate portion (polysaccharide or oligosaccharide) of a glycoconjugate. Glycoconjugate is a collective term for several molecules including saccharides, glycoprotein, glycans, glycolipids and proteoglycans (Caldwell and Pagett, 2010). Glycans are similar to proteins in that they have very diverse functions, many of which are found in the marine environment. These vary from enzymes to hormones, transporters and structural elements. Glycans are classified into three groups according to the chain they carry (Brooks et al., 2002): glycans attached to lipids, those attached to a protein via a nitrogen atom (known as *N*-linked) and those linked to a protein through an oxygen atom (*O*-linked) (Taylor and Drickamer, 2003). The glycoproteins in Chapter 3 are *N*-linked and consequently the core protein is linked to a nitrogen via a GlcNAc and β -*N*-glycosidic bond (Brooks et al., 2002).

Glycans or cell surface oligosaccharides play an important role in recognition (Ambrosi et al., 2005). This is true for the glycans and glycoproteins being studied as part of this project (adhesion and signalling) and thus react with protein receptors called lectins (see 1.1.13). Lectins are proteins of nonimmune origin that bind to carbohydrates. Lectins recognise specific sugars, and consequently are thought to function in cell recognition (Caldwell and Pagett, 2010). It is through the use of these lectins that scientists have been able to examine complex carbohydrates both on cell surfaces and in solution (Ambrosi et al., 2005).

Glycomics is the compilation and study of the glycome or carbohydrate code, a catalogue of all the sugars of an organism, and the information conveyed in them. Studies of this nature are essential as sugars perform important roles such as cell-cell interactions and protein folding (Spain et al., 2006). It is the interaction between the carbohydrate moiety of cells and the lectins that bind to them, which has formed the basis for part of this research. Studying these interactions is becoming increasingly more accessible through the ultra-high sensitivity mass spectrometric strategies being developed to define the primary structures of glycoproteins (Dell and Morris, 2001). Once this has been achieved, it may be possible to manipulate the sugar structures presented on cells through the interruption of carbohydrate

biosynthetic pathways (Bertozzi and Kiessling, 2001). This would have a profound effect on the way that lectins react. There are also steps to increase the ease of synthesising glycoproteins through several methods, including coupling short peptides and using cells to produce them through fermentation (Sears and Wong, 2001).

1.1.9 The settlement-inducing protein complex

The settlement-inducing protein complex (SIPC) has been identified as the chemical cue to gregarious settlement in *B. amphitrite* and is implicated in both adult-larva and larva-larva interaction (Matsumura et al., 1998c). The SIPC is a water soluble cuticular glycoprotein contact pheromone (Crisp and Meadows, 1963) and appears to be synonymous with arthropodin which is mentioned in earlier papers (Crisp and Meadows, 1962, Yule and Crisp, 1983, Crisp et al., 1985, Crisp, 1990). Arthropodin was the name given to the SIPC before it was more fully understood due to its similarity to the cuticular proteins of insects (Dreanno et al., 2006c).

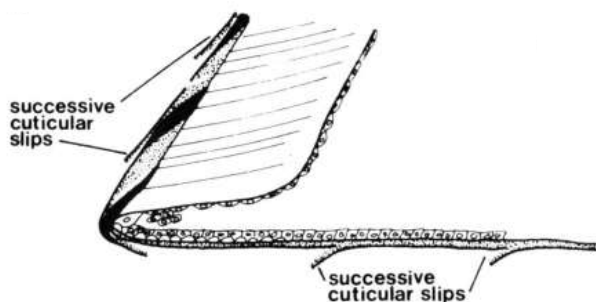


Figure 6 - Lateral section of an adult *Balanus* barnacle showing the successive cuticular slips exposing new SIPC (Bourget, 1987).

The SIPC is found in the cuticles of all larval stages as well as the adult (Matsumura et al., 1998c). However the concentration and site varies depending on the developmental stage. In the nauplius there is highest concentration in the mouthparts and hindgut, whereas in the cyprid it is found in the thoracopods, antennules and carapace. In the adult barnacle, when the exposure of the SIPC is most crucial, the glycoprotein is found in all internal cuticular tissues as well as the successive cuticular slips on shell. As shown in Figure 6 it is suggested that this is due to production by epidermal cells (Dreanno et al., 2006a) as there is continual growth of shell plates and secretion of epicuticle. The new cuticle is secreted

underneath the current epicuticle and both layers expand until the old membrane breaks, exposing the new cuticle to the searching cyprids (Bourget, 1987).

Knight-Jones (1953) endeavoured to test the stability and chemical nature of the settlement substance, then referred to as arthropodin. This led to conclusions on the probable nature of the SIPC as it was discovered that the chemical was unaffected by heat up to 200 °C, exposure to fat and protein solvents, contact with cold acids and alkalis, and treatment with protein reagents and oxidising agents. Further experiments attempted to gain more understanding of the SIPC as Larman et al. (1982) found the ‘active component’ was non-dialysable and could be fractionated with ammonium sulphate.

Following SDS-electrophoresis of boiled and unboiled extracts, it was concluded that the protein consisted of a polymorphic group of closely related protein subunits, as three distinct bands were observed on SDS-PAGE gels. While the sequence of *B. amphitrite* would suggest a molecular mass of ~170 kDa, the sum of the three subunits leads us to estimate a native mass of ~260 kDa, though this includes an approximate 15% carbohydrate content (Matsumura et al., 1998c, Matsumura et al., 1998b). Further complicating understanding, size exclusion chromatography indicates a native mass of between 200-400 kDa (Dreanno et al., 2006c), possibly suggesting a dimer.

The three polypeptide subunits of the SIPC protein (masses of 76, 88 and 98 kDa) have each shown to be capable of inducing *B. amphitrite* cyprid settlement as effectively as the intact SIPC (Matsumura et al., 2000, Matsumura et al., 1998b, Matsumura et al., 1998c). While it is known that the same gene encodes all three subunits, exactly how these three subunits are formed remains unknown. One possible solution is that post-translational cleavage of the SIPC gene product into three subunits that are then joined by disulphide bonds to form the complex. However, other processes cannot be ruled out, consequently this is an ideal area for future research.

Following the cloning and successful sequencing of the SIPC gene, 5202 base pairs were shown to encode a 1547-amino-acid protein with 7 potential *N*-glycosylation sites. As this single protein appears on denaturing gels as three subunits. It is thought that after the protein is expressed, it is post-translationally cleaved into three peptide subunits that then form the complex, joined by disulphide bonds. However, this is an idea area of future reach

as the mechanisms behind the mechanisms are far from clear. The SIPC was shown to be similar to thioester proteins with 30% sequence homology to the α_2 -macroglobulin protein family (A2M) (Dreanno et al., 2006a). There are similar instances of the A2M-type surface associated proteins performing SIPC-like roles in other marine organisms (Dreanno et al., 2006c), but specifically in the copepod, *Tigriopus japonicus*, where a sequentially similar protein to A2M has been shown to assist in mate recognition through chemical contact (Ting and Snell, 2003).

When a cyprid is exploring the substratum, it is thought that the SIPC in the basal margin and cuticular cover on the outer shell surface of adults is recognised (Clare and Matsumura, 2000). The cue must be adsorbed onto the substratum surface to be effective (Finelli and Wetthey, 1999) however an adsorbed monolayer appears to be adequate for cyprid response (Yule and Crisp, 1983). This may be because the cyprid responds to surface chemistry only, thus the thickness is irrelevant (Crisp, 1965). This research was reinforced when adults were covered in a barrier of bolting silk or nitrocellulose and cyprids did not settle, showing the need for contact with the cue for settlement (Knight-Jones, 1953). However, in the natural environment, layers of adsorbed macromolecules and microbial slimes cover submerged surfaces and consequently cyprids must be able to detect the SIPC through these (Crisp, 1985).

When cyprids were presented with the crude extract (adult protein containing the SIPC) treated and untreated panels for settlement in a solution of barnacle extract, they were able to distinguish between the two types of panel, and favoured the treated panels. However, over time the untreated panels became more favourable as it appeared that the extract in the solution was adsorbing onto the panel surface, forming a layer of protein and modifying the surface. It was found that attachment of cyprids to treated surfaces is immediately more tenacious than to untreated surfaces (Crisp and Meadows, 1963).

In some marine organisms the settlement cue must come from live animals, such as in the case of *Ostrea edulis*, however in barnacles the cue appears to effect a settling response from living, dead or preserved animals (Crisp, 1965). However, the SIPC was higher in concentration in newly moulted or recently settled individuals (Crisp and Meadows, 1962), and it has been observed that even old cement bases on surfaces still attract cyprids (Knight-Jones, 1953). Dreanno et al. (2007) found that the EC₅₀ (50% settlement) of *B.*

amphitrite SIPC was around $125\mu\text{g m}^{-2}$ in comparison to the 25mg m^{-2} found by Crisp (1990). It is thought this 200-fold difference is related to the purity of the cue. The more crude extracts used in Crisp's experiments would have contained higher contaminating protein concentrations as well as having degraded and denatured the glycoprotein through the preparation process (boiling and ammonium sulphate precipitation).

Studies comparing the proteomes of *B. amphitrite* larval stages; nauplius, swimming cyprid, attached cyprid and metamorphosed cyprid, using two-dimensional electrophoresis found marked differences and some similarities. The swimming cyprid proteome contained many more protein spots than other larval stages; this is perhaps related to the production of lectins for the detection of the SIPC during searching behaviour. Corroborating this theory, attached and metamorphosed cyprids both had a lower number of major proteins, implying the majority of those found in the swimming cyprid were no longer needed or produced (Thiyagarajan and Qian, 2008).

1.1.10 Cyprid Temporary Adhesive

The cyprid leaves behind 'footprints' of a proteinaceous secretion from the ambulatory antennules. These 'footprints' are detected using the high protein-binding membrane of nitrocellulose and the stain Coomassie Brilliant Blue (Walker and Yule, 1984) as seen in Figure 7.

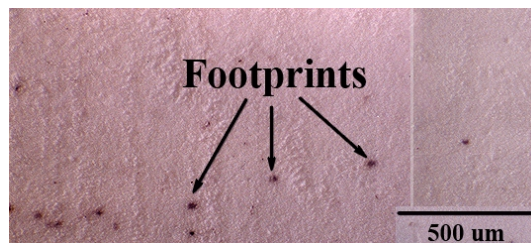


Figure 7 – The proteinaceous cyprid footprints of *Balanus amphitrite* stained on nitrocellulose membrane (from Phang et al., 2007).

The secretion appears to form a temporary adhesive but also has a secondary function as a chemical cue for larval settlement as foot-printed areas are more attractive to cyprids (Clare et al., 1994). The tenacity of the temporary adhesive is in the range of $2\text{-}3 \times 10^5 \text{Nm}^{-2}$ as this adhesive must allow movement over the substratum whilst still remaining strong enough to resist the flow of seawater (Yule and Walker, 1987). Some of the adhesive force is likely to be provided by cuticular villi.

Tests using excised antennules showed that there was no attachment (Crisp et al., 1985, Yule and Walker, 1987). Thus antennular attachment is not passive and requires a living animal demonstrating specific behaviour for adhesion to occur (Crisp, 1985, Aldred and Clare, 2008). It has been suggested that the antennular secretion is not an adhesive and the cyprid uses the nanotextured attachment disc like a gecko's foot relying solely on van de Waals forces. Aldred (2007) suggested that cyprids actually use a 'dry' mechanism for adhesion and that the antennular secretions are solely to enhance this rather than provide the adhesion itself. These theories are supported by the lack of footprints on low protein binding surfaces such as glass. It may be that the nitrocellulose, as a high protein binding surface, encourages excessive binding (Dreanno et al., 2006b). However, where they do occur, the cyprid footprint can persist on glass for up to three weeks, which is roughly the duration of some species' settlement seasons (Yule and Walker, 1985).

As it is found in the shell, hypodermis and soft tissues of adult barnacles, it is thought that the SIPC may be a structural protein that has acquired a secondary role in inducing settlement. Similarly, the cyprid temporary adhesive may be primarily for exploratory attachment and secondarily for attracting further cyprids. Explored surfaces with larger numbers of 'footprints' appear more attractive to cyprid larvae even without the presence of adults (Clare et al., 1994, Matsumura et al., 1998c).

Using polyclonal antibodies raised against peptides at the N- and C- termini of the SIPC, Dreanno et al. (2006b) discovered that this temporary adhesive was either a component of or related to the SIPC.

1.1.11 Waterborne cue

There has been much debate over the presence of a waterborne cue and it is widely considered to be a hypothesis. Early on in the research into settlement cues, the thought was very much against the concept. Crisp and Meadows (1963) argued that this cue would be diluted too quickly and that the spatial scale on which the cyprid larvae were interacting was too small for a waterborne cue. When water flows over a surface, a substance diffusing from it forms only a thin layer where the concentration is substantial, thus further from this layer the concentration in the water would be negligible (Crisp, 1965). As the cyprids are so small, the distance between sense organs is very small thus a chemical gradient would not be detectable (Crisp and Meadows, 1962). Further experiments showed that solutions of the

settling factor show no evidence of chemotaxis and have little effect on exploring cyprids. This led to the hypothesis that it must be bound to the surface (Crisp and Meadows, 1962, Crisp and Meadows, 1963).

After developments in experimental procedures, opinions began to change over the presence of a waterborne cue. Clare et al. (1994) surmised that the cue may be the water soluble SIPC from moulted adults, newly settled spat and the temporary adhesive. Later Matsumura et al. (1998b) postulated that water soluble peptides could be derived from the adult barnacles. It appears that the cue does originate from the adult (Clare and Matsumura, 2000) but only appears to alter the behaviour of cyprids encouraging temporary attachment and exploratory behaviour. Clare et al. (1994) showed that *B. amphitrite* did not permanently attach in response to a waterborne cue but changed exploratory behaviour. In this case, the purpose of the waterborne cue had been fulfilled, as the cyprids were encouraged to explore the surface. Although settlement was not directly induced, it would be provoked through contact with cyprid footprints or adults. Elbourne and Clare (2010) also experimented with the waterborne cue through conditioning seawater with adult barnacles. In conditioned seawater, cyprids did display increased swimming and searching behaviour, however this was also the case in some blank seawater standards. Evidence for the presence of the waterborne cue is varied but it has been hypothesised that bacteria may degrade the SIPC into peptide fragments which once in the water column are detected by free swimming cyprids (Dreanno et al., 2006a). In other marine species, such as the crayfish *Pacifastacus leniusculus*, a water borne pheromone is produced in the urine of females that initiates male courtship (Berry and Breithaupt, 2008).

1.1.12 Taxonomic Affinity

Taxonomic affinity is the rationale behind this research as all barnacle species appear to produce an SIPC-like protein, each with a different molecular mass. Although these proteins are specific to each species, there is some cross-reactivity and consequently ensures that developing an antagonistic antifouling surface based on *B. amphitrite* would also be effective on other barnacle species. This implies that either the SIPC receptor of cyprids is broadly tuned or that each species' SIPC is sufficiently similar (Clare and Matsumura, 2000). The variation appears to be in the amino acid composition and carbohydrate moiety of the different species' SIPC. This variation may contribute to species

recognition; this was tested using three different species' SIPC and also a human α_2 -macroglobulin (hA2M) as a negative control. There was no settlement induced on the hA2M. It is interesting that while allospecific SIPCs were similar enough to be recognised by all barnacle cyprids they were sufficiently different to allow discrimination at settlement (Dreanno et al., 2007).

There have been varying results in the area of the taxonomic affinity of cyprids. Interaction was first shown by Knight-Jones (1955) when the majority of cyprids settled on stones bearing conspecific elements (live adults or shell plates) but also that there was significant settlement on stones bearing elements from other Balanidae. This was not the case for different families such as Verrucidae and Chthamalidae. However, the results of Kirby (2006) contradicted this, showing that there was no significant difference in settlement on different species. It is thought that the response to allospecific cues enables barnacles to colonise new geographic areas more easily.

Crisp and Meadows (1962) showed in several independent experiments that extracts from other arthropods promoted settlement but not to the same extent as the same species. Barnett and Crisp (1979) noted that settlement is reduced by the presence of previous allospecific colonizers but increased by conspecific colonisers. This stimulation to settle gregariously with conspecifics but a distance away from newly settled allospecific larvae, achieves a density suitable for successful reproduction and growth. Barnett et al. (1979) and Hui and Moyse (1982) showed that *Elminius modestus* appears to be less discriminatory than *Semibalanus balanoides* as when presented with adult extract-treated plates of both species, *E. modestus* settled on both but preferentially its own. Kato-Yoshinaga et al. (2000) also found that the extracts of allospecific adults induced settlement of *B. amphitrite*, however the activity observed was less than that on conspecific extracts. Matsumura et al. (2000) found that there was a significantly higher rate of settlement on conspecific SIPC-coated surfaces than untreated areas. There was exploratory behaviour on both con- and allospecific SIPC-treated areas, however, exploration was slower and more prolonged on conspecific surfaces. Areas that had been treated corresponded with intense searching activity but longer assays were needed for settlement to occur. Higher concentrations also caused increased settlement of conspecifics.

1.1.13 Inhibition of settlement

Lentil lectin, known as LCA from *Lens culinaris* agglutinin, is a naturally occurring glycoprotein that inhibits settlement induced by adult extracts. It has been shown that sugar chains within the SIPC bind with the LCA, which suppresses the settlement-inducing activity of the pheromone (Matsumura et al., 1998b, Matsumura et al., 1998a). Treatment of cyprids with LCA did not affect settlement indicating it solely affects the SIPC (Matsumura et al., 1998a). It was concluded that it is the glycans within the SIPC protein that bind with the LCA, making these glycoproteins important for settlement-inducing activity. Further experiments were carried out by Matsumura et al. (1998b) using other commercially available proteins, some containing LCA-binding sites. These did not induce settlement as expected and it was concluded that the active sugar chains of the SIPC glycoproteins were specific and not simply LCA-binding glycoproteins.

Using diatoms to investigate settlement, Jouuchi et al. (2007) found that of 23 strains, two induced and nine inhibited the settlement *B. amphitrite*. They first concentrated on those which induced settlement, finding that the settlement factor, not to be confused with the SIPC, was a stable surface bound compound whose effectiveness was affected by a film of LCA. This led to the conclusions that an LCA-binding sugar chain compound in the inducing species plays an important role in inducing settlement of *B. amphitrite* and thus may be similar to the SIPC of barnacles. By removing bacteria from the diatom culture, the inductive effects were enhanced. The nine species that inhibited settlement were from seven different genera, indicating that the effects on settlement were not genus specific (Jouuchi et al., 2007).

1.1.14 Biofouling

Since the use of boats and ships to cross oceans and seas, biofouling has proved a problem. Biofouling is the process where a structure that is permanently or temporarily submerged in coastal, shallow water, becomes settled by organisms. Biofouling was originally thought to follow the successional hypothesis, beginning with the adsorption of molecular organic 'biochemical conditioning' films which are followed by 'slimes' of microscopic organisms (Jenkins and Martins, 2010). These slimes, organic detritus and bacteria provide a suitable physical surface for the colonisation of yeasts, protozoa and diatoms leading to the successful settlement of macrofoulers such as barnacles (Wahl, 1989, Nair, 1999,

Yamamoto, 1999). It is often found that larger macrofoulers such as oysters and mussels settle on the stable surface that the barnacles provide (Satpathy et al., 1999). However, Clare et al. (1992) emphasised that the successional hypothesis is too simplistic as barnacles will settle on non-biofilmed surfaces or form several layers with juveniles settled on larger adults, oysters and mussels (Mary and Mary, 1999).

In fouling communities, barnacles are frequently the primary colonisers (Foster, 1987). Barnacles are the group of marine fauna that are renowned for the problems caused by fouling; this is due to their substantial contribution to the surface coverage, volume and weight of fouling. There are around 1220 species of barnacles, of which 25 are common foulers (Nair, 1999). These crustaceans are not inhibited by the lack of light and thus foul the entire submerged portion of a structure (Lunn, 1974). Other fouling organisms include tunicates, worms, sponges, anemones and mussels. The shipworm, *Teredo navalis*, was a bigger problem before the introduction of metal hulled ships. This worm bores into the wood of ships and simultaneously lines the tube with a calcareous deposit, which temporarily supports the structure before complete collapse (Lunn, 1974).

For ships, the consequence of fouling on the hull is a reduction in speed of up to 30% (Ruppert and Barnes, 1994) due to the drag and weight increase caused by the fouling organisms and also the damage caused to the ship hull once removed, this was particularly true on older ships with softer paints. This drag can increase the amount of fuel needed by as much as 40% (Christie and Dalley, 1987) as well as impede manoeuvrability. This requirement to transport additional fuel in turn reduces amount of cargo that can be shipped. In addition, it is predicted that, when compared to a smooth hull, heavy calcareous fouling on boat hulls increases the required shaft power by 86% (Schultz, 2007). All of the above cost shipping companies time and money (Lunn, 1974). Fouling on the hulls of ships is also an important vector in the movement of invasive species (Fusetani and Clare, 2006).

Barnacles are a particular problem as they form a corrosive micro-environment beneath their bases. This area is ideal for the growth of sulphate-reducing bacteria which accelerates localised corrosion. In addition, the cyprid larvae are known to settle preferentially in cracks and fissures on surfaces. The consequential outward and downward growth of the shell increases the cracks and can lead to the ships' unprotected surface coming into contact with both the barnacle and seawater leading to further localised corrosion resulting in the

pitting of the surface. This proves particularly difficult to rectify during repairs (Christie and Dalley, 1987).

Biofouling also occurs on stationary structures such as buoys and pilings (Ruppert and Barnes, 1994) as well as aquaculture structures including nets (Eno and Clark, 1997). It is not considered to be as great a problem with the external sections of stationary structures such as oil platforms, although it can cause safety issues with overloading and does impede inspection by divers (Matsumura, 2006, Giúdice, 1999). Serious problems can arise in cooling intake pipes for electric power stations as fouling decreases water flow and increases the cost of maintenance with closure for cleaning (Christie and Dalley, 1987).

However, it should be noted that biofouling can also be a profitable business, for example the farming of oysters and mussels from naturally settled spat on intentional artificial structures (Giúdice, 1999). Even in these circumstances, incidental fouling organisms reduce the flow of water through cages, depleting oxygen as well as sometimes outcompeting the farmed foulers for food (Armstrong et al., 2000a). The additional weight of macrofoulers can sink aquaculture rafts as well as affecting land based aquaculture through the blocking of pipes pumping water to ponds (Armstrong et al., 2000a).

1.1.15 Antifouling Approaches

Fouling organisms can be plant, animal or prokaryote. Green and brown algae can prove difficult to remove due to their ability to reproduce sexually, asexually and vegetatively. Traditional underwater cleaning of ship hulls simply led to a rapid increase in algal fouling due to the increased spread of spores and fragmentation of adult parts (Lunn, 1974). Marine algae will only foul to a level on a structure where there is sufficient sunlight for photosynthesis, reducing the surface area affected. Antifouling technologies have been studied and summarised in recent years (Yebra et al., 2004) and a brief outline of the techniques used is presented below.

Early antifouling techniques were crude but nonetheless began steps to finding effective antifouling agent. As far back as Roman times, wax and lead were used to protect ships from fouling (Almeida et al., 2007). In the 15th century, it is thought that a mixture of pitch and whale grease was used to prevent fouling organisms from settling on ships (Lunn, 1974). There are several early patents dating from around this time covering the use of tar,

ground glass, arsenic, sulphur and zinc ores (Lunn, 1974). Toward the end of the 18th century it was shown that copper was effective against both *T. navalis* and surface foulers. At a similar time the use of zinc alloys were shown to reduce the concentration of fouling organisms and allow easier removal (Lunn, 1974). These methods, although most effective could increase the weight of the ship by around 5%, a heavy price to pay in loss of cargo weight (Lunn, 1974).

In the 20th century, the introduction of toxic antifouling paints began to revolutionise the antifouling of marine structures. These paints are made by dispersing a slightly toxic material in a natural varnish, and consist of several layers: a pre-treatment primer (corrosion inhibitor), an ordinary primer or anticorrosive paint, an intermediate or sealing coat and a finishing paint (Giúdice, 1999). Antifouling paints release toxins which kill the cyprid at the point of settlement, however to remain effective they must release the toxin at a constant rate, known as the Critical Leaching Rate ($\mu\text{g}/\text{cm}^2/\text{day}$). The maintenance of this has been the most difficult objective for current antifouling development. However, with the development of new vinyl, chlorinated rubber and epoxy resins physically tougher products were developed.

There are three approaches to paint systems. Firstly, the soluble matrix paint, developed in the 1950's, was a copper, arsenic or zinc toxin in a rosin matrix. The matrix dissolves over time thus releasing a steady rate of toxin but when the paint has gone, the surface is left unprotected. These coatings lasted only 12 to 15 months and were also sensitive to oil pollution and oxidation (Almeida et al., 2007).

The second approach is the insoluble matrix also developed in the 1950's, which leached toxins (copper or zinc oxides and/or organo-metallic compounds) out of an insoluble binder (an acrylic rosin or chlorinated rubber polymer) using seawater. Unfortunately this leads to the exponential release of toxins (Almeida et al., 2007) and the lifetime was only 12 to 24 months (Central Directorate of Environmental Protection, 1986). This method proved less reliable as the matrix remains when the toxin had been leached out leaving the surface unprotected but with a layer of now ineffective coating (Giúdice, 1999).

The third approach was the self-polishing organotin copolymer paint, developed in the 1970's and 1980's. This was an acrylic polymer bonded with tributyltin acrylate (TBT),

other oxides (e.g. cuprous oxide) and biocides (Christie and Dalley, 1987). The entire coating was soluble in seawater, thus gradually eroded away giving a constant release. The biggest advantage of this was that there was always a fresh surface to repaint (Almeida et al., 2007). Self-polishing paints containing TBT can remain effective for up to seven years (Armstrong et al., 2000a).

In regard to the toxins used, one chlorinated hydrocarbon; dichloro-diphenyl-trichloroethane (DDT) was particularly effective against barnacles. However, due to its persistence in the environment and food chains, it was banned from use in 1977. Following this and during reviews of the effects of the environment and human health, it was decided to reduce volatile organic compounds and toxic and carcinogenic components from paints (Almeida et al., 2007). The environmental consequences of TBT soon appeared as build up in estuaries led to excessive bioaccumulation due to its lipophilic nature (Central Directorate of Environmental Protection, 1986). TBT was finally banned in January 2008 (Almeida et al., 2007). An alternative to TBT was the herbicide Irgarol[®], which was a successful antifoulant increasing mortality of *Balanus albicostatus* (Khandeparker et al., 2005), however it was found to have negative impacts on aquatic and salt marsh plants (Armstrong et al., 2000b).

1.1.16 Modern Antifouling Approaches

In the last century there have been many novel ideas to combat the problem of biofouling. The suggestion of using ultrasonics to prevent settling was discarded due to the detrimental effect on the health of the crew. Teflon was also put forward as an idea, to include integrating synthetic microfibers, first to provide a coating that was difficult for foulers to attach to, then to assist with the flexibility of self-polishing coats (Almeida et al., 2007). However, there were problems with these coatings adhering to the hulls of ships. Radioactive paints, loudspeakers, air bubbles, toxins derived from decomposing cyprids and hormones have all been suggested (Crisp, 1976b) but none have proved worthy of serious experimentation. Recently, the use of electrodes to deliver pulsing electric fields (100ms duration and 10V) has been shown to reduce settlement of *B. amphitrite* from an average of 40% to 5% (Pérez-Roa et al., 2008).

In 1987, Intersleek, a low surface energy ‘self-cleaning’ coating was tested, and was introduced for use in the fast ferry market in 1996. The high speeds of these vessels made

them ideal for the antifouling properties of Intersleek (Anderson et al., 2003). Intersleek type products are termed as ‘foul release’ and have pioneered the biocide-free range of antifouling paints. However, the requirement of high speeds for effective release means that the technology is only suitable for a small proportion of the antifouling market.

Following problems with DDT and TBT, and the failure of other novel solutions, the move towards developing naturally occurring toxins was made. These are more environmentally acceptable, likely to be less persistent, are required to be inactive against non-target species, safe for humans and biodegradable (Christie and Dalley, 1987, Dobretsov et al., 2006). Aquatic organisms that remain un-fouled employ a combination of behavioural, physical, mechanical and chemical mechanisms, introducing the concept of natural chemical antifoulants (de Nys et al., 2010). Consequently, the prospect of producing a natural antifoulant has been the subject of several reviews covering the multitude of avenues for research and commercial potential (Rittschof, 2000). As many of the physical and mechanical defences were impracticable for antifouling, the use of extreme pH-values and exuded secondary metabolites was developed (Wahl, 1989). Sessile marine organisms such as live sponges and octocorals remain free of fouling organisms despite the lack of a mechanical antifouling mechanism. However dead colonies rapidly become fouled by algae and other organisms thus it appeared that a compound was being produced which deterred settlement (Mary and Mary, 1999, Armstrong et al., 2000a). Rittschof et al. (1986) found that settlement of laboratory reared barnacles was inhibited by products from sea pansies *Renilla reniformis* and whip corals *Leptogorgia virgulata*. The sponges studied by Mary and Mary (1999) contained up to two active compounds that inhibited the settlement of *B. amphitrite* larvae without killing cyprids. Similarly, isethionic acid and floridoside extracted from the red algae *Grateloupia turuturu* both inhibited cyprid settlement (Hellio et al., 2004). It was hoped to develop commercial analogues of these natural products and through experimentation in mixing different compounds, increase their effectiveness and spectrum (Nair, 1999). Burgess et al. (2003) have gone some way to investigating the application of water based paints containing bacterial extracts which proved effective at reducing barnacle and algal settlement. Water based paints required additional specialist chemistry to ensure appropriate drying times and film integrity and as such is the subject of current research by both academia and industry.

Other marine animals have inspired novel approaches that have the potential to be used in new antifouling technology. Lee et al. (2006) developed work on the observation that mussels can adhere to both organic and inorganic surfaces, even those renowned for being adhesion resistant, such as polytetrafluoroethylene (PTFE). They found that the adhesive pad of the mussel contained five specialised adhesive proteins in varying concentrations. These proteins contained lysine amino acids and 3,4-dihydroxy-L-phenylalanine (DOPA). Inspired by this composition, they found that by dipping objects in an aqueous solution of dopamine, it was possible to form multifunctional polymer coatings. These coatings were of the same composition regardless of the substratum used thus provided a versatile platform for secondary reactions. It is thought that through the selection of appropriate secondary reactants, the polydopamine surface can be adapted to have specific properties. In this case the suppression of biological interactions was the focus for further work rather than the practical application of the research (Lee et al., 2007).

Armstrong et al (2000b) began work on extracting active compounds from bacterial cells and adding them to acrylic resin base paints, which appeared to inhibit fouling bacteria. Interestingly, bacterial films of *Vibrio* sp. continued to remain inhibitive even in the presence of settlement cues such as the SIPC (Lau et al., 2003). The development of other enzymatic-based natural biocides from secondary metabolites produced by marine organisms is in progress but not yet at the testing stage (Almeida et al., 2007). The advantage of producing products from bacteria is that production is rapid and possible in large quantities (Armstrong et al., 2000b). Issues with systems of this nature appear producing a practical solution for mixing the extracts with paints to form effective coatings.

1.1.17 Stationary Structures

Antifouling paints are not practical for oil platforms and similar long-lived stationary structures as they cannot be removed for repainting. Currently rig operators use sacrificial anodes to protect from corrosion and use divers with heavy gauge wire brushes to remove fouling. This results in the surface being roughened by the remains of the previous growth which encourages more fouling to occur, resulting in successive scrubblings becoming increasingly frequent (Christie and Dalley, 1987). However, barnacle bases can be removed using sodium hypochlorite or covered using paint or nitrocellulose (Knight-Jones and Crisp, 1953). Milne submitted patents in the mid 1970's for a combined silicone-rubber and

silicone-oil system intended for ships. However, this was only developed on a small scale on fish farms. This worked on the principle that the initial adhesion of the organism was so poor that it was inadequate for the larger adult form. Silicone based fouling-release coatings now account for nearly 5% of the vessel based antifouling market (Yebra et al., 2004). This has been developed by Beigbeder et al. (2008) by adding synthetic multiwall carbon nanotubes in small quantities (0.05%) to silicone elastomer which causes a reduction in adhesion strength of *B. amphitrite*. Although this system reduced settlement when compared to unfilled control, it was not as effective as current commercial coatings.

There are several methods of antifouling for power plant systems; these include physical and mechanical cleaning, osmotic shock, deoxygenation, heat treatment, and the addition of biocides to the water. These biocides consisted of copper and bromine-based compounds, ozone, iodine, chlorine dioxide, tributyltin oxide, acrylamides and tannic acid (Satpathy et al., 1999). The addition of such treatments to cooling systems led to altered levels in surrounding natural watercourses affecting local ecosystems. Matsumura (2006) developed methods to assist in the antifouling of cooling systems. This was through the detection and identification of the species of larvae present in the water before settlement, to determine the settlement period and then take appropriate measures to stop settlement. This identification was through deoxyribonucleic acid (DNA) analysis of larvae, using a simple polymerase chain reaction (PCR) method without DNA extraction developed for individual larvae. This proved effective but was highly uneconomical from both a time and cost perspective. Further removal of the cyprids can be controlled using chlorination equipment which generates chlorine from the seawater and systematically flushes it through the system (Christie and Dalley, 1987). Alternately, the reversal of flow through cooling pipes is an effective method of killing organisms through subjection to high temperatures (Giúdice, 1999).

An alternative approach is the manipulation of surface topography to deter settling cyprids, as investigated by Schumacher et al. (2007). This is achieved by changing the height and width of features on the settlement surface, in this case a polydimethylsiloxane elastomer (PDMS_e). The attachment disc on the antennule of *B. amphitrite* is 25-30µm by 15µm. It was discovered that the critical dimensions for the feature spacing for *B. amphitrite* were 20µm wide and 40µm high. These parameters reduced cyprid settlement by 97% in

comparison to smooth PDMSe surfaces. From this work it was hoped that it might be possible to determine the critical dimensions for roughness required to reduce settlement. However, to define appropriate roughness to act as broad-spectrum antifouling surface is still a problem faced by those developing surfaces of this nature. An additional problem that is faced on such nanotextured surfaced occurs during field trials when algal spores fill the troughs, to once again form a suitable surface for settlement by smoothing the textured surface.

1.2 Project Rationale

This chapter has introduced the basics of barnacle biology and reproduction. The financial and ecological consequences of hard fouling by organisms such as barnacles highlight the importance of this research.

This research primarily consists of two main components. The first part centred on the carbohydrate portion of the SIPC. This initially focussed on characterising the carbohydrate moiety of the SIPC is outlined in Aims 1 and 2:

Aim 1 - To purify and isolate the SIPC of *Balanus amphitrite*.

Objective - The SIPC is partially purified by ammonium precipitation, ion exchange chromatography and gel filtration. At each step in the purification, the protein fractions are run on SDS-PAGE gels and the SIPC fractions are detected by immunoblotting with antibodies previously raised against purified SIPC. Bands are eluted from preparative gels for carbohydrate characterisation.

Aim 2 - To fully characterise the carbohydrate moiety of the SIPC.

Objective - Full *N*-glycan characterisation of the SIPC carbohydrates using combined HPLC and exoglycosidase digestions in collaboration with Professor Pauline Rudd's Group at the National Institute for Bioprocessing and Research, University College Dublin.

Following Aims 1 and 2, the next part of the research was to confirm the findings through the production and bioassay of an SIPC mimic, as outlined in Aim 3:

Aim 3 - To develop and test carbohydrate-functionalised polymers that are antagonistic to the SIPC and the cyprid temporary adhesive.

Objective - Surface bound SIPC mimics involving commercially available polymers to be developed at Professor Neil Cameron's Synthetic Chemistry Laboratory, Durham University, followed by bioassays based in the Invertebrate Reproduction and Development Laboratory, Newcastle University.

The second focus for this project was the deglycosylated SIPC protein, as outlined in Aim 4:

Aim 4 - To develop further understanding of the SIPC protein core.

Objective - Further analysis of the amino acid sequence and the core protein was carried out using techniques commonly used in structural biology, such as transmission electron microscopy and atomic force microscopy.

Chapter 2. Settlement Bioassay Development

2.1 Introduction

A series of preliminary experiments involving adult barnacles or the SIPC were carried out at the start of this research to provide suitable background and understanding of the topic and subject species. Other researchers have previously carried out these experiments using different species of barnacle. In this case, they provide a solid foundation on which to develop the novel research within this project. By looking at the basics of settlement and the effect of adult barnacles or the SIPC on cyprids it was possible to construct a suitable research plan to tackle the hypothesis under scrutiny.

In the recent decades that have seen closer examination of the contribution of barnacles to the biofouling problem, assays to measure and quantify the significance have been developed. Currently a suite of adaptable bioassays exists which can be adjusted to investigate settlement in barnacles of different species. Each of the assays mentioned in this chapter has been used in this research to provide insight into the settlement of *Balanus amphitrite*.

2.1.1 24-well plate assays

Settlement assays using polystyrene containers was first developed by Rittschof et al. (1984). The first iterations of this experimental design used small (30mm) non-treated polystyrene petri dishes, sometimes referred to as Falcon #1006 dishes. This was later refined by Rittschof et al. (1992) for observing inhibition of settlement. Each Falcon dish contained 25-30 barnacle cyprids in 5ml of artificial seawater or treatment solution and was incubated at 28 °C on a 15:9 L:D cycle. After 22 hours, the cyprids were counted as dead, free, attached or metamorphosed with the aid of a microscope. This system of bioassay provided accurate and repeatable results suitable for high statistical rigour. However, the nature of the individual dishes and lids meant that the assay was not space or time efficient. Consequently, Matsumura et al. (1998a) further developed this protocol to increase the throughput of replicates. This involved using polystyrene multi-well plates, either 24 or 96 wells depending on the experiment. For a 24-well assay, 4ml of treatment solution or artificial seawater was placed in each well with 14-18 cyprids and incubated for 8, 24 and 48 hours. As either 24 or 96 treatments could be observed in rapid succession the use of multi-well plates became commonplace. This method was adapted for experiments during

this research as outlined in Chapter 2.2.5. In the case of the research carried out by Matsumura et al. (1998a) larval settlement was promoted in the presence of adult extract in concentrations above 1µg protein/ml.

One area of discussion in the field of barnacle research for some time, has been the number of replicate cyprids in an assay. Due to the variation in larvae and the inductive effect of newly settled individuals, it has often been suggested that single-larva-per-well assays are the most appropriate to give representative and rigorous data. Several papers centring on the statistical differences between single-larva and multi-larva assays with barnacle cyprids have been published. The research carried out by Elbourne et al. (2008) centres around the interaction of conspecific cues in settlement assays, and explains the rationale behind the multi-larva assays employed during this research. In an ideal world, one-animal-per-well trials would be the best solution. However, in reality, these are not practical for several reasons. Primarily, the settlement rate (for example 15% after 24 hours) means that hundreds of replicate wells of each treatment are required to get statistical power, as demonstrated by Elbourne et al. (2008). This is rarely practical or time and cost appropriate. Secondly, the statistics that could be applied to these data would not be considered robust because there is no measure of variance. The most appropriate statistical analyses to be carried out on this data would be non-parametric chi-square-based evaluations. These are normally considered to be a less rigorous statistical analysis, as the data produced is not suitable for more robust analyses. Finally, it may be that any variation in the assays is not due to conspecific interactions, and simply due to natural variability in surface preference and settlement rate. Elbourne et al. (2008) showed that more than 10 cyprids per 2ml well could be used without seeing these effects. Consequently, the 24-well plate method as outlined in Chapter 2.2.5 has become a standard method.

2.1.2 Video Tracking

The ability to track individual larvae, whether barnacle cyprids or not, was a key step forward in understanding the modes of action in settlement. The system developed by Noldus et al. (2001) was primarily used for the behavioural tracking of small mammals and insects. However this has been developed and refined by Marechal et al. (2004) to include the tracking of much smaller, faster organisms such as barnacle cyprids. The protocol developed by Marechal (2004) tracked individual cyprids in small (30mm) nontreated

polystyrene petri dishes (Falcon #1006). Two of these dishes were used simultaneously over a 5-minute period to track individuals, with a minimum of 20 individuals being observed in total. This was found to be an appropriate number of replicates to remove individual variability within a larval batch and provide reliable measurements. The EthoVision 3.0 software analyses the cyprid's position within the petri dish arena and by measuring several parameters (distance moved, meander, turn angle, velocity and angular velocity), can distinguish between the different exploratory behaviours of individual cyprids. The distance covered and speed is indicative of a cyprid swimming or searching. The drawback of this method, is that it is very time consuming and intensive, thus for application in this research, some modifications were made to the protocol as laid out in Chapter 2.2.6.

2.1.3 Post tracking settlement assay

The post tracking settlement assay uses the 30mm petri dishes (Falcon 1006) from the video tracking of cyprids. The methods of using these larger dishes for settlement assays was first developed by Rittschof et al. (1984). In this case, the dishes were used in 22-hour settlement assays of different aged cyprids to allow analysis of the effect of age and presence of settlement cues on cyprid settlement. Cyprids were aged in the dark at 6 °C from 0 to 21 days old. Under these conditions, the cyprids did not settle on the storage containers and the effects of age could be tested. After 22 hours at 25 °C on a 15:9h light:dark cycle, the number of settled cyprids was counted and compared with the number still swimming in the media. This assay type also proved useful for assessing metamorphosis competence in different aged cyprids.

Clare et al. (1994) further developed this methodology where the same sterile Falcon dishes were used for high-density cyprid settlement assays. In this case up to 250 cyprids were added per 5ml of 100kDa-filtered seawater, following storage under similar aging conditions. Again, both the free-swimming larvae (emptied through a filter) and cyprids that had successfully settled in the dishes were counted to provide a percentage settlement per treatment.

This methodology has been adopted for the analysis of cyprid behaviour in conditioned petri dishes, whether the conditioning is the presence of an adult barnacle or an algal biofilm. The protocol used has been explained in Chapter 2.2.7.

2.1.4 Nitrocellulose Membrane Spot Assay

The nitrocellulose membrane assay was developed by Matsumura (1998a). Here, dot blotting apparatus was used to create 10mm diameter concave wells on a sheet of nitrocellulose. Some wells had the proteinaceous adult extract (See Chapter 1.1.6) applied, as nitrocellulose membrane is highly protein binding. This allows discrimination between wells by a cyprid exploring the surface. In the assay developed in 1998, after partially drying the membrane at 4 °C, it was fixed to a polypropylene container with carbon adhesive tape. 100ml of artificial seawater was added before two hundred cyprids were incubated for 48 and 72 hours. This methodology was built on further by Matsumura (1998b) using four commercially available purified proteins and the barnacle SIPC, in four separate assays, to observe the attractive effect of the SIPC against other proteins. Fetuin, ovalbumin, lysozyme and BSA, at concentrations of 100µg/spot, resulted in significantly less settlement than the SIPC (at 10µg/spot). This assay was repeated using similar parameters (see Chapter 2.2.8) with the SIPC purified during this research to ensure results were comparable to previous studies.

2.1.5 Drop Assay

The protocol for drop assays has been used in several iterations; the first drop assay methodology was developed by Pechenik et al. (1993), however other research led by Tang (2005), Perez-Roa (2008) and Petrone (2011) have adapted the design to suit the requirements of the assay. Tang et al. (2005), focussed on zoospores of the algae *Ulva linza*, where $1.5 \times 10^6 \text{ ml}^{-1}$ spores were placed on treated glass slides. These slides were then incubated in the dark for 1 hour, washed and then incubated in the light for 3 hours. The density of attached spores was then analysed via fluorescence detection.

Perez-Roa et al. (2008) and Tang et al. (2005), used similar designs for the study of barnacle cyprids; 200µl of seawater was placed as a drop onto a treated glass slide with ~28 cyprids and was incubated under ambient light. Despite 100% humid conditions, it was essential to incubate the slides in a lidded container with wet paper towels to prevent desiccation of the water drop. Petrone et al. (2011) plated glass slides with gold before treating with further SAM (self assembled monolayer) surface modifications. Here, ~2ml of filtered natural seawater was used for each drop along with 20 cyprids. The protocol used in

this research is based on that of Pechenik et al. (1993) and similar to the work of Perez-Roa et al. (2008) and Tang et al. (2005), see Chapter 4.2.7.

2.1.6 Aims and Objectives

The general aims for Chapter 2 are to investigate the previous research into experimental design of bioassays and the analyses that are commonly used to analyse behaviour as well as gain understanding of subject species. Although this will not include novel research, it can provide a solid foundation on which to develop further innovative research within this project.

2.2 Materials and Methods

2.2.1 Barnacle husbandry

The appropriate maintenance of an adult barnacle population was essential for this research as a supply of healthy cyprids was required. This maintenance included basic husbandry conditions, predictable production of juveniles and cyprid culture.

2.2.2 Laboratory maintenance of *B. amphitrite* adults

Brood stock supply of adult striped acorn barnacle, *B. amphitrite*, from North Carolina, USA were maintained in aquaria. Individual broods of barnacles were kept in separate plastic tanks containing natural seawater at 26 °C, on a 12:12 light:dark cycle. Tanks were aerated using air-stones and the water changed daily. Tanks were fed 24 hour hatched *Artemia* sp. (Artemia International, USA) nauplii each day and occasionally the algae *Tetraselmis suecica*.

For the release of nauplii to produce cyprids for assays, barnacles were encouraged to release in the dark, using a fibre-optic light source at one end of the tank. The photosensitive nauplii were removed from the tank and incubated at 28 °C, on a 12:12 light:dark cycle with aeration in 10 litres of 0.45µm filtered natural seawater. Initially 1 litre of the algae *Skeletonema* sp., 21.9mg/l of penicillin and 36.5mg/l of streptomycin were added to the water and 0.5 litre *Skeletonema* sp. was added each day. After 3 to 4 days, the presence of stage V nauplii (3-eyed nauplii, see Figure 2) was noted indicating that cyprid metamorphosis would occur within 12-24 hours. When more than 50% of nauplii metamorphosed into cyprids, the culture was filtered through 300, 250 and 160µm mesh to separate cyprids from the remaining nauplii. Once filtered, cyprids were stored at 6 °C in

cold 0.45µm filtered natural seawater before being left to the appropriate age for the assay and used for experimentation. 0-day-old cyprids (filtered that day) were most useful for experiments that aimed to examine induction of settlement as they are less inclined to settle. Experiments designed to reduce settlement used 5-day-old cyprids as these have a higher rate of settlement. Although this practice seems overly manipulative, the correct choice of cyprid age more clearly defines the efficacy of an experimental treatment (Clare et al., 1995).

2.2.3 Petri dish rearing of barnacles

In 30x10mm polystyrene petri dishes (Sterilin, UK), ten 5-day-old cyprids were added in a 200µl droplet of 0.45µm filtered natural seawater. Dishes were incubated at 28 °C for 48 hours until the cyprids had metamorphosed into the adult form. The barnacles were grown up over 25 days, washed three times weekly in artificial seawater and fed 2ml of *Tetraselmis suecica*, *Skeletonema* sp. or *Isochrysis galbana* depending on availability. After 7 days, weaker barnacles were removed, leaving the dominant adult remaining. At 25 days old, these adults were used for further assays.

2.2.4 Resin barnacle mimics

Using the 25-day-old petri dish reared adults, resin mimics of the adults were made. Using dental adhesive (Extrude medium, Kerr, USA) impressions were taken of the barnacles in order to make epoxy mimics as per the manufacturer's instructions (Epiglass HT9000 epoxy resin, International Paint, UK). These mimics were glued to clean dishes using epoxy and treated after this as if the dish contained a real barnacle to ensure similar growth of biofilm (i.e. incubated in seawater with the other biofilm treated dishes for 25 days).

2.2.5 24-well plate assays

In all settlement assays, an internal laboratory standard of polystyrene was included to provide an indication as to the larval quality and overall settlement potential of cyprids used in the main assay, i.e. whether the batch would settle or not regardless of the test conditions. Briefly, the sterile non-treated polystyrene 24-well plate (Iwaki, Japan) can hold a maximum of 2.5ml per well. Aliquots of 2ml of 0.45µm filtered natural seawater were placed in 6 wells and ten cyprids were added to each well. The well plate lid was replaced to avoid excessive evaporation and all of the well plates wrapped together in tin foil. The

assay was incubated at 28 °C in the dark for 48 hours. After the initial 24-hour point and after an additional 24 hours, cyprid settlement was recorded with the number of dead, floating, settled, metamorphosed and swimming cyprids noted.

2.2.6 Video Tracking

The ability to remotely observe and quantitatively assess cyprid behavioural changes under different circumstances was conceptualised by Noldus et al. (2001) and further developed by Marechal et al. (2004). Using camera hardware (digital colour charge-coupled device camera) (Panasonic CCD camera with a 50mm telecentric lens (Computar Ltd.) connected via c-mount) and EthoVision software (Noldus, UK) the coordinates of a cyprid were tracked and this data used to create five parameters: total distance moved, velocity, turn angle, angular velocity and meander. The camera lens was placed 125 mm above the experimental arena, which contained six 30x10mm petri dishes (Sterilin, UK). The arena was placed on a light box to give better contrast to the cyprids. Four treatments were used for the assessment of the effect of the presence of adult barnacles on cyprids: a real adult with biofilm, produced as described in Chapter 2.2.3, where one 25-day-old adult was grown in a petri dish and consequently had a thin algal biofilm present; a resin mimic of an adult with biofilm, produced as described in Chapter 2.2.4; an empty petri dish that had been left to soak in natural seawater to build up a biofilm over the same 25 day period as other dishes; and a new clean petri dish. In those dishes with biofilm, the excess visible algae on the bottom of the dishes were removed with a soft sponge to allow clarity whilst tracking. One cyprid was introduced to each dish in 5ml of 0.45µm filtered seawater. The treatments were tracked in sets of 6 with each treatment repeated 6 times with different cyprids giving 36 replicates. A 5 minute tracking time was used.

After tracking was completed, the same dishes were retained and used for the settlement assay in Chapter 2.2.7. For the analysis of video tracking data, each track was assessed to remove errant, non-representative tracks where cyprids were not swimming or exploring or where tracking had lost them. In addition, to remove outliers and retain representative results, the top and bottom five results were removed. This apparently arbitrary methodology of ‘data smoothing’ is used frequently in this protocol to eliminate slight ‘apparent’ movements if a lower sample rate describes the path better Noldus et al. (2001). As a high throughput method, there are a small number of outliers per experiment. If the

distribution is normal, the removal of a few points does not affect the mean or significantly change the variance. Occasionally, there may be significant outliers and these are generally 'caught' by this technique and only the central 'more normal' portion of the frequency distribution is used in the analysis. This smoothing technique is applied on a case-by-case basis.

2.2.7 Post tracking settlement assay

Using the same dishes as in the video tracking experiments (see Chapter 2.2.6), the settlement rate and proximity of cyprids can be assessed. Six replicate petri dishes of each treatment were used: a real barnacle with biofilm, a resin mimic barnacle with biofilm, a dish with no barnacle present but with a biofilm and a clean empty dish (no barnacle or biofilm). Twenty cyprids were put into each dish, which to reduce evaporation were wrapped in aluminium foil. The dishes were incubated at 28 °C for 48 hours with the number of cyprids settled and metamorphosed being counted at 24 and 48 hours. In addition, digital photographs were taken at 48 hours using the same equipment as used for tracking and EasyGrab software. No scale was needed for the analysis as the dishes used were 30mm diameter. In the case of those treatments where there was no barnacle or resin mimic in the dish, a sheet of acetate was placed underneath to indicate the position. ImageTool software (UTHSCSA, USA) was used to measure distances from settled cyprids to the barnacle in the centre of the dish.

2.2.8 Nitrocellulose Membrane Spot Assay

Assays carried out using nitrocellulose were based on those from Matsumura et al (1998b), Kirby (2006) and Dreanno et al. (2007). In this case it was used for testing the efficacy of the SIPC as an attractant in comparison to another protein; bovine serum albumin (BSA) which is not glycosylated. In brief, the nitrocellulose membrane (0.45µm plain white membrane, MFS Advantec, USA) was cut to 135mm x 95mm pieces and soaked in 50mM TrisHCl pH7.5 for 10 minutes. The membrane was sandwiched between plates of a dot-blotting apparatus with 10mm diameter wells (Atto Immunodot AE-6190, Atto Co. Ltd, Japan). The dot-blotting apparatus allows for 24 wells, of which two sets of 12 were used. In each 12 there were 4 wells each of the SIPC, BSA and TrisHCl. The allocation of wells to each treatment was determined using random number generation. A control set of 24 wells contained only TrisHCl but had falsely assigned SIPC, BSA and TrisHCl labels to

give ‘expected’ values. The SIPC was diluted with 50mM TrisHCl pH7.5 to 10µg/ml of which 1ml was added to each of the appropriate wells. Likewise, 10µg/ml of control protein BSA (Sigma, UK) and ‘blanks’ of 50mM TrisHCl pH7.5 buffer were added to wells. The apparatus was then attached to a vacuum manifold and the nitrocellulose membrane was subjected to gentle suction for 10 minutes allowing the proteins present in the well solutions to bind to the membrane. The membrane was then removed from the apparatus and double-sided carbon tape (Agar Scientific, UK) was applied around the edge of the membrane. Due to the action of the vacuum, the wells in the apparatus formed concave depressions in the membrane, referred to as ‘spots’, and it was in these areas that the treatments were present. The membrane was taped to the bottom of a new polypropylene container that closely matched its dimensions. 200ml of 0.45µm filtered natural seawater was added to the container followed by approximately 200 cyprids. After replacing the lid to ensure no evaporation occurred, the container was wrapped in aluminium foil and placed in an incubator at 28 °C for 48 hours. At the same time, a 24-well plate (Iwaki, Japan) was used to assess general settlement levels and allow appropriate interpretation of results. This plate contained 10 cyprids in each of 12 wells of 0.45µm filtered natural seawater and 12 wells of 1×10^{-5} 3-isobutyl-1-methylxanthine (IBMX) (Clare et al., 1995). Cyprid settlement behaviour was recorded at 24 and 48 hours, with the number of settled and metamorphosed cyprids recorded on each concave spot, the surrounding membrane, the carbon tape and the container itself.

The total number settled in each well was counted in comparison to the total settled in all wells. Cyprids that had not settled in a well were ignored due to the prevalence of edges, corners and sticky carbon tape.

2.3 Results

2.3.1 Video Tracking Assay

The parameters were total distance moved (cm), mean velocity (cm/s), total turn angle (°), mean angular velocity (°/s) and mean meander (°/cm). Figure 8 shows the results of the video tracking for each of the parameters, with those results that are significantly different from each other indicated with a letter. For example, two treatments both with an A are significantly different from each other, similarly those treatments with B indicates that they

are significantly different from each other. Where a treatment has two letters, e.g. AB, this indicates that this result is significantly different from two others.

For velocity, data were normal (Kolmogorov-Smirnov test statistic = 0.052, $p > 0.150$) and equally variant (Bartlett's test statistic = 3.06, $p = 0.382$). An ANOVA showed that the dish with no barnacle and with biofilm was significantly different from the dishes with no barnacle and no biofilm and a resin barnacle with biofilm (ANOVA $F = 7.13$ $P = <0.001$), as shown in Figure 8(a).

For distance moved, data were normal (Kolmogorov-Smirnov test statistic = 0.051, $p > 0.150$) and not equally variant (Bartlett's test statistic = 8.21, $p = 0.042$). A Kruskal-Wallis test showed that the dish with the real barnacle and biofilm was significantly different from the dish with no barnacle or biofilm ($H_{19} = 14.89$ $P = 0.0019$) as indicated in Figure 8(b).

For turn angle, data were normal (Kolmogorov-Smirnov test statistic = 0.073, $p > 0.150$) and not equally variant (Bartlett's test statistic = 12.00, $p = 0.007$). A Kruskal-Wallis test showed that the dish with a real barnacle and biofilm was significantly different from both dishes not containing a barnacle ($H_{19} = 12.96$, $P = 0.0047$), as shown in Figure 8(c).

For angular velocity, data were normal (Kolmogorov-Smirnov test statistic = 0.087, $p > 0.150$) and equally variant (Bartlett's test statistic = 5.78, $p = 0.123$). An ANOVA showed that the dish with no barnacle and with biofilm was significantly different from the dish with a resin barnacle and biofilm (ANOVA $F = 3.89$ $P = 0.012$), as shown in Figure 8(d).

For meander, data were normal (Kolmogorov-Smirnov test statistic = 0.079, $p > 0.150$) and equally variant (Bartlett's test statistic = 4.27, $p = 0.234$). An ANOVA showed that the dish with no barnacle and with biofilm was significantly different from the dish with a resin barnacle and biofilm (ANOVA $F = 3.98$ $P = 0.011$), as shown in Figure 8(e).

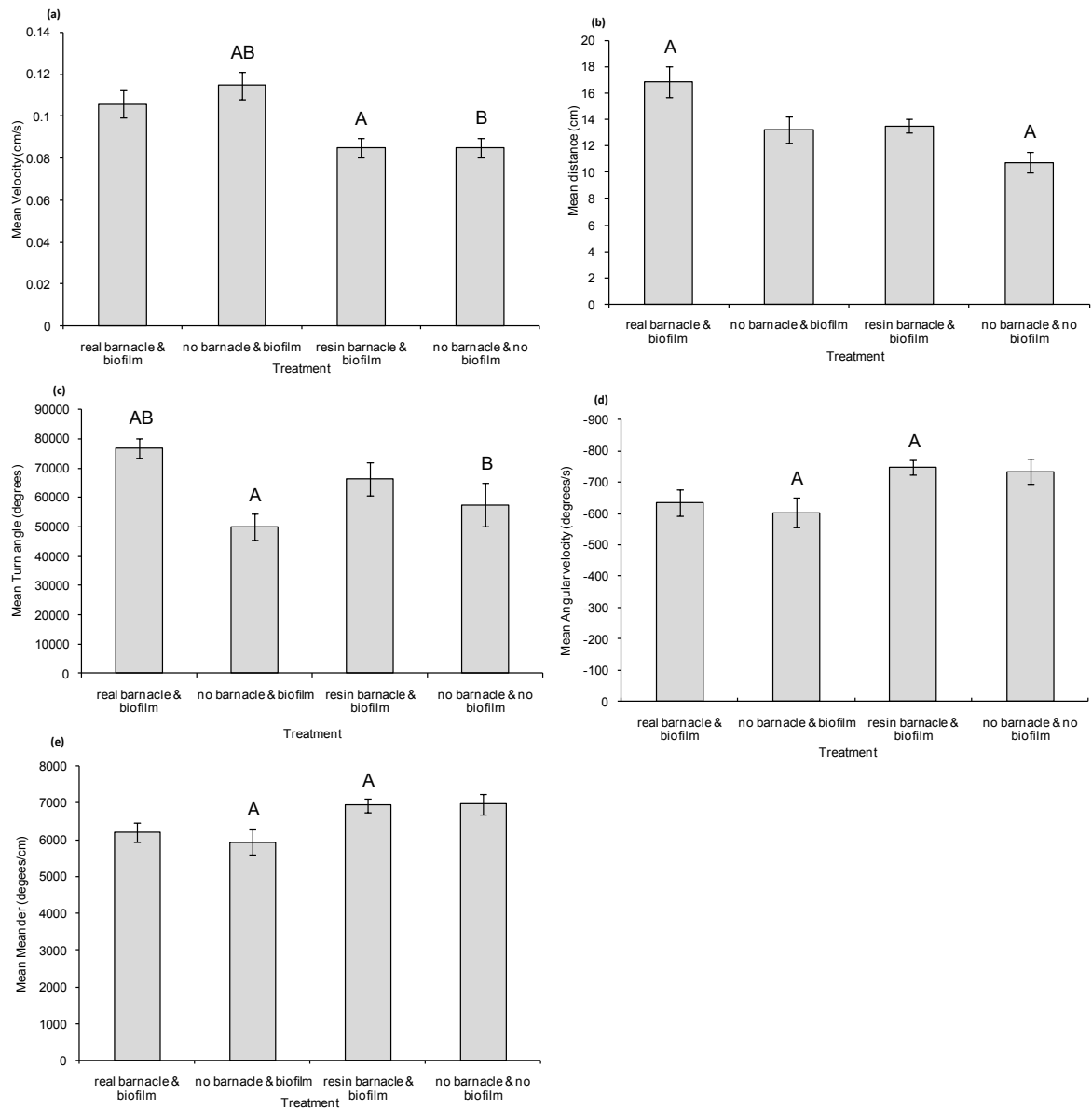


Figure 8 - Behavioural parameters measured for *Balanus amphitrite* cyprids when tracked for 5 minutes with EthoVision 3.1. (a) mean velocity (cm/s), (b) mean distance (cm), (c) mean total turn angle ($^{\circ}$), (d) mean angular velocity ($^{\circ}$ /s) and (e) mean meander ($^{\circ}$ /cm). The letters indicate which treatments are significantly different from each other (i.e. treatment with A is significantly different to the other treatment with A). Error bars are \pm standard error.

In summary, the mean distance travelled when a cyprid was in the vicinity of a real barnacle was significantly more than when there was no barnacle or biofilm present. This is most likely to be due to the cyprid detecting the presence of the adult via the SIPC and searching the dish to locate the adult and settle. The lack of biofilm may also play a part. Similarly, the total turn angle when an adult barnacle is present is much higher than for the

non-barnacle treatments. This is due to the characteristic ‘close searching’ employed by cyprids to pinpoint the source of a settlement cue. For the speed of exploration, the presence of an adult barnacle does not affect velocity as it is the dish with no barnacle present that has the highest average speed of exploration. This may be the case because the cyprid is using a fast searching technique to allow coverage of a large area to find a cue rather than the close surface exploration observed when a cue is present. For both angular velocity and mean meander the results are similar, where the resin mimic is different from dishes with no barnacle present. This is likely to be due to searching patterns reflecting the detection of the biofilm indicating a suitable surface (unlike the clean dish) but not the presence of a cue.

2.3.2 Settlement Assay

In regard to the number of cyprids settled and metamorphosed after 24 hours, the data were normal (Kolmogorov-Smirnov test statistic 0.170, $p=0.072$) but not equally variant (Bartlett’s test statistic =11.78, $p=0.008$). The results were significantly different, with both dishes with a real barnacle and resin mimic being significantly different from the dish with no barnacle or biofilm (Kruskal-Wallis test statistic $H=11.18$, $p=0.011$). These results are shown in Figure 9(a).

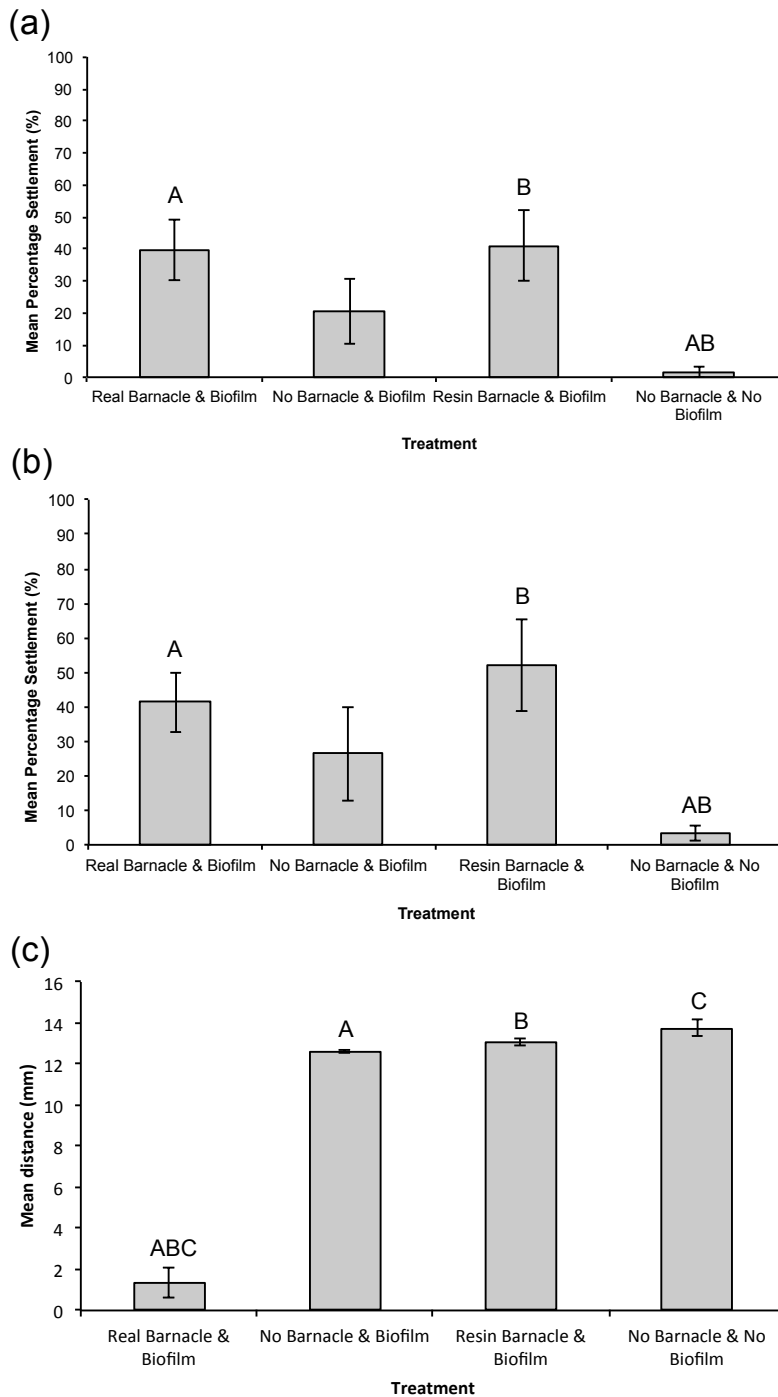


Figure 9 - Settlement of *Balanus amphitrite* cyprids in the presence of adult barnacles, resin mimics of barnacles and no adult (a) Mean percentage settlement of cyprids after 24 hours in dishes with four treatments. (b) Mean percentage settlement of cyprids after 48 hours in dishes with four treatments. (c) Proximity of cyprid settlement to an adult barnacle in the centre of a petri dish. The letters indicate which treatments are significantly different from each other (i.e. treatment with A is significantly different to the other treatment with A). Error bars are \pm standard error.

After 48 hours, the data were again normal (Kolmogorov-Smirnov test statistic 0.164, $p=0.09$) and not equally variant (Bartlett's test statistic =12.07, $p=0.007$). Again the data were significantly different, with dishes containing both a real barnacle and a resin mimic being significantly different from the dish with no barnacle or biofilm (Kruskal-Wallis test statistic $H=12.20$, $p=0.007$). These results are shown in Figure 9(b).

In addition to the total settlement of cyprids, the distance of settlement from an adult barnacle was also measured after 48 hours. The data were neither normal (Kolmogorov-Smirnov test statistic 0.329, $p<0.010$) nor equally variant (Levene's test statistic =1.03, $p<0.05$). However, as shown in Figure 9(c), the dish with the real adult barnacle was significantly different to all of the other three treatment conditions (Kruskal-Wallis test statistic $H=45.09$, $p<0.001$).

2.3.3 Nitrocellulose Membrane Spot Assay

After 24 hours, this data was not normally distributed (Kolmogorov-Smirnov test statistic = 0.240, $p<0.01$) or equally variant. Settlement on either of the control membranes spots showed no significant difference between wells; $\chi^2=0.503$, $df=2$, $p=0.776$ and $\chi^2=0.26$, $df=2$, $p=0.878$. For the test assays, one assay was significantly different ($\chi^2=6.52$, $df=2$, $p=0.0383$) and one was not ($\chi^2=3$, $df=2$, $p=0.2231$).

After 48 hours, data were again not normally distributed (Kolmogorov-Smirnov test statistic = 0.259, $p<0.01$) and not equally variant (Levene's test statistic = 9.25, $p=0.001$). Data from both controls showed no significant difference; $\chi^2=0.823$, $df=2$, $p=0.6626$ and $\chi^2=0.5$, $df=2$, $p=0.7788$. However, both of the test assays showed a significant difference; $\chi^2=7.33$, $df=2$, $p=0.0256$ and $\chi^2=6.75$, $df=2$, $p=0.0342$.

The non-parametric Chi-square test is less powerful than other statistical tests as it does not require the data to be normal or equally variant. Due to the less robust nature of Chi-square, it could not be determined which of the three treatments was significantly different using the statistical tests above. However, Figure 10 clearly shows the increased settlement in proximity to wells containing the SIPC in comparison to Tris or BSA.

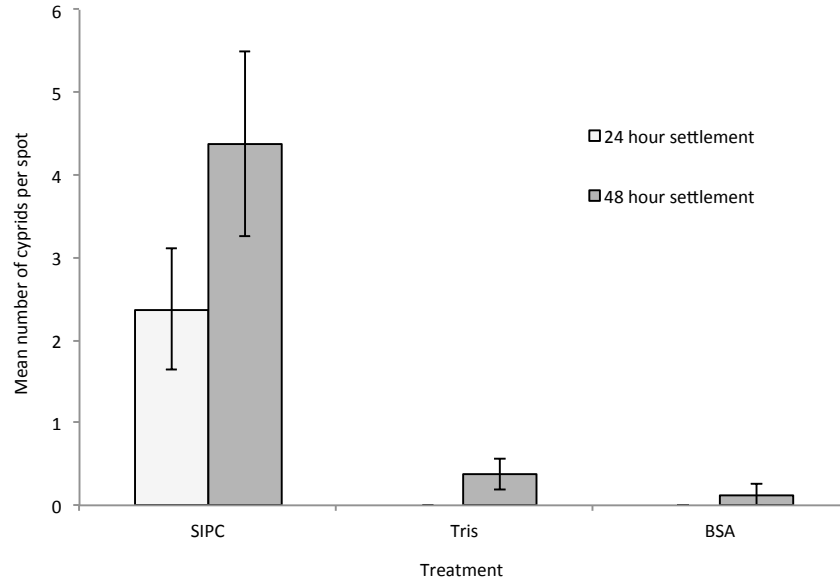


Figure 10 - Mean number of *Balanus amphitrite* cyprids settled in a nitrocellulose membrane spot assay treated with the SIPC, Tris and BSA. Error bars are \pm standard error.

2.4 Discussion

This chapter focuses on the results of preliminary experiments carried out during this research. These initial stages of research have been outlined to explain the rationale behind the project and set the scene for further research chapters.

The video tracking and following settlement assays showed the effect of the presence of an adult barnacle on the exploratory behaviour and settlement pattern of cyprids. Video tracking of *B. amphitrite* cyprids revealed that the adult caused cyprids to travel further, turn more times and slow down showing a distinct change in exploratory behaviour. The previous research using video tracking software to monitor cyprid movement was by Marechal et al. (2004). As this was the first application of this methodology to small, fast moving larvae, more problems were experienced than in current research. However, the results provided clear guidelines for future use of the software, and many were used during this research. Examples of these problems include; acclimation time, it was found that cyprids required a minimum of 2 minutes; temperature shock, minimum change in temperature from storage to analysis should be maintained; tracking time, as it was

statistically indistinguishable, a period of 5 minutes was thought appropriate; replication, to account for individual behaviour variability, a minimum of 20 replicate cyprids was considered suitable.

The post-tracking settlement assay showed that the presence of a resin mimic providing simulated topography of an adult increased settlement as well as presence of biofilm. The most significant result from this data set is the effect of an adult on the position of settling cyprids. When there was an adult present, the cyprid settled on or immediately next to the adult. This was not the case in any of the other treatments and was caused by the exploratory behaviour of the cyprid identifying the SIPC settlement cue on the adult shell. These results follow the outcomes of Rittschof et al. (1984) where settlement in the presence of the settlement factor, or in this case the adult barnacle, lead to significantly higher settlement levels. Due to the modifications in experimental design to observe the proximity of settlement to a cue source, however, the results cannot be directly compared. The authors have been unable to find a similar study for comparison. Similarly, the results from Clare et al. (1994) show that as the number of cyprids in a dish increases, so does the percentage settlement. Clare et al. (1994) hoped to show the effect of footprints on settlement, however despite the replicates used, this was inconclusive. It was surmised that this was linked to the positive feedback effect of cyprid settlement on other non-attached cyprids. This was not a problem in the research carried out during this study as the experiments only used one cyprid per petri dish.

As previously shown by Matsumura (1998a, 1998b), the nitrocellulose spot assay showed the significantly attractive properties of the SIPC to cyprids as there was over eight times higher settlement in wells containing the SIPC.

These results have set the scene for further experiments and the following chapters document the progress of this project from the characterisation of glycans associated with the SIPC (Chapter 3.3.3), the production of the SIPC mimics (Chapter 4.2.3) and the beginnings of research into the structure of the SIPC core protein (Chapter 5.2). It is hoped that though the progress made in this research there will be increased understanding of the mechanisms behind gregarious barnacle settlement.

Chapter 3. Purification and characterisation of glycan moiety of the settlement-inducing protein complex (SIPC) of *Balanus amphitrite*

3.1 Introduction

Chapter 3 focuses on the purification and characterisation of the settlement-inducing protein complex (SIPC) with respect to the glycan moiety, specifically *N*-linked glycans. The SIPC is expressed throughout the barnacle life cycle (Matsumura et al., 1998c) and has been localised to the cuticle (Dreanno et al., 2006a). *Balanus amphitrite* SIPC has an estimated molecular mass of around 200 kDa and consists of three major polypeptide subunits of 76, 88 and 98 kDa (Matsumura et al., 1998b). These polypeptide chains play an important role in the settlement of *B. amphitrite* larvae (Matsumura et al., 1998b) as each subunit when assayed, induced cyprid settlement as effectively as intact SIPC (Matsumura et al., 1998c). As mentioned in Chapter 1.1.9, there is significant homology to the highly *N*-glycosylated α_2 -macroglobulin (A2M) and insect thioester-containing proteins (TEP) (Dreanno et al., 2006c). Cyprid temporary adhesive (see Chapter 1.1.10) also appears to be glycoprotein based (Clare and Matsumura, 2000). Consequently glycoproteins potentially function as both settlement cues and assist attachment in the processes of barnacles and other hard fouling organisms. Boone et al. (2003) found that the cypris larvae of the parasitic barnacle *Loxothylacus texanus* search for and recognise glycoproteins on the carapace of potential host crabs. Similarly to barnacles, the quagga mussel *Dreissena bugensis*, produces a glycoprotein termed ‘foot protein 1’ which is a major constituent of the mussel’s byssus thread. Foot protein 1 contains *N*-acetylgalactosamine *O*-linked to a threonine residue (Anderson and Waite, 2002). The larval metamorphosis of the nudibranch *Eubranchus doriae* is induced by the glycoconjugate-containing solutions extracted from their prey, hydroid *Kirchenpauria pinnata* (Bahamondes-Rojas and Dherbomez, 1990). This is also seen in herbivores, such as the nudibranch *Alderia modesta*, where larvae metamorphose in response to glycoproteins produced by the algae on which they feed (Krug and Manzi, 1999). Sponges are also known to produce the glycoprotein fibronectin as an adhesive from the basal lamina (Pahler et al., 1998). Another adhesive glycoprotein, tenascin, has been shown to be produced by sponges (Humbertdavid and Garrone, 1993). Raphid diatoms produce glycoprotein-rich mucilage as an aid to motility and adhesion on surfaces (Lind et al. 1997) and female rotifers produce a glycoprotein pheromone to trigger

mating behaviour in males (Dingmann and Snell, 1999, Rico-Martinez et al., 1996). Similarly, daphnid females display glycoproteins for contact recognition after male-female encounters (Carmona and Snell, 1995).

The characterisation of glycans involved in aquatic animals has become an increasingly appealing area of research in recent years. In the blue lobster, *Cherax quadricarinatus*, the yolk glycolipoprotein, vitellin, is preceded by vitellogenin which itself consists of high mannose oligosaccharides, specifically M5-9 (Khalaila et al., 2004). These oligomannose moieties are similar to the carbohydrate components of haemocyanin from the freshwater crayfish, *Astacus leptodactylus* (Tseneklidou-Stoeter et al., 1995). A marine example of a similar oligomannose moiety is the glycosylated proteins found in the haemoglobins of *Riftia pachyptila*, the deep-sea tubeworm (Zal et al., 1998). Serum immunoglobulins are important for immune response in vertebrates, including fish. The immunoglobulin of the Atlantic cod, *Gadus morhua*, is similar to the mammalian counterpart as it contains complex, heterogenic *N*-linked glycans; however, it contains lower levels of oligomannose glycans than mammalian immunoglobulin (Magnadóttir et al., 2002). Research on Atlantic salmon, *Salmo salar*, also highlights the importance of glycans for fish immunoglobulins (Magnadóttir et al., 1997). The channel catfish, *Ictalurus punctatus*, was found to express high-mannose *N*-glycans leading to further research into teleost immune systems (Thankappan et al., 2006).

Glycans on the cell surface play an important role in recognition both on cell surfaces and in solution (Ambrosi et al., 2005). There are similar instances of other surface-associated proteins playing similar roles to the SIPC in other marine organisms. A conceptual model as reviewed in Snell (2011), shows how the harpacticoid copepod, *Tigriopus japonicus*, secretes a protein with sequence similarities to A2M which has been shown to assist in mate guarding and spermatophore transfer through chemical contact (Kelly and Snell, 1998, Ting and Snell, 2003). This copepod also uses glycoproteins to distinguish the species, sex and female developmental stage of potential mates when stroking another with their antennules (Ting et al., 2000). The efficacy of these glycoproteins in regard to mate guarding was inhibited through the addition of mannose binding pea lectin, *Pisum sativum* (PSL) (Lonsdale et al., 1996). Glycoproteins are also important for mate recognition in calanoid copepods (Snell and Carmona, 1994) and can function as attractants for

allospecifics. For example, eggs of the horseshoe crab, *Limulus polyphemus*, are used as bait in eel fisheries and it is thought that egg-derived glycoproteins act as chemo-attractants (Ferrari and Targett, 2003). In some marine organisms the settlement cue must come from live animals, such as the case of the European flat oyster, *Ostrea edulis* (Crisp, 1965). However living, dead or preserved barnacles induce a settling response from cyprids. This implies the cue is effective long after the death of the barnacle producing it (Crisp, 1965). Newly moulted or recently settled individuals strongly induce settlement activity (Crisp and Meadows, 1962, Hills and Thomason, 1996), and it has been observed that even old cement bases on surfaces still attract cyprids (Knight-Jones, 1953).

An understanding of the mechanisms behind the gregarious settlement of organisms such as barnacles may highlight ways to reduce unwanted fouling by these animals. In fouling communities, barnacles are frequently the primary colonisers (Foster, 1987). Several marine organisms are known for producing natural antifouling agents and glycoproteins also appear to have a function in antifouling. Mucus secretions are a common mechanism utilized by marine animals to prevent fouling (McKenzie and Grigovale, 1996). The mucus may contain toxins which act to deter settling organisms (Fontaine, 1964). Bavington et al. (2004) identified mucin-type glycoproteins produced by seastars and brittlestars which prevent fouling at the cellular level. Meikle et al. (1987) determined the structure of oligosaccharide side chains from glycoproteins from a marine coral which may potentially have antifouling properties.

3.1.1 Aims and Objectives

The aims of Chapter 3 focus on the early stages of carbohydrate analysis of the SIPC.

Aim 1 - To purify and isolate the SIPC of *Balanus amphitrite*.

Objective - The SIPC is partially purified by ammonium precipitation, ion exchange chromatography and gel filtration. At each step in the purification, the protein fractions are run on SDS-PAGE gels and the SIPC fractions are detected by immunoblotting with antibodies previously raised against purified SIPC. Bands are eluted from preparative gels for carbohydrate characterisation.

Aim 2 - To fully characterise the carbohydrate moiety of the SIPC.

Objective - Full *N*-glycan characterisation of the SIPC carbohydrates using combined HPLC and exoglycosidase digestions in collaboration with Professor Pauline Rudd's Group at the National Institute for Bioprocessing and Research, University College Dublin.

3.2 Materials and Methods

Preparation of the SIPC samples was carried out at Newcastle University. Glycan analysis and characterisation was carried out at the Rudd Group Laboratory at the National Institute for Bioprocessing, Research and Training in Dublin, Ireland.

3.2.1 Purification of a 'Crude Extract' of Adult Barnacles

The 'crude extract', as referred to in Clare and Matsumura (2000) is an extraction of all proteins present in the barnacle including the desired SIPC. It acts as a settlement cue as it contains SIPC but is not a pure extract. The extraction protocol was based on Matsumura et al. (1998b). All purification was carried out on ice during the procedure and samples stored at -80 °C when not used immediately to ensure minimal protein denaturing. For the recipes of solutions required during the purification process, see Appendix A. When carrying out the purification of molecules containing glycans, whether they are glycolipids or glycoproteins, it is essential to use non-powdered gloves during experimental procedures. The powder in the gloves contains a polysaccharide that produces a ladder on the HPLC which can obscure the true nature of other glycans present (Royle et al., 2006). *Balanus amphitrite* were removed from different substrates (oyster shell and plastic piping), cleaned thoroughly in tap water, briefly dried, weighed and frozen for extraction of the SIPC. The barnacles were ground for 30 minutes in a pestle and mortar. A 150% volume of 50mM TrisHCl pH7.5 was added and crushing continued with more liquid if necessary. The protein mixture was stirred for 2 hours before filtering through 200µm paper (Whatman, UK) to remove the larger particles. The filtrate was centrifuged at 13000xg for 30 minutes, retaining the supernatant before further filtering with glass fibre filter paper (Whatman No. 3, Whatman, UK). 472g of ammonium sulphate, for every litre of filtered supernatant, was added slowly and stirred overnight before centrifuging at 13000xg for 30 minutes, retaining the pellet. The pellet was re-suspended in a small volume of 50mM TrisHCl pH7.5 and transferred into dialysis tubing, dialysed in 3 litres of 50mM TrisHCl pH7.5 overnight after changing the buffer after 3 then 6 hours. The contents of the dialysis tubing were centrifuged for 3 hours at 13000xg, retaining the supernatant and filtered using 0.2µm

cellulose acetate filter (Whatman, UK), under vacuum. This filtrate constitutes the total protein from the crushed barnacles.

3.2.2 Total protein assay

The total protein assay indicates the amount of protein in a sample, based on comparison to the colour change of a dye (Total Protein Reagent, BioRad, UK) to known protein concentrations. The filtrate from the crude purification process was diluted to 1:10, 1:50 and 1:100 and was compared to six dilutions from 0mg/ml to 1mg/ml of Bovine Serum Albumen (BSA) (Sigma, UK) at the same dye concentration. Results were obtained spectrophotometrically using a microplate reader (Emax precision, Molecular Devices, USA) and were averaged to produce a calibration curve with a corresponding equation. As long as the R^2 value was more than 0.98, the results were considered acceptable. The equation was rearranged to find the protein concentration ('x') when 'y' is the known absorbance.

3.2.3 Ion Exchange Chromatography

An EconoPump system and EconoSystem fraction collector (Bio-Rad, UK) for Ion Exchange Chromatography was used to separate the proteins contained in the crude extract based on their differing charge. A 15mm diameter, 100mm long column containing Q-sepharose cation exchanger (Pharmacia Biotech, UK) was equilibrated with 1 litre of 50mM TrisHCl pH7.5. 100mg of crude extract was diluted in 30ml of 50mM TrisHCl pH7.5. Gradient buffers of 2 litres 1M NaCl and 3 litres 50mM TrisHCl pH7.5 were used to run the gradient as shown in Figure 11 at 1ml min^{-1} . Fractions of 3ml were collected and stored on ice for the duration of the elution.

To identify which of the collected fractions contained protein, a total protein assay was conducted, as in 3.2.2, using 10 μ l from every 5th fraction tube after vortexing. After spectrophotometric analysis, this can also be represented graphically. The fractions containing the protein were retained and frozen at -80 °C in individual vials. As only 100mg could be run on the ion exchange column at any one time, chromatography was repeated until all of the dialysed extract was fractionated.

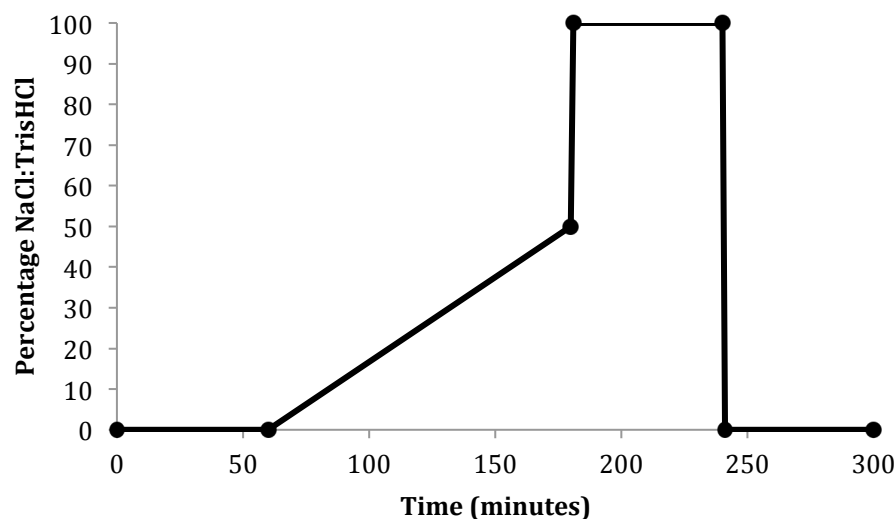


Figure 11 – An example of the ion exchange gradient used to separate the *Balanus amphitrite* SIPC proteins by charge

3.2.4 Protein precipitation

Chloroform:methanol precipitation is a simple method of precipitating proteins from suspension. These proteins can then be used as required for SDS-PAGE gels and Western blotting. 30µg of protein was required from each fraction and the appropriate volume of liquid was transferred from the ion exchange fractions containing protein. Roughly every 10th fraction was chosen for chloroform:methanol precipitation. To the protein samples of known volume, 4 volumes of cold methanol were added and vortexed, followed by 1 volume of cold chloroform then 3 volumes of dH₂O. The samples were vortexed, then centrifuged for two minutes at 15000xg. The aqueous top layer was removed, and 4 volumes of methanol added before vortexing again. This was then centrifuged at 15000xg for two minutes and as much liquid as possible was removed without disturbing the protein precipitate. All samples were dried down under vacuum and were then suitable for immediate use or freezing. Samples were re-solubilised in a compatible buffer, for example Laemmli Buffer, for use in gels.

3.2.5 SDS-PAGE gel electrophoresis

SDS-PAGE (sodium dodecyl sulphate polyacrylamide gel electrophoresis) 10% acrylamide gels were run using a mini-gel system (Atto Co. Ltd, Japan). These mini-gels were 90mm x

80mm x 1mm and a 12 sectioned comb was used in the stacking gel to create the appropriate number of wells. The previously chloroform:methanol precipitated protein samples (see 3.2.4) were boiled for five minutes with 20µl Laemmli buffer (containing 0.1% β-mercaptoethanol to denature the protein if required). 19µl of the protein solution was added to a gel well and 10µl of See Blue Plus2 Pre-Stained Standard (Bio-Rad, UK) was also run. The gel was run for 2-3 hours at 30mA (approximately 150V). If required, gels were stained using Coomassie Brilliant Blue (CBB) for 1 hour and de-stained overnight in CBB de-stain. Alternative stains were also used, depending on the amount of protein present, and carried out according to the manufacturers' instructions. SilverQuest Silver staining is a more sensitive protein stain than CBB thus is most suitable when very small amounts of protein are being run on a gel. For Western blot gels, no stain was used.

3.2.6 Western blots

A Western blot or protein immunoblot was the process employed to transfer the proteins from the unstained SDS-PAGE gels to polyvinylidene fluoride (PVDF) membrane (PALL Europe Ltd, UK) using a semi-dry TransBlot cell (Bio-Rad, UK). A piece of membrane 9cm x 6.5cm was rinsed in methanol to make the surface hydrophilic, before soaking both the membrane and the gel in pH11 n-cyclohexyl-3-aminopropanesulphonic acid buffer (CAPS) for one hour. Six pieces of 9cm x 6.5cm x 3mm chromatography paper (Whatman, UK) were also soaked in the CAPS for 5 minutes to ensure complete saturation. The sheets were then placed on the anodal plate of the transfer cell as follows: three sheets of filter paper, the PVDF membrane, the gel and finally three sheets of filter paper. The cathode plate was then placed on top of this stack and the system run for two hours at 2mA cm⁻² of the membrane (voltage not exceeding 25V). To confirm protein transfer, the SDS-PAGE gel was stained with Coomassie Brilliant Blue, de-stained and examined for protein staining. The PVDF membrane was not stained as it was to be used for immunostaining.

3.2.7 Immunostaining

The PVDF membrane was immunostained using polyclonal antibodies for *B. amphitrite* (Matsumura et al., 1998c). Previously, SIPC had been purified from crude adult extracts by Matsumura et al. (1998c). The methods used were very similar to those outlined above. Following purification, antibodies (antisera) were produced from the 76, 88 and 98 kDa subunits via inoculation into rabbits. Consequently, three antisera (anti-76, anti-88, and anti-

98) were produced. The anti-76kDa antibody had highest-titre and was confirmed specific to 76kDa subunit of SIPC. The antibody used here for the immunostaining is the same anti-76 kDa antisera. The membrane was washed in Tris-buffered saline (TBS) for 10 minutes, washed in blocking buffer overnight, again washed for an hour in TBS (changing the TBS solution every 15 minutes) then incubated at room temperature in a 1:1000 solution of the antibody buffer and primary antibody for 2 hours. The membrane was rinsed in dH₂O, washed for 20 minutes in Tris-Tween buffered saline (TTBS) (changing the TTBS solution every 10 minutes) then incubated in 1:3000 solution of antibody buffer and secondary antibody (anti-rabbit IgG, Sigma, UK) for 1 hour. The membrane was rinsed in dH₂O, washed in TBS for 20 minutes (changing the TBS solution every 10 minutes) and finally rinsed in dH₂O. The stain used was 5-bromo-4-chloro-3-indolyl phosphate/nitro blue alkaline phosphatase (BCIP/NBT, Sigma, UK) until the immunostained bands became visible. The stained membrane was washed in dH₂O and dried on tin foil. Active fractions, those that were immunostained, were pooled.

3.2.8 Ultrafiltration

Using an Amicon filtration system under nitrogen (Amicon, UK), the pooled active fractions were ultrafiltered through a YF-30 cellulose hydrophilic membrane (Millipore, UK) to reduce the total volume of the active fraction to less than 10ml. Following this, the filter was changed and the volume reduced to less than 3ml.

3.2.9 Gel filtration chromatography

As with the ion exchange chromatography, an EconoPump system and EconoSystem fraction collector (Bio-Rad, UK) was used for gel filtration chromatography to separate the proteins based on their size. A 1.5cm diameter, 100cm long column containing Sephacryl S-200 size exclusion media (Pharmacia Biotech, UK) was first cleaned with 1M sodium hydroxide (NaOH) solution for 1 hour (Selkirk, 2004). Buffer consisting of 250ml 2M NaCl, 100ml 500mM TrisHCl pH7.5 and 650ml dH₂O was used to equilibrate the column, running one column's volume of buffer through before collection started. The column was run at 0.5ml min⁻¹ collecting fractions of 3ml which were stored on ice for the duration of the elution. To ensure that protein was eluted and to confirm the end point, a simple protein test was carried out on every 2nd tube, similar to Total Protein Assay (see 3.2.2) but purely to confirm presence of protein rather than quantify it. When there was no longer protein

showing in the fractions, the elution was stopped. A total protein assay was carried out on every 5th fraction.

Following the column fractionation, samples containing protein were precipitated using chloroform:methanol, run on SDS-PAGE gels and Western blots then immunostained as before.

To reduce the volume of SIPC solution, it was again ultra filtered under nitrogen to reduce the volume to approximately 10ml and another total protein assay carried out giving a concentration of 0.74mg/ml. This solution was then suitable for further analysis and SDS-PAGE gels were run if required.

3.2.10 Sodium periodate glycan removal

Initially, it was hoped to deglycosylate the SIPC using sodium periodate (Boone et al., 2003). Briefly, 10mM sodium periodate was added to 50mM sodium acetate pH 4.5. 1ml of this periodate solution was added to 25µg of the SIPC and incubated for 1 hour at room temperature on a rocker. Proteins were precipitated using chloroform:methanol precipitation in the periodate sample and also denatured SIPC. An SDS-SAGE gel was run and stained with Coomassie Brilliant Blue to see if the protein was deglycosylated. As Figure 12 shows, the denatured SIPC (B) gave the three expected subunits. However the periodate-treated SIPC (C) appeared as just a smear down the gel. This is most likely an artefact of the presence of proteins because the protein was completely denatured and broken into small peptides so the original subunits were not distinguishable. In order to deglycosylate SIPC, glycans were removed using the enzyme *N*-Glycosidase F (PNGaseF), see Chapter 3.2.13.

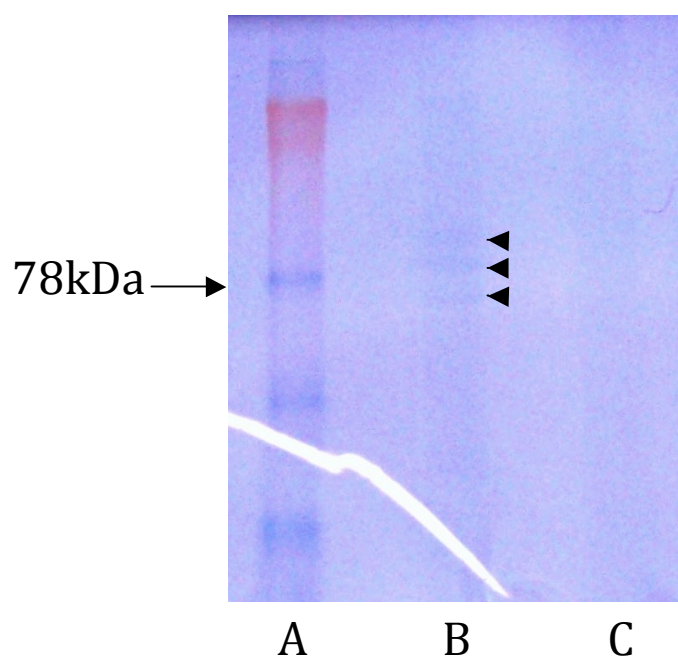


Figure 12 - SDS-PAGE gel of *Balanus amphitrite* SIPC (A) molecular standard showing the 78kDa band, (B) native denatured SIPC showing the 76, 88 and 98 kDa subunits (arrowheads) and (C) sodium periodate treated SIPC

3.2.11 Confirmation of glycan presence

30µg native SIPC in 12µl dH₂O was prepared as described previously for SDS-PAGE gel methodology (see Chapter 3.2.5) and run on a pre-cast gradient gel (NuPAGE 4-12% BT 1.0). Bio-Rad Precision Plus Dual Colour Protein Standard was run alongside as a reference. The gel was washed and stained with Pro-Q Emerald 300 according to manufacturer's instructions and viewed under the Gene Genius BioImaging System, causing any glycans present to fluoresce.

3.2.12 Preparation of samples for release of N-glycans

Where glycoprotein samples were not already in a gel, the in-gel block method was used. In brief, the SIPC samples (totalling 50µg) were dried down in 1.5 ml microcentrifuge tubes under vacuum for 1 hour. The samples were then reduced by adding 7 µl of dH₂O, 2 µl of sample buffer (0.625 ml of 0.5 M Tris pH 6.6, 1 ml of 10% sodium dodecyl sulphate (SDS) and 3.375 ml dH₂O) and 1 µl of 0.5 M dithiothreitol (DTT) and were incubated at 70 °C for 10 minutes. The samples were then alkylated by adding 1µl of 100mM iodoacetamide (IAA) and then incubated in the dark at room temperature for 30 minutes. Next, samples were set into a gel block by adding 22.5 µl Protogel (National Diagnostics, UK), 11.25 µl

of gel buffer (1.5 M Tris pH 8.8), 1 μ l of 10% SDS, 1 μ l of 10% ammonium persulphate (APS) and 1 μ l tetramethylethylenediamine (TEMED). The samples were mixed and left to set for 15 minutes. After setting the gel block was cut into 1mm cubes.

Where glycoprotein samples had already been run on an SDS-PAGE gel, the sections containing the desired protein bands were cut to 1mm cubes for washing. Regardless of which method was used to set the glycoproteins in the gel, washing was necessary. The gel cubes were transferred to a microcentrifuge tube and then washed with 1ml acetonitrile while shaking on an orbital platform shaker (Heidolph, Germany) for 15 minutes. The liquid was removed and the washing procedure was repeated twice with 1ml 200mM ammonium bicarbonate (pH7.2) followed by 1 ml acetonitrile. The gel pieces were then dried in a vacuum centrifuge.

3.2.13 Release of N-glycans from gels

N-glycans were released from the SDS-PAGE gels or gel blocks using a protocol previously outlined by Rudd et al. (2001) and developed by Royle et al. (2006). After washing, glycans were liberated by adding 2 μ l of N-glycosidase F (PNGaseF, Prozyme, San Leandro, CA, USA) and 48 μ l of 20mM sodium bicarbonate buffer (pH 7.0), mixed and incubated overnight at 37 °C. The glycans released from the gel were collected by washing and sonicating the gel pieces for 15 minutes at 37 °C and retaining the liquid. This was repeated three times with 200 μ l of dH₂O then 200 μ l of acetonitrile. The released glycans were combined and concentrated by drying overnight by vacuum centrifugation. To each dry glycan sample, 20 μ l of 1% v/v formic acid was added to convert the released glycosylamines back to reducing sugars before being vortexed and spun down. The glycans were incubated for 40 minutes at room temperature and then dried in a vacuum centrifuge for 30 minutes. For further analysis, 50 μ l of dH₂O was added, vortexed and spun to re-dissolve the glycans. This was divided into 25 μ l aliquots for fluorescent labelling.

For in-solution digests, 20 μ l of N-glycosidase F (PNGaseF, Prozyme, San Leandro, CA, USA) was added to 200 μ l of native SIPC and incubated overnight at 37 °C. The protein was separated from the sugars and PNGaseF using a 50kDa Amicon Ultra 0.5 ml spin filter (Millipore, USA).

3.2.14 Labelling of N-glycans

Glycans required for HPLC analysis were labelled using a LudgerTag™ 2AB (2-aminobenzamide) labelling kit (Ludger, Abingdon, UK). 5µl of labelling solution was added to the glycans and vortexed for 5 minutes before being incubated for 30 minutes at 65 °C. Samples were vortexed again for 5 minutes and incubated for 90 minutes at 65 °C. Excess 2AB label was removed using solid-phase extraction with 'I' shaped pieces of prewashed and dried Whatman 3MM chromatography paper (Whatman, USA). The 5µl of 2AB-labelled samples were pipetted onto the chromatography paper and left to dry for 10 minutes. Using a holder to keep the filter paper in an upright position, acetonitrile was used to remove the excess 2AB by carrying it up the filter paper away from the labelled glycan spot. The labelled spot was cut out for removal of the glycans. The labelled glycans were eluted from the paper by syringing dH₂O through the paper spot, in 4x 500 µl aliquots of dH₂O, leaving the water in contact with the paper for 10 minutes in between water changes. All of the water was retained, combined and dried down overnight.

3.2.15 HILIC-fluorescence glycan profiling

Samples were resuspended in 80:20 acetonitrile:water prior to analysis by HILIC (hydrophilic interaction liquid chromatography) with fluorescence detection. Separations were performed on a Waters Alliance 2695 Separations Module with a Waters 2475 Multi Wavelength Fluorescence Detector (Waters Corporation, Millford, MA, USA). HILIC is a type of partition chromatography within high performance liquid chromatography (HPLC). The HILIC separation arises due to the interaction of polar functional groups i.e. hydroxyls, on the oligosaccharides with the polar stationary phase (in this instance amide functionalised silica) in a high solvent environment. Retention increases with increasing glycan size and therefore, associated presentation and interaction of hydroxyls with the stationary phase. A TSKgel Amide-80 5µm (250 x 4.6mm) column was used with a 152 minute 20-48% gradient of 50mM ammonium formate pH4.4 and acetonitrile. Detection wavelengths used were $\lambda_{ex} = 330\text{nm}$ and $\lambda_{em} = 420\text{nm}$. The system was calibrated by running an external standard of 2AB-dextran ladder (5µl dextran, 15µl dH₂O and 80µl acetonitrile) (2AB-glucose homopolymer, Ludger, Abingdon, UK) alongside the sample runs for time based normalisation and subsequent annotation of the analytical peaks with

Glucose Unit (GU) values using Empower GPC (gel permeation chromatography) software add-in.

3.2.16 Exoglycosidase digestions

The exoglycosidase digestion enzymes used were bovine kidney α -fucosidase (BKF) and Jack bean α -mannosidase (JBM) (Prozyme, San Leandro, CA, USA) in 50 mM sodium acetate buffer, pH 5.5. 25 μ l aliquots of the 2AB-labelled glycan protein pool were dried down in microcentrifuge tubes. For the BKF digestion, 1 μ l enzyme, 1 μ l of buffer and 8 μ l of dH₂O were added to one tube. For the JBM digestion, 4 μ l enzyme, 2 μ l of buffer and 4 μ l of dH₂O were added to another. These were incubated overnight at 37 °C and then centrifuged at 7000rpm for 10 minutes through a 10kDa enzyme filter (MWCO, Millipore, USA). To obtain the proteins, the filter was reversed, 200 μ l of phosphate buffered saline (PBS) added and centrifuged at 1000g for 3 minutes. To precipitate the proteins, 800 μ l of ice cold acetone was added and the samples frozen for 30 minutes before spinning down at 8000g for 10 minutes and retaining the pellet. Digested samples were dried down completely for HILIC-fluorescence as outlined in Chapter 3.2.15. Structural assignments were made based on expected enzyme activity and incremental shifts in GU.

3.2.17 Sugars in solution

Following the characterisation of the glycans on the SIPC, experiments were carried out using sugars in solution to investigate the efficacy of the dominant sugar, mannose, as a cue when in solution. 1-day-old *B. amphitrite* cyprids were exposed to different concentrations of two sugars (methyl- α -mannopyranoside and methyl- β -galactopyranoside) in artificial seawater (ASW), 3-isobutyl-1-methylxanthine (IBMX) and native SIPC for 24 hours. An ASW standard was also included. Settlement of 10 cyprids per well in a 24-well plate was measured as a percentage of cyprids settled or metamorphosed compared to total number present at 24 hours. Traditionally assays were run for 48 hours however, due to the positive feedback of newly settled cyprids providing the natural SIPC cue, the effect of treatments becomes less distinct and negates or reduces any inductive effect of a settlement cue after the initial 24 hour period.

The following dilutions were used to produce 6 replicates of each dilution; for mannose, galactose and IBMX: 1mM, 0.1mM, 0.01mM, 1 μ M and 0.1 μ M and for the SIPC: 50nM,

25nM, 5nM, 2.5nM and 0.5nM. To achieve the dilutions required for the sugars and IBMX a stock solution of 10mM was made for serial dilutions. From this stock a second stock of 0.01mM was made for the later dilutions due to the small volumes involved. Due to the potential of the sugars to degrade during the freeze-thaw processes, these solutions were freshly made up for each experiment. Minitab Probit analysis on the mannose and galactose data used the concentrations and number settled to give an EC₅₀ estimate for each replicate; these were then averaged to give the mean EC₅₀ for each treatment.

3.3 Results

3.3.1 Protein purification

A calibration curve for determining the protein concentration in crude extract was carried out using the first set of wells in Figure 13. In this case the concentration of protein in the SIPC crude extract was 7.5mg/ml. Figure 13 also shows the protein content of fractions after ion exchange chromatography, indicated in blue.

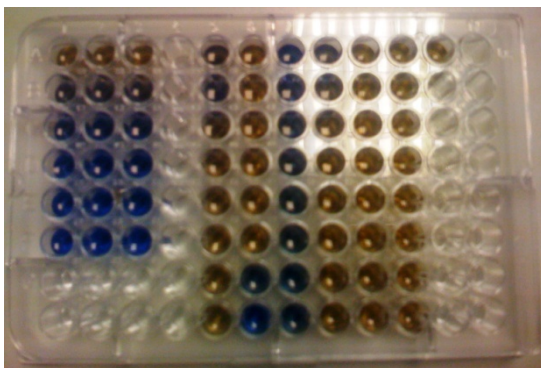


Figure 13 - Total protein assay of *Balanus amphitrite* SIPC protein fractions using a 98-well plate and every 5th fraction from the ion exchange column. The standards are on the left and fraction samples on the right. Fractions showing protein present are blue.

After spectrophotometric analysis, Figure 13 can be represented graphically, as shown in Figure 14 where the protein is indicated in grey.

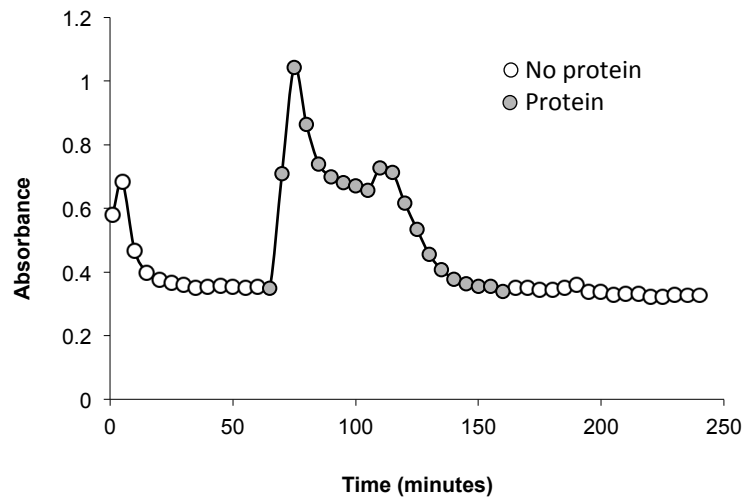


Figure 14 - Total protein from the crude extract of *Balanus amphitrite* proteins after charge separation by ion exchange chromatography.

The dark staining on the PVDF immunoblotting membrane in Figure 15 shows that SIPC was found in those fractions from the ion exchange column eluted at 100 to 120 minutes. This information can also be overlaid on to the absorbance graph (Figure 16) to indicate the active fractions (SIPC). These active fractions, shown in black, were pooled and all other fractions, shown in white and grey, were discarded.

Following gel filtration chromatography, a full total protein assay was carried out on every 5th fraction giving the absorbance spectrum shown in Figure 17.

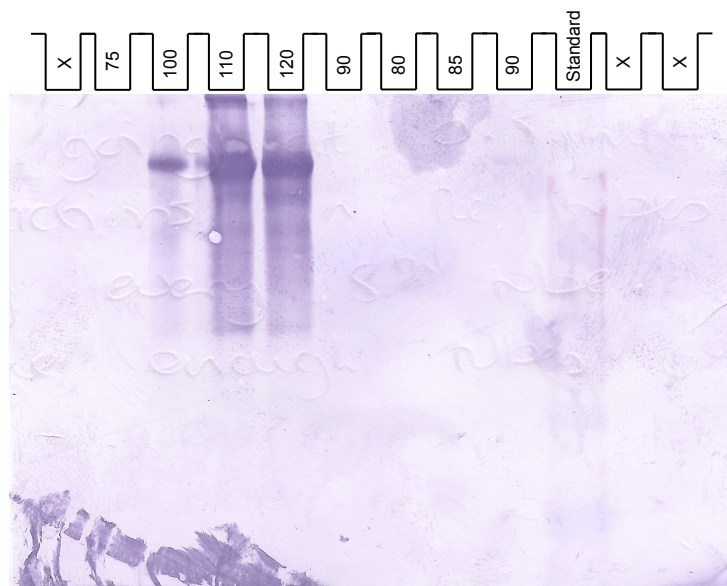


Figure 15 - Stained PVDF membrane Western blot of ion exchange chromatography separated fractions of *Balanus amphitrite* crude protein extract. The numbers refer to the time of elution in minutes.

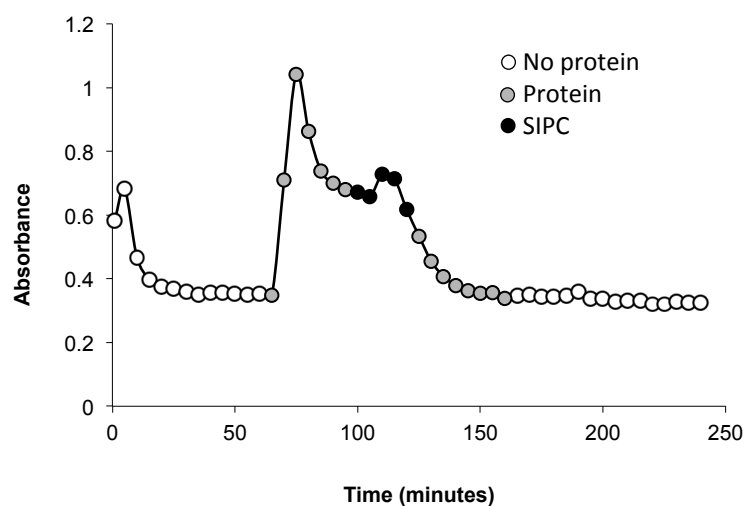


Figure 16 - Total protein from the crude extract of *Balanus amphitrite* after charge separation by ion exchange chromatography with the fractions containing SIPC indicated.

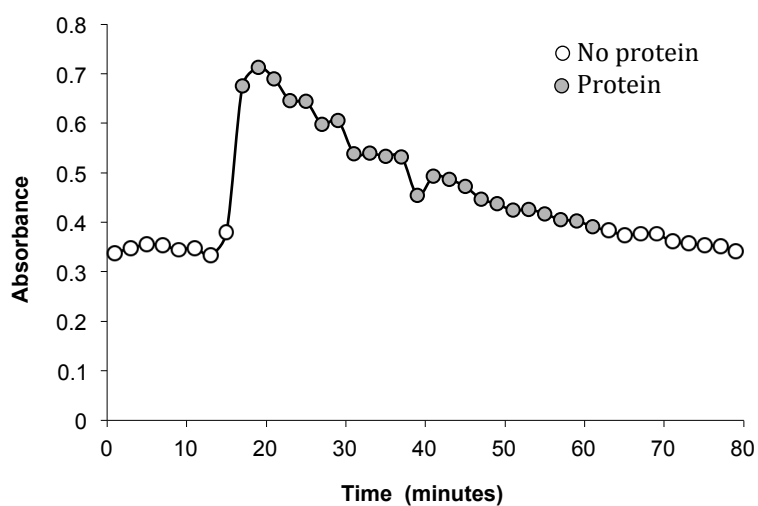


Figure 17 - SIPC active fractions (from antibody immunoblotting) of *Balanus amphitrite* after size separation by gel filtration chromatography, with the fractions containing protein indicated.

From these protein fractions, a second Western blot (Figure 18) again shows the SIPC active fractions eluting between 25 and 37 minutes. The dark smear at 21 minutes was caused by protein overloading on the gel rather than a positive response for the SIPC. These

SIPC fractions were pooled and a total protein assay carried out giving a concentration of 0.15mg/ml. The other fractions, shown in white and grey in Figure 19 were discarded.

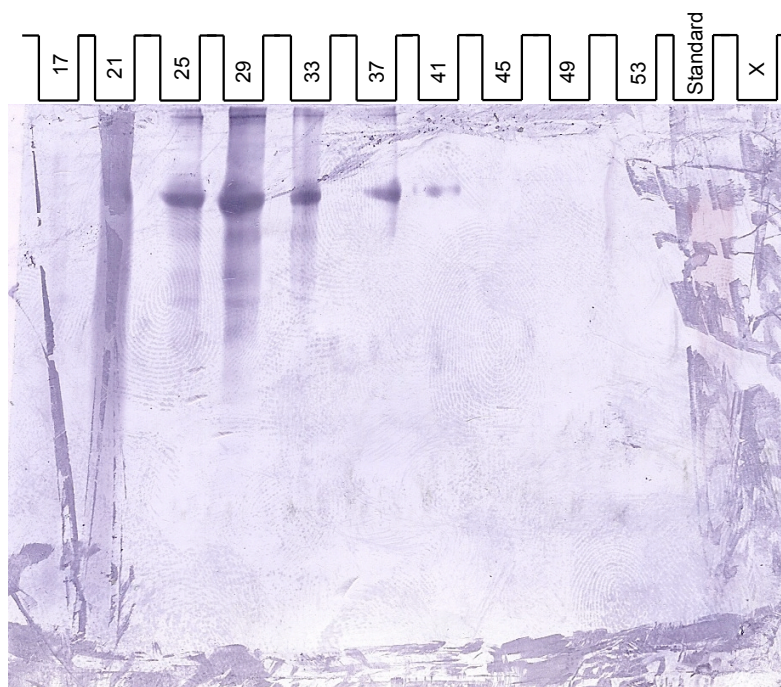


Figure 18 - Stained PVDF membrane Western blot of gel filtration chromatography separated fractions of *Balanus amphitrite* proteins, active fractions indicate SIPC. The numbers refer to the time of elution in minutes.

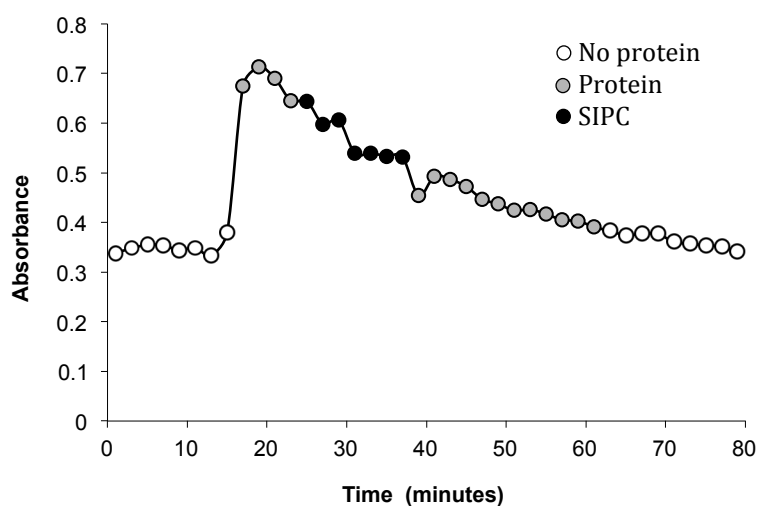


Figure 19 - SIPC active fraction of *Balanus amphitrite* after size separation by gel filtration chromatography with the fractions containing SIPC indicated.

An SDS-PAGE gel was run on this final solution (Figure 20) and with the use of β -mercaptoethanol, the disulphide bonds were broken between the major subunits forming the three distinct bands in the region of the 78kDa standard (B, C and D as 98, 88 and 76 respectively). In addition, it was noted there were several further fainter bands at the base of the gel; these were referred to as bands E and F.

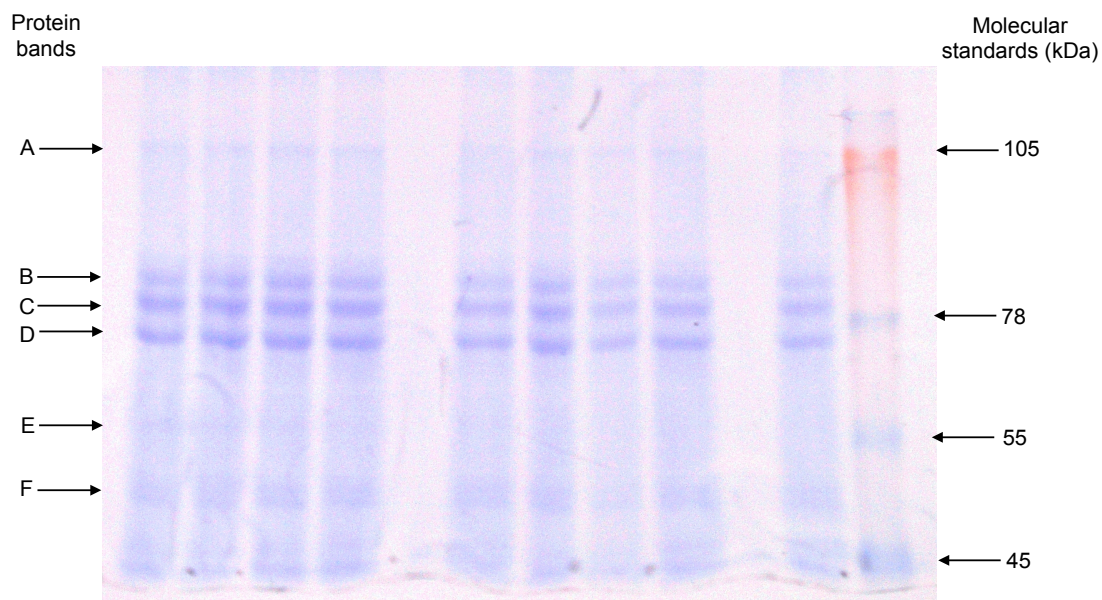


Figure 20 - SDS-PAGE gel of denatured *Balanus amphitrite* SIPC showing a band of higher mass (A), the three major subunits (B, C and D) and two fainter bands (E and F).

3.3.2 Confirmation of glycan presence

The Pro-Q Emerald stained gel (Figure 21) indicated the presence of glycans in native SIPC as the gel fluoresced green when viewed under the Gene Genius BioImaging System. Due to excess protein on the gel and the large size of the native (not denatured into subunits) SIPC, there was a smear rather than individual bands, although this was adequate for confirming that glycans were present and further analysis was appropriate.

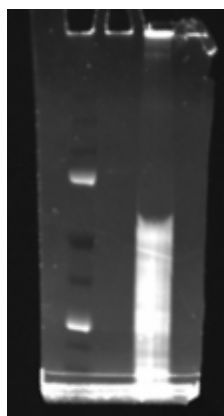


Figure 21 - Pro-Q Emerald stained gel showing glycans present in *Balanus amphitrite* SIPC as well as the 75 and 25 kDa bands from the protein standard on the left.

Along with the standard Bio-Rad Precision Plus Dual Colour Protein Standard, Human Immunoglobulin G (IgG) was also used as a comparison as this had known glycosylation. These gels all show the presence of the protein subunits and glycan fluorescence. It can also be seen that there are other bands as well as the three expected subunits. These are most likely the subunits with smaller peptides removed as a consequence of additional denaturing. For HPLC analysis, these bands were also analysed and referred to as bands E and F.

3.3.3 HILIC-fluorescence

The initial HILIC outputs were assessed for artefact peaks from the blank gel. Figure 22 shows the stacked traces and the highlighted area (grey) indicates peaks to be disregarded. Peaks present in the highlighted region of the chromatogram were noted to be artefacts from the polyacrylamide gel matrix (the black trace), based on the comparison with resulting chromatogram following the analysis of a gel blank. Furthermore, only peaks that subsequently digested with the exoglycosidase enzymes used were considered real.

Once the gel blank artefacts were removed from the traces, the remaining peaks were allocated numbers. In the native SIPC (red trace) there were 11 major peaks as shown in Figure 23.

GU values for each of the peaks for the native SIPC and each gel band were allocated using the HPLC output, dextran hydrosylate ladder and Empower software, as shown in Figure 24. It was noticeable that some of the peaks were not present in all gel bands, indicated with an ✕.

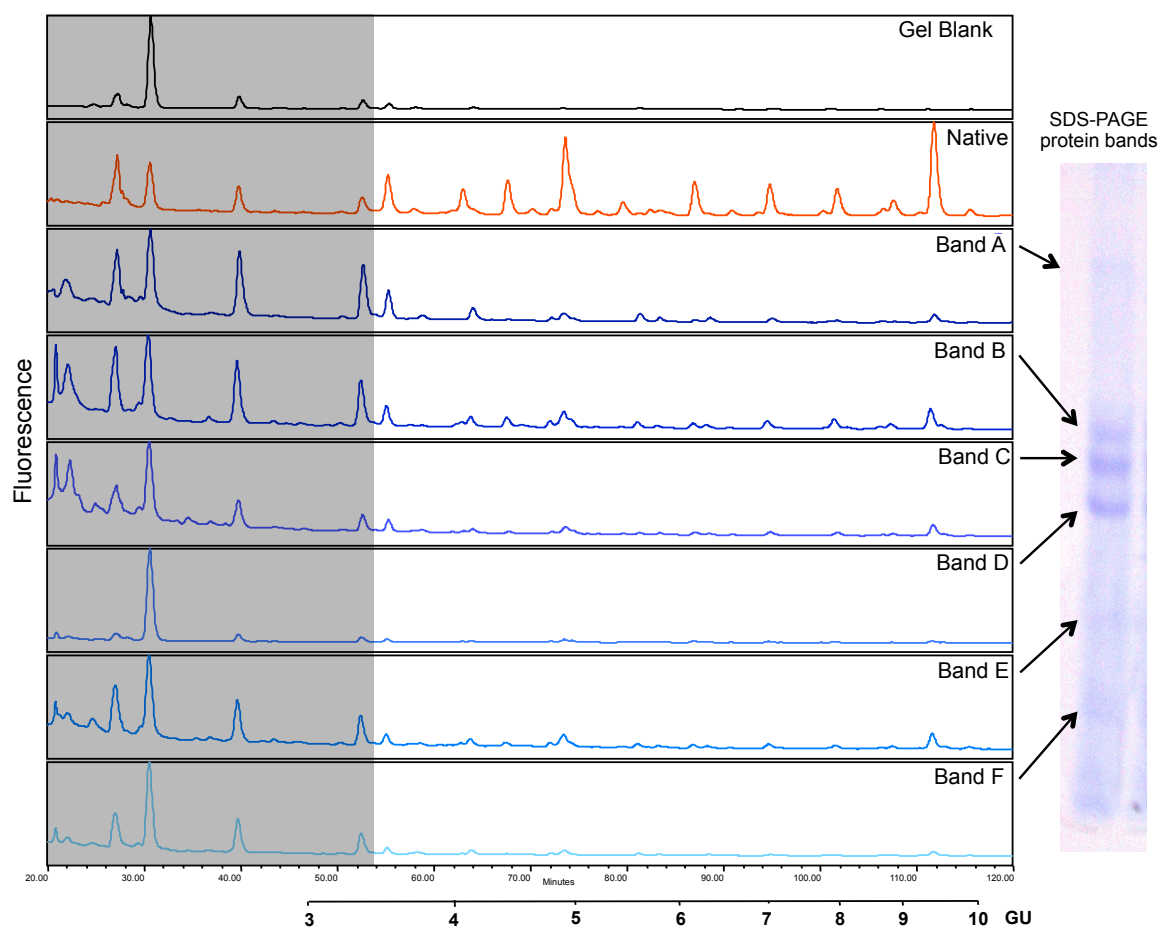


Figure 22 - HPLC chromatograms of *Balanus amphitrite* SIPC including the gel blank. The grey area shows peaks that are artefacts from the gel blank to be discarded. Bands A to F are subunits of the Native SIPC, as shown in the adjacent SDS-PAGE gel (see Figure 20 for the full gel)

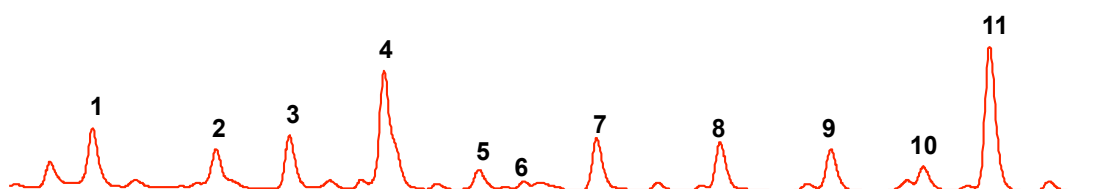


Figure 23 - HPLC chromatogram of total *N*-glycans released from native *Balanus amphitrite* SIPC

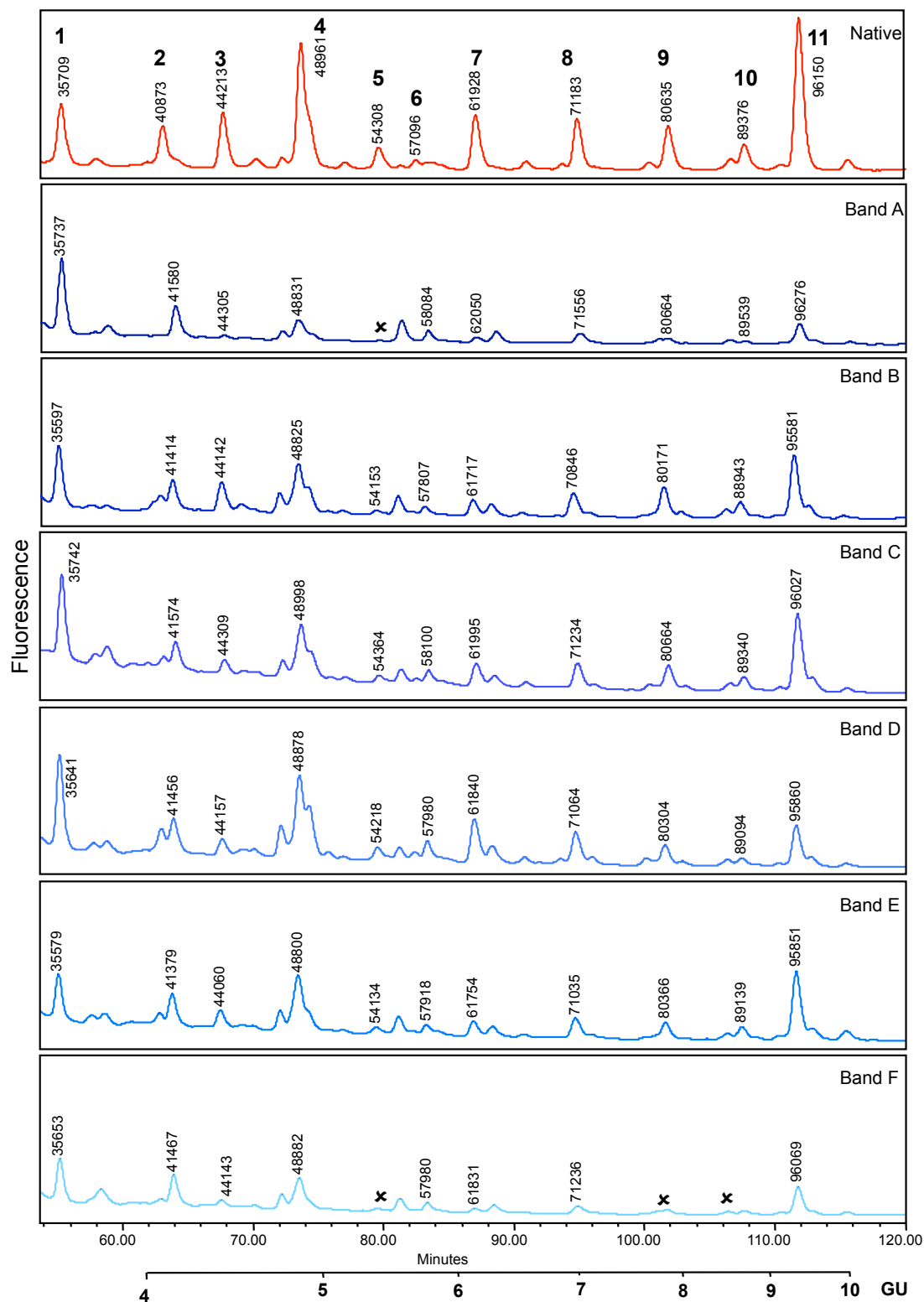


Figure 24 - HPLC chromatograms of total *N*-glycans released from the native *Balanus amphitrite* SIPC and gel fractions A-F with Dextran ladder assigned GU values. These GU values are displayed here as vertical values in thousands (e.g. 96069). GU value is rounded to the nearest thousand as shown on the GU scale below the x-axis. For further analysis the GU values are similarly displayed (e.g. 9.61). * indicates absence of a peak.

A tentative glycan structural assignment was carried out using the GU values and GlycoBase (Campbell et al., 2008), are shown in Figure 25 along with the representative proportions of each glycan (Table 1). In addition, Table 2 shows the proportions of the glycans in each of the gel bands A to F. These results indicate that high-mannose type glycans are the most prevalent glycans present in the native SIPC, forming a ‘mannose ladder’ consisting of the oligomannose series M2-9, with each ‘rung’ of the ladder representing an oligosaccharide, here a GlcNAc, containing one additional mannose residue. Monofucosylated oligomannose species (F(6)M2-4) also appear to be present but in considerably lower quantities. Where ‘shoulders’ appear beside a peak, this can be due to one or more isomers of the parent peak. This provides a base for further confirmation using enzymes and additional HILIC.

The structures and names used throughout this analysis are as per the nomenclature system outlined in Harvey et al. (2009), the key to which is shown in Figure 26. Exoglycosidase digestions of the *N*-glycan pool liberated from the SIPC were performed to refine and confirm the preliminary glycan assignments, see Figure 27.

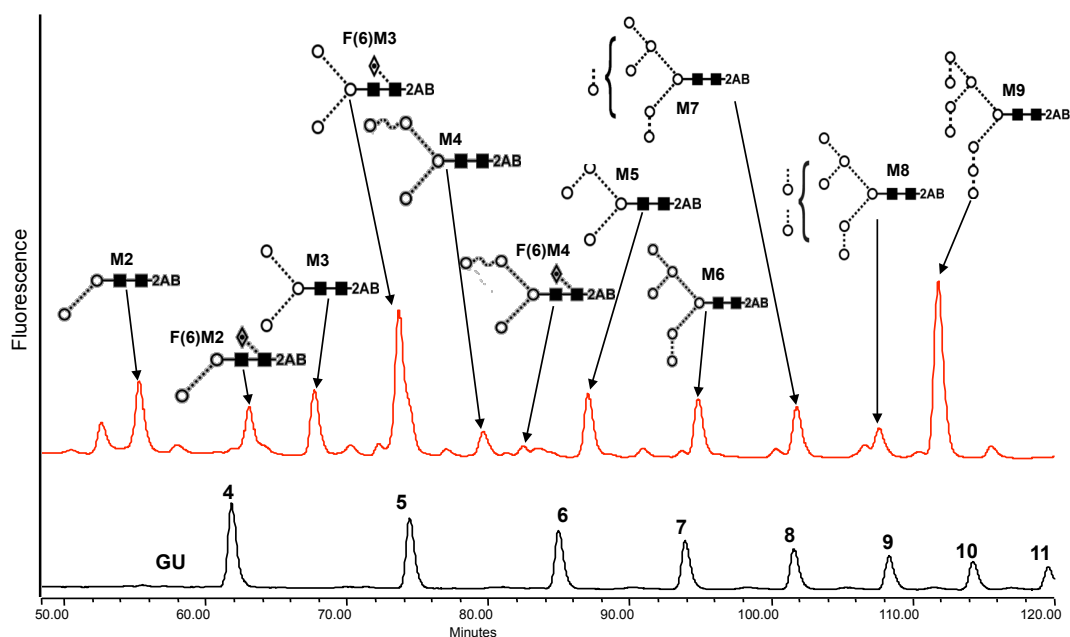


Figure 25 - HILIC chromatogram showing the glycans released from the native *Balanus amphitrite* SIPC from the in-gel block showing the oligomannose series M2-9 along with a dextran ladder to find the GU values. Molecular representations of the sugars are included. The individual monosaccharides are represented as follows: open circle, mannose; dotted diamond, fucose, dotted line, α linkage; solid line, β linkage.

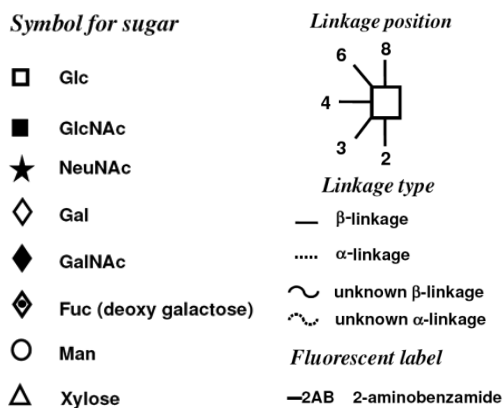


Figure 26 - Key to carbohydrates, linkages and structures as used in this research as used in Harvey et al. (2009)

Table 1 - Structure details of the glycans of *Balanus amphitrite* SIPC with glucose unit (GU) and percentage area from the HILIC-fluorescence data. ^a Allocated peak numbers, see Figure 23. ^b Glucose Unit. ^c The amount of glycan present as a percentage of the total glycans measured by HPLC.

Peak ^a	Glycan	HPLC GU ^b	% area ^c
1	M2	3.57	6.7
2	F(6)M2	4.08	4.9
3	M3	4.42	5.2
4	F(6)M3	4.89	15
5	M4	5.43	2.1
6	F(6)M4	5.7	0.7
7	M5	6.19	5.3
8	M6D3	7.11	5.1
9	M7	8.06	4.4
10	M8	8.93	2.8
11	M9	9.61	15.5

Table 2 - Structural assignment with relative percentage areas of peaks present in native *Balanus amphitrite* SIPC and gel fractions A-F. ✖ indicates absence of a peak.

Peak	HPLC GU	Possible GU	Possible glycan	% Area						
				Native	A	B	C	D	E	F
1	3.57	3.46	M2	6.7	2.9	3.5	3.2	2.2	1.2	2.9
2	4.08	3.95	F(6)M2	4.9	1.4	0.9	0.9	0.5	0.3	2.1
3	4.42	4.4	M3	5.2	0.1	1.7	0.4	0.3	0.4	0.4
4	4.89	4.89	F(6)M3	15	1.2	1.0	2.2	1.9	1.9	2.8
5	5.43	5.31	M4	2.1	✖	0.2	0.3	0.3	0.2	✖
6	5.7	5.7	F(6)M4	0.7	0.4	0.4	0.2	0.3	0.3	0.4
7	6.19	6.19	M5	5.3	0.2	1.0	0.9	1.1	0.4	0.6
8	7.11	7.06	M6D3	5.1	0.5	1.6	1.0	0.8	0.5	0.5
9	8.06	8.02	M7	4.4	0.2	2.2	1.1	0.6	0.4	✖
10	8.93	8.83	M8	2.8	0.1	1.0	0.6	0.1	0.3	✖
11	9.61	9.49	M9	15.5	1.0	3.9	3.3	1.0	1.9	1.4

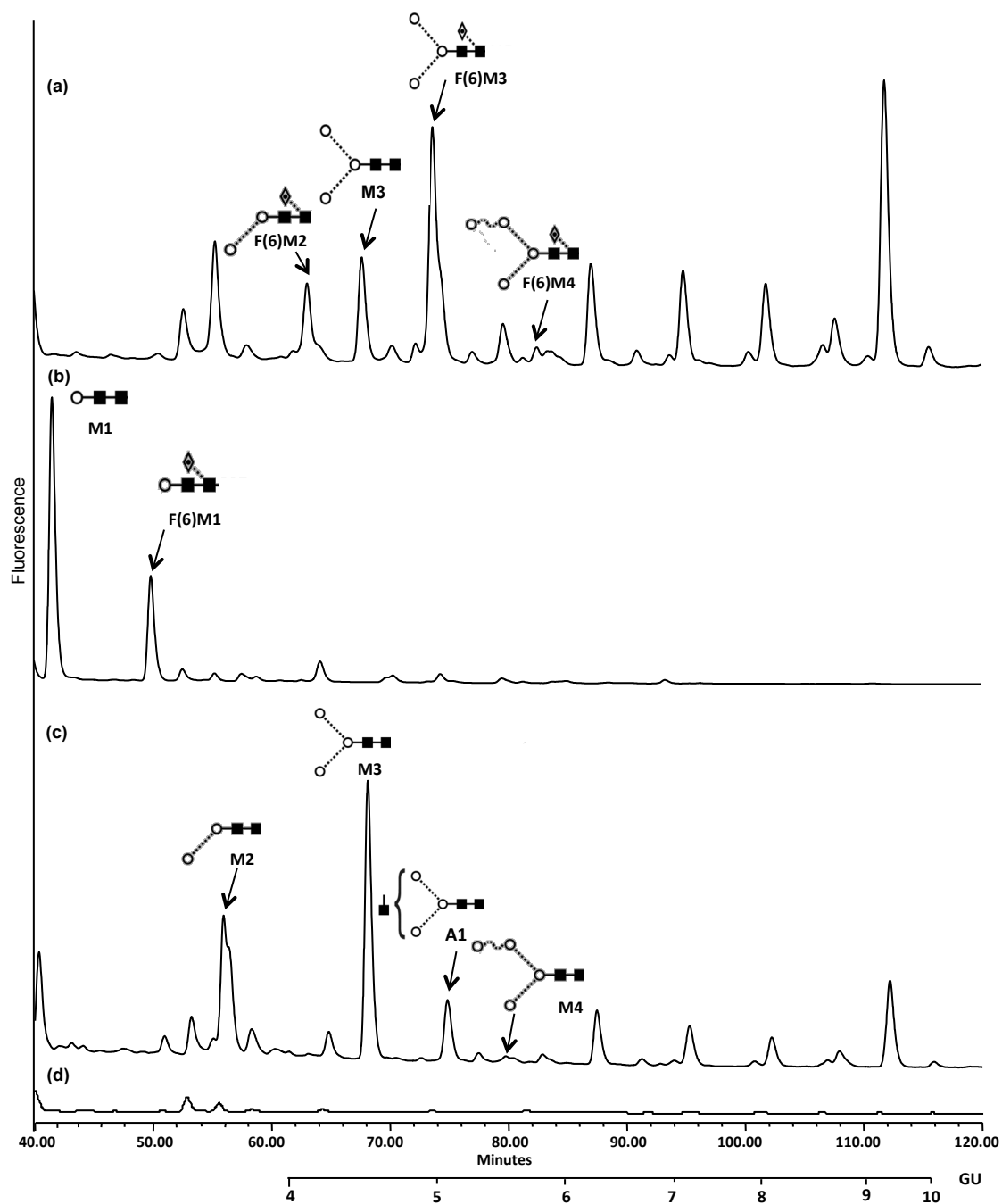


Figure 27 - HILIC-fluorescence chromatogram of *Balanus amphitrite* SIPC (a) glycans released from the native SIPC from the in-gel block showing the oligomannose series M2-9 with F(6)M2-4. Chromatogram (b) shows the JBM digest of the glycans. Chromatogram (c) shows the BKF digest of the glycans. Chromatogram (d) shows the gel blank. Molecular representations of the sugars are included. The individual monosaccharides are represented as described by Harvey et al. (2009).

The sequencing of the *N*-glycan pool after exoglycosidase digestion using the same HILIC-fluorescence results in the traces depicted in Figure 27. Figure 27(a) shows the oligomannose series M2-9 and core fucosylated oligomannose glycans F(6)M2-4 released from the native SIPC while Figure 27(b) shows the jack-bean mannosidase (JBM) digest of the glycans. All peaks present were found to be trimmed back yielding only M1(GU of 2.7) and F(6)M1. This is because JBM removed all but the terminal mannose (M1). Figure 27(c) is the resulting HILIC-fluorescence chromatogram following digestion with bovine kidney α -fucosidase (BKF), which depicts the removal of the α -(1-6)-linked fucose residue present on the reducing terminal GlcNAc residue in F(6)M2-4 to yield M2, M3 and M4 respectively. In addition, the digestion of the F(6)M4 peak revealed a previously masked peak corresponding to a monoantennary glycan (A1). All other peaks associated with the oligomannose series M2-M9 were unaffected by the presence of α -fucosidase indicating the absence of an α -(1-6)-linked fucose residue on their reducing terminal GlcNAc residue. Figure 27(d) shows the gel blank.

3.3.4 Sugars in solution

Figure 28 shows the changing response of settling cyprids in response to different concentrations of sugars and other controls. Figure 28(a) indicates that cyprids settle at a higher rate when exposed to exogenous mannose than to galactose. The settlement response to 1mM mannose is significantly different to 0.1mM, 1 μ M and 0.1 μ M galactose but not in comparison to the artificial seawater control (data was not normal; Kolmogorov-Smirnov test statistic = 0.121, $p < 0.01$, equally variant; Levene's test statistic = 0.37, $p = 0.320$ and significantly different; Kruskal-Wallis $H_{10} = 26.37$, $p = 0.003$). Cyprids exposed to the SIPC, Figure 28(b), elicited a similar maximum response as compared to mannose; however the concentrations involved are very different. To achieve around 40% settlement, 1mM of mannose is required, only 25nM of the SIPC produces the same settlement. It is noticeable in Figure 28 that in solutions that cue settlement (mannose and the SIPC) there is a decline in settlement with decreasing concentration. However in the case of galactose, the settlement remains roughly constant at all concentrations, indicating it does not provoke settlement. Figure 28(c) is the exception to this and as IBMX is known to be a strong chemical inducer for cyprid settlement, the high levels of settlement are expected. IBMX is thought to induce settlement by raising intracellular concentrations of cAMP (Clare et al., 1995). However, it appears that at the highest concentrations, IBMX stops all settlement.

These results corroborate those of Clare et al. (1995) where concentrations of more than 0.01mM show very little or zero settlement. This was followed by a peak in settlement of around 70% at 0.01mM then a gradual decline with decreasing concentration to 0.1 μ M.

From the settlement data, the half maximal effective concentration (EC50), where half the population settled, was determined using Minitab Probit analysis. After 24 hours, galactose EC50 is 2.29 \pm 1 mM, mannose EC50 is 1.548 \pm 0.23 mM and the SIPC EC50 is 102 \pm 40.1 nM.

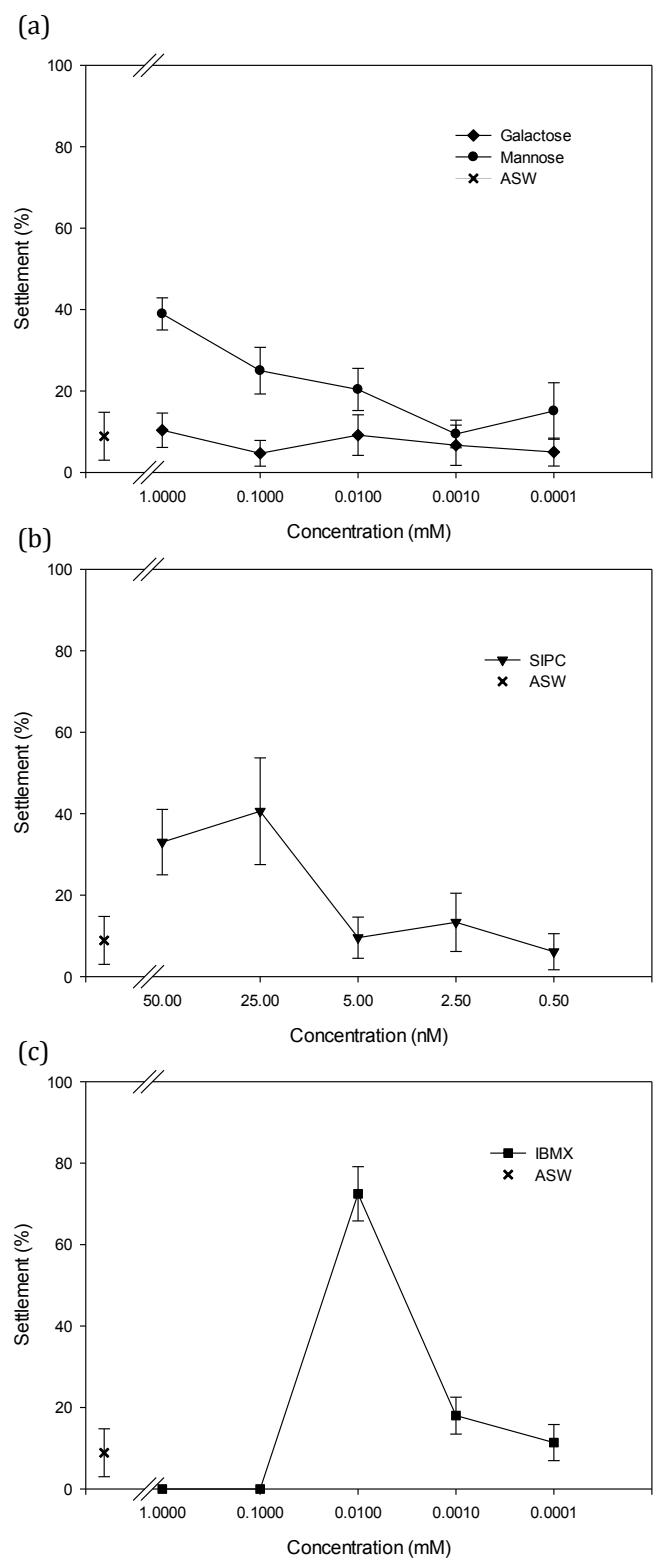


Figure 28 - Effect of exogenous sugars on the settlement of 1-day-old *Balanus amphitrite* cyprids when compared to artificial seawater (ASW). (a) mannose and galactose at 24 hours (b) SIPC at 24 hours (c) IBMX at 24 hours. Note the different scales on the x axes.

3.4 Discussion

3.4.1 SIPC purification

The established nature of the protein purification protocol (Matsumura et al., 1998b) ensures that the methodologies used are appropriate and successful. The result of the immunoblotting and Western blots after both size and charge separation indicate that the extraction and consequent purification of the SIPC from the barnacle crude extract was a success.

3.4.2 SIPC glycan characterisation

Cell surface oligosaccharides play an important role in recognition both on cell surfaces and in solution (Ambrosi et al., 2005, Caldwell and Pagett, 2010) and the presence of the glycoprotein SIPC in barnacle cuticle is key to the gregarious settlement and colonisation of surfaces. This research has confirmed that the SIPC is indeed a glycoprotein and through the exoglycosidase digestions has identified the oligosaccharide content to be mannose. *N*-linked glycans enzymatically liberated from the SIPC were found to be high-mannose-type ranging from M2 to M9. Previous research has reported similar structures in other freshwater and marine organisms such as haemocyanin from the crayfish *Astacus leptodactylus* (Tseneklidou-Stoeter et al., 1995) and haemoglobins from *Riftia pachyptila* (Zal et al., 1998). Matsubara et al. (2005) found the same oligomannose and α -1-6 fucose structures in *Megabalanus rosa* haemolymph.

The confirmation of high-mannose oligosaccharides in the SIPC is in agreement with previous research on the inhibition of conspecific settlement in *B. amphitrite* by certain lectins. Both lentil lectin (LCA) and jack-bean lectin (ConA) were reported to inhibit settlement (Matsumura et al., 1998a). Both LCA and ConA are mannose binding lectins (Sharon and Lis, 1989). It is thought that these lectins impede the cyprid detecting the SIPC by preferentially binding to the mannose. Kornfeld et al. (1981) also found that LCA required fucose to be present in addition to mannose for successful binding. As the SIPC also has a small proportion of core fucosylated oligomannose structures, this would again encourage the LCA to bind. Conversely, glucosamine and galactose binding lectins, wheat germ agglutinin (WGA) and peanut agglutinin (PNA) (Sharon and Lis, 1989), did not inhibit settlement (Matsumura et al., 1998a). It is suggested this may be because they are

not specific to the mannose and therefore leave it available for detection by the cyprid antennules. Following inhibition of settlement by mannose specific lectins, it was found that adding α -D-mannopyranoside ‘reversed’ the inhibition and caused settlement to increase. This process was not undoing the effect of the lectin but simply providing the cyprid with additional mannose in solution thus supplying the cue to settle. The original mannose on the SIPC was still ‘hidden’ by the lectin.

Some progress has been made to this end, as the percentage proportions of each of the oligomannose peaks is shown in Table 1. It may be possible for further mass spectrometry work to be carried out in the future using methods outlined by Kaji et al. (2003) and Zhang et al., (2003). These two methods outlined involve replacing the sugars on peptides with heavy isotope tags then identifying the peptides using mass spectrometry. This avoids the issues associated with putting the variably sized glycans through MS and potentially remedying the problem that was experienced.

It is possible that the SIPC may contain α -(1-3)-linked core fucose. Due to the choice of exoglycosidase used in this initial study, such oligosaccharides, if present, will not have been liberated due to the inability of PNGaseF to liberate glycans containing α -(1-3)-linked core fucose. Further characterisation using PNGaseA to determine if *O*-glycans are present would be required to fully characterise the carbohydrates present on the SIPC. At the time this research was carried out, an appropriate optimised protocol for using PNGaseA for *O*-glycan release was still in development and thus could not be employed. As shown in Chapter 5.3.3 there is the possibility that *O*-linked glycans are present.

The current study on the characterisation of the carbohydrate moiety of the SIPC has attempted to identify the glycans involved in barnacle gregariousness and builds on the study of Dreanno et al. (2006b). The identification of high-mannose-type oligosaccharides present on the SIPC is in agreement with previous studies (Khandeparker et al., 2002, Matsumura et al., 1998a) and has provided the first steps towards fully understanding the role of glycans in contact-based pheromone cues in barnacles.

3.4.3 Sugars in solution

The concentrations of mannose used in these experiments ranged from 1000 to 0.1 μ M and similar (mM) concentrations of mannose in this range have been used in inhibitory

experiments in the past (Calarese et al., 2003). Johnson et al. (1977) showed that a representative concentration of mannose in natural seawater is around $2.23\mu\text{M}$, thus the range used here covers this value. In addition, assays in this experiment were run with artificial seawater (ultra pure water and TropicMarin Sea Salt), which as outlined in Nussbaumer et al. (2004) does not contain any mannose.

Mannose in solution has also been shown to act as a settlement cue whereas galactose and glucose do not (Khandeparker et al., 2002). These findings were reinforced by the EC_{50} data collected during this research. The EC_{50} for mannose is less than half that of galactose. The large standard errors seen with these EC_{50} values are common in bioassays where there is positive feedback mechanism from newly metamorphosed barnacles providing additional settlement cues to exploring cyprids (Aldred and Clare, 2009).

The SIPC, Figure 28(b), induces consistently high settlement as it is the barnacles' natural settlement pheromone. The efficacy of the SIPC reduces with decreasing concentration, implying the more there is present on a surface the more inductive it will be, although the curve would asymptote to a maximum response as shown by Crisp (1990). The pattern of results is very similar to those found by Matsumura et al. (1998a) in both settled and metamorphosed cyprids. Similarly, the same result was observed by Dreanno et al. (2007) who investigated the settlement response of *B. amphitrite* cyprids to the SIPC but used the SIPC glycoprotein bound to nitrocellulose membrane, which gave better control of concentration. Stelzer and Snell (2003) showed a similar reduction in reproduction with decreasing concentration of female conditioned water in rotifer species. However, this settlement is only approximately half of the maximal response to IBMX, which may be due to SIPC forming the initial part of the cascade to initiate settlement whereas IBMX may bypass this cascade and initiate settlement directly, a theory proposed by Clare et al. (1995). IBMX, Figure 28(c), is known to induce settlement in barnacles and the results shown match the results of Clare et al. (1995) where concentrations of more than 0.1mM show very little or zero settlement. This is followed by a peak in settlement of around 70% at 0.01mM then a gradual decline with decreasing concentration to $0.1\mu\text{M}$. From Figure 28(a) it appears that mannose does induce settlement more than galactose, reinforcing the glycan analysis (Chapter 3.3.3), which showed that the SIPC consists of mannose oligosaccharides. Figure 28 shows that a high concentration of mannose is required to observe a similar level

of settlement to SIPC. This is most likely because the mannose monosaccharide, a monovalent ligand, has lower affinity with the cyprid receptors. The SIPC, as a multivalent ligand, would have much higher affinity due to the avidity effect of the combined strength of all the bonds. This would be the case if the larval receptor were a lectin, as these proteins bind with high affinity to a multivalent ligand such as SIPC. This suggests that the receptor for SIPC is a lectin.

Cyprid settlement in the control monosaccharide, galactose is not significantly different (Kruskal-Wallis $H_{10} = 26.37$, $p = 0.003$, where only mannose was significantly different) from that of cyprids in artificial seawater at all concentrations assayed. In addition, the percentage settlement of cyprids when exposed to galactose does not change with decreasing concentration, as is the case with mannose. The cyprids were clearly unaffected by the presence of galactose and consequently it did not act as a cue.

3.4.4 Conclusion

The bioassay results, taken together with the glycan analysis data, suggest that the mannose oligosaccharides of the SIPC contribute to the settlement-inducing activity of the SIPC, as published in Pagett et al. (2012). It may be possible that there are other glycans present in SIPC that were not characterised using this research. It is feasible that the SIPC may contain α -(1-3)-linked core fucose. Due to the choice of exoglycosidase used in this initial study, such oligosaccharides, if present, will not have been liberated due to the lack of ability of PNGaseF to liberate glycans containing α -(1-3)-linked core fucose. Further characterisation using PNGaseA, when a protocol has been established, could be used to determine if *O*-glycans are present and fully characterise the carbohydrates present on the SIPC.

Chapter 4. Functionalised glycopolymers

4.1 Introduction

Preliminary experiments looking at the effect of carbohydrates in solution on the settlement of cyprids provided a focus for research throughout this project. This was followed by the characterisation of the glycans in the SIPC confirming the presence of high mannose oligosaccharides. Further research then continued into the effect of surface bound carbohydrates in an effort to reproduce the natural presentation of glycans on the barnacle cuticle. The aim of this experimental chapter was to create a synthetic mimic of the SIPC glycans.

There has been considerable research into surfaces that repel or attract barnacles and to understand the mechanisms they use to adhere. Pettitt et al. (2004) found that commercially available serine proteases reduced fouling by *Ulva linza* (green algae), *Navicula perminuta* (diatom) and *Balanus amphitrite* (barnacle) through hydrolysing the adhesive polymers. Conversely, earlier research by Morse and Morse (1984) found that small peptides on the surface of red crustose algae induced settlement of larvae of the abalone *Haliotis rufescens*. Other approaches have involved searching for chemicals that can be incorporated into the paint. Aldred et al. (2008) found that the addition of the serine endopeptidase, Alcalase[®], reduced the effectiveness of cyprid adhesives, removed cyprid footprints from glass but the permanent cement became resistant after curing. Through researching the physical and chemical properties of surfaces, other surfaces that decreased *B. amphitrite* cyprid settlement were found. One example of this was a fouling-release coating of poly(dimethyl siloxane) (PDMS). This surface provided a low modulus surface with a fluorinated copolymer giving low surface tension (Marabotti et al., 2009). The zwitterionic polymers poly(sulphobetaine methacrylate) and poly(carboxybetaine methacrylate) also affected *B. amphitrite* cyprids, as both polymers completely stopped settlement and changed the surface exploratory behaviour (Aldred et al., 2010). The hydrophilic polymer poly(ethylene)glycol (PEG), when coated on surfaces including aminated glass, showed antifouling properties against *B. amphitrite*, *U. linza*, *N. perminuta* as well as several bacterial species. This efficacy was attributed to its high protein resistance (Ekblad et al., 2008). Similar work which was based on the physical properties of poly[poly(ethylene

glycol)methyl ether methacrylate]-*block*-poly(2,3,4,5,6-pentafluorostyrene) forming brush-type copolymers discouraged barnacle settlement (Tan et al., 2010).

In a natural occurrence of molecular mimicry, pathogens in multicellular animals can create a thick coating of lipopolysaccharides (LPS) on their outer membrane surface which appear similar to those of the host cell and avoids triggering an immune response (Varki and Lowe, 1999). One specific example of this is *Yersinia pestis*, the plague. This particular bacteria alters the structure of LPS to mimic that of the mammalian host and avoid detection (Nizet and Esko, 1999). It is hoped that this research could lead to a similar mimic to emulate the presence of the SIPC and cue settlement so adding to the understanding of gregarious settlement mechanisms. One previous approach to produce analogues of the SIPC was that of Tegtmeier and Rittschof (1989), who experimented with a series of peptides to further understand the mechanisms behind pheromone receptor interactions. They discovered six peptides that mimicked pheromone activity, the most effective being L-leucyl-L-arginine and L-histidyl-L-lysine, highlighting the importance of the basic carboxy-terminal amino acid.

The favoured protocol for creating a synthetic mimic of the SIPC was based around 'carbohydrate functionalised polymers'. There are several techniques for attaching thin films of molecules to surfaces, including self-assembly (Ulman, 1996), deposition of reactive layers (Stouffer and McCarthy, 1988) and graft polymerization (Zhou et al., 1996). Research of this nature focusing on the immobilisation of thin films on glass using maleic anhydride copolymers was instigated by Liu et al. (1997) where a reactive copolymer, in this case poly(methyl vinyl ether-*co*-maleic anhydride) or Gantrez[®], was attached to a surface to form a brush-like layer of dense, semi-organised and readily modified polymer. Following the success of this research, other studies on immobilizing molecules on surfaces have been successful (Pompe et al., 2003, Uzawa et al., 2005, Freudenberg et al., 2005).

There has also been progress in binding sugars to surfaces, such as the experiments carried out by Maciel et al. (2007) using the galactose-rich polysaccharide, cashew gum. Thin films of cashew gum were added to silicon wafers and amine-terminated wafers to immobilize desired biological molecules. This strategy provided galactose-terminated surfaces as required for bioassaying. More suited to the synthetic approach to work for this chapter, Yin et al. (2003) and Ying et al. (2003) attached 1-O-(6'-aminohexyl)-D-galactopyranoside

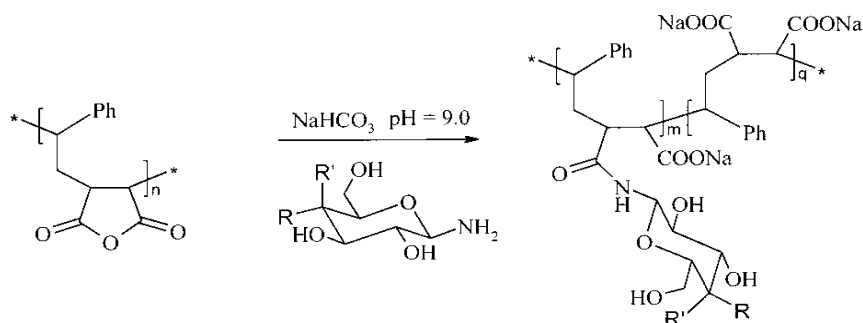
(AHG) to polyethylene terephthalate (PET) to produce surfaces with a high density of immobilized galactose.

Introducing the use of polymers to the surface modification in addition to the sugars mentioned above increases the density of carbohydrates as well as the flexibility of the molecule. The use of maleic anhydride copolymers to form an easily reactive surface has become an area of increasing popularity and is the approach that was used for the surface modification in this chapter. Firstly, the surface e.g. glass, has to be aminosilated (Wieringa and Schouten, 1996) then modified with a layer of Gantrez[®]. This provides anhydride groups for additional reactions and was confirmed to be successful in more recent studies by Evenson et al. (2000) using X-ray photoelectron spectroscopy (XPS). Following this, Grombe et al. (2006) used 2-aminoethoxyl- β -D-glucopyranoside and poly(propylene-*alt*-maleic anhydride) copolymer to form a carbohydrate-based polymer layer. XPS was used to confirm that the glucopyranoside was incorporated into the polymer rather than forming a separate layer. By bonding 1-amino-1-deoxy- β -D-galactose, glucose and lactose to the anhydride of the poly(styrene-*co*-maleic acid), Donati et al. (2002) formed the first steps towards carbohydrate functionalised polymers as shown in Figure 29(a).

Drawing on this research, using poly(styrene maleic anhydride) Galgali et al. (2007) added various regio-specific ester derivatives of glucose to form carbohydrate-linked synthetic biodegradable polymers Figure 29(c). Similarly, as shown in Figure 29(b), micellar mannose nanoparticles based on poly{styrene-*co*-[(maleic anhydride)-*alt*-styrene]} were developed for understanding the protein-carbohydrate interactions in cell surface biology (Su et al., 2009). Mannosylated Gantrez[®] AN nanoparticles were developed by Salman et al. (2006) for use in oral drug delivery. Binding to the lectin Concanavalin A confirmed successful coating of the particles with mannosamine, corroborating another methodology of creating carbohydrate-terminated polymers. Arbos et al. (2002) developed Gantrez[®] AN and 1,3-diaminopropane nanoparticles, giving a binding efficacy of 68%, six times more than conventional nanoparticles. This was measured using the black elder lectin, *Sambucas nigra* agglutinin (SNA). This research showed Gantrez[®] was a suitable copolymer to use for creating biologically active nanoparticles.

Synthesis pathways of maleic anhydride polymers

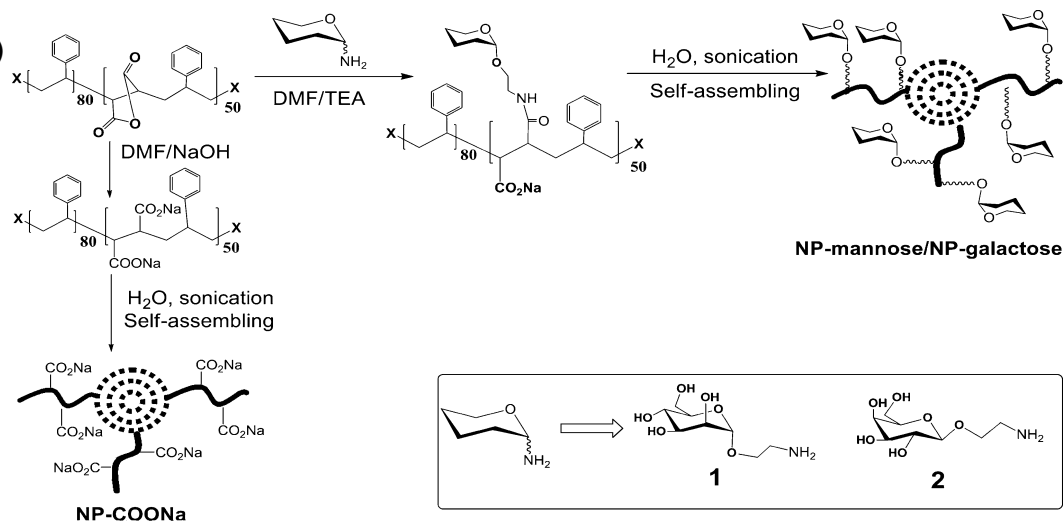
(a)



	R'	R	DS ^a	1-DS ^a
SMA-Gal	OH	H	0.56	0.44
SMA-Gluc	H	OH	0.54	0.46
SMA-Lac	H	O-β-Gal	0.94	0.06

^a DS = degree of substitution

(b)



(c) 1

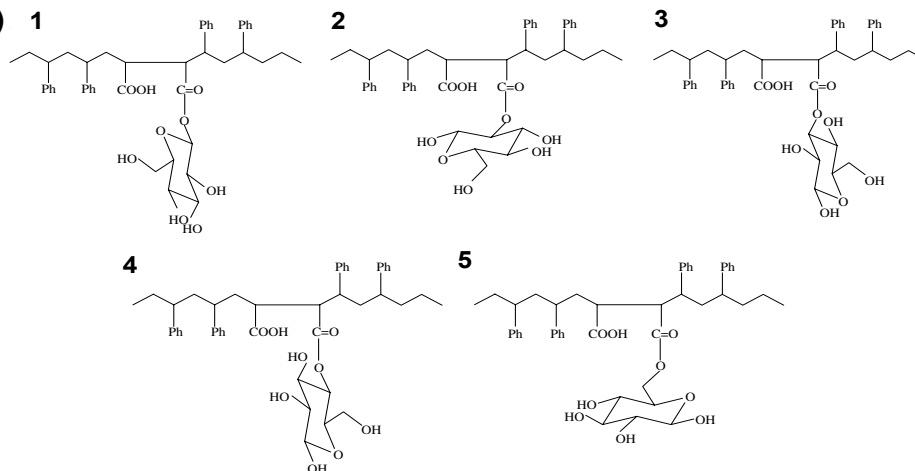


Figure 29 - Synthesis pathways for maleic anhydride polymers (a) Reaction scheme for the production of poly(styrene-co-maleic acid) glycopolymers from Donati et al. (2002) (b) Synthesis and assembling of 'hairy' glycol-nanoparticles from poly{styrene-co-[(maleic anhydride)-*alt*-styrene]} from Su et al.(2009) (c) Polymer structures formed by carbohydrate-polymer attachment via 1) the anomeric hydroxyl, 2) C2 hydroxyl, 3) C3 hydroxyl, 4) C4 hydroxyl and 5) C6 hydroxyl, in the reaction of glucose with poly(styrene maleic anhydride) from Galgali et al. (2007)

Building on the success of maleic anhydride polymer surface modification, the pre-formed polymer used during this research was a commercially available amine-reactive polymer, Gantrez[®] AN119 (International Specialty Products, NJ, USA). To provide a suitable link and additional flexibility within the structure, an amino alcohol was used as a linker between the polymer and carbohydrates. The polymers were functionalised with α -mannose residues, predicted to cue settlement, as mannose is a major constituent of the SIPC. In addition, comparison treatments with β -galactose and β -glucose units were also created, as these carbohydrates were predicted not to cue, as they are not present in the SIPC. Synthesising molecules containing glycans requires stereochemical and regiochemical control which is achieved using protecting groups to determine the orientation of bonds (Bertozzi and Kiessling, 2001). This work was based around similar projects being pioneered in the structural chemistry laboratory of Professor Neil Cameron at the University of Durham (Hazelhurst, 2009, Brogdon, 2010).

Work on the carbohydrate portion of the SIPC showed *N*-linked glycans (see Chapter 3.3.3), as it is asparagine, the N of NX_{≠P}S/T, which forms the *N*-glycosidic bond at the glycosylation sites on the amino acid sequence. The NX_{≠P}S/T rule states that glycosylation sites must consist of NX_{≠P}S/T sequons, i.e. an asparagine plus any amino acid plus serine or threonine. The structure of a possible glycosylation site is shown in Figure 30. Here, the amine group on one amino acid forms a peptide bond with the carboxyl group on the next, as indicated with the blue circles. Once the NX_{≠P}S/T has been formed, it is the terminal amine (circled in red) that bonds to the sugar through the nitrogen, therefore all *N*-linked glycans need this terminal amide. At the other end of the molecule, the hydroxyl (circled in green) hydrogen bonds hold the glycan in the correct position for the enzyme to attach the glycan to the amine, thus the molecule must end with S or T to provide the hydroxyl group. However as NX_{≠P}S/T is only a requirement of glycosylation, not a guarantee, its presence is not always sufficient for the asparagine to be glycosylated.

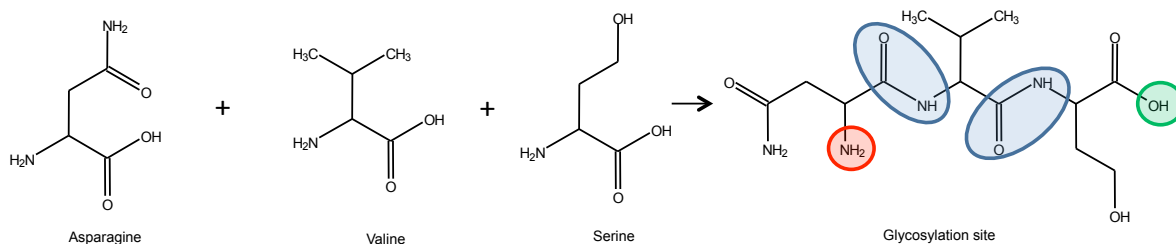


Figure 30 - The structure of a glycosylation site using the $NX_{\neq p}S/T$ rule; where Asn-Xaa(\neq Pro)-Ser or Asn-Xaa(\neq Pro)-Thr (where Xaa is any amino acid except Pro, as it renders the Asn inaccessible).

However, the above proposals will produce *O*-glycans. It is very difficult to make *N*-linked glycans under laboratory conditions due to the enzymatic reactions required. Nonetheless, when there is more than one glycan present, they are *O*-linked to each other at the anomeric position. As the SIPC contains M2 to M9, these glycans are *O*-linked. In addition, Chapter 3.2.17 shows cyprid settlement in carbohydrate solutions which are also *O*-linked glycans. Consequently, producing *O*-linked glycans is expected to produce a similar settlement effect and will be the approach taken for this experimental chapter.

4.1.1 Aims and objectives

A single aim is the subject of the research in Chapter 4, this covers the use of the analysis of the SIPC from Aims 1 and 2 to incorporate the carbohydrate into an SIPC mimic.

Aim 3 - To develop and test carbohydrate-functionalised polymers that are antagonistic to the SIPC and the cyprid temporary adhesive.

Objective - Surface bound SIPC mimics involving commercially available polymers to be developed at Professor Neil Cameron's Synthetic Chemistry Laboratory, Durham University, followed by drop bioassays based in the Invertebrate Reproduction and Development Laboratory, Newcastle University.

4.2 Materials and Methods

Due to the unusual nature of the polymer and carbohydrate work, there was no precedent of optimised protocol upon which to base experimental work. Using similar works in progress with other polymers and carbohydrates, several approaches were taken to develop a suitable methodology for creating the desired carbohydrate functionalised polymers. The initial approach under these circumstances was to produce proof of concept products in solution to

ensure the chemistry employed created the desired product. Therefore, Method 1 involved developing a synthetic sequence, which allowed for the addition of a linker to the carbohydrate, deprotection of protecting groups and the addition of the carbohydrate to the polymer. Method 2 was based on Method 1, again creating an in-solution proof of concept but starting the reaction at the other end of the molecule; adding a linker to the polymer then adding the carbohydrate. Method 3 involved a different technique of directly layering the reactants onto a surface rather than in solution.

4.2.1 Carbohydrate functionalised polymers - method development 1

The initial step when working with this type of reaction is to create an in-solution proof of concept of the desired product. The method employed to create a galactose derivative was first to produce 1-O-(6'-Fmoc-aminoethyl)-2,3,4,6-tetra-O-acetyl- β -D-galactopyranoside, Figure 31(a). Fmoc is fluorenylmethyloxycarbonyl chloride, a chloroformate ester, used here to protect the amine group. Once the correct stereochemistry was achieved and confirmed, the carbohydrate was deprotected (Figure 31b) and attached to the polymer (Figure 31c).

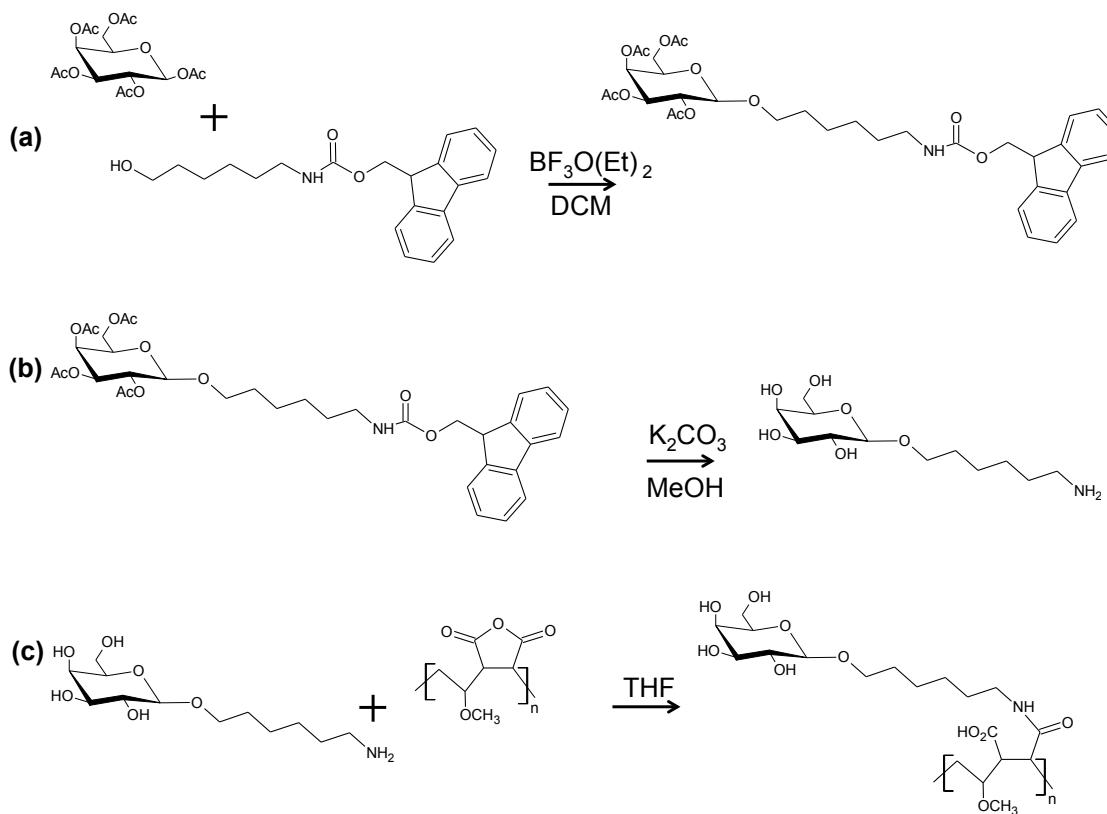


Figure 31 - Three steps of Method 1 for the synthesis of *Balanus amphitrite* SIPC mimic (a) The desired product of the first step; 1-O-(6'-Fmoc-aminoethyl)-2,3,4,6-tetra-O-acetyl- β -D-galactopyranoside (b) Step two; deprotection of the carbohydrate and removal of Fmoc (c) Step three; addition of Gantrez[®] polymer.

In Method 1, firstly boron trifluoride diethyl etherate ($\text{BF}_3\text{O}(\text{Et})_2$) was used to promote the glycosylation. Due to the sensitivity of this promoter to water, all equipment was oven dried overnight at 200 °C and experiments were carried out under nitrogen using Schlenk-line apparatus and nitrogen flushed needles. 6-(Fmoc-amino) hexan-1-ol (0.50 g, 1.48 mmol) and β -D-galactose pentaacetate (0.65 g, 1.66 mmol) were dissolved in anhydrous dichloromethane (DCM) (10 ml) and the mixture was stirred for 10 minutes under nitrogen. The use of the pentaacetate in DCM promotes the preferential formation of the desired β -anomer over the α -anomer. This is due to the neighbouring group participation of the acetate group on C2. To the stirring solution, boron trifluoride diethyl etherate (1.25 ml, 10 mmol) was slowly added drop-wise via syringe, creating a pale yellow solution. The mixture was then sonicated in an ultrasonic bath (Ultrawave, UK) under nitrogen for a total of 45 minutes (5 min on, 5 min off). After this period the solution was solubility washed with brine (2 x 10 ml) and the organic layer dried with anhydrous magnesium sulphate, filtered (Whatman Qualitative Circles, Grade 1, 185mm), and the solvent removed *in vacuo* to yield a pale yellow oil.

The reaction was confirmed using several methods. First, ultra violet thin layer chromatography (UV TLC) on plastic backed TLC plates (Polygram, SilG/UV254, 0.25mm silica gel plates with fluorescent indicator) was used. The solvent system used was ethyl acetate: hexane at a 1:1 (v:v) ratio in a capped beaker to produce a solvent filled atmosphere. The filtrate and Fmoc starting material were both spotted onto the plate for comparison. There should not have been any Fmoc remaining in the product, as it was not in excess to the galactose. The plate was observed under short wave UV light and fraction spots indicated in pencil.

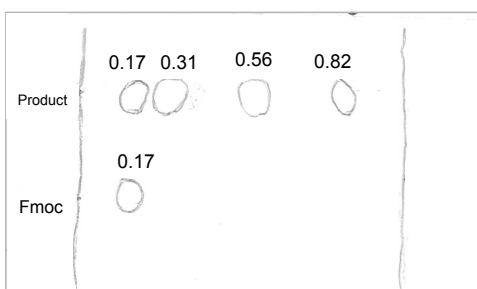


Figure 32 - A thin layer chromatograph of the product of the 1-O-(6'-Fmoc-aminoethyl)-2,3,4,6-tetra-O-acetyl- β -D-galactopyranoside reaction, clearly showing residual Fmoc and unwanted products. Rf values for each are quoted.

Figure 32 shows the TLC for the desired product with the retention factor (Rf) values of the spots calculated by dividing the spot height by the solvent height. The Fmoc appears at 0.17 which indicates that the 0.17 spot in the product is also Fmoc. There should not have been an excess of Fmoc, implying the reaction did not run to completion. The desired product (β sugar) was expected to have an Rf of approximately 0.40 so was allocated the 0.31 spot. The other spots are probably the galactose pentaacetate (0.82) and possibly the galactose hemiacetal (0.56), where the acetate on C1 is replaced by an OH as this structure often has an Rf of around 0.5.

To separate unwanted compounds from the product, purification by column chromatography was next employed. The volume of the product was reduced using a rotary evaporator to remove as much solvent (DCM) as possible. The product was purified using flash column chromatography (ethyl acetate: hexane 1:1v:v), (Biotage SP1™ Flash Purification System: flow rate 12 ml/min; Samplet™ cartridge: FLASH 12+M; UV Wavelength Collection 252 nm). The Biotage flash system calculates an appropriate gradient elution according to the Rf values from the TLC which are inputted during setup. The auto-column samplets are composed of a silica matrix and work in the same way as the TLC plates, with the non-polar molecules eluting first, i.e. the first peak on the auto-column output is the same as the spot furthest right on the TLC.

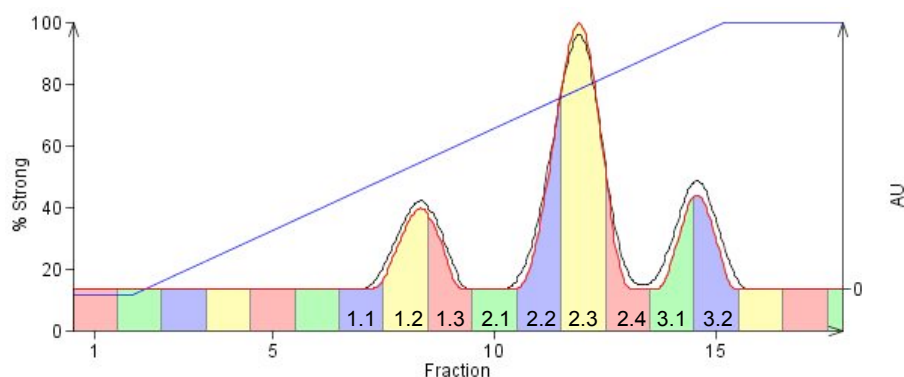


Figure 33 - Auto-column trace of the 1-O-(6'-Fmoc-aminohexyl)-2,3,4,6-tetra-O-acetyl- β -D-galactopyranoside reaction, clearly showing unwanted peaks along with the desired product (Peak 2)

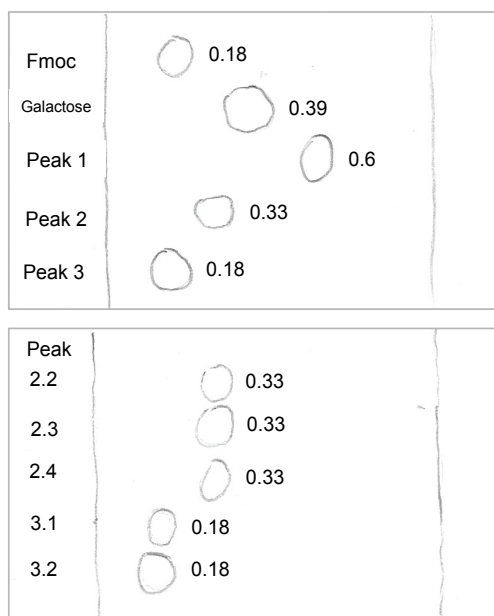


Figure 34 - TLC plate showing (top plate) the three auto-column peaks from Figure 33 (1-O-(6'-Fmoc-aminohexyl)-2,3,4,6-tetra-O-acetyl- β -D-galactopyranoside reaction). (bottom plate) TLC plate suggesting that there is no contamination between peaks.

From Figure 33 and Figure 34 once again the lower spot (peak 3) with an Rf value of 0.18 is excess Fmoc. Peak 2 is the desired product (0.33) and peak 1 (0.60) is not galactose pentaacetate as this possessed an Rf of 0.39.

Following the TLC analysis, the next step to discover the purity and constituents of a product was Nuclear Magnetic Resonance (NMR) spectroscopy. Again, to ensure as much water as possible was removed, all glassware was acetone-washed and oven dried at 200 °C. In this case, the water interferes with the NMR traces, giving an extra peak. In addition, the product was vacuum evaporated to remove all traces of solvent, as any hydrogen in the

solvent will also give errant peaks. A very small amount of product was added to 2ml of deuterated chloroform. This solvent has 99.9% deuterium atoms instead of hydrogen atoms so only shows a small peak in the NMR trace, despite being present in great excess to the solute.

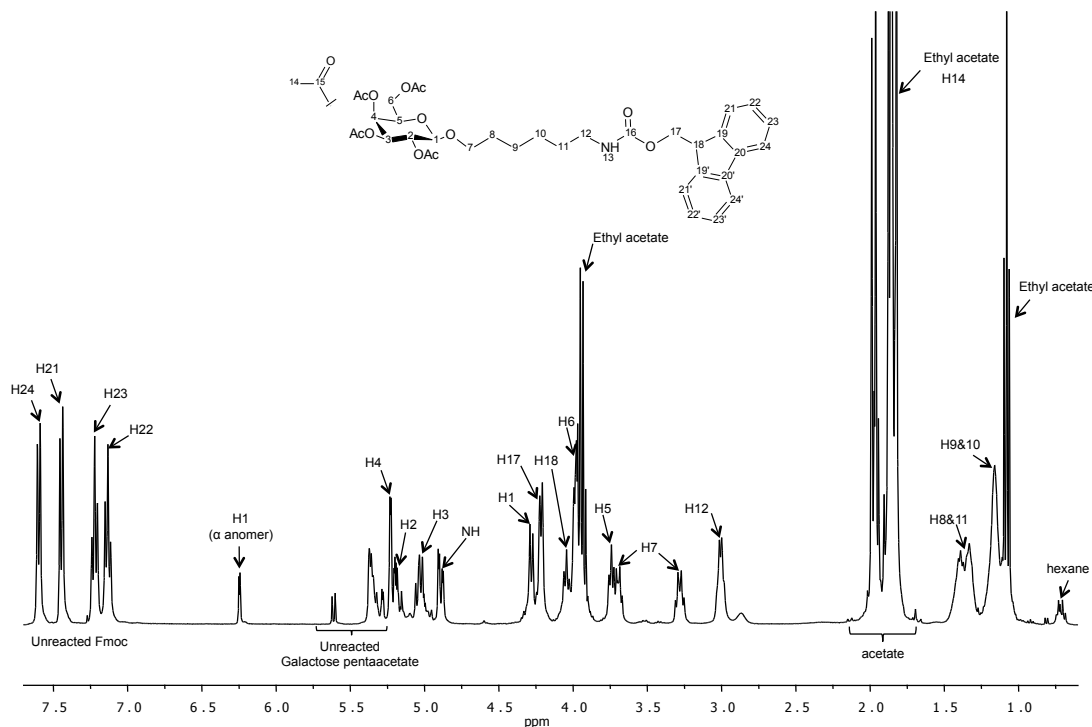


Figure 35 - Proton ^1H NMR spectrum for 1-O-(6'-Fmoc-amino)hexyl-2,3,4,6-tetra-O-acetyl- β -D-galactopyranoside showing unreacted galactose pentaacetate, Fmoc and unwanted peaks

Figure 35 is the ^1H NMR spectrum for the product, showing peaks that correspond with the TLC (Figure 34). There are undesired reactants still in the product in the form of unreacted galactose pentaacetate. Errant solvent peaks were easily identified by referring to Gottlieb et al. (1997), and ethyl acetate and hexane can be seen. The interpretation from the ^1H NMR in Figure 35 is shown below. For clarity the peaks attributable to the product are quoted separately from those peaks originating from other sources.

Product: ^1H NMR (400 MHz, CDCl_3) δ 7.60 (d, $J = 7.5$ Hz, 2H, H^{24}), 7.45 (d, $J = 7.4$ Hz, 2H, H^{21}), 7.22 (t, $J = 7.4$ Hz, 2H, H^{23}), 7.13 (t, $J = 7.4$ Hz, 2H, H^{22}), 5.23 (d, $J_{4-5} = 3.0$ Hz, 1H, H^4), 5.19 (dd, $J_{2-1} = 7.7$, $J_{2-3} = 4.4$ Hz, 1H, H^2), 5.07 – 5.00 (m, 1H, H^3), 4.89 (dd, $J = 10.5$, 3.2 Hz, 1H, NH), 4.28 (d, $J_{1-2} = 7.8$ Hz, 1H, H^1), 4.22 (d, $J_{17-18} = 7.0$ Hz, 2H, H^{17}), 4.04 (t, $J_{18-19} = 6.9$ Hz, 1H, H^{18}), 3.99 (d, $J_{6-5} = 6.6$ Hz, 2H, H^6), 3.74 (t, $J_{5-6} = 6.6$ Hz, 1H, H^5), 3.72-3.64 (m, 1H, H^7), 3.33-3.23 (m, 1H, H^7), 3.01 (dd, $J_{12-11} = 12.3$, $J_{12-\text{NH}} = 6.1$ Hz,

2H, H¹²), 1.99, 1.96, 1.88, 1.82 (4 x s, 4 x 3H, 4 x OCH₃), 1.51 – 1.25 (m, 4H, H⁸, H¹¹), 1.24 – 1.11 (m, 4H, H⁹, H¹⁰).

Impurities: ¹H NMR (400 MHz, CDCl₃) δ 6.25 (d, *J* = 3.0 Hz, 1H), 5.61 (d, *J* = 8.3 Hz, 1H), 5.39 – 5.27 (m, 6H), 3.94 (dd, *J* = 14.3, 7.1 Hz, 13H), 1.97 (s, 2H), 1.94 (s, 3H), 1.91 (s, 2H), 1.86 (s, 25H), 1.83 (s, 4H), 1.08 (t, *J* = 7.1 Hz, 15H), 0.76 – 0.66 (m, 1H).

Unfortunately the impurities shown in the ¹H NMR could not be completely accounted for. It is likely however that the doublet at 5.61ppm is residual galactose pentaacetate starting material, as this is also observed in the mass spectrum (see Figure 37). The doublet at 6.25ppm is perhaps most likely to belong to the anomeric proton of the α-anomer of the desired product, as α-protons have much smaller *J* values than the same proton in the β-anomer. This peak could also be from the talo isomer, where the acetate on C2 is positioned axially rather than equatorially.

The ¹H NMR spectra of Fmoc containing compounds are often complicated by the formation of rotational isomers in solution. A resonance structure (Figure 36) occurs due to the delocalisation of the nitrogen lone pair, thus restricting the rotation of the C=N bond. This causes a slight shift in local ¹H protons because of their occupation of an altered chemical environment. In an affected ¹H NMR spectrum, multiple signals can often be seen for signals when only one would be expected.

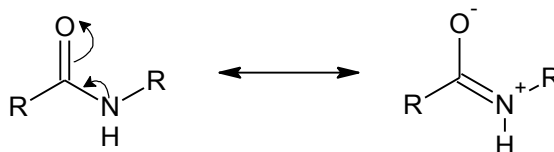


Figure 36 - Resonance structure resulting from the delocalisation of a nitrogen lone pair. The rotation about the C-N bond becomes fixed thus resulting in a different chemical environment for the NH and other local protons.

In addition to the TLC and auto-column, mass spectrometry (MS) can also be employed to assess the structure of the desired product and identify any unwanted products. 1mg of the product was dissolved in 1ml of acetonitrile for ES+ (positive electrospray) using an LCT Premier XE orthogonal acceleration time-of-flight mass spectrometer (Waters, UK).

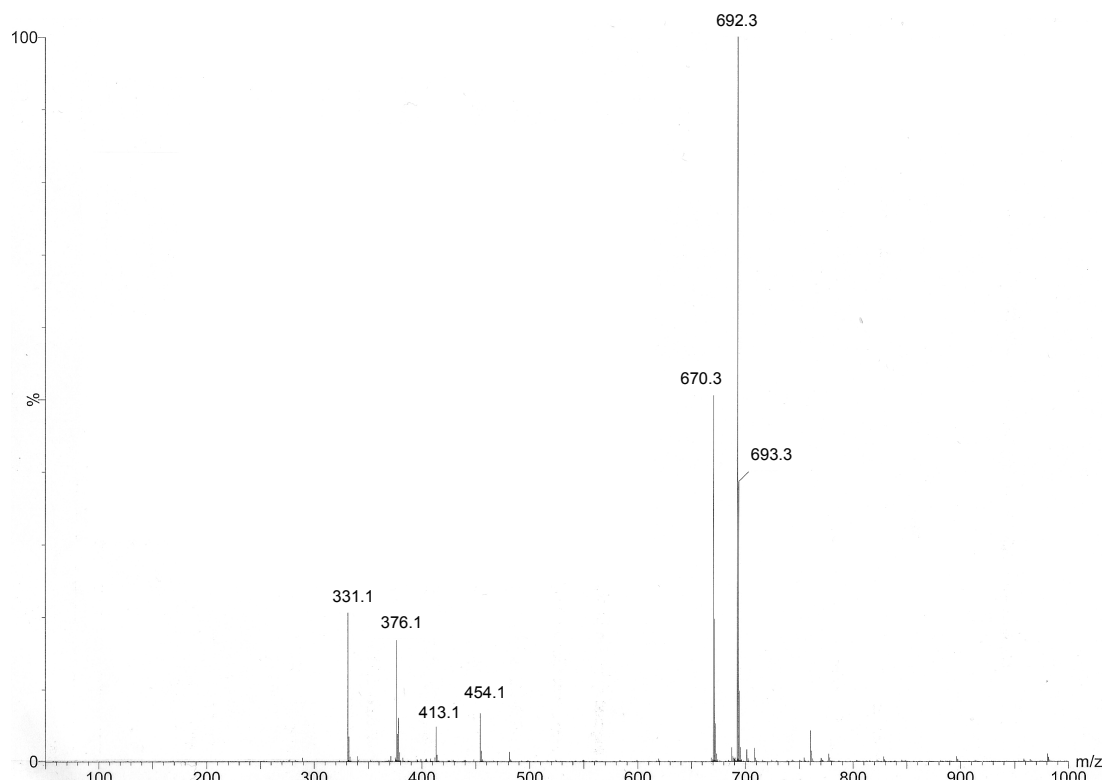


Figure 37 - Low Resolution Mass Spectrometry trace of 1-O-(6'-Fmoc-aminohexyl)-2,3,4,6-tetra-O-acetyl-β-D-galactopyranoside

The output of Figure 37 is shown below:

LRMS; (ES+) m/z; 692.3 (100%) $[M+Na]^+$, 670.3 (50%) $[M+H]^+$, 331.1 (25%) [glycosyl cation] $^+$, 376.1 (18%) $[M-Fmoc]^+$, 454.1 (8%) $[?]^+$, 413.1 (5%) [galactose pentaacetate] $^+$.

As described in the MS output above, peak 692.3 is the base peak (100%) of the product molecular ion plus sodium; peak 670.3 is the product molecular ion plus hydrogen; peak 331.1 is the glycosyl cation (the galactose pentaacetate with the anomeric -OR group missing); peak 376.1 is the product molecular ion minus Fmoc; peak 454.1 could not be attributed to a specific molecular ion; and peak 413.1 is galactose pentaacetate. If there were α sugars present in the sample, as visible from the 1H NMR (Figure 35) these are undetectable from β sugars on the spectrum (Figure 37). However, as demonstrated, any impurities and unused reactants are revealed.

As the 1H NMR and MS showed unwanted peaks, changing the solvent mix may help to separate these fractions. Figure 38 shows a TLC using a 9:1 chloroform:methanol mix where there are two spots, the impurity and product. TLC plates were developed with 5% sulphuric acid in ethanol, dried and developed with a heat gun. Here the R_f of the impurity

is 0.28 and the R_f of the product is 0.62. This shows that the unwanted product is more polar than the desired product.



Figure 38 - TLC plate showing the product (peak 2 from Figure 33 the 1-O-(6'-Fmoc-aminoethyl)-2,3,4,6-tetra-O-acetyl- β -D-galactopyranoside reaction) and impurity as separated using 9:1 chloroform:methanol solvent mix.

As changing the solvent mix for TLC separated the two components, removal of the impurity by auto-column using the same solvent system was expected (chloroform:methanol 1:1v/v), (Biotage SP1™ Flash Purification System: flow rate 40 ml/min; Samplet™ cartridge: FLASH 40+M; UV Wavelength Collection 252 nm).

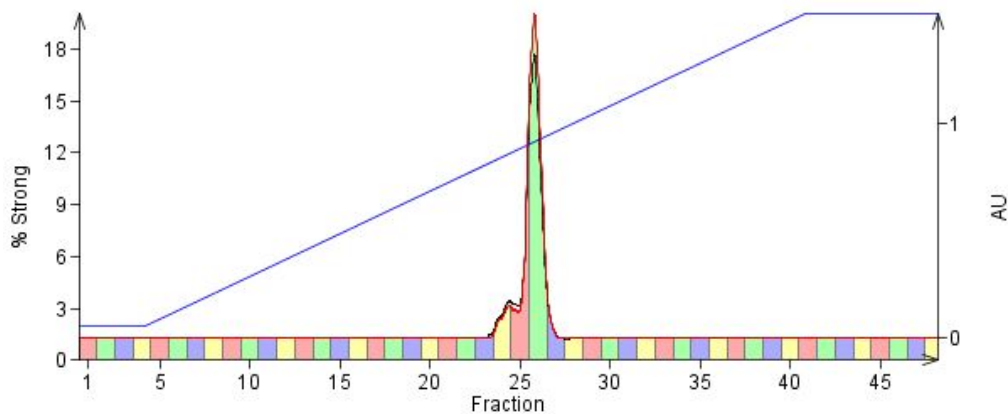


Figure 39 - Auto-column trace of the product peak 1-O-(6'-Fmoc-aminoethyl)-2,3,4,6-tetra-O-acetyl- β -D-galactopyranoside, clearly showing unwanted products with the desired product

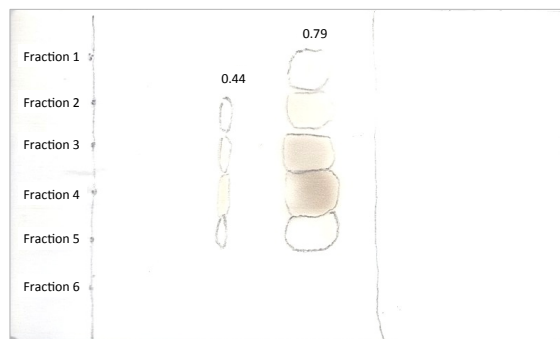


Figure 40 - TLC plate showing the six fractions of the peak in Figure 39, the unwanted product and the desired 1-O-(6'-Fmoc-aminoethyl)-2,3,4,6-tetra-O-acetyl- β -D-galactopyranoside.

Figure 40 shows that fraction 1 was the only product fraction (R_f of 0.79) not contaminated by the unwanted peak as fractions 2-5 have the impurity spot (R_f of 0.44) as well. Fraction six did not contain any reactants or products, so was discarded.

As fraction 1 was the only uncontaminated fraction from the auto-column (Figure 39), a ^1H NMR was run on this fraction only to ensure it was pure.

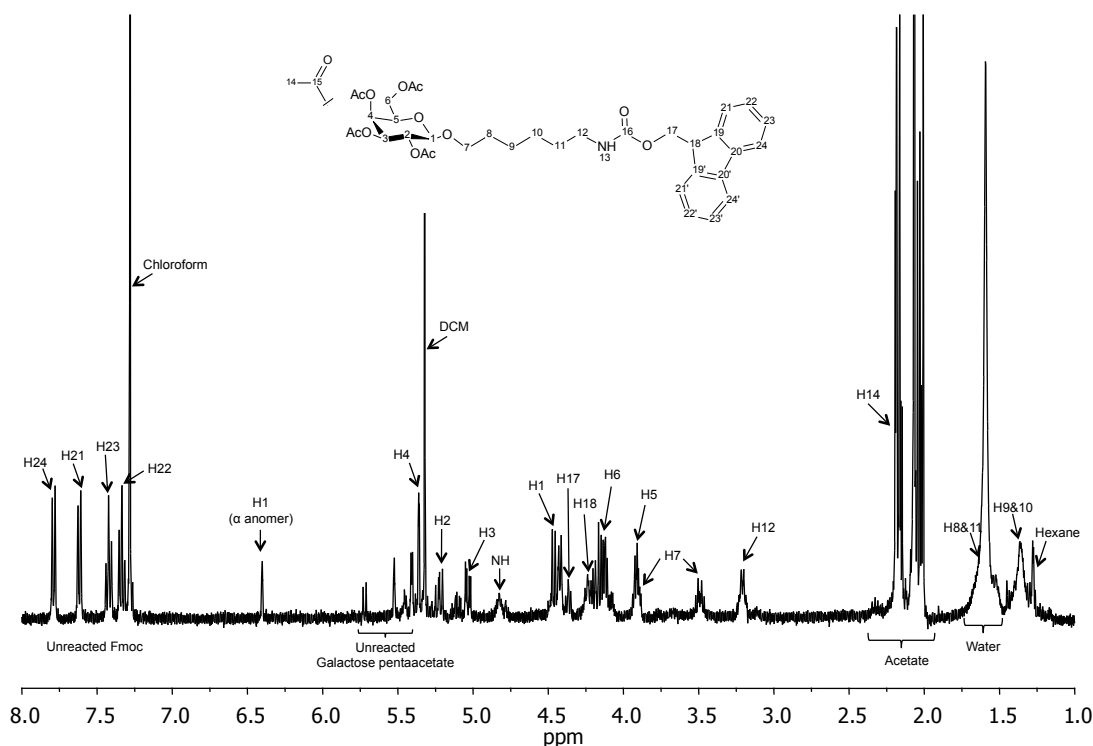


Figure 41 - Proton ^1H NMR spectrum on the uncontaminated product peak (1-O-(6'-Fmoc-aminohexyl)-2,3,4,6-tetra-O-acetyl- β -D-galactopyranoside) still showing unwanted products

As Figure 41 is very similar to Figure 35, the characterisation data will be similar too. Again there are unwanted products present in the desired product, in this case unreacted galactose pentaacetate as well as solvents (chloroform, DCM, water and hexane). It seems that the unwanted peak is hidden under the main peaks as is often be the case with anomers.

In order to retain as much of the product as possible, fractions 2-5 were pooled and run on the auto-column (chloroform:methanol 95:5v/v), (Biotage SP1TM Flash Purification System: flow rate 40 ml/min; SampletTM cartridge: FLASH 40+M; UV Wavelength Collection 252 nm).

It was expected from the TLC (Figure 40) that the auto-column (Figure 42) would show two peaks, the product and the impurity. However, Figure 42 shows only one peak, thus changing the solvent mix did not separate the two. Another TLC of the peak below was carried out using the same solvent mix, to confirm this (as shown in Figure 43).

Figure 43 shows that despite the fact that the product and impurity separate on the TLC plate, this does not occur on the auto-column (Figure 42). The impurity and product must be so similar that they cannot be separated by polarity; as would be the case if the unwanted peaks were from the α -anomer and/or talo-isomer.

The ^1H NMR (Figure 44) and correlation spectroscopy (COSY) (Figure 45) also show the impurity that has been persistent throughout the methodology.

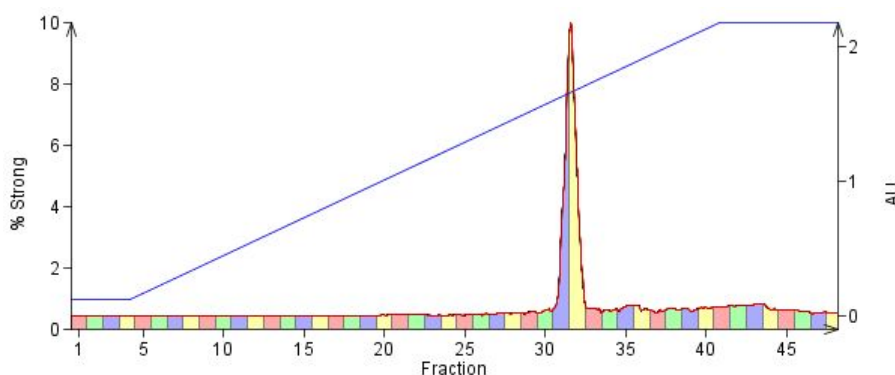


Figure 42 - Auto-column trace of the contaminated product peak 1-O-(6'-Fmoc-aminohexyl)-2,3,4,6-tetra-O-acetyl- β -D-galactopyranoside, showing only one peak despite the previous TLC showing impurities

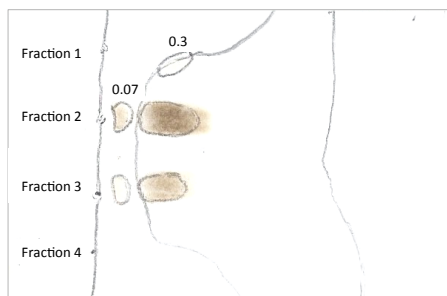


Figure 43 - TLC plate showing the four fractions of the peak in Figure 42, the contaminated 1-O-(6'-Fmoc-aminohexyl)-2,3,4,6-tetra-O-acetyl- β -D-galactopyranoside.

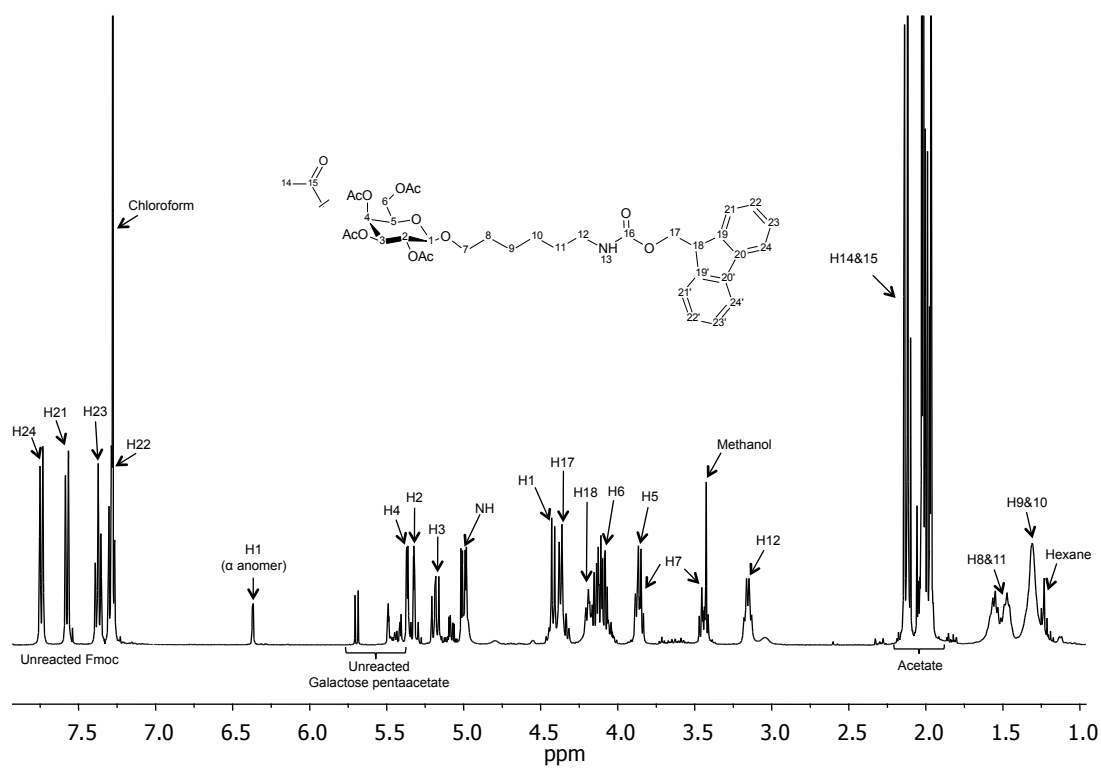
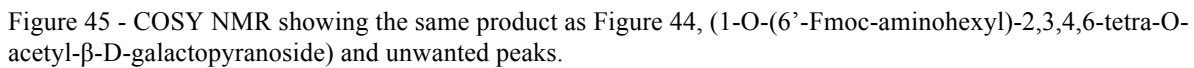


Figure 44 - Proton ^1H NMR spectrum of the product peak (1-O-(6'-Fmoc-aminoethyl)-2,3,4,6-tetra-O-acetyl- β -D-galactopyranoside) still showing unwanted peaks



All of the NMR results have consistently confirmed the product, 1-O-(6'-Fmoc-aminohexyl)-2,3,4,6-tetra-O-acetyl- β -D-galactopyranoside, was present as a yellow-brown oil, which also contained unreacted galactose pentaacetate and other unwanted products. The product is impure due to the presence of the unreacted galactose pentaacetate but also because it has not been possible to isolate the product in the desired stereochemistry i.e. solely β anomer without the α -anomer. To assess the success of the reaction, the percentage yield was calculated. The reaction produced 479.3mg of product or 0.7156mmol (molecular mass of product 669.7827). Maximum yield (assuming 100% efficiency) would be 1.48mmol, therefore the yield was 48%.

The small amount of product synthesised (0.473g), low reaction yield (48%) and expected loss of mass of almost 60% during deprotection steps as well as issues with the presence of the α sugar led to the decision to try other methods.

4.2.2 Carbohydrate functionalised polymers - method development 2

Method 2 is similar to Method 1 as an in-solution proof of concept, but starts at the other end of the molecule. Method 1 involved adding the carbohydrate to the linker then deprotecting it before adding the polymer. Method 2 involved starting with the polymer (Gantrez[®]) and adding the linker (6-amino-1-hexanol), then adding the galactose pentaacetate using BF₃O(Et)₂ and deprotecting the acetate groups.

For this in-solution reaction, a round bottomed flask was set up in an oil bath heated to 70 °C with a reflux condenser to retain the solvent. 1.6g Gantrez[®] was added to 50ml THF and stirred until dissolved. Next 0.702g aminohexanol (linker) was added with 0.84ml triethylamine (catalyst) and stirred for 2 hours to give a solid purple agglomerate in a white liquid. This reaction gave approximately 3.5g of product. 50ml dH₂O was added to break up the solid giving a gelatinous pink clear gel. 10g of this gel was dialysed in slightly acidic water (hydrochloric) to retain the polymer but release any triethylamine salts or aminohexanol. The water was changed at 1, 2, 4 and 24 hours. The polymer product was frozen using liquid nitrogen before freeze drying for 24 hours in a freeze-dryer (SciQuipAlpha2-4 LSC) to give a white/yellow powder. This reaction gave 0.08g of product. 5mg of the product was dissolved in dimethyl sulphoxide (DMSO) for NMR to ensure the product is Gantrez[®] with aminohexanol attached.

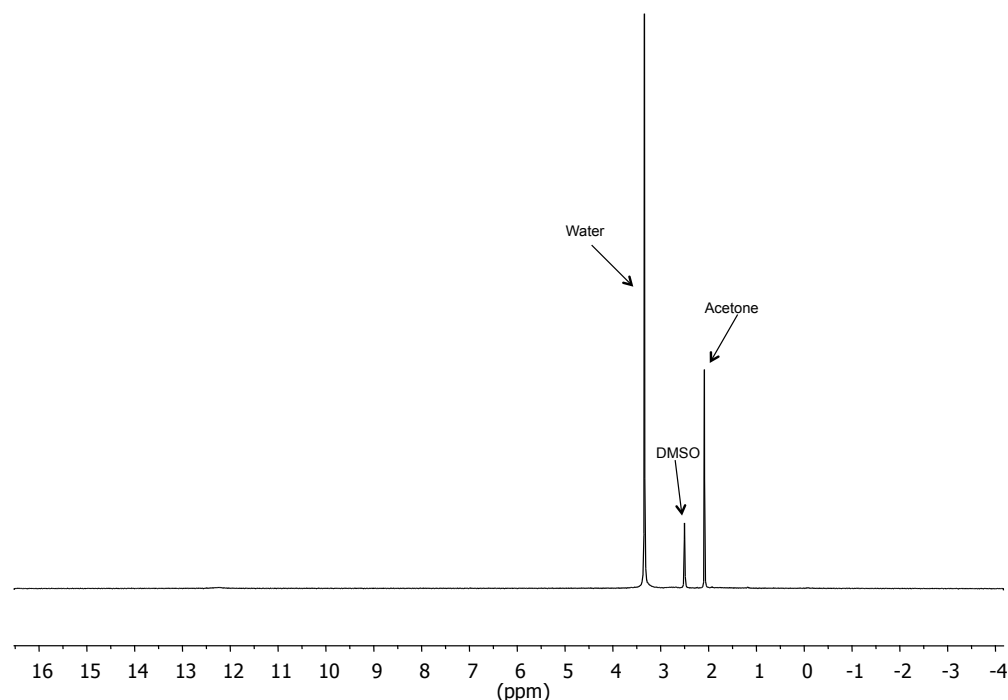


Figure 46 - Proton ^1H NMR spectrum of the Gantrez[®]-aminohexanol product. Only solvents are visible as the product was insoluble in dimethyl sulphoxide.

Figure 46 shows only solvents in the ^1H NMR and no product as it was not soluble in DMSO. As a consequence of the solubility issues in DMSO, the following solvents were tried: chloroform, methanol, chloroform and methanol (0.05:0.65), deuterated water, tetrahydrofuran, dichloromethane, isopropanol, ethylacetate, acetonitrile, acetone and toluene. All of the above solvents formed a suspension and by working back through the chemistry involved in the methods it was possible to trouble-shoot the causes leading to the insolubility. Initially, dissolving the Gantrez[®] was encouraged by heating the reactants in the oil bath, however as Figure 47 shows the polymer cross-links, forming an interchain network, which is insoluble.

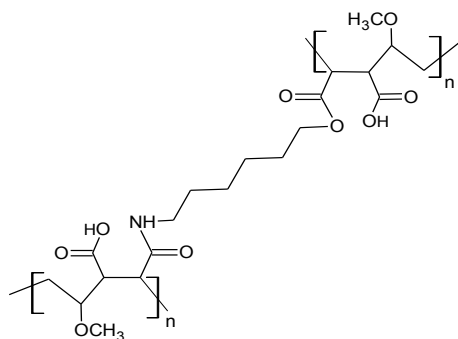


Figure 47 - The undesired insoluble interchain network formed by heating the Gantrez[®] and reactants

In addition, during the dialysis of the product, slightly acidic water is used, and as a consequence the polymer is ring opened so two carboxylic acids form rather than the oxygen closing the ring as shown in Figure 48.

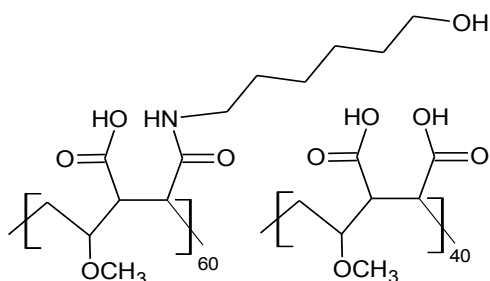


Figure 48 - The undesired ring-opened Gantrez[®] as a consequence of dialysis with water

Ordinarily, heating the undesired product in Figure 48 would remove the water and close the ring. However, in this case the hydroxyl on the linking chain binds to the oxygen (Figure 49) to form the same cross-linked interchain network in Figure 47.

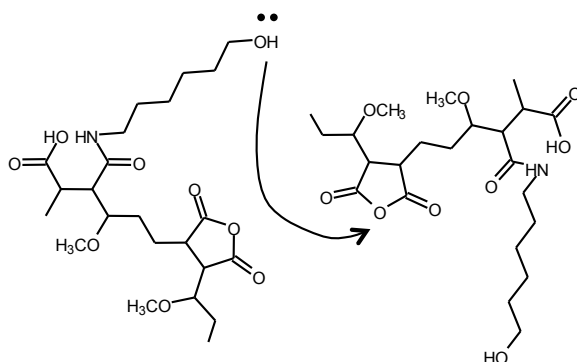


Figure 49 - Hydroxyl binds to the oxygen to again form the undesired interchain network

This method development section has shown that running experiments in solution is suitable for proof of reaction concept but not for surface use due to all of the problems faced during method development. This has been overcome in method 3 by directly binding layers onto the surface.

4.2.3 Carbohydrate functionalised polymers - method development 3

The final method involved the binding of reactants to a surface in layers to form the carbohydrate functionalised polymer. In brief, as shown in Figure 50 the reaction is begun with clean glass, adding an aminated layer, then adding Gantrez[®], followed by a linker, then adding the carbohydrate and finally deprotecting.

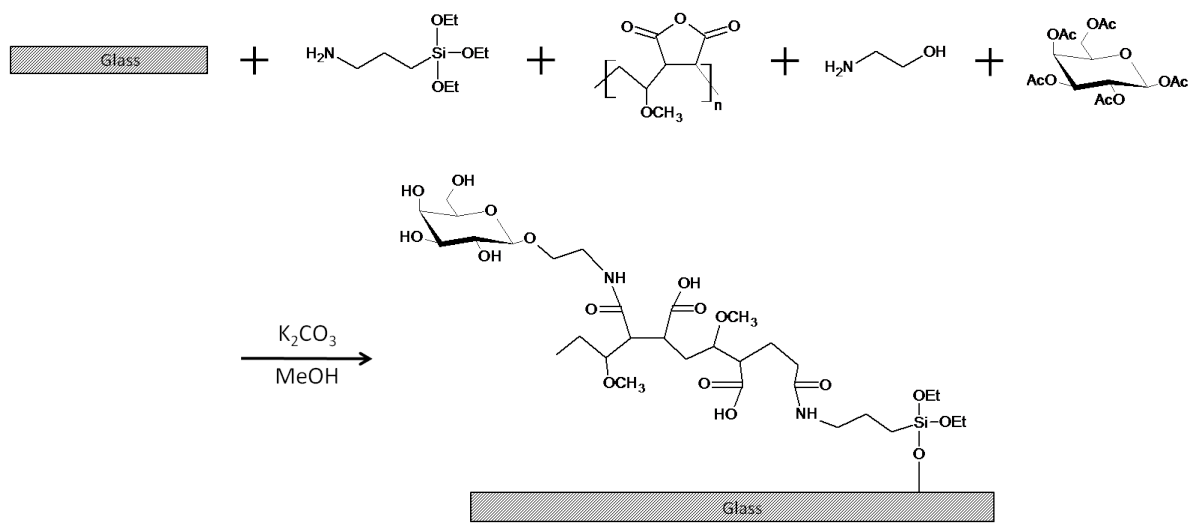


Figure 50 - Immobilisation of the reactant layers (glass, APTES, Gantrez[®], aminoethanol, galactose pentaacetate) and final product creating the carbohydrate functionalised polymers to mimic *Balanus amphitrite* SIPC

This method required the use of standard glass microscope slides for the bioassays. However, when used for confirmation of surface modification (ellipsometry and XPS) single side polished, 500m thick silicon wafers (Si-Mat Silicon Materials, Germany) were used, as the surface must be reflective and conductive.

For drop bioassays (see Chapter 4.2.7), 4 slides were required for each treatment. After each layer of surface modification, they were retained and stored for bioassaying. In addition, 8 slides were required to be acid cleaned due to the high hydrophilicity of the surface. Initially, the first step of the surface modification was thorough cleaning of the glass slides using ‘Piranha’ solution (sulphuric acid and hydrogen peroxide). The strongly acidic and oxidising nature of this solution makes it an effective cleaner, although, it was essential to remove all organic materials and solvents from the fume hood to avoid the risk of fire. Coplin jars were washed with dH₂O followed by tetrahydrofuran (THF), then the glass microscope slides were added to each jar. The slides were washed with hexane then methanol for 5 minutes each. In a clean beaker, 250ml methanol was added to 250ml 36% hydrochloric acid (1:1 mix) and the jars filled with this mixture. After 2 hours the slides were washed three times with dH₂O then once with methanol. Using a Dewar bowl ice bath, 375ml sulphuric acid was cooled in a clean beaker for 30 minutes before slowly

adding 125ml 30% hydrogen peroxide. This Piranha Solution was added to the Coplin jars containing the slides and left overnight.

The slides were thoroughly washed ten times with dH₂O as any residual acid on the surface can prevent bonding of further layers. The next step was amino silation of the clean surface as outlined in Kitano et al. (2006). The slides were washed first with methanol then twice with toluene. In a clean beaker, 1ml (3-aminopropyl)triethoxysilane (APTES) was thoroughly mixed with 400ml toluene, before covering the slides and leaving for 6 hours. Next, the slides were washed four times with toluene and once with THF. To ensure that more terminal amines are exposed on the surface, the aminosilated slides were heated in a vacuum oven at 120 °C overnight. At the same time 3g Gantrez[®] was heated in the same oven, to guarantee the Gantrez[®] had not hydrolysed while in contact with air. In a clean beaker, 400ml THF was added to the 4g baked Gantrez[®] and added to the Coplin jars before leaving for 10 minutes. The slides were washed three times with THF and allowed to dry. In a clean beaker, 2ml ethanolamine was added to 400ml THF and the mixture added to the slides and left for 30 minutes, before washing twice with THF, three times with dry methanol and twice with dry DCM. The use of dry solvents is essential due to the sensitivity of the boron trifluoride diethyl etherate to water. Using a Dewar bowl ice bath, a clean dry two neck flask was cooled before adding 0.65g of one of the carbohydrates (either galactose, mannose or glucose pentaacetate) and 100ml dry DCM. Using Suba-Seal rubber septa, the flask was flushed with nitrogen before adding 1.25ml boron trifluoride diethyl etherate (reaction promoter) through the side seal. This mixture was added to one third of the remaining slides before repeating the step with the other carbohydrates. The Coplin jars containing the slides and carbohydrate mixtures were flushed with nitrogen, sealed with parafilm and left to incubate for 24 hours. Following this the slides were washed twice with DCM. Due to the reactivity of boron trifluoride diethyl etherate to water, excess carbohydrate mixture was disposed of with drops of first isopropanol, then methanol and finally water. The surface modification of the slides was then complete but the carbohydrate hydroxyl groups remained protected by the four acetates. The final step of the method was to deprotect the carbohydrate. In a round-bottomed flask, 3g potassium carbonate was dissolved in 300ml methanol when stirred vigorously for 30 minutes. The slides were covered with this mixture and left for 1 hour before washing twice with methanol.

In order to confirm the chemical modification of the surface, additional slides and silicon wafers were prepared for contact angle measurements, ellipsometry and XPS.

4.2.4 Contact Angle

Contact angle is a semi-empirical measurement used to show the progression of the surface modifications as, depending on how hydrophobic or hydrophilic a surface is, the shape of a droplet of water on the surface changes. This allows discrimination between polar and non-polar surfaces and some characteristics of the surface to be estimated (Murray and Darvell, 1990). As water was used to measure the contact angle it was possible to deduce if the surface was hydrophobic (large angle) or hydrophilic (small angle). The sessile drop method used consists of the direct measurement of the angle at the point of contact of a pure liquid (dH₂O) on a solid substratum (glass). This was measured by a contact angle goniometer using an optical subsystem at 4 volts with 10µl of dH₂O, in triplicate.

4.2.5 Ellipsometry

Ellipsometry measures film thickness, and was most useful to compare aminated surface to Gantrez[®] surface as this is the biggest increase in thickness. This analysis requires silicon wafers as they are reflective. Measurements were carried out using a SE500 Sentech GmbH with laser wavelength set to 632.8 nm and spot size of 80µm was used. Alignment was carried out using one of the blank piranha clean wafers to get correct stage height and tilt. Ellipsometry required the use of the following assumptions for equipment setup: the thickness of the silicon oxide is 3.827nm, the refractive index of the layers is 1.5 and the dielectric constant of the film is 1.2.

4.2.6 XPS

X-ray photoelectron spectroscopy (XPS), also referred to as Electron Spectroscopy for Chemical Analysis (ESCA), is a technique that probes the top ten to twenty atomic layers and measures the elemental composition in the top 10nm of a surface. Spectra were acquired by irradiating surface modified samples of silicon wafer with a beam of X-rays then measuring the number and energy of electrons emitted from the samples. These emitted photoelectrons create a series of peaks, each of which are characteristic of different elemental bonds. This analysis was used to provide further evidence to the contact angle and ellipsometry data (See Chapter 4.3.3) to confirm the chemical surface modification

carried out (See Chapter 4.2.3). This modification is shown in Figure 51, where each step of the modification is indicated by a coloured circle. Six sample surfaces were analysed: aminated, Gantrez[®], aminoethanol, mannose, galactose and glucose. Consequently, as well as a wide (survey) scan on each surface, high resolution scans on the elements silicon, carbon, oxygen and nitrogen were carried out on each treatment surface. Similarly to ellipsometry, these samples were on silicon wafer in this case, as the surface was required to be conductive.

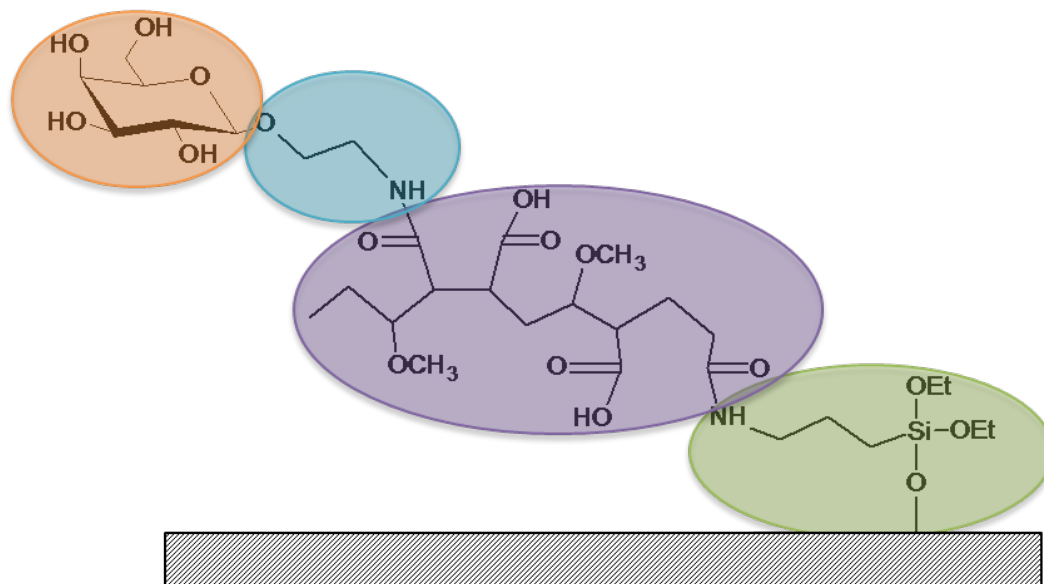


Figure 51 - Structure of the carbohydrate functionalised polymer surface modification to mimic *Balanus amphitrite* SIPC, showing the progress from silicon wafer (striped box), aminated (green), polymer (purple), linker (blue) and carbohydrate (orange). This figure shows galactose as the terminal carbohydrate.

Using Figure 51, a summary of predicted bonds can be formed. The four elements analysed by XPS were carbon, nitrogen, oxygen and silicon and the bonds involving these elements are summarised in Table 3. Hydrogen is not detected by XPS, thus any hydrogen bonds will not show up on the trace as a peak and these bonds can be disregarded.

Table 3 - Predicted bonds at each stage of the carbohydrate functionalised polymer surface modification to mimic *Balanus amphitrite* SIPC, as indicated by Figure 51 showing aminated (green), polymer (purple), linker (blue) and carbohydrate (orange) terminated surfaces.

Element	Aminated	Gantrez [®]	Aminoethanol	Carbohydrates
Carbon	C-C C-O C-Si C-N	C=O C-C C-O C-Si C-N	C=O C-C C-O C-Si C-N	C=O C-C C-O C-Si C-N
Nitrogen	N-C	N-C	N-C	N-C
Oxygen	O-C O-Si	O=C O-C O-Si	O=C O-C O-Si	O=C O-C O-Si
Silicon	Si-O Si-C Si-Si	Si-O Si-C Si-Si	Si-O Si-C Si-Si	Si-O Si-C Si-Si

Samples were kept under vacuum at approx. 10^{-10} Torr for the period between submission and analysis to reduce degradation of surface chemistry. The system used was a Kratos AXIS Ultra 165, X-ray setup was 10mA current and 15kV anode voltage. The X-ray source consisted of an Al $k\alpha$ mono-chromated source of photon energy of 1486.6 eV with an energy resolution of 0.3 eV. Pressure inside the chamber was of the order 10^{-9} Torr whilst the X-rays were active. The surface area sampled was 700 μm x 300 μm . All XPS scans were done at room temperature with 0.1 eV step size and 60s sweep time. There was no additional in situ processing and no forced oxidation method was employed.

The silicon wafer used as a substratum is a semi-conductor, although the chemical surface modification causes the surface to become non-conductive. The consequence of this was that during analysis, positive charge built up on the surface as the X-rays liberate electrons. This charge build up caused the peaks to shift an unknown amount, so methods were employed to dissipate this charge build-up and reduce shifting; these are illustrated in Figure 52. Briefly, double-sided carbon tape (low silicone) was used to hold the sample to the platform and was wrapped around one edge to contact the modified surface to provide a conductive path. A charge neutraliser (electron gun) underneath the platform supplied a flux of low energy electrons to again compensate for any charging of the sample. Gold foil was placed in a position of good electrical contact with the silicon surface for each sample providing a conductive path from the surface to the platform to again help dissipate charge. In addition, this foil is used to provide an indicator of the shift as it is conductive and non-reactive and is expected to peak at 84 eV. A gold (Au 4f) spectrum was taken for 1 sweep.

This was used to calibrate the energy scale and determine any energy shifts associated with charging effects as the samples are non-conductive (Seah et al., 1998). Peaks were normalised to aliphatic carbon (C1s) at 285eV.

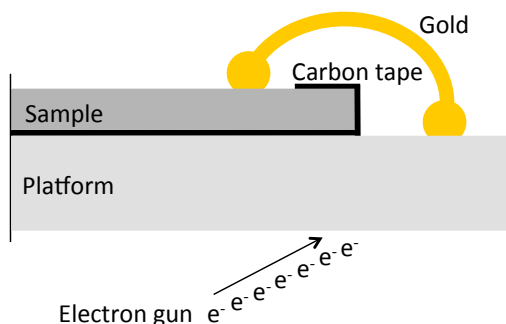


Figure 52 - Sample set up inside XPS chamber to reduce charging using an electron gun and gold

All data were divided by the number of sweeps for that element to normalise data for graphical comparison. The XPS photoemission spectra were fitted with the predicted bonds to give chemical information. This was completed using the programme WINSPEC (developed at the University of Namur, Belgium) which runs iterations to achieve the best fit using the predicated peaks positioned by the user. For the majority of peaks, a Gaussian profile of mixed singlets was used, which takes into account the instrumental energy resolution as well as broadening due to chemical disorder (Yeganeh et al., 2007). Metallic materials (in this case only the gold sample) were fitted with a Doniach-Sunjic profile (Doniach and Sunjic, 1970). All backgrounds were subtracted using the Shirley background method (Shirley, 1972).

Unless the chemical modifications are completed within the chamber and sequential scans taken to compare the data *in situ*, a direct comparison between spectra cannot be made, as there is too much variation in homology and conductivity between the surfaces. Due to the nature of the chemistry involved in this experiment it is impossible to carry out modifications within the chamber. However, the shape of spectra, position and apparent ratio of peaks will change predictably with the surface modification so graphs can be visually compared.

Following fitting peaks to the spectrum, the peaks were assigned and confirmed using the NIST X-ray Photoelectron Spectroscopy Database, Version 3.5 (National Institute of Standards and Technology, Gaithersburg, 2003); <http://srdata.nist.gov/xps/>.

4.2.7 Drop Assay

Microscope slides were modified to give the following surfaces: clean glass, aminated, Gantrez[®], aminoethanol, galactose, mannose and glucose (See Chapter 4.2.3). Standard drop assay methodology was employed, based on protocol by Pechenik et al. (1993). Four slides of each surface treatment were used with two 250µl drops of 0.2µm filtered natural seawater on each. Ten 0-day-old *B. amphitrite* cyprids were added to each droplet. 0-day-old cyprids were used as low settlement is expected (5-10%) and stimulatory effects are more noticeable. The assay was incubated under damp conditions (to avoid evaporation of the droplets) in the dark at 28°C in labelled quadriPERM cell culture dishes. Standards to ensure cyprids were healthy, settling batches were also carried out in polystyrene 24-well plates (Iwaki, Japan) using 10 cyprids in 2ml of seawater. Settlement (including both settled and metamorphosed cyprids) was recorded after 24 and 48 hours.

4.3 Results

4.3.1 Carbohydrate functionalised polymers

The lack of success with the first two methods led to the change of approach with the final method. This appeared successful and this was confirmed by assessing the surfaces with contact angle, ellipsometry and XPS.

4.3.2 Contact Angle

Figure 53 shows the change in contact angle ($^{\circ}\pm\text{SE}$) with the changing surface properties. The piranha clean glass had a very low contact angle, in this case $4.7^{\circ}\pm 0.7$. The aminated surface had a much increased contact angle of $72.7^{\circ}\pm 0.3$. The contact angle of the Gantrez[®] surface was $37.3^{\circ}\pm 0.9$. The aminoethanol surface had an observed contact angle of $48.0^{\circ}\pm 1$. The carbohydrate surfaces, galactose, mannose and glucose had contact angles of $31.7^{\circ}\pm 0.7$, $29.3^{\circ}\pm 3.5$ and $25.7^{\circ}\pm 0.7$ respectively.

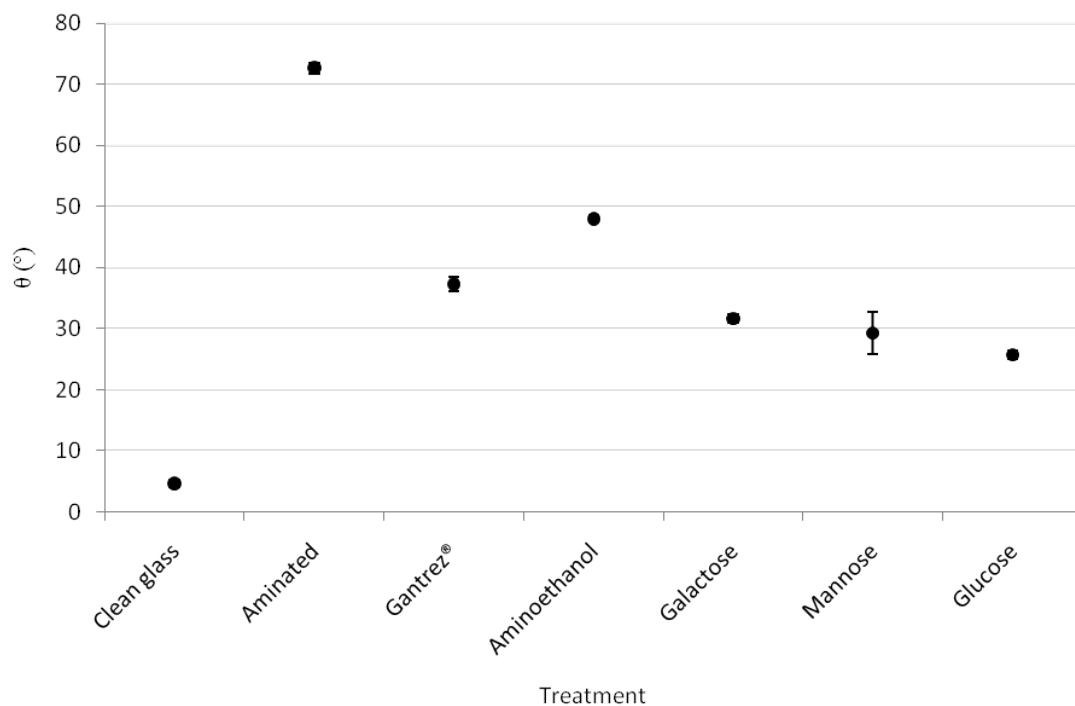


Figure 53 - Contact angle results, mean angle or θ (°) \pm SE) for each of the carbohydrate functionalised polymer surface modifications to mimic *Balanus amphitrite* SIPC. Error bars are \pm standard error

4.3.3 Ellipsometry

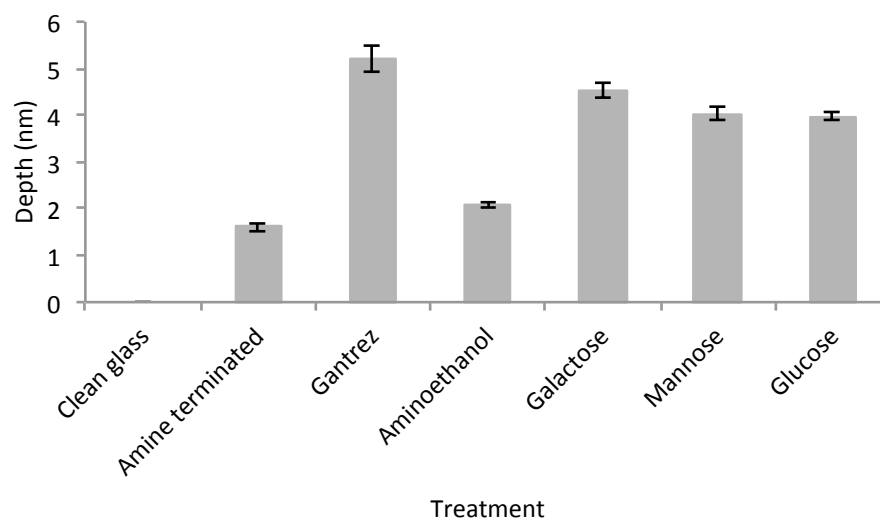


Figure 54 - Ellipsometry results for each of the carbohydrate functionalised polymer surface modifications to mimic *Balanus amphitrite* SIPC indicating the change in depth of surface layers. Error bars are \pm standard error.

Figure 54 shows the changing depth of the surface layers as determined by ellipsometry. As the piranha cleaned glass has no surface chemistry, this surface was used to calibrate the equipment. The aminated surface had a thickness of $1.6\text{nm}\pm0.1$ and the Gantrez[®] a thickness of $5.2\text{nm}\pm0.3$, the largest change in thickness. The aminoethanol surface had a thickness of $2.1\text{nm}\pm0.1$. As with the contact angle, each of the carbohydrate surfaces should be similar; galactose, mannose and glucose were $4.5\text{nm}\pm0.2$, $4.0\text{nm}\pm0.2$ and $4.0\text{nm}\pm0.1$ in thickness respectively.

4.3.4 XPS

The wide scan survey spectra, Figure 55, shows the full elemental spectrum for each of the modified surfaces. These spectra are useful for assessing all of the elements found on the surfaces, particularly for identifying any errant compounds.

The graphical results for XPS (Figure 56 to Figure 59) are based around individual elements with graphs for each element and each surface.

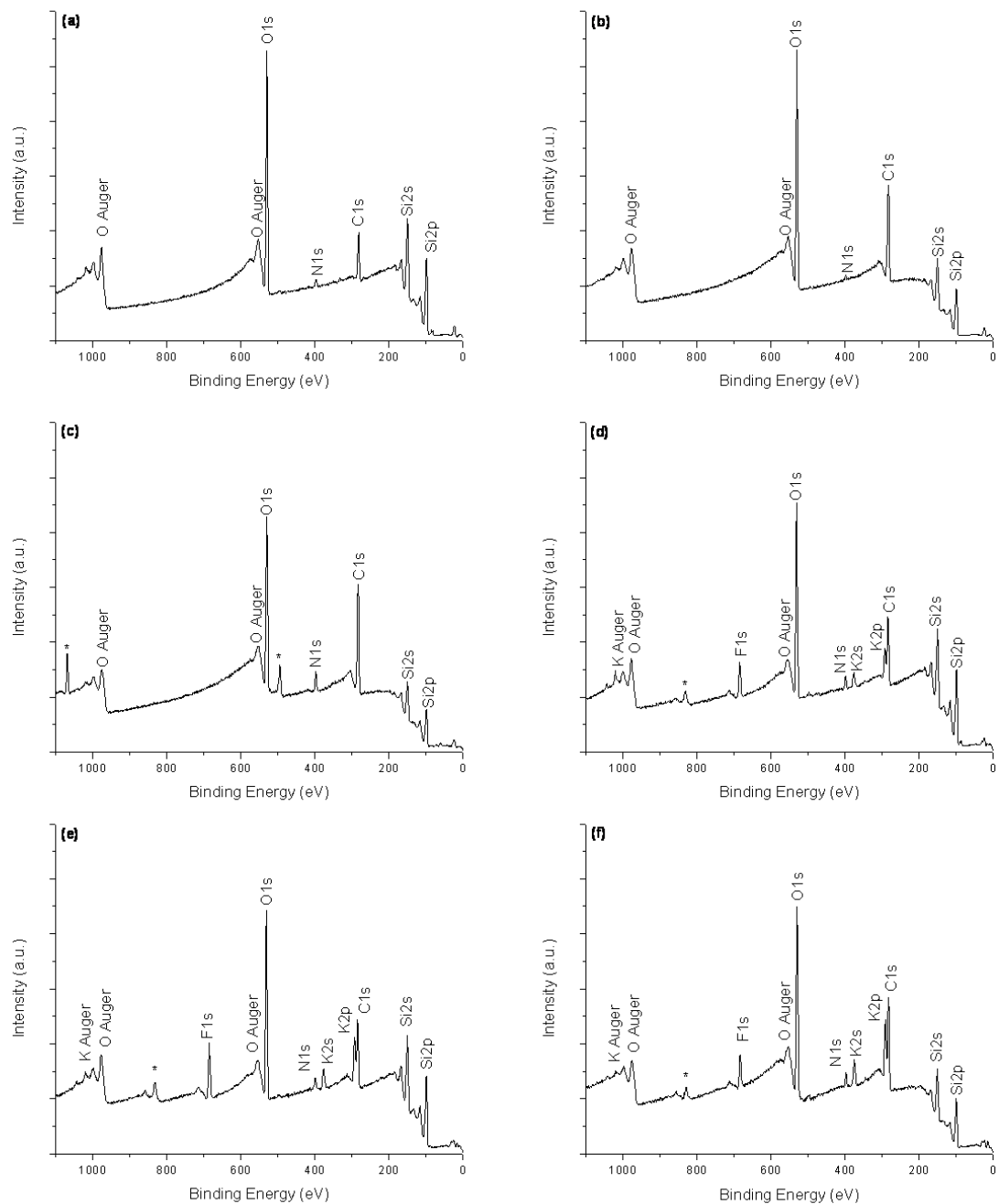


Figure 55 - Wide scan survey spectra for all elements for all samples of the carbohydrate functionalised polymer surface modification to mimic *Balanus amphitrite* SIPC; (a) aminated, (b) Gantrez[®], (c) aminoethanol, (d) glucose, (e) mannose and (f) galactose. * indicates an unidentifiable peak not found in the elemental database.

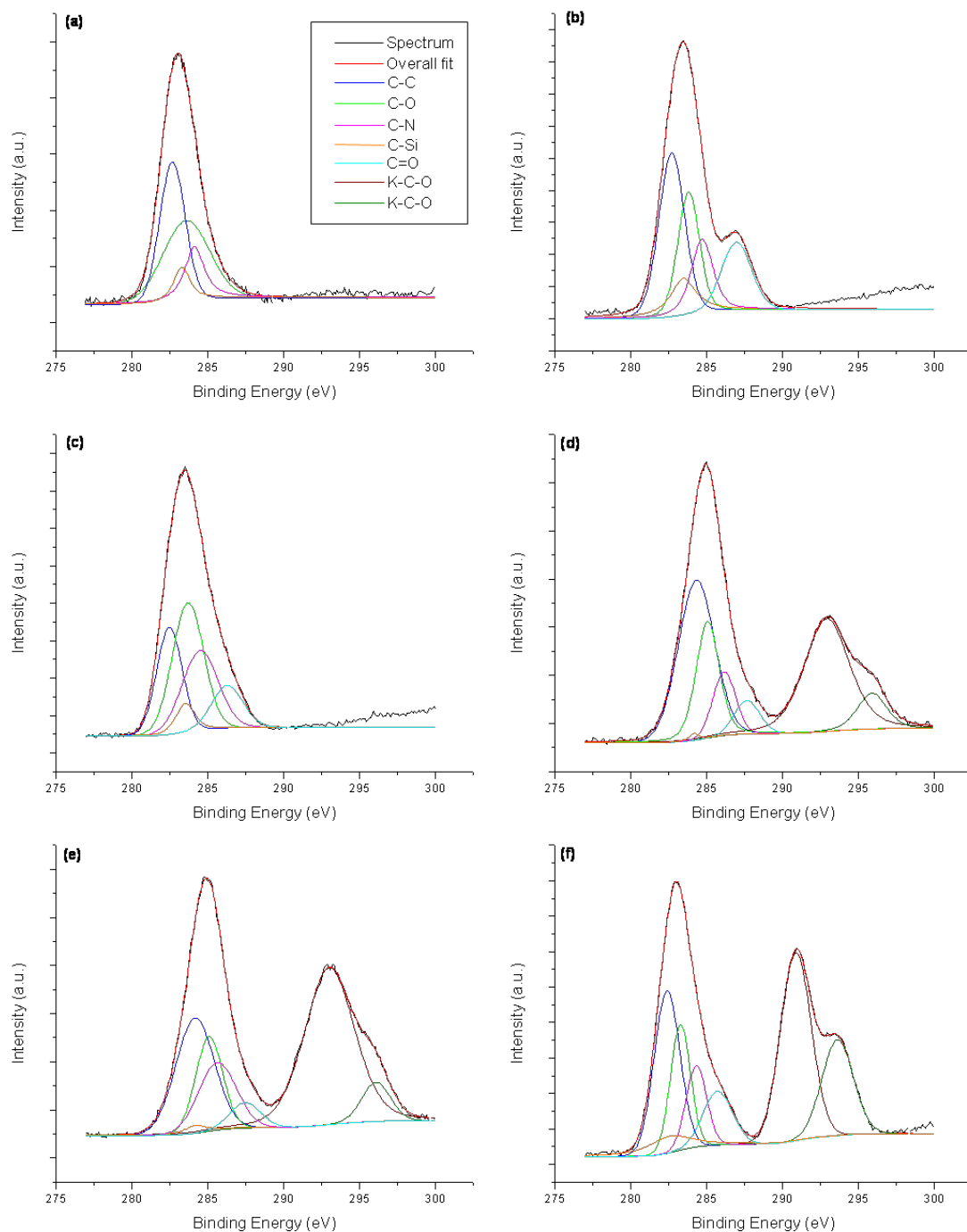


Figure 56 - High resolution spectra for carbon(1s) for all samples of the carbohydrate functionalised polymer surface modification to mimic *Balanus amphitrite* SIPC; (a) aminated, (b) Gantrez[®], (c) aminoethanol, (d) glucose, (e) mannose and (f) galactose.

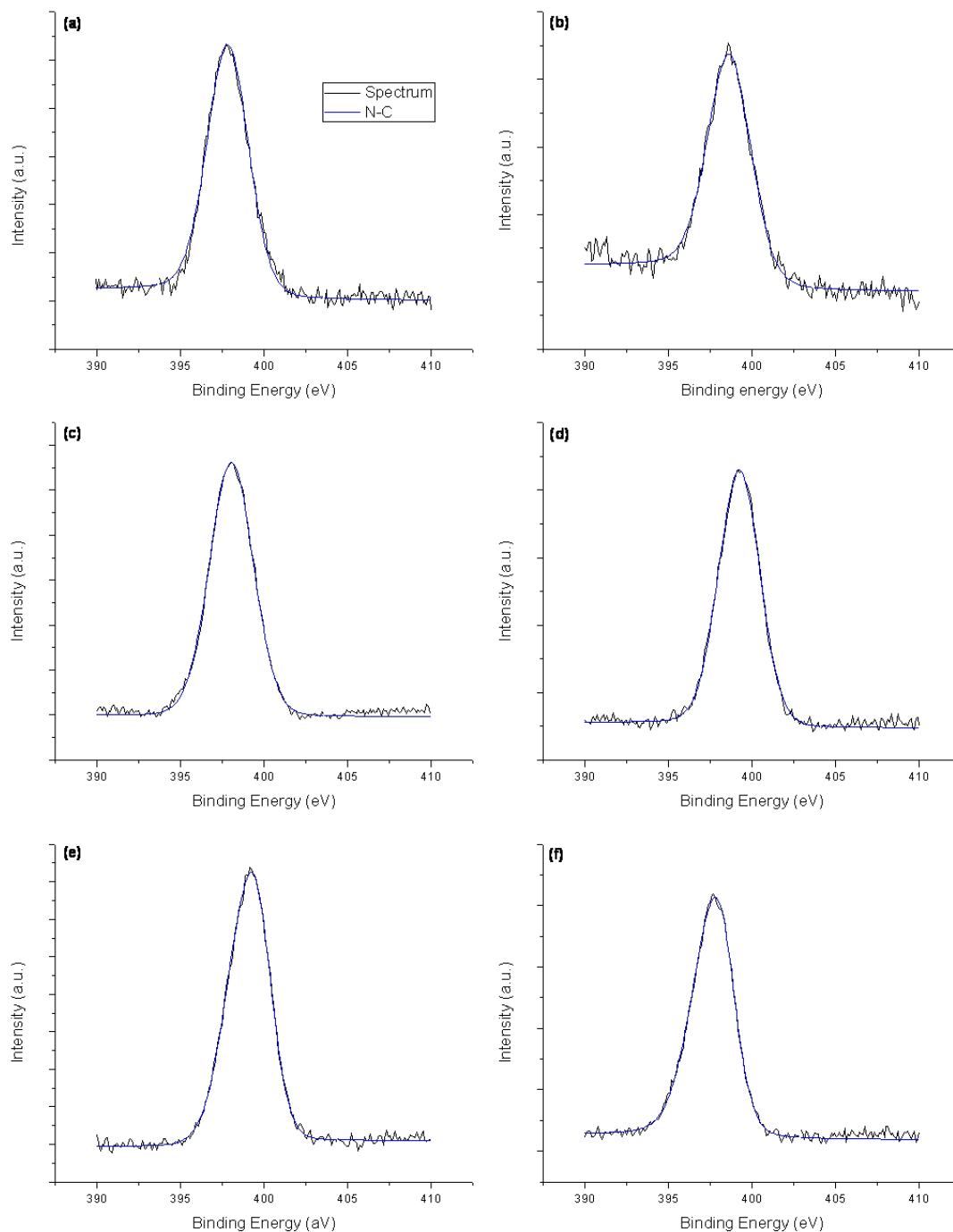


Figure 57 - High resolution spectra for nitrogen(1s) for all samples of the carbohydrate functionalised polymer surface modification to mimic *Balanus amphitrite* SIPC; (a) aminated, (b) Gantrez[®], (c) aminoethanol, (d) glucose, (e) mannose and (f) galactose.

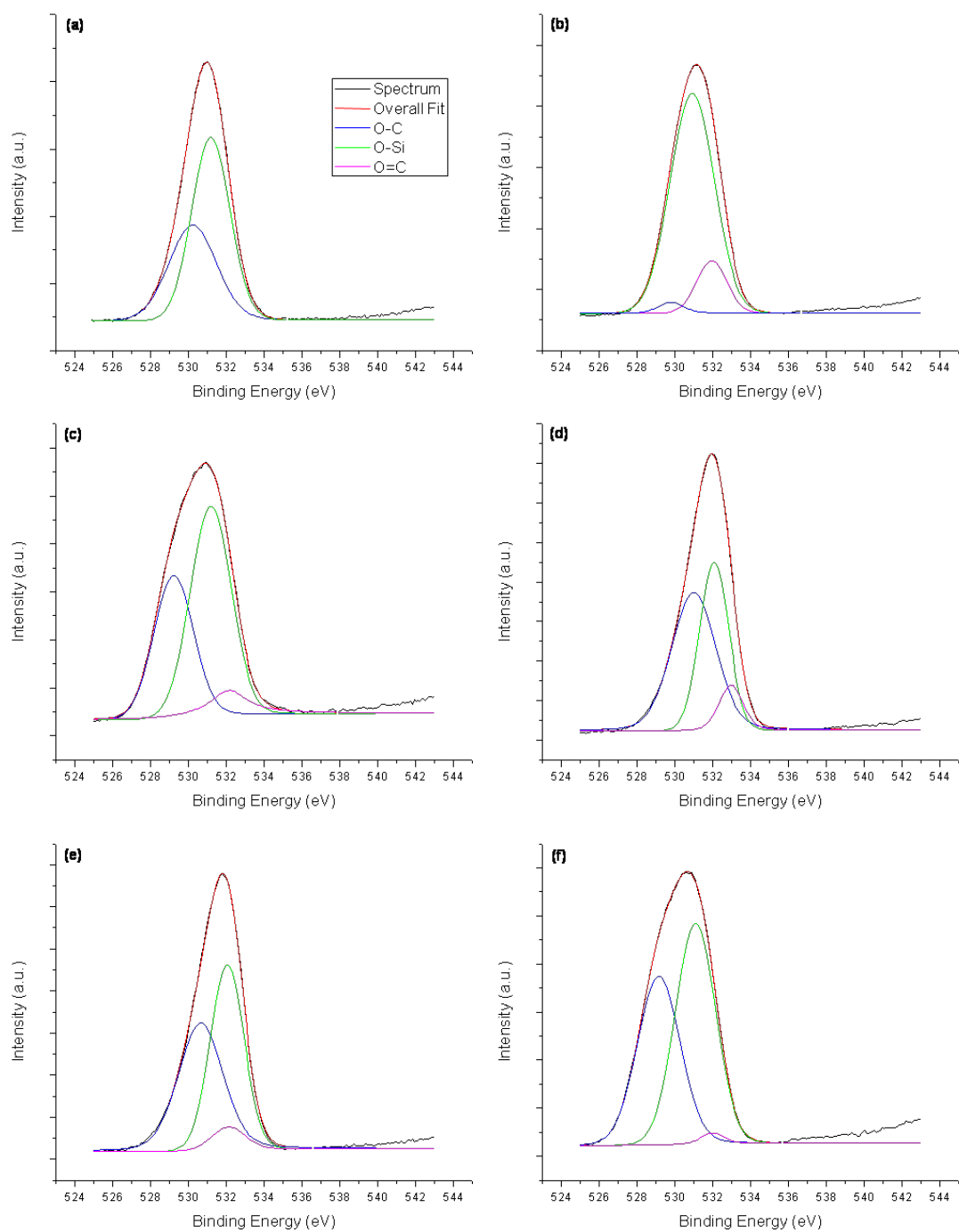


Figure 58 - High resolution spectra for oxygen(1s) for all samples of the carbohydrate functionalised polymer surface modification to mimic *Balanus amphitrite* SIPC; (a) aminated, (b) Gantrez®, (c) aminoethanol, (d) glucose, (e) mannose and (f) galactose.

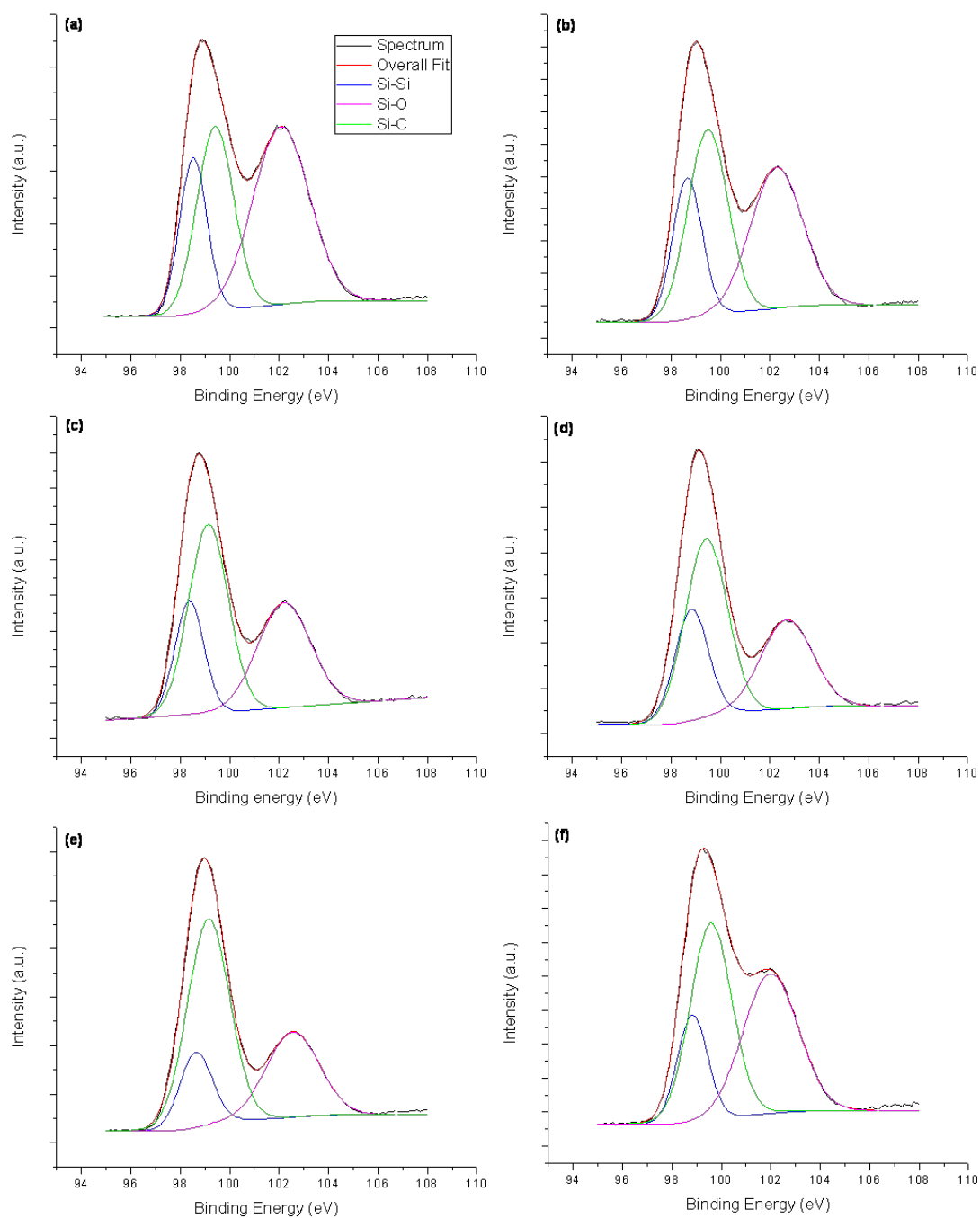


Figure 59 - High resolution spectra for silicon(2p) for all samples of the carbohydrate functionalised polymer surface modification to mimic *Balanus amphitrite* SIPC; (a) aminated, (b) Gantrez[®], (c) aminoethanol, (d) glucose, (e) mannose and (f) galactose.

The tabular results for XPS (Table 4 to Table 9) relate to each surface and the elements within that surface. The tables are formed in conjunction with Figure 56 to Figure 59, and they also provide more detail as to the binding energy of each peak and evidence from peer reviewed sources that the bond has been confirmed at that binding energy in previous literature.

Table 4 - High-resolution spectrum component positions for carbon (1s), nitrogen (1s), oxygen (1s) and silicon (2p) signals on the aminated surface of the functionalised polymer surface modification to mimic *Balanus amphitrite* SIPC

Binding energy	Width	Predicted bond	Shift	Adjusted binding energy	Predicted bond binding energy	Evidence
282.647	1.97094	C-C	1.9	284.6	284.6	Palchan I., Crespin M., Estrade-Szwarckopf H., Rousseau B. Chem. Phys. Lett. 157, 321 (1989)
283.258	1.2948	C-Si	1.9	285.158	285.0	DiCastro V., Polzonetti G., Contini G., Cozza C., Paponetti B. Surf. Interface Anal. 16, 571 (1990)
283.545	3.62264	C-O	1.9	285.445	285.4	Kishi K., Ehara Y. Surf. Sci. 176, 567 (1986)
284.107	1.5308	C-N	1.9	286.007	286.0	Yoon S.C., Ratner B.D. Macromolecules 19, 1068 (1986)
397.82	2.93833	N-C	1.9	399.72	399.7	Zanoni R., Boschi T., Licoccia S., Paolesse R., Tagliatesta P. Inorg. Chim. Acta 145, 175 (1988)
530.227	2.94669	O-C	1.9	532.127	531.9	Burger K., Buvári A. Inorg. Chim. Acta 11, 25 (1974)
531.185	2.37681	O-Si	1.9	533.085	532.84	Wagner C.D., Passoja D.E., Hillery H.F., Kinisky T.G., Six H.A., Jansen W.T., Taylor J.A. J. Vac. Sci. Technol. 21, 933 (1982)
98.5227	1.30611	Si-Si	1.9	100.4227	99.61	Ingo G.M., Zacchetti N., della Sala D., Coluzza C. J. Vac. Sci. Technol. A 7, 3048 (1989)
99.4134	1.75456	Si-O	1.9	101.3134	101.1	Aarnik W.A.M., Weishaupt A., van Silfout A. Appl. Surf. Sci. 45, 37 (1990)
102.078	2.68715	Si-C	1.9	103.978	103.8	Morra M., Occhiello E., Marola R., Garbassi F., Humphrey P., and Johnson D. J. Colloid Interface Sci. 137, 11 (1990)

Table 5 - High-resolution spectrum component positions for carbon (1s), nitrogen (1s), oxygen (1s) and silicon (2p) signals on Gantrez[®] surface of the functionalised polymer surface modification to mimic *Balanus amphitrite* SIPC

Binding energy	Width	Predicted bond	Shift	Adjusted binding energy	Predicted bond binding energy	Evidence
282.679	1.99265	C-C	1.9	284.579	284.6	Palchan I., Crespin M., Estrade-Szwarckopf H., Rousseau B. Chem. Phys. Lett. 157, 321 (1989)
283.432	2.00368	C-Si	1.9	285.332	285.3	Asakawa T., Tanaka K., Toyoshima I. Langmuir 4, 521 (1988)
283.787	1.67063	C-O	1.9	285.687	285.7	Grunze M., Lamb R.N. Chem. Phys. Lett. 133, 283 (1987)
284.686	1.71146	C-N	1.9	286.586	286.6	Lalitha S., Manoharan P.T. J. Electron Spectrosc. Relat. Phemon. 49, 61 (1989)
286.946	2.33673	C=O	1.9	288.846	288.8	Gelius U., Heden P.F., Hedman J., Lindberg B.J., Manne R., Nordberg R., Nordling C., Siegbahn K. Phys. Scripta 2, 70 (1970)
398.643	3.0745	N-C	1.9	400.543	400.5	Peeling J., Hruska F., McKinnon D.M., Chauhan M.S., McIntyre N.S. Can. J. Chem. 56, 2407 (1978)
529.768	1.55601	O-C	1.9	531.668	531.60	Hammond J.S., Holubka J.W., Devries J.E., Duckie R.A. Corros. Sci. 21, 239 (1981)
530.889	2.73879	O-Si	1.9	532.789	532.7	Clarke T.A., Rizkalla E.N. Chem. Phys. Lett. 37, 523 (1976)
531.921	1.87289	O=C	1.9	533.821	533.84	Beamson G., Briggs D. High Resolution XPS of Organic Polymers: the Scienta ESCA300 Database (1992)
98.6631	1.39683	Si-Si	1.9	100.5631	99.61	Ingo G.M., Zacchetti N., della Sala D., Coluzza C. J. Vac. Sci. Technol. A 7, 3048 (1989)
99.4873	1.90175	Si-O	1.9	101.3873	101.7	Finster J., Klinkenberg E.-D., Heeg J. Vacuum 41, 1586 (1990)
102.275	2.47899	Si-C	1.9	104.175	103.8	Morra M., Occhiello E., Marola R., Garbassi F., Humphrey P., and Johnson D. J. Colloid Interface Sci. 137, 11 (1990)

Table 6 - High-resolution spectrum component positions for carbon (1s), nitrogen (1s), oxygen (1s) and silicon (2p) signals on aminoethanol surface of the functionalised polymer surface modification to mimic *Balanus amphitrite* SIPC

Binding energy	Width	Predicted bond	Shift	Adjusted binding energy	Predicted bond binding energy	Evidence
282.447	1.96689	C-C	2.2	284.647	284.6	Palchan I., Crespin M., Estrade-Szwarckopf H., Rousseau B. Chem. Phys. Lett. 157, 321 (1989)
283.496	1.47656	C-Si	2.2	285.696	285.3	Asakawa T., Tanaka K., Toyoshima I. Langmuir 4, 521 (1988)
283.673	2.42839	C-O	2.2	285.879	285.8	Jordan J.L., Kovac C.A., Morar J.F., Pollak R.A. Phys. Rev. B 36, 1369 (1987)
284.474	2.7895	C-N	2.2	286.674	286.6	Lalitha S., Manoharan P.T. J. Electron Spectrosc. Relat. Phemon. 49, 61 (1989)
286.263	2.40591	C=O	2.2	288.463	288.4	Salyn Y.V., Nefedov V.I., Makarova A.G., Kuznetsova G.N. Zh. Neorg. Khimii 23, 829 (1978)
398.033	3.09553	N-C	2.2	400.233	400.22	Beamson G., Briggs D. High Resolution XPS of Organic Polymers: the Scienta ESCA300 Database (1992)
529.201	2.45123	O-C	2.2	531.401	531.4	Lindberg B., Berndtsson A., Nilsson R., Nyholm R., Exner O. Acta Chem. Scand. A 32, 353 (1978)
531.152	2.53775	O-Si	2.2	533.352	533.4	Taylor J.A., Lancaster G.M., Ignatiev A., Rabalais J.W. J. Chem. Phys. 68, 1776 (1978)
532.089	2.30807	O=C	2.2	534.289	534.3	Clark D.T., Thomas H.R. J. Polym. Sci. Polym. Chem. Ed. 14, 1701 (1976)
98.3712	1.38293	Si-Si	2.2	100.5712	99.61	Ingo G.M., Zacchetti N., della Sala D., Coluzza C. J. Vac. Sci. Technol. A 7, 3048 (1989)
99.1402	1.89049	Si-O	2.2	101.3402	101.7	Finster J., Klinkenberg E.-D., Heeg J. Vacuum 41, 1586 (1990)
102.202	2.53621	Si-C	2.2	104.402	103.8	Morra M., Occhiello E., Marola R., Garbassi F., Humphrey P., and Johnson D. J. Colloid Interface Sci. 137, 11 (1990)

Table 7 - High-resolution spectrum component positions for carbon (1s), nitrogen (1s), oxygen (1s) and silicon (2p) signals on glucose surface of the carbohydrate functionalised polymer surface modification to mimic *Balanus amphitrite* SIPC

Binding energy	Width	Predicted bond	Shift	Adjusted binding energy	Predicted bond binding energy	Evidence
284.302	2.81072	C-C	0.3	284.6	284.6	Palchan I., Crespin M., Estrade-Szwarckopf H., Rousseau B. Chem. Phys. Lett. 157, 321 (1989)
284.136	0.642915	C-Si	0.3	284.436	284.39	Beamson G., Briggs D. High Resolution XPS of Organic Polymers: the Scienta ESCA300 Database (1992)
285.04	1.7913	C-O	0.3	285.34	285.33	Beamson G., Briggs D. High Resolution XPS of Organic Polymers: the Scienta ESCA300 Database (1992)
286.139	1.76352	C-N	0.3	286.439	286.4	Lee T.H., Rabalais J.W. J. Electron Spectrosc. Relat. Phenom. 11, 123 (1977)
287.635	1.96796	C=O	0.3	287.935	287.9	Gelius U., Heden P.F., Hedman J., Lindberg B.J., Manne R., Nordberg R., Nordling C., Siegbahn K. Phys. Scripta 2, 70 (1970)
292.908	3.47837	K-C-O	0.3	293.208	294.0	Jerome R., Teyssie Ph., Pireaux J.J., Verbist J.J. App. Surf. Sci. 27, 93-105 (1986)
295.878	2.2656	K-C-O	0.3	296.178	296.8	Jerome R., Teyssie Ph., Pireaux J.J., Verbist J.J. App. Surf. Sci. 27, 93-105 (1986)
399.227	2.9033	N-C	0.3	399.527	399.5	Lindberg B.J., Hedman J. Chem. Scr. 7, 155 (1975)
530.967	2.73185	O-C	0.3	531.267	531.25	Beamson G., Briggs D. High Resolution XPS of Organic Polymers: the Scienta ESCA300 Database (1992)
532.046	1.82033	O-Si	0.3	532.346	532.23	Wagner C.D., Passoja D.E., Hillery H.F., Kinisky T.G., Six H.A., Jansen W.T., Taylor J.A. J. Vac. Sci. Technol. 21, 933 (1982)
532.954	1.53762	O=C	0.3	533.254	533.26	Beamson G., Briggs D. High Resolution XPS of Organic Polymers: the Scienta ESCA300 Database (1992)
98.3712	1.38293	Si-Si	0.3	98.6712	98.7	Franklin G.E., Rich D.H., Hong H., Miller T., Chiang T.-C. Phys. Rev. B 45, 3426 (1992)
99.1402	1.89049	Si-O	0.3	99.4402	99.4	Aarnik W.A.M., Weishaupt A., van Silfout A. Appl. Surf. Sci. 45, 37 (1990)
102.202	2.53621	Si-C	0.3	102.502	102.4	Vargo T.G., Gardella J.A., Jr. J. Vac. Sci. Technol. A 7, 1733 (1989)

Table 8 - High-resolution spectrum component positions for carbon (1s), nitrogen (1s), oxygen (1s) and silicon (2p) signals on mannose surface of the carbohydrate functionalised polymer surface modification to mimic *Balanus amphitrite* SIPC

Binding energy	Width	Predicted bond	Shift	Adjusted binding energy	Predicted bond binding energy	Evidence
284.14	2.99627	C-C	0.46	284.6	284.6	Palchan I., Crespin M., Estrade-Szwarckopf H., Rousseau B. Chem. Phys. Lett. 157, 321 (1989)
284.159	1.7205	C-Si	0.46	284.619	284.70	Beamson G., Briggs D. High Resolution XPS of Organic Polymers: the Scienta ESCA300 Database (1992)
285.061	2.10761	C-O	0.46	285.521	285.55	Beamson G., Briggs D. High Resolution XPS of Organic Polymers: the Scienta ESCA300 Database (1992)
285.607	2.91766	C-N	0.46	286.067	286.0	Yoon S.C., Ratner B.D. Macromolecules 19, 1068 (1986)
287.437	2.3885	C=O	0.46	287.897	287.9	Gelius U., Heden P.F., Hedman J., Lindberg B.J., Manne R., Nordberg R., Nordling C., Siegbahn K. Phys. Scripta 2, 70 (1970)
292.999	3.87208	K-C-O	0.46	293.459	294.0	Jerome R., Teyssie Ph., Pireaux J.J., Verbist J.J. App. Surf. Sci. 27, 93-105 (1986)
296.068	2.22338	K-C-O	0.46	296.528	296.8	Jerome R., Teyssie Ph., Pireaux J.J., Verbist J.J. App. Surf. Sci. 27, 93-105 (1986)
399.227	2.9033	N-C	0.46	399.687	399.7	Doring M., Rudolph M., Uhlig E., Nefedov V.I., Salin J.V. Z. Anorg. Allg. Chem. 554, 217 (1987)
530.616	2.74568	O-C	0.46	531.076	531.0	Llopiz P., Maire J.-C. Bull. Soc. Chim. Fr. 457 (1979)
532.016	2.09454	O-Si	0.46	532.476	532.4	Shalvoy R.B., Reucroft P.J., Davis B.H. J. Catal. 56, 336 (1979)
532.075	2.0541	O=C	0.46	532.535	532.5	Sugama T., KuKacka L.E., Carciello N., Hocker N.J. Cement and Concrete Research 19, 857 (1989)
98.6393	1.53995	Si-Si	0.46	99.0993	99.1	Chao S.S., Takagi Y., Lukovsky G., Pai P., Caster R.C., Tyler J.T., et al. Appl. Surf. Sci. 26, 575 (1986)
99.1404	2.01428	Si-O	0.46	99.6004	99.5	Cros A., Saoudi R., Hewett C.A., Lau S.S., Hollinger G. J. Appl. Phys. 67, 1826 (1990)
102.551	2.51974	Si-C	0.46	103.011	103.4	Laoharajanaphand P., Lin T.J., Stoffer J.O. J. Appl. Polymer Sci. 40, 369 (1990)

Table 9 - High-resolution spectrum component positions for carbon (1s), nitrogen (1s), oxygen (1s) and silicon (2p) signals on galactose surface of the carbohydrate functionalised polymer surface modification to mimic *Balanus amphitrite* SIPC

Binding energy	Width	Predicted bond	Shift	Adjusted binding energy	Predicted bond binding energy	Evidence
282.371	1.99256	C-C	2.2	284.6	284.6	Palchan I., Crespin M., Estrade-Szwarczkopf H., Rousseau B. Chem. Phys. Lett. 157, 321 (1989)
282.515	3.30932	C-Si	2.2	284.715	284.70	Beamson G., Briggs D. High Resolution XPS of Organic Polymers: the Scienta ESCA300 Database (1992)
283.251	1.5457	C-O	2.2	285.451	285.43	Beamson G., Briggs D. High Resolution XPS of Organic Polymers: the Scienta ESCA300 Database (1992)
284.298	1.59991	C-N	2.2	286.498	286.6	Lalitha S., Manoharan P.T. J. Electron Spectrosc. Relat. Phemon. 49, 61 (1989)
285.698	2.28695	C=O	2.2	287.898	287.9	Gelius U., Heden P.F., Hedman J., Lindberg B.J., Manne R., Nordberg R., Nordling C., Siegbahn K. Phys. Scripta 2, 70 (1970)
290.862	2.38568	K-C-O	2.2	293.062	294.0	Jerome R., Teyssie Ph., Pireaux J.J., Verbist J.J. App. Surf. Sci. 27, 93-105 (1986)
293.609	2.43078	K-C-O	2.2	295.809	296.8	Jerome R., Teyssie Ph., Pireaux J.J., Verbist J.J. App. Surf. Sci. 27, 93-105 (1986)
397.834	2.52644	N-C	2.2	400.034	400.0	Salyn J.V., Zumadilov E.K., Nefedov V.I., Scheibe R., Leonhardt G., Beyer L., Hoyer E. Z. Anorg. Allg. Chem. 432, A275, (1977)
529.129	2.63906	O-C	2.2	531.329	531.3	Christie, A.B., Lee J., Sutherland I., Walls J.M. Appl. Surf. Sci. 15, 224 (1983)
531.06	2.48868	O-Si	2.2	533.26	533.2	Paparazzo E., Fanfoni M., Severini E. Appl. Surf. Sci. 56, 866 (1992)
531.955	1.35554	O=C	2.2	534.155	532.4	Yoon S.C., Ratner B.D. Macromolecules 19, 1068 (1986)
98.826	1.43995	Si-Si	2.2	101.026	99.61	Ingo G.M., Zacchetti N., della Sala D., Coluzza C. J. Vac. Sci. Technol. A 7, 3048 (1989)
99.5786	1.96566	Si-O	2.2	101.7786	101.7	Finster J., Klinkenberg E.-D., Heeg J. Vacuum 41, 1586 (1990)
101.989	2.61095	Si-C	2.2	104.189	103.8	Morra M., Occhiello E., Marola R., Garbassi F., Humphrey P., and Johnson D. J. Colloid Interface Sci. 137, 11 (1990)

4.3.5 Drop Assay

The drop assays were analysed at 24 and 48 hours to assess the longer-term efficacy of surface chemistry modification as shown in Figure 60. After 24 hours the data were found to be normal (Kolmogorov-Smirnov test statistic=0.105, $p<0.123$) and equally variant (Bartlett's test statistic=8.71, $p=0.121$). A one-way ANOVA test showed there was no significant difference in the mean percentage settlement of cyprids on the seven surfaces tested ($F_{6,49}=1.66$, $p=0.150$). After 48 hours the data were found to be normal (Kolmogorov-Smirnov test statistic=0.110, $p=0.088$) and equally variant (Bartlett's test statistic=3.36, $p=0.645$). A one-way ANOVA test showed there was a significant difference in the mean percentage settlement of cyprids on the seven surfaces ($F_{6,49}=5.55$, $p<0.001$). This significant difference was found between the aminoethanol and clean glass. Average settlement in the 24-well plate standard was low ($14.12\% \pm 3.51$) as expected from 0-day-old cyprids.

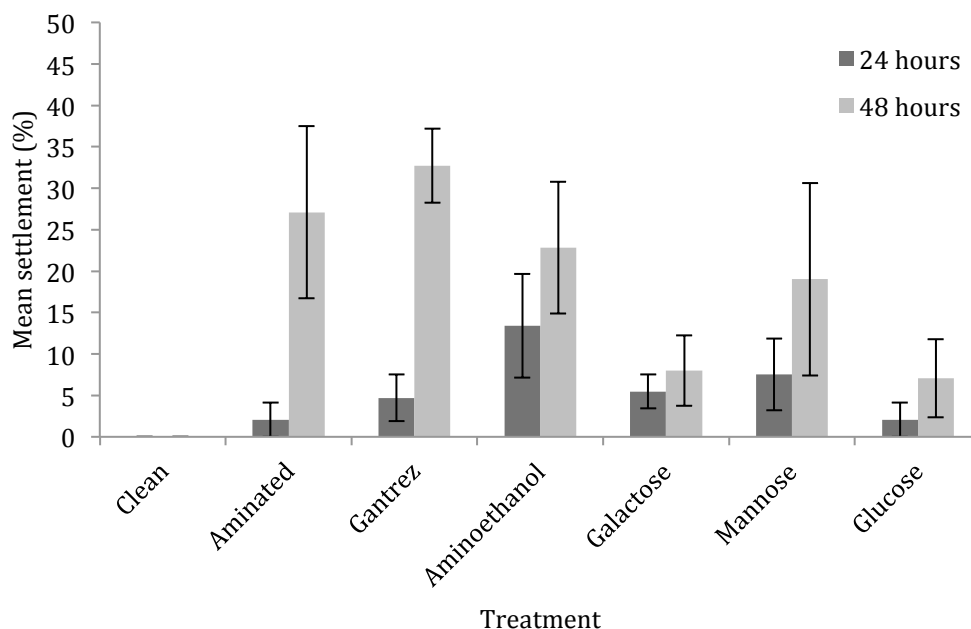


Figure 60 - Mean cyprid settlement on the carbohydrate functionalised polymer surface modification to mimic *Balanus amphitrite* SIPC at 24 and 48 hours. Error bars are \pm standard error.

Figure 61 shows only the carbohydrate surfaces after 48 hours and when other surfaces were removed from the analysis, the data were again found to be normal (Kolmogorov-Smirnov test statistic = 0.107, $p<0.15$) and equally variant (Bartlett's test statistic=0.27,

$p=0.873$). A one way ANOVA test showed there was no significant difference in the mean percentage settlement of cyprids on the three carbohydrate surfaces ($F_{2,21}=0.29$, $p=0.749$).

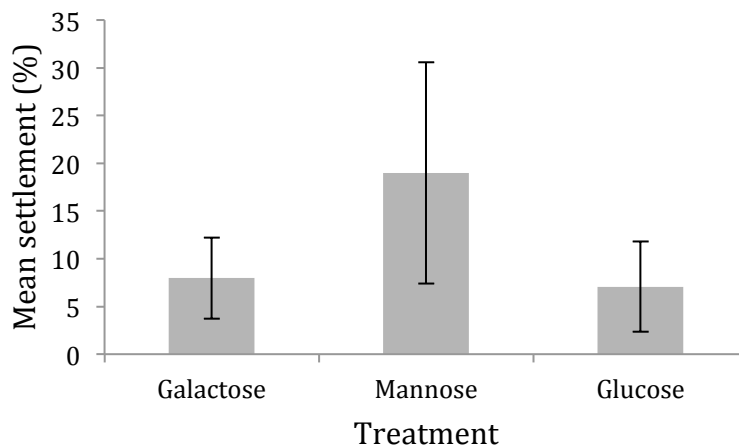


Figure 61 - Mean cyprid settlement on the carbohydrate functionalised polymer surface modification to mimic *Balanus amphitrite* SIPC at 48 hours. Error bars are \pm standard error.

This experiment was also repeated using 6-week-old slides. These slides had very little settlement most likely due to the degradation of the surface chemistry over time. However, the batch of cyprids used was a very low settling batch as they did not settle well in the 24-well plate standard.

4.4 Discussion

The successful functionalisation of polymers with carbohydrates on surfaces was the aim of this experimental chapter. Despite some difficulties initially, contact angle, ellipsometry and XPS all provided evidence that the modification of the surface has been achieved, confirmed and finally bioassayed.

The contact angle measurements showed the expected changes in surface wettability. The piranha-cleaned glass was expected to have a very low contact angle due to the high hydrophilicity of the surface. The aminated surface is hydrophobic and consequently the contact angle reflects this. The Gantrez[®] surface is less hydrophobic with a contact angle of $37.3^{\circ} \pm 0.9$. It was expected to be in the region of 48° as this has been found in other maleic anhydride polymers (Johnson, 2009). The aminoethanol surface was expected to be more hydrophobic than the Gantrez[®] with a value of around 52° (Johnson, 2009). The contact angle observed was $48.0^{\circ} \pm 1.2$ which is slightly lower than expected. However, as the

Gantrez[®] surface reading was also comparably lower, it was considered acceptable. As expected, each of the carbohydrate surfaces were expected to be approximately the same value as the surfaces would all be similar. Some variation in observed contact angles is inevitable under normal circumstances due to particle contamination and general heterogeneity of the surface (Murray and Darvell, 1990).

As ellipsometry analyses the depth of a surface layer, this is most useful to examine the increase between the amine terminated and Gantrez[®] surface as this is where the largest depth increase occurs due to the size of the Gantrez[®] polymer. This increase was demonstrated as expected in Figure 54. The aminoethanol surface had a depth lower than anticipated. As with the contact angle, each of the carbohydrate surfaces was expected to be similar in depth, which was the case here. Again, these values were lower than the Gantrez[®] layer. There are several explanations for this; firstly it could be that the area of Gantrez[®] surface analysed had longer polymer chains than others. Additionally, as ellipsometry relies on the change in polarity of polarised laser light as it interacts with the different components on the surface, any erroneous results could be due to scratches on the wafer or dust on the surface.

During XPS analysis, gold was used to provide an indication of the shift caused by charge build up on samples. Gold is expected to have two peaks caused by splitting due to degeneracy of the orbital levels, with one peak around 84eV and the other around 87.7eV (Seah et al., 1998). In the carbohydrate functionalised Gantrez[®] samples, the gold spectra are very unusual indicating two Doniach-Sunjic doublets, where only one is expected, being elemental gold. It is possible that the extra peak is gold nitride but under normal circumstances, the nitrogen is present in very small amounts and decomposes under the vacuum leaving no peak on the spectrum. As these results are so unusual, the gold data was disregarded and the carbon shift from the expected 284.6eV (Yeganeh et al., 2007) was used to assess any shift that may be found. This approach of using the carbon peaks is commonly used.

The wide scan spectra (Figure 55) show peaks from carbon, oxygen, silicon and nitrogen as expected when compared to spectra from Johnson (2008). However, there are also peaks from the Auger process; these have the characteristic shape as shown in the graphs. Auger de-excitation occurs in XPS when the X-rays remove an electron in the 1s level (forming

the expected elemental peak) but then an electron from the 2s level drops in to fill the space left by the 1s electron. The energy involved in this transition is then passed on to a 2p electron, which is emitted, creating the Auger peaks. Also present in the wide scan spectra are unknown peaks, marked with *, not present in the elemental database. Consequently, these peaks are most likely to be compounds from the surface modification process such as boron trifluoride diethyl etherate or potassium carbonate.

When compared to the closest literature cited values, it is noted that some of the binding energies are sometimes different. This is due to the complexity of the surface chemistry of samples and consequently, there may not be an exact match to the chemistry present in these samples, so the binding energies are only approximate.

Figure 56 shows the high-resolution carbon spectra for all surface samples. Figure 56(a) is the aminated spectrum and shows the presence of the four carbon bonds as expected; C-C, C-O, C-Si and C-N. Here, the C-Si peak is small as there are very few of these bonds present on the surface in comparison to C-C and C-O bonds. Figure 56(b) is the spectrum with the addition of Gantrez[®], and as shown in Figure 51, this structure contains C=O bonds and the spectrum reflects this with the appearance of an additional peak. Figure 56(c) shows the aminoethanol spectrum, showing the presence of all 5 carbon bonds as in Figure 56(b) but more C-O and C-N bonds due to presence of aminoethanol. The C=O peak is still present but the shoulder of the peak is less obvious in the spectrum because of the increase in the presence of C-N bonds in the aminoethanol. Figure 56(d-f) are the spectra for glucose, mannose and galactose. These carbohydrates are very similar from an elemental point of view but possess different stereochemistry (position of O-H bonds on carbons 2 and 4) so the XPS cannot be used to detect differences between them. Consequently, the spectra for the three carbohydrates are predicted to look similar. When compared to the three previous spectra, Figure 56(a-c), it is obvious that a second set of peaks is present. It was first thought that these peaks may potentially be satellite peaks from the carbon (Gardella et al., 1986). However, when studying the wide survey spectra, Figure 55(d-f) shows unexpected peaks relating to potassium. Potassium carbonate was used as the final step in the surface modification during the deprotection of the carbohydrates. It is most likely that, despite rigorous washing stages, some of the potassium carbonate remained on the surface. If this is the case then these peaks are the K2p peaks from a K-C-O complex.

The two peaks are present due to degeneracy or splitting of the 'p' orbitals of potassium. Jerome and colleagues (1986) also found binding energies of around 292.9eV for a compound containing K, C and O. This is similar to the values found before the appropriate shifting was added, although the reference paper does not match exactly but shows the peaks are in the correct region. The peaks are also predicted to be approximately 2.8eV apart for potassium bromide as potassium is too unstable to use in the XPS chamber. The distances between these peaks were 2.97, 3.07 and 2.75eV for glucose, mannose and galactose respectively. Due to the difference in chemical complexity between these samples and the reference, these values are within the $\pm 0.5\text{eV}$ variability and are considered acceptable. In conclusion, the XPS has confirmed the success of the surface modification at each step. However, there was presence of contamination by potassium carbonate. In future, this could be remedied by increasing the washing of the samples and varying the solvents used in the final washing stages to ensure no residue remains.

Figure 57 shows the high resolution spectra for nitrogen. Figure 57(a) is the spectrum for the aminated surface, showing the N-C bond expected from the addition of APTES. Figure 57(b) shows the surface after the addition of Gantrez[®], and as expected there is no change as only the N-C bonds from the APTES are present. Figure 57(c) was expected to have more N-C bonds, and accordingly the peak appears larger in comparison to the previous two graphs (Figure 57 a-b) due to increased presence of the N-C bond from the aminoethanol. Similarly to the carbon spectra, the nitrogen spectra for glucose, mannose and galactose are expected to have approximately the same spectrum as the structures are so similar. Comparing the spectra confirms this.

Figure 58 shows the high resolution spectra for oxygen, Figure 58(a) the aminated surface, shows the presence of two oxygen bonds (O-C and O-Si) as expected from the addition of APTES. The spectra for the Gantrez[®] surface, Figure 58(b), again shows the presence of two oxygen bonds as expected from APTES but in addition, the presence of the O=C bond from the addition of Gantrez[®]. Figure 58(c) has increased presence of O-C bonds due to the aminoethanol. Figure 58(d-f) are again expected to appear similar as they show the spectra for glucose, mannose and galactose, and again there is an increased proportion of O-C bonds due to the presence of carbohydrates.

The high resolution spectra for silicon are shown in Figure 59. It was expected that all spectra for silicon bonds would remain the same for each of the samples a-f as silicon only appears in the substratum (silicon wafer) and APTES. Consequently, the first spectrum showing the aminated surface Figure 59(a), confirms the presence of the three silicon bonds (Si-C, Si-O and Si-Si) and the following spectra for Gantrez[®], aminoethanol, glucose, mannose and galactose (Figure 59b-f) all appear very similar.

The XPS analysis of the surface modified samples has supported the data from contact angle and ellipsometry that the surface modification using carbohydrate functionalised polymers has been successful. It has also highlighted issues of contamination during the final stages of the modification and so changes to the washing protocol at the end of the carbohydrate deprotection step were made. By increasing the number of washes and also changing the solvent used, this will hopefully ensure that future repeats using this protocol will not have the same contamination concerns.

As a result of all of the confirmation steps; contact angle, ellipsometry and XPS, it can be concluded that the desired surface modification of carbohydrate functionalised polymers was successful.

The drop assay, Figure 60, shows mean settlement appears to differ but it is not statistically significant due to the large standard error. Previously, mannose has been shown to cue settlement in solution (see Chapter 3.3.4) but the considerably higher induction of settlement on the aminated, Gantrez[®] and aminoethanol surfaces is at first surprising. However, if the chemistry of the individual surfaces is scrutinized, possible hypotheses for this increased settlement can be arrived at. The aminated surface is amine terminated and thus creates a positively charged surface; on the other hand, the Gantrez[®] anhydride ring provides a negatively charged surface. Assays with cyprids (Aldred, unpublished) showed settlement is increased on charged surfaces, with higher settlement on negatively charged surfaces. Corroborating this, Holm et al. (1997) found aminopropylsilyl (APS) treated glass, providing a similar surface chemistry to the aminated surface assayed here, had higher settlement than glass during field trials. In regard to the aminoethanol surface, which is OH terminated, cyprids have shown increased settlement in solution where a small quantity of alcohol is present in the water (Aldred and Clare, 2009). However, it is considered that although surface energy is important for initial settlement, over time, the

effect of this may not be as significant as first thought (Holm et al., 1997). Figure 61 indicates that there is a small difference in settlement between the carbohydrates. However this is not significant although visually it appears that mannose induces settlement more than the other carbohydrates,. It is the large standard errors associated with this data that remove the significance. These errors are common when using inductive surface compounds due to the positive feedback created by settling cyprids and variation in larval quality. There is visually no indication of nauplii and cyprid quality, so the natural variation in the size of cyprids (Emlet and Sadro, 2006), organic content, metamorphic success, feeding rate and growth capacity (Jarrett and Pechenik, 1997) vary greatly and can mask the true results in assays. The reliability of larvae also changes, larvae were selected if they look healthy and have fed, and unhealthy batches are discarded. This type of selection would normally be considered over selective. However, as the protocol for producing the modified slides is so extensive, using every cyprid batch produced would have resulted in time and resources outside the scope of this research.

The presentation of glycans and how they are exposed on the surface is thought to be very important. Carbohydrates displayed on the SIPC move a lot in relation to the core protein and are flexible in comparison so this may be why the SIPC mimic surfaces did not cue as much as expected, as this flexibility is absent in the polymer structure. In addition, the carbohydrate may not be the only inducer; there may be some inductive effect from the presence of the protein structure.

Chapter 5. Physical characteristics of the settlement-inducing protein complex

5.1 Introduction

Following the progress of the previous experimental chapters, some preliminary steps towards further structural characterisation of the SIPC core protein were attempted. Adding to the knowledge of the protein structure has increased understanding of how the newly characterised sugars are presented, how these sugars might interact with binding partners and importantly, what can be learnt from structural homology with other proteins.

The SIPC core protein has been the subject of previous studies, the most detailed of which is the confirmation of the amino acid sequence by Dreanno et al. (2006c). The results of this research are briefly touched upon in Chapter 1.1.9.

Atomic force microscopy (AFM) studies of the prepared SIPC samples were carried out by Dr In Yee Phang in Professor Julius Vancso's 'Materials Science and Technology of Polymers Group' at the University of Twente, Netherlands. There has been some previous research into the cyprid temporary adhesive of *Balanus* species. Phang et al. (2007) began work on the morphology of footprints using AFM and proposed that both 'wet' and 'dry' mechanisms are employed to provide the attachment tenacity of cyprids. Work in the same group studied the cyprid footprints of *Semibalanus balanoides*, recreating the interactions of the footprint protein with chemically different surfaces (Phang et al., 2009). There is thought to be some possible relation between the SIPC and cyprid temporary adhesive, this is briefly touched upon in Chapter 1.1.10. Other biological adhesives, have also been researched, for example, the amyloid fibres in the terrestrial algae, *Prasiola linearis*, have revealed detailed information about the mechanisms behind the mechanical strength and structure of biopolymers (Mostaert et al., 2006).

AFM work in this chapter also involved the use of lectins - specific sugar binding proteins. As the SIPC is a glycoprotein, it has been shown previously that certain lectins react with the SIPC, inhibiting settlement (Matsumura et al., 1998a). Research in earlier chapters has shown that mannose is the main oligosaccharide present on the SIPC and this induces settlement, therefore the cyprid antennule must detect or bind to specific sugars, in this case

mannose. Lentil lectin binds to mannose and consequently to the mannose-containing SIPC, reducing settlement. Non-mannose binding lectins such as peanut lectin do not bind to the SIPC so do not inhibit settlement. Six lectins were used in this research: *Lens culinaris* (lentil) agglutinin (LCA) and Concanavalin Agglutinin (ConA) were expected to inhibit settlement as they are mannose-binding lectins. Wheat germ agglutinin (WGA), phytohaemagglutinin from the kidney bean (PHA), soybean agglutinin (SBA) and peanut agglutinin (PNA) were not expected to affect settlement as they are N-acetylglucosamine, N-acetyl galactosamine and galactose binding (Sharon and Lis, 1989). As methyl α -D-mannopyranoside has been shown to reverse the LCA inhibitory effect (Matsumura et al., 1998a), it was also introduced during AFM measurements. It was hoped that through observing the interactions with lectins and methyl α -D-mannopyranoside it may be possible to discover more detail on the adhesive properties, unfolding characteristics, structure and composition of the SIPC.

Transmission electron microscopy (TEM) was conducted using both native and deglycosylated SIPC. This research is novel for barnacle species however there has been considerable research into the protein structure of other aquatic organisms, using similar TEM protocols to that used here (Harris and Horne, 1991), mainly focusing on haemoglobins and haemocyanins. Micrographs of haemoglobin from the annelid worm *Nereis virens* showed intact hexameric molecules as well as dissociated molecules (Harris et al., 2006) (Figure 62a). Studies on the branchiopod crustacean *Triops cancriformis* showed detailed information on the structure and function of the haemoglobin. TEM images revealed both circular shapes of 14nm diameter and rectangular structures of 16x9nm (Rousselot et al., 2006). Again focusing on haemocyanin, Meissner et al. (2003) presented the structure for the haemocyanin of the European spiny lobster, *Palinurus elephas*, using a combination of cryoelectron microscopy (Figure 62b) and analysis of the amino acid sequence. The comparison of the sequence to that of the American counterpart, *Panulirus interruptus*, showed more than 80% sequence homology. Similarly, Dube et al. (1995) and Gebauer et al. (2002) also characterised the protein structure of a haemocyanin, this time from the Californian keyhole limpet, *Megathura crenulata*. This study found cylindrical structures consisting of ten globular masses or subunits that made up the wall of the haemocyanin (Figure 62c). Following this work and that of others such as Meissner et al. (2000), the structure of the molluscan haemocyanin was determined to be constructed

from ten ‘banana’ shaped subunits of around 400kDa, which are arranged to form hollow cylinders. Using the chiton *Acanthochiton fascicularis*, further three-dimensional reconstruction was carried out to confirm previous work and generate greater detail. This work led to the visualisation of the ‘man-in-the-boat’ structure of a subunit dimer (Harris et al., 2004) (Figure 62d).

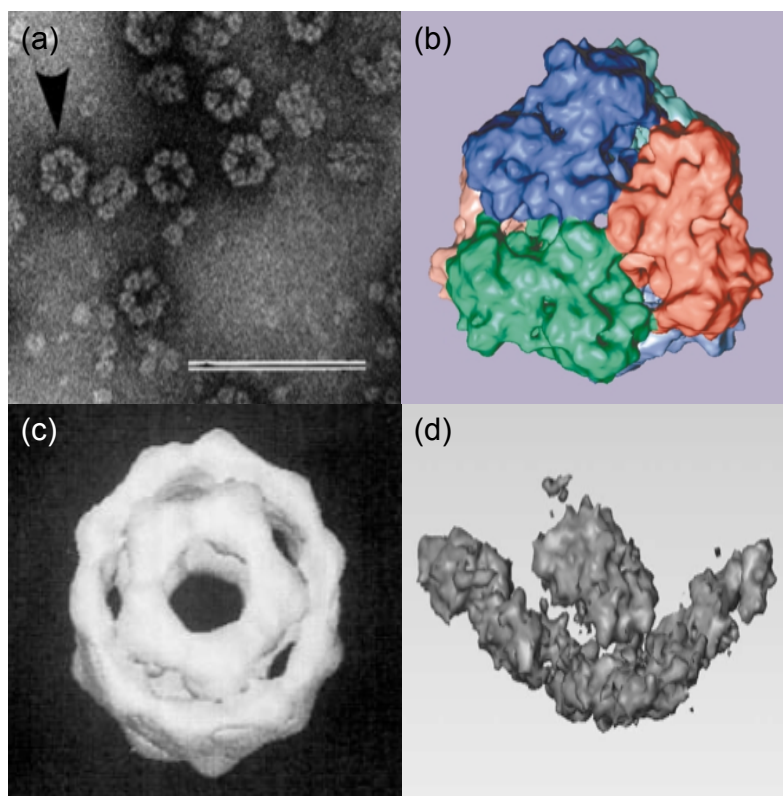


Figure 62 - Examples of characterised protein structures from other aquatic organisms; (a) haemoglobin from the annelid worm *Nereis virens* showing hexameric molecules (from Harris et al., 2006) (b) haemocyanin from the European spiny lobster, *Palinurus elephas* showing three subunits (from Meissner et al., 2003) (c) haemocyanin from the Californian keyhole limpet, *Megathura crenulata* showing cylindrical structures consisting of ten globular masses (from Dube et al. 1995) (d) haemocyanin from the chiton *Acanthochiton fascicularis* showing the ‘man-in-the-boat’ structure (from Harris et al. 2004)

5.1.1 Aims and Objectives

Following the success of the purification and characterisation of the SIPC carbohydrates as well as the development of a synthetic mimic for the SIPC, the second focus for this project was the structure of the deglycosylated SIPC protein, as outlined in Aim 4:

Aim 4 - To develop further understanding of the SIPC protein core.

Objective - Further analysis of the amino acid sequence and the core protein was carried out using techniques commonly used in structural biology, such as transmission electron microscopy and atomic force microscopy.

5.2 Materials and methods

5.2.1 Atomic force microscopy

The protocol employed was similar to that of Phang et al. (2009). 50µl native SIPC (5.76mg/ml), 1ml 50µg/ml of lectins: *Lens culinaris* (lentil) agglutinin (LCA), wheat germ agglutinin (WGA), peanut agglutinin (PNA), Concanavalin Agglutinin (ConA), phytohaemagglutinin (PHA) from kidney bean and soybean agglutinin (SBA) and 1ml 0.5M methyl α -D-mannopyranoside were sent to the University of Twente for analysis. The SIPC was diluted in 0.45µm filtered artificial seawater to 1:100, 1:500 and 1:1000 to ensure a suitable concentration for imaging was established. The protein was immobilised for 2 hours on four different surfaces chosen for their differing properties. Methyl terminated glass (CH₃-Si) and highly ordered pyrolytic graphite (HOPG) are both hydrophobic. Mica (sheet silicate mineral) and amine-terminated glass (NH₂-Si) are both hydrophilic. Standard triangular silicon nitride tips (Digital Instruments, USA) were used to probe the immobilised protein using dry tapping mode under nitrogen. AFM measurements were carried out using a Dimension D3100 atomic force microscope with NanoScope IVa controller and hybrid scanner H-153 (Veeco, USA). The lectins and methyl α -D-mannopyranoside were added to the surface after initial measurement with the SIPC.

5.2.2 Transmission electron microscopy (TEM)

Native and deglycosylated samples of the SIPC (purified as in Chapter 3.2.1-3.2.9) were diluted to approx. 0.7mg/ml and 0.07mg/ml with 50mM TrisHCl pH7.5. Two methods were used. Firstly, samples were prepared for TEM by the 'single-droplet' parafilm procedure (Harris and Horne, 1991). Briefly, a carbon film coated copper formvar support mesh (400-mesh grid) was surface activated by glow discharge (Edwards Coating Unit) before loading the 10µl sample, washing and staining with 2% uranyl-acetate at pH 4.2-4.5. This heavy metal-containing cation forms a layer of negative stain, whereby the proteins are surrounded by the stain which scatters electrons revealing the protein as white particles on a darker background. In addition, holey carbon microgrid films were used. These produced very thin carbon films supported on holey carbon grids and were stained with 2%

ammonium molybdate (pH7). This approach imparts lower electron density but results in higher resolution than the grainy uranyl acetate images (Harris and Horne, 1991).

TEM was performed with a Philips CM100 transmission electron microscope with charge-coupled device camera. Digital images of areas of interest were taken at 130,000x instrumental magnification. Protein concentration and sample conditions were optimised to generate grids with a homogeneous coverage of single particles before image processing. The glycosylated form of the SIPC protein aggregated under the conditions used for imaging, therefore the protein was deglycosylated to produce optimal loading on electron microscopy grids for imaging. Deglycosylated SIPC in a 10% solution was chosen as the optimal dilution. Two-dimensional image processing provided preliminary image averaging to give a qualitative assessment of the protein structure. Two-dimensional processing involved selection of individual protein particles that were processed by multivariate analysis to determine the shape of the protein and define any surface projections. To produce two-dimensional class averages, digital micrograph images were processed in e2boxer to select individual particles of interest and then EMAN2 to extract the boxed particles and stack them. As particles lay at random orientations in the micrographs, to remove noise and create class averages, multivariate analysis was run on individual protein particle images, again using EMAN2 as described in Tang et al. (2007).

5.2.3 Protein Structure Analysis

In order to compare the SIPC to previously fully characterised proteins, a search of the Research Collaboratory for Structural Bioinformatics (RCSB) Protein Data Bank (www.pdb.org) was carried out using the SIPC amino acid sequence as identified in Dreanno et al. (2006c). Again using this sequence, MultAlin sequence alignment analysis (<http://multalin.toulouse.inra.fr/multalin/>) as in Corpet (1988) and ESPript sequence alignment (<http://esprict.ibcp.fr/ESPript/ESPript/index.php>) as developed by Gouet et al. (1999) were completed.

Using the amino acid sequence along with internet-based prediction software, further investigation of the SIPC core protein took place. To assess which, if any, of the cysteines in the SIPC can potentially form disulphide bonds, the DiAminoacid Neural Network Application (DiANNA) (<http://clavius.bc.edu/~clotelab/DiANNA/>) cysteine classification and disulphide connectivity prediction was used as developed by Ferre and Clote (2005).

In addition, using the DomPred system (UCL Bioinformatics Group <http://bioinf.cs.ucl.ac.uk/dompred>), it is possible to predict putative protein domains and their boundaries for a given protein sequence as shown in Marsden et al. (2002).

Further computational analysis of the protein was possible through use of the ExPASy Proteomics Server (www.ExPASy.ch), the accession number (AY423545) and corresponding FASTA sequence from Dreanno et al. (2006c). Using the ExPASy NetNGlyc in Post Translational Modification Prediction (<http://www.cbs.dtu.dk/services/NetNGlyc/>) (Gupta et al., 2004), it was possible to show likely *N*-glycosylation sites within the amino acid sequence. In short, glycosylation sites occur where the amino acid sequons obey to the Asn-Xaa(≠Pro)-Ser or Asn-Xaa(≠Pro)-Thr consensus (where Xaa is any amino acid except Pro, as it renders the Asn inaccessible) (Zuber and Roth, 2009). Similar prediction software can be used for *O*- and *C*-glycosylation prediction using <http://www.cbs.dtu.dk/services/NetOGlyc/> (Julenius et al., 2005) and <http://www.cbs.dtu.dk/services/NetCGlyc/> (Julenius, 2007) respectively.

In order to visualise the impact of glycan removal on the position of the SIPC on an SDS-PAGE gel, native, denatured and deglycosylated SIPC were simultaneously run on gels. 30µg of each sample were suspended in 12µl dH₂O as previous SDS-PAGE gel methodology (Chapter 3.2.5) and run on two gels, one 6% and one 10% acrylamide. A Bio-Rad Precision Plus Dual Colour Protein Standard was run alongside as a reference. The gels were washed and stained with Pro-Q Emerald 300 according to the manufacturer's instructions. The gels were viewed under a Typhoon 9200 Variable Mode Imager set at Blue2 (488nm excitation wavelength, 520 band pass and 700V detector voltage).

To identify which glycans are present on different parts of the protein, using ExPASy Peptide Cutter (<http://expasy.org/tools/peptidecutter/>), it was possible to see which enzymes cleave the sequence between the glycosylation sites, separating them, following a protocol similar to Geyer and Geyer (2006). To find the size of the peptides, amino acids in the cleaved section were entered into ExPASy Compute pI/MW (http://expasy.org/tools/pi_tool.html) to give values in kDa. This was required if the peptides were to be run on a gel or for LC-MS. This data is shown in Appendix B.

Using the information gathered using the ExPASy server, the following enzymes were chosen for digestions; Lys-C (Endoproteinase Lys-C from *Lysobacter enzymogenes*, Sigma), Glu-C (Endoproteinase Glu-C from *Staphylococcus aureus* V8, Sigma), Arg-C (from mouse submaxillary gland, Sigma) and trypsin (Promega) based on the predicted cleaving. Native SIPC was set in a gel as in Chapter 3.2.12. In addition, control proteins from the molecular weight standard were extracted from an SDS-PAGE gel. These standards were the 210kDa band (myosin), 105kDa band (phosphorylase B) and the 55kDa band (glutamic dehydrogenase). All gel blocks were washed as in Chapter 3.2.12. SIPC samples were treated under three conditions: trypsin, Glu-C and Lys-C, and Arg-C. Enzymes were prepared as per individual instructions. 100µl of enzyme was added to each microcentrifuge tube containing gel pieces, vortexed and spun down before 50µl of 100mM ammonium bicarbonate was added and samples were incubated at 37 °C overnight. To recover the peptides, the solution was removed from each tube and dried down. 50µl of 30% acetonitrile and 0.2% trifluoroacetic acid (TFA) was added to the tubes containing the used gel pieces and sonicated for 10 minutes before pooling with the enzyme solution and drying down. The process was repeated with 50µl of 60% acetonitrile and 0.2% TFA. The pooled samples were dried down for use in a mass spectrometer.

5.2.4 Mass Spectrometry of proteins and N-glycans

For running the peptides on MALDI-MS, a 384 spot metal MALDI plate was first cleaned using detergent, metal polish and methanol with delicate task wipes (Spilfyter). Dry samples of digested proteins were re-suspended in 5 µl of 0.1% formic acid and spotted in 1µl aliquots onto the plate. Calibration standards were spotted using 1µl of standard calibration mix, 12µl matrix and 12µl dH₂O. The matrix consisted of α -cyano-4-hydroxycinnamic acid (HCCA) in acetonitrile and 0.1% TFA. The plate was run in an Applied Biosystems 4800 proteomics analyser MALDI-TOF/TOF.

5.3 Results

5.3.1 Atomic force microscopy

Experiments using the different lectins and α -D-mannopyranoside were inconclusive due to the low concentrations used. However, representative images from each of the four surfaces; methyl terminated glass, HOPG, amine terminated glass and mica, are shown in Figure 63. The SIPC on methyl terminated glass, Figure 63(a), shows globular proteins with a high adsorption and affinity of the SIPC to the surface. The HOPG surface, Figure 63(b), shows no adsorption of the SIPC to the surface at all. The amine-terminated glass, Figure 63(c), shows less adsorption than the methyl-terminated glass but does show globular proteins. The mica surface, Figure 63(d), required extra incubation time, totalling 4.5 hours in comparison to 2 hours for the other surfaces to see adsorption of the SIPC to the surface. Even after this time, slow and low-density adsorption was observed. The proteins were elongated on the surface showing that certain domains of the protein had strong affinity for the surface.

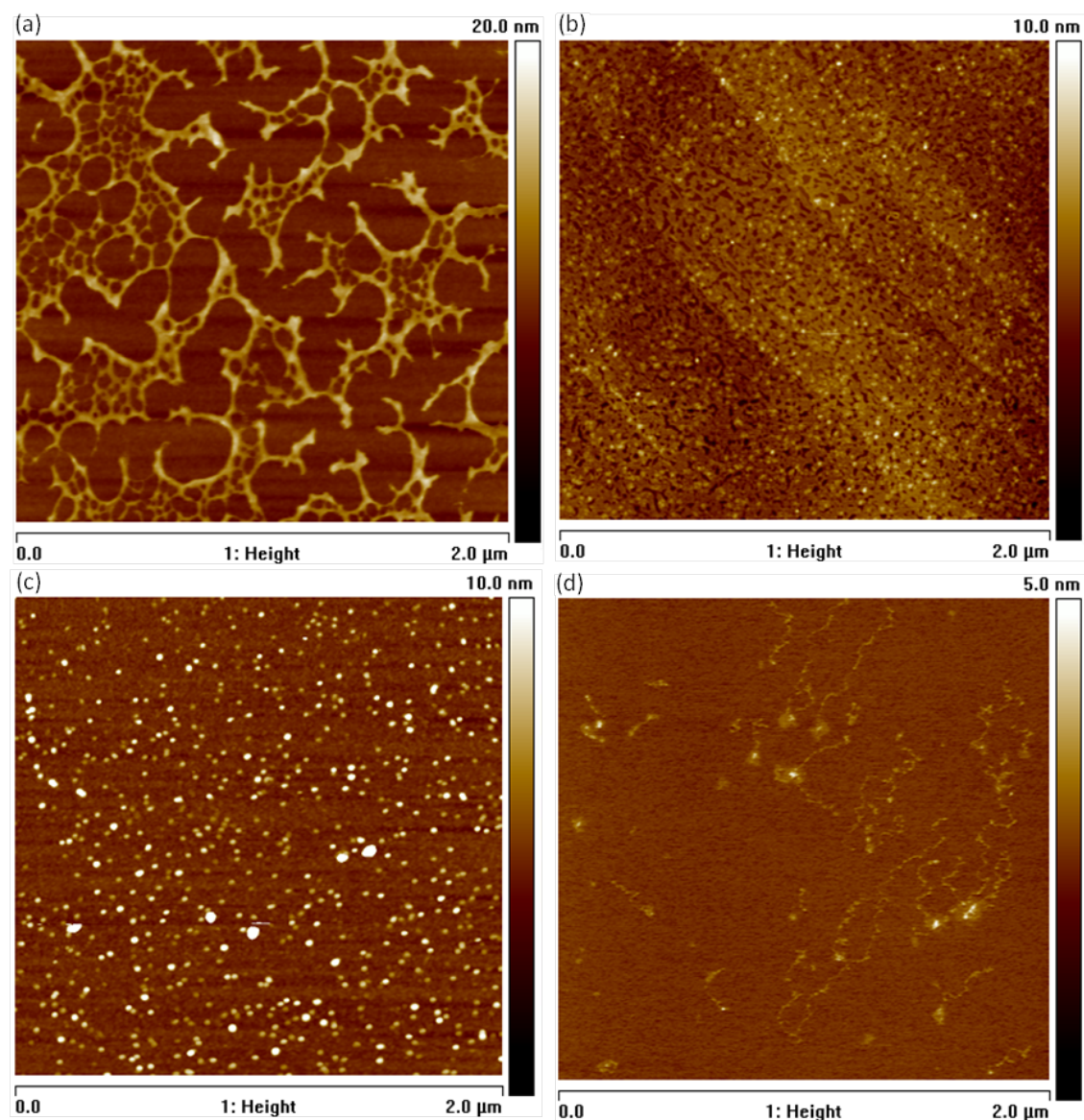


Figure 63 - Representative AFM micrographs of *Balanus amphitrite* SIPC (a) 1:500 dilution on methyl-terminated glass, (b) 1:500 dilution on highly ordered pyrolytic graphite, (c) 1:500 dilution on amine-terminated glass and (d) 1:500 dilution on Mica 1:1000.

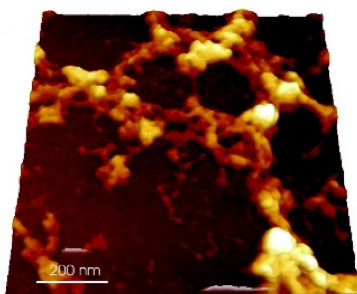


Figure 64 - High resolution three-dimensional TEM micrograph of *Semibalanus balanoides* protein adhesive showing properties similar to Figure 63(a) (from Phang et al., 2009).

5.3.2 *Transmission electron microscopy*

The holey carbon microgrid films produced very fragile grids and under the conditions used images showed features that were consistent with distortion of the film on the grid and breakage. Intact sections of broken film displayed image distortion due to stretching of the layer during breakage, as shown in Figure 65(a). When compared to the other images in Figure 65, the proteins appear stretched oval rather than round as in all other images. Arrows (<) on each of the images indicate an individual protein particle. The poor quality of images and very low number of useable grids mean that this method did not yield many images.

The use of standard carbon grids yielded better quality images. Initially native SIPC was imaged, however the glycans caused the proteins to aggregate into globular clusters or filamentous chains, see Figure 65(b). This is not ideal for further TEM analysis as individual proteins cannot be easily identified due to the particle superimposition.

Deglycosylation of the SIPC removed the complication of the aggregatory sugars ensuring that individual proteins were clearly identifiable on a surface. Protein concentration and sample conditions were optimised to give grids with a homogeneous coverage of single particles before image processing. The precipitated pellet of the SIPC, Figure 65(e), was also imaged. However, the 100% solution did not contain sufficient particles for further imaging. The deglycosylated SIPC in a 10% solution, Figure 65(d), was chosen as the most representative sample set as protein particles in the 100% solution, Figure 65(c) were too crowded to distinguish.

The preliminary images provide a qualitative assessment of the protein by TEM. Two dimensional image processing averaged individual protein particles by multivariate analysis to give some idea of the diameter and potential shape of projections. In summary the two-dimensional reconstruction of 266 individual SIPC proteins show that, under these conditions, the protein appears homogeneous and globular, has no obvious symmetry and is non-filamentous on the surface. The SIPC did form a roughly spherical, multilobed, globular structure of approximately 8nm diameter. When deglycosylated, the SIPC did not aggregate but when the sugars were present the individual proteins tended to aggregate.

In total, nine two-dimensional class averages of the SIPC were formed during image processing based on the different orientations of the protein (Figure 66). Due to limitations in the quantity of the SIPC available for analysis there were inadequate individual proteins to carry out a full reconstruction.

One of the class averages shows a twisted shape, implying the protein may be a multi-domain structure, possibly to expose more of the glycans to the environment, as shown in Figure 67.

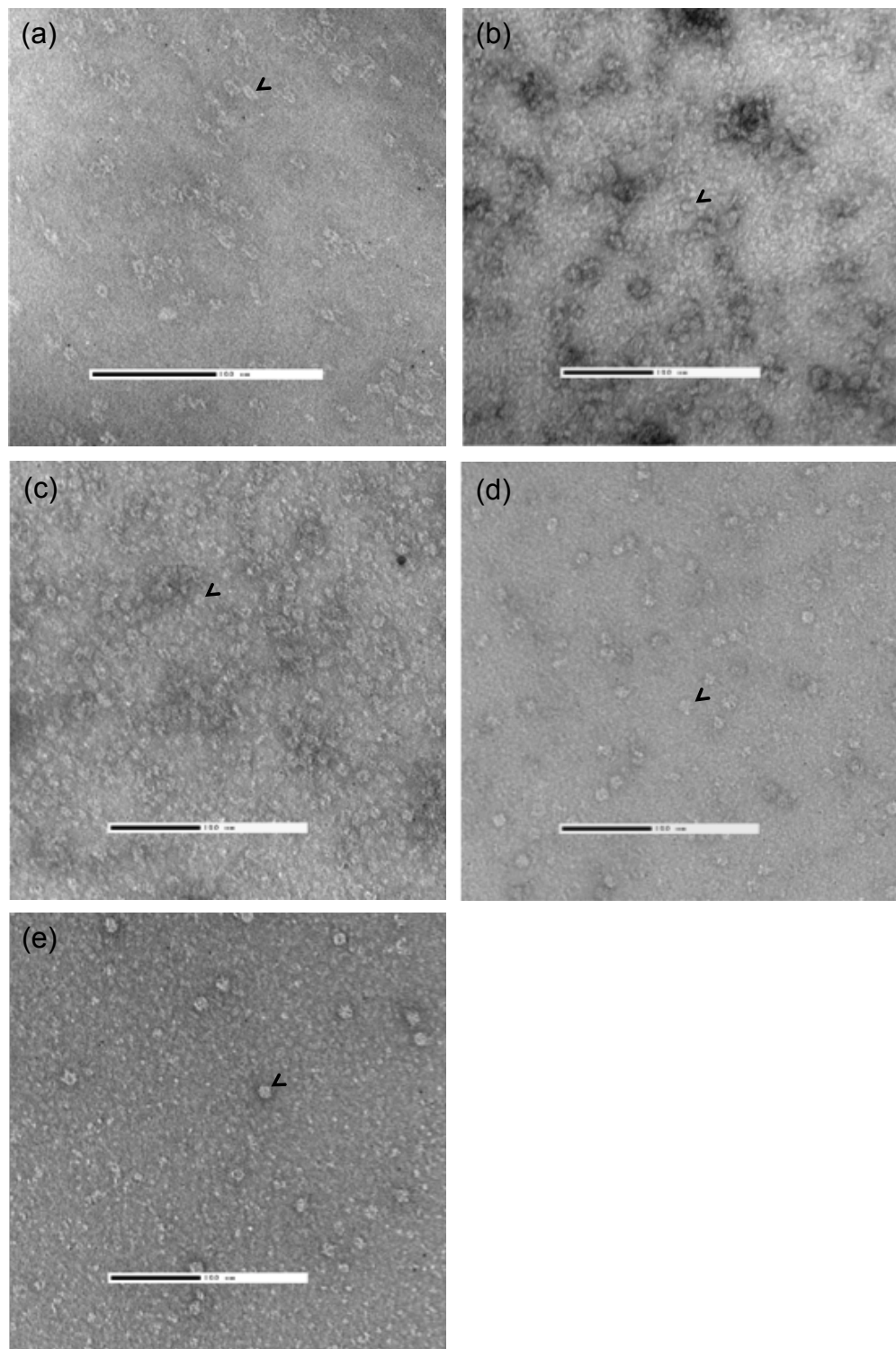


Figure 65 - A representative TEM micrograph of *Balanus amphitrite* SIPC (a) deglycosylated (100% solution) showing distortion, (b) native (glycosylated) (100% solution) showing clustering, (c) deglycosylated (100% solution) (d) deglycosylated (10% solution) and (e) deglycosylated precipitated pellet (100% solution). All scale bars indicate 100nm. < indicates an individual particle.

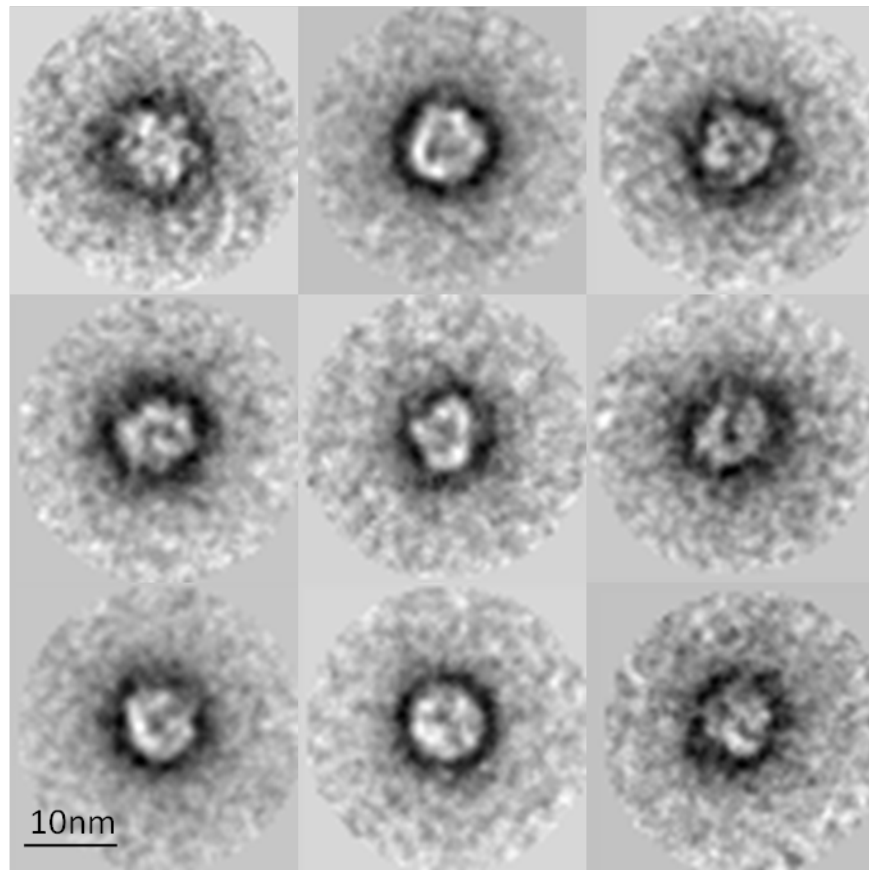


Figure 66 - Nine 2D class averages of TEM images of deglycosylated *Balanus amphitrite* SIPC from 266 particles. Each class average contains approximately 15 particles.

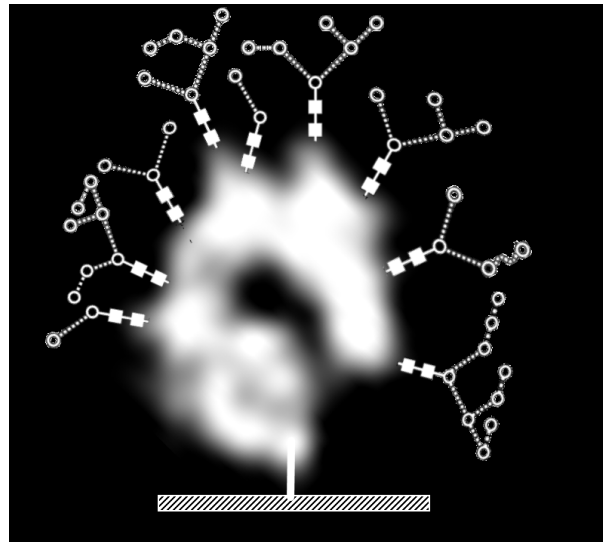


Figure 67 - A hypothetical model of *Balanus amphitrite* SIPC on a surface, showing a membrane anchor, protein backbone and exposed sugars. Components not shown to scale.

5.3.3 Protein Structure Analysis

Previously, Dreanno et al. (2006c) found that the SIPC appeared analogous to proteins of the α 2-macroglobulin family. The main difference between these is that the SIPC does not contain the 'GCGEQ' amino acid signature sequence of the thioester bond. In order to obtain a full three-dimensional reconstruction of a protein homologous to the SIPC for structural comparison, the SIPC amino acid sequence was input into a protein database. The closest homologue was the TEP1r protein with which the SIPC has 26% sequence identity. This protein belongs to a distinct group of the α 2-macroglobulin family, contains a thioester bond, and forms part of the anti-parasite immune system of the mosquito *Anopheles gambiae* (Baxter et al., 2007). This hints at the role of the protein in self/non-self recognition as the complement system functions as a defence mechanism in invertebrates (Kawabata and Tsuda, 2002). The MultAlin sequence alignment analysis and following ESPript sequence alignment are shown in Figure 68. This shows where the sequences are identical and also indicates the glycosylation sites in the SIPC and thioester bond in TEP1r.

Figure 69 shows the physical appearance of TEP1r including the presence of disulphide bonds (shown as red spheres). This along with similar folding as demonstrated in Figure 70 indicates the distinct physical similarities between the SIPC and TEP1r.

ESPrift alignment output of *Balanus amphitrite* SIPC and *Anopheles gambiae* TEPlr (Baxter et al., 2007). The alignment shows the two sequences with identical amino acids shaded in black. The sequence is divided into blocks of 10 residues, with positions 1 to 900 indicated at the top. The SIPC sequence is shown in the first column, and the TEPlr sequence is shown in the second column. The alignment is as follows:

```

1      10      20      30      40      50      60      70      80      90
SIPC  MGPPVVVLLVALATASAVKVPESGYLFTAKVQLQAGTDERACLSLFNLPGPNRALKLFVYERDVPSSLSSTLTKSDFLFETNTAVPDSV
TEPlr  ...WQFIRSRILTVIIFIGAAGHLVVGKFRIRANQOYELVLVSNFSLSKVDLLKLLSGETDNGLSVL.....NVTKMVDV

100     110     120     130     140     150     160     170
SIPC  AENGEYCFDITIFSKVVARSADMMELTAGEGVMKESVVLKRSSETFLT.VOTDKSKYOPCQKVIFRVVTL.SHDLTALNNDLNE.VWLT
TEPlr  RRMNMRMNFNMHEELTAGNYKITIDGQGFSGFKAEELVLLSKSISGLHOVDKPVFKPGDTVNFVILLDTEKPPARVKSIVYVTRD

180     190     200     210     220     230     240     250     260
SIPC  PDNIRVAQKKNVKTNTCMVLELQLTEEPFLGSMTHV.LTTQDTYKRFVVEFYVLPFFLEIEAPESLESNEKTVTVKVGAKYVFGKP
TEPlr  PQRNVIRKSTANLYAGVFESDLOIVPTMLGVNNISVEVEGEELVSKTEVVKFYVLSSTFDVOVMPSPVPLEEHOAVNLTIEANVHFGKP

270     280     290     300     310     320     330     340     350
SIPC  LIAANVSINATARGIGSQWYNNPDLRLNISDYQFSDEOCGAIFDLVVSKIGIGHRNIGGGNTVIITIDVEEOCHGLROVEVKEVSQAYS
TEPlr  V.....OCVAKVELYLDDDKLNQKK.....ELTVYKGL..OVELR.....

360     370     380     390     400     410     420     430     440
SIPC  FINLRQSDNAOKFLKFLFVYGEYTLMSMRDGKAAKNEIVKVCYFARVYKERVISDEKKPTDDPVYSTHKKYESVKTEFGYTPFFWSESE
TEPlr  FDNFAM.DADQODVRVKVSEIEQYTL...NRTVVKQSQITV.VRYARVVELIKESPOFRGLP.FKCALQFTHDGTAKGKITGVKEVSD

450     460     470     480     490     500     510     520     530
SIPC  PNRRITGGECREYKTDENCRIVYIIPQALDIDSIDLSTSTSVGGSDSSSHSTLTAFSPSHSVLSIDAHLEPELPCSGDVTVKLLSIE
TEPlr  VGFETTT.....TSNDGLIKLELOP.SEGTEOLGTFNFNAV...DGGFFFYEDVNVKVEVTDAIKLELKS....PIKRNKLMRFMVQC

540     550     560     570     580     590     600     610     620
SIPC  EGPVPAMVVKILSRRTIRACNNNTTLTPPVLP....KMGPEFFKLVYIYIKESCEVVSDSRVFKVDKCFNNTVQVSWDQKTVKPGDSA
TEPlr  TERMFTFVYVMSKGNIDAGFMRFNKKKYLQOLNATEKMIKAMLIATV..AGRTVVYDADLDFQELRNNDLSIDEQEIKPGROI

630     640     650     660     670     680     690     700     710
SIPC  SFTVRASPNVSCGISAVDKSTELGTSNQITLDTVFSKLOQFIINSFESPNQVRSDGDYCRELQLSLVDTLRSGGATVAELTGQSTPEGT
TEPlr  ELSMSGRPDGAAYVGLAAYDKALLFNKNHDLFWEDI.....

720     730     740     750     760     770     780     790     800
SIPC  PESETSGAAHSSLFIPPPTRSQRFRTRDREDAIKPFDEAGLVLVSNLALETNFCYKRVKAEKELPELTEDKIQASRDGEEELDDLDSPVPA
TEPlr  .....GQVF.....DGFHAINENEDIFHSLGLFART.....LDDI.....

810     820     830     840     850     860     870     880     890
SIPC  LAFSKESADASRFAGEGVSGGGGAAPPQEDQVDFPEAFLSIETLDAEGVKTVTSEMPDTHTSWVGSIAICTNSKDGFGISNKT.SIT
TEPlr  LFDANEXTGRNALQSGKPIGLKLV.....YRTNFOESWLNKWNVIGRSKSRKLEIVPDTHTSWVLTGFSIDPVGGLGIKPIQFT

900     910     920     930     940     950     960     970
SIPC  FPKPFFTEVSLPYSMKRGEILMSVSVFNFLLDSSLSVYLEV.GASDQVEISG..EVAMGLCIAAGRTVEVSFPVNFGLGGEVNITVTAHA
TEPlr  TVOPFYIENLPYSHKRGDAVVLQFTLFLNMLGAEYIADVTLYNVANDEFFVGRPDTLSTYKSVSVPPKVGVPISFLKARKLGEMAVRV

980     990     1000    1010    1020    1030    1040    1050    1060
SIPC  QDGYCDEGNTIAPGSDTVIRPILVVKPEGFPOEVTHSRFTCLDRDDDDHHTETVNLFPVEGLVPDSORAYFVSVIGDLTGQTQGLEGLIKS
TEPlr  KASIM....LGHEIDALEKVIKVMPESLAOPKMDTSFFCFD.DYKHOQFFFNEDINKKADNGSKKIEFRLNPNLLTMVVKLNDN.LLAV

1070    1080    1090    1100    1110    1120    1130    1140    1150
SIPC  PTGAGEPNMTITVPNIYIRRYLETTCOLNERQRRLHNNKSGYORLFRFRVYDGSFSSYGNEDPQGSMMLTAFVVKAFREASEYI.EID
TEPlr  PTGCGEQNNVVKFVPNLVLVDYLATCSKEQHLDKATNLLROGYQONMRRRQTDGSGFVW..EKSGSVVLTAFVATSMQATASKMNDID

1160    1170    1180    1190    1200    1210    1220    1230    1240
SIPC  ETIINKAKDWILKKONTTCQFPRFGLIHHELKGGTERGGEAALTAFVMLALKDIATTNE..LANGFACLEDGELLPNKTLTSEILLAY
TEPlr  AAMVEKALDWLASKOHSRFDDETGVKVVHDMOGGLRNGVALTSVYLTALLENDDIAKVKKHAVVIONGMNYSNOTAFINNP.YDLSIATY

1250    1260    1270    1280    1290    1300    1310    1320    1330
SIPC  TYLNMQODVKGRLVNKLMSKAKREGDDIILYWEGRDLSLFGGSRRAVDVEMTAYMALSLMHISGKGNMEEAARAIRWINTORNSNGGFKST
TEPlr  AMMLNGHTMKKFAIDKLIDMSISDNKKKERVW.....GTTNQIETATAYALLSEVMAE...KYLDGIPVMNWLNVNQRVYVTSFPRPT

1340    1350    1360    1370    1380    1390    1400    1410    1420
SIPC  QDTIVAVEALSEFASRTFASDLATSVSVTAGGETVQRMVDGDNRLLYQESKVPDLTLPGTMNFDVSPPGCVVYQSIFRFSSTLEVPDPAPF
TEPlr  QDTFVGLKALTCLAEKISPSRNDYTVOLKYKKNTKYFNNINSEQIDVQNFLEIPEDTKK..LEINVGGIGFGLLEVYIYQDLNLVNFENRF

1430    1440    1450    1460    1470    1480    1490    1500    1510
SIPC  SGVAAKKKRT.GVLELVCTSFRLN..SGAVDRAITETLPSGYVAVDSTLRDLRRGSVAVRVSEIKEC..KVIFTLQGVADKTCLEFR
TEPlr  KDLEKONTGSDYELRLRVCANIPELTDSQSNMALIEVTLPSGYVVDNRNPISQTTVNPIONMEIRYGGTSVVLVLYYKMGTERNCFTVT

1520    1530    1540
SIPC  TIQENEVEQLKPSIVHVVHDFYRPEERNIQEYELTPAA.....
TEPlr  AYRRFKVALKRPAVYVVVYVYNTNLNAIKVYVVDKQNVCEICEEDCPAECKK

```

Figure 68 - ESPrift alignment output of *Balanus amphitrite* SIPC and *Anopheles gambiae* TEPlr (Baxter et al., 2007). Black shading denotes identical amino acids when comparing the two sequences giving the 26% homology. The ▲▲ indicates the NX₂P/S/T sequence for glycosylation and □ represents the 'GCGEQ' sequence indicative of a thioester bond.



Figure 69 - PyMOL representation of *Anopheles gambiae* TEP1r (Baxter et al., 2007) showing disulphide bonds as red spheres

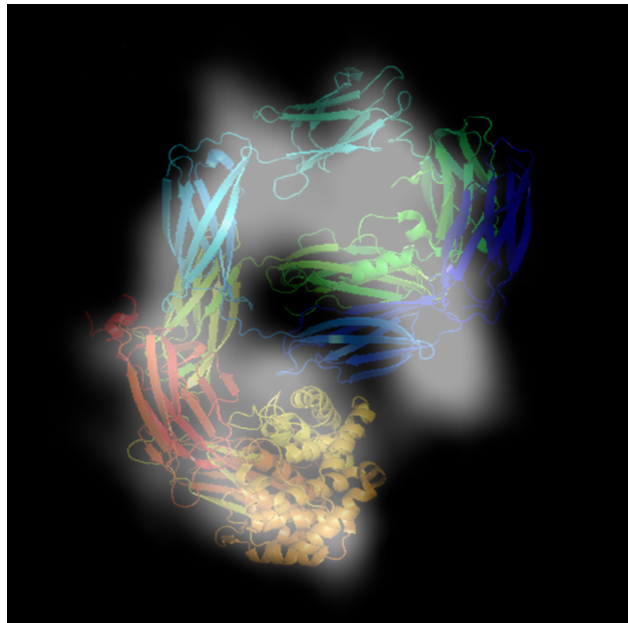


Figure 70 – TEM image of *Balanus amphitrite* SIPC (white shadow) and *Anopheles gambiae* TEP1r (colour) (Baxter et al., 2007) overlaid show the structural and folding similarities

As indicated in Figure 71 there are twenty cysteines (shown in green) within the SIPC amino acid sequence, potentially forming ten disulphide bonds. However, there are only three subunits, implying only two disulphide bonds between four cysteines. Yet, after denaturing with β mercaptoethanol in an SDS-PAGE gel, the SIPC shows there are also several other smaller peptides identified on the gel (See Figure 20). It may be that the three subunits are the most dominant cleavage sites on the SIPC but there are also other disulphide bonds that break to form the other peptides. Appendix C shows the DiANNA cysteine predictions. In brief, when applied to the SIPC sequence, it is indicated that the SIPC protein has 20 cysteines that form 10 disulphide bonds, with the connectivity pattern 1-16, 2-15, 3-13, 4-14, 5-7, 6-10, 8-18, 9-17, 11-12, 19-20 (between cysteines 42 and 1225, 1178 and 635, 97 and 603, 1019 and 1405, 260 and 309, 950 and 526, 984 and 876, 400 and 766, 458 and 683, 1444 and 1506). Due to the splitting of the SIPC into three major subunits, it was proposed that the SIPC contained only two disulphide bonds. However as the prediction has shown, all 20 cysteines present are expected to form disulphide bonds.

```

MGGPVVLLVALATASAVKVPESGYLFTAPKVLQAGTDERACLSLFLNLPGNRALKLKFY
ERDVPSSLSTLTKSDFLLFETNTAVPDSVAENGEYCFDITIPSKVVARSAADMHELTAG
EGVWKEESVVTLKSETFLTTLVQTDKSKYQPGQKVLFRVVTLSHDLTALNNDLNEVWITP
DNIRVAQWKNVKTNTGMVQLELQLTEEPPLGSWTIHVLTQDITYTKRFTVEEYVLPTEFEL
EIEAPESLESNEKTVTVKVCAKYTFGKPLIAANVSINATARGIGSWQYNNNPDLRNISD
YQFSDEQGCAIFDLVSKIGIGHRNIGGNTVITIDVEEQGTGLRQVEVKEVSQAYSFI
NLRQSDNAQKFLPKPLPFYGEYTLNMRDGKAAKNEIVKVCYTAKYKERVISDEKKPTPDD
PVYSTHKKYESHVKTEFGYTPFFWETSEPNRRTTGGECREYKTDENGRIVYYIIPPQAEDI
DSIDISTSTSVGGSDSSSHSTLTAFSPSHSYLSIDAHELPEQLPCSGDVTVKLLSTEEG
PVPAMVYKILSRGKIIKAGNMNTNTLTFPVLPMGPEFKLLVYYIKESGEVVS2SRVFKV
DKCFPNTVQVSWDQKTVKPGDSASFTVRASPNSCGISAVDKSTELLGTSNQITLDTVFS
KLQQFIINSFESPNQVRSDGDYCRELQLSLVDTLRSGGATVAELTGQSTPEGTPESETSG
AAHSSLFIPPPTRSQRFR2TDREDAIKPFDEAGFLVLSNLALETRPCYKRVEAKELPELTE
DKIQASRDGEEELLDDLDSPVPALAFSKESADASRFAAEGGVSGGGGAAPPQEDQVRDFF
PEAFLFSIETLDAEGVKTVTSEMPDITISWVGSACTNSKDGFGISNKTSITTFKPPFFTE
VSLPYSMKRGEILSMSVSVFNFLDSSLSVYLEVGASDQYEISGEVAMGLCIAAGRTEVRS
FPVNFLGLGEVNITVTARAQDGYCDEGNTIAPGSDTVIRPIVVKPEGFPQEVTHSRFICL
DKDDDDHHTETVNLVPPEGLVPDSQRAYFSVIGDLLGQTFQGLEGLIKSPTGAGEPNMIT
LVPNIYIRRYLETGTGLNERQRRQLEHNMGSGYQRQLRFRRYDGFSFYSGNEDPQGSMWL
TAFVVKAFREASEYIEIDETIINKAKDWILKKQNTTGCFPRFGELIHKELKGGTERGGEA
ALTA2FVMLALKDIATTNELANGFACLEDGLLLPNKTLYSEILLAYTYLNMGDVKGERLV
NKLMSKAKREGDDILYWEGDRDSLFGGSRAVDVEMTAYMALSLMHISGKGNMEEAARAIR
WINTQRNSNGGFKSTQDTIVAVEALSEFASRTFASDLATSVSVTAGETVQRMVDGDNRLLY
QESKVPDLTLPGTMNFDVSPPGCVVYQSIFRFSSTLEVDPAPFSLGVAACKRGRTGYE
LEVCTSFLRNSGAVDRAILETELPSGYVAVDSTLRDLRRGSAVRSYEIKEGKVIFTLQGV
AEDKTCLEFRIIQENEVEQLKPSIVKVHDFYRPEERNIQEYELTPAA

```

Figure 71 - FASTA amino acid sequence of *Balanus amphitrite* SIPC from Dreanno (2006c) showing the possible glycosylation sites. NX_pS/T sequons are shown in blue with asparagines predicted to be *N*-glycosylated shown in red. In addition, possible disulphide bond sites (cysteines) are shown in green.

Figure 72 shows the results of the DomPred protein domain predictor. The graph is derived from the N- and C-termini positions from PSI-BLAST local alignments as outlined by Marsden et al. (2002). Here, peaks in the graph show regions where sequence discontinuities occur, and consequently indicate predicted boundaries. In this case 8 domains are predicted with the boundaries at residue positions 292, 504, 652, 849, 936, 1118, 1343 and 1449. Following this domain prediction it was possible to complete Secondary Structure Element Alignment where structural relationships within the sequence are detected and folding within the protein predicted. This is shown in Appendix D.

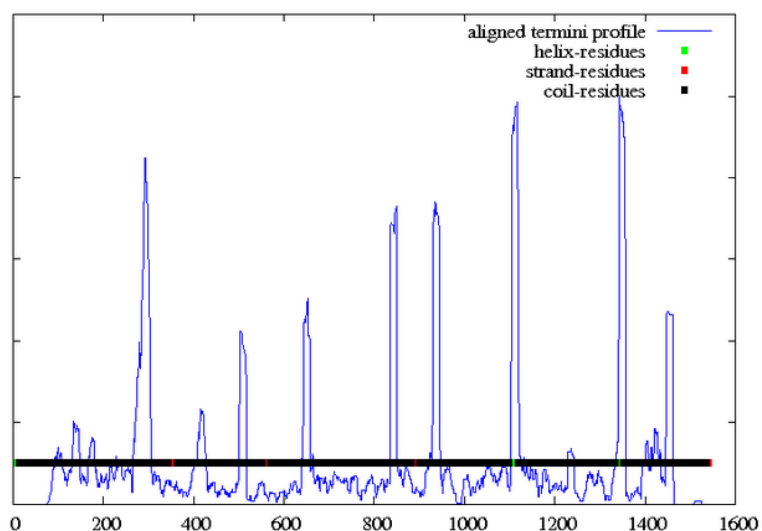
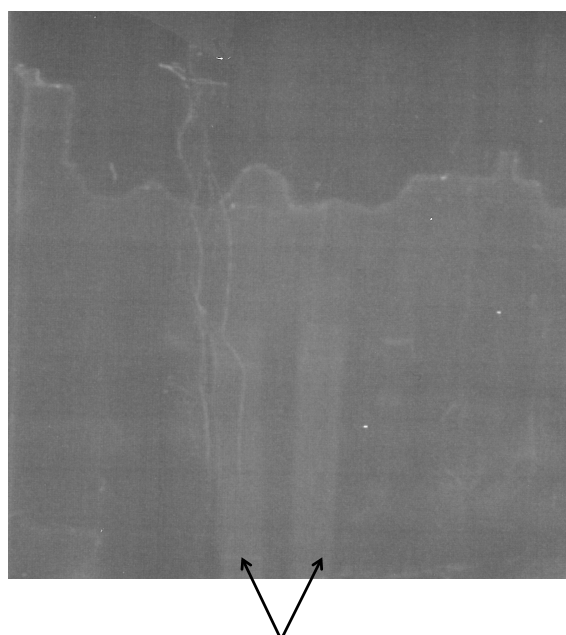


Figure 72 - The DomPred prediction of sequence discontinuities (Marsden et al., 2002) in the *Balanus amphitrite* SIPC amino acid sequence, indicating where domains occur. The x-axis represents the amino acid sequence.

The SDS-PAGE gel of native, denatured and deglycosylated SIPC to illustrate the shift in band location following the removal of glycans from the protein subunits was unsuccessful as shown in Figure 73.



Fluorescent bands

Figure 73 - Pro-Q Emerald stained SDS-PAGE gel of native, denatured and deglycosylated *Balanus amphitrite* SIPC, showing some fluorescence but no band detail.

However, using the *B. amphitrite* amino acid sequence, as detailed by Dreanno et al. (2006c), some manipulation of the SIPC protein can be achieved. The ExPASy server allowed access and manipulation of the amino acid sequence, showing that the SIPC had a deglycosylated mass of 170,717 Da and an amino acid length of 1,547. Also in agreement with previous research, 7 possible *N*-glycosylation sites were identified thorough the $\text{NX}_{\neq}\text{P}\text{S}$ or $\text{NX}_{\neq}\text{P}\text{T}$ rule. Figure 71 shows the position of these sequons identified as glycosylation sites in *B. amphitrite* SIPC. As well as cysteines (marked in green) as the thiol groups from disulphide bonds between two cysteines form a cystine. When denatured using β -mercaptoethanol, three subunits form, indicating there are two disulphide bonds in the SIPC. Consequently not all of the 20 cysteines are used to form disulphide bonds. These bonds are particularly important in the display of glycans on the protein core as they create the particular folding found in the SIPC by forming links between different sections of sequence.

Further research into the protein and disulphide bonds in Chapter 5.3.3 shows the likelihood of the sequons being glycosylated. The ‘*N*-glyc agreement result’ is an indication of the possibility of an *N*-glycosylation where + shows predicted *N*-glycosylation and – would mean a negative site. The agreement result is a combination of the potential (the averaged output of nine neural networks) and the jury agreement (how many of the nine networks

support the prediction). For + (> 0.5 only), ++ (> 0.5 and (9/9) or >0.75), +++ (> 0.75 and (9/9)) and ++++ (> 0.90 and (9/9)).

Figure 74 illustrates predicted *N*-glycosylation sites across the protein chain; here the graph x-axis represents protein length from N- to C-terminal. A position with a potential for *N*-glycosylation (vertical blue lines) crossing the threshold (horizontal red line at 0.5) is predicted to be glycosylated. In the case of *B. amphitrite*, all potential sites cross the threshold line and consequently all are predicted to be *N*-glycosylated. Sequons indicated with + or above have high specificity and consequently it is very likely that all seven sequons are glycosylated.

Similarly, the ‘*O*-glyc agreement result’ is an indication of the possibility of *O*-glycosylation. The score is the result from the best general predictor. If the score is greater than 0.5 the residue is predicted as glycosylated. The greater the score the more confident the prediction. As indicated in Figure 75, two *O*-glycosylation sites are predicted, both threonine, at position 205 and 718 with scores of 0.567 and 0.547 respectively. Likewise, the *C*-glyc predictor indicates potential *C*-glycosylation. As shown in Figure 76, no site in the SIPC amino acid sequence achieved a score above the required 0.5 threshold and thus there is no predicted *C*-glycosylation.

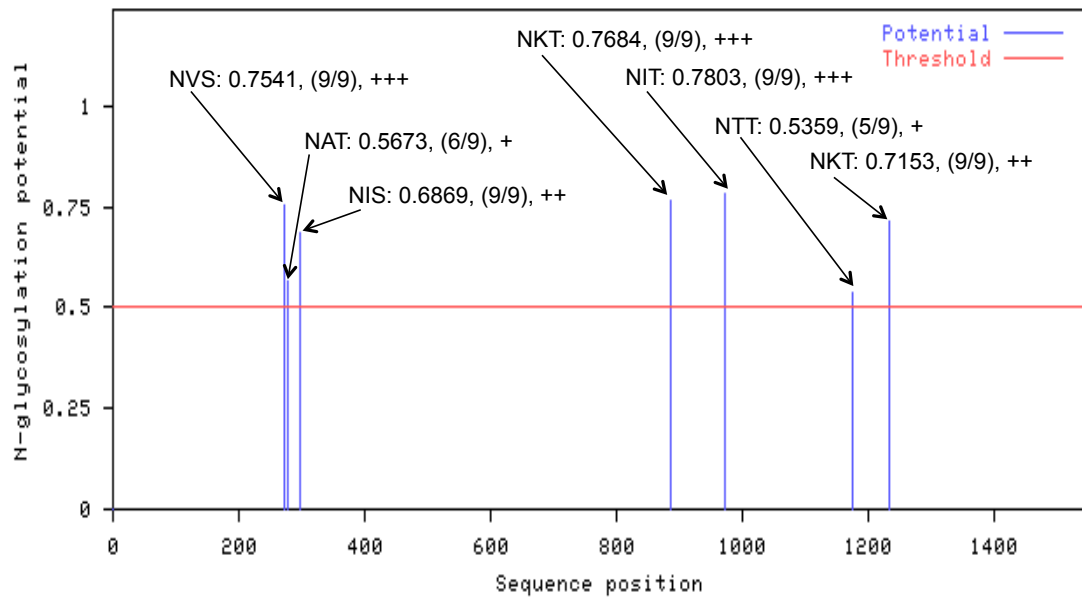


Figure 74 - Graphical output of the potential *N*-glycosylation sites on *Balanus amphitrite* SIPC from NetNGlyc 1.0 (Gupta et al., 2004). The blue line indicates the potential for the site and the red line shows the potential above which glycosylation is considered likely. The site potential, jury agreement and consequent *N*-Glyc agreement result are shown by each site.

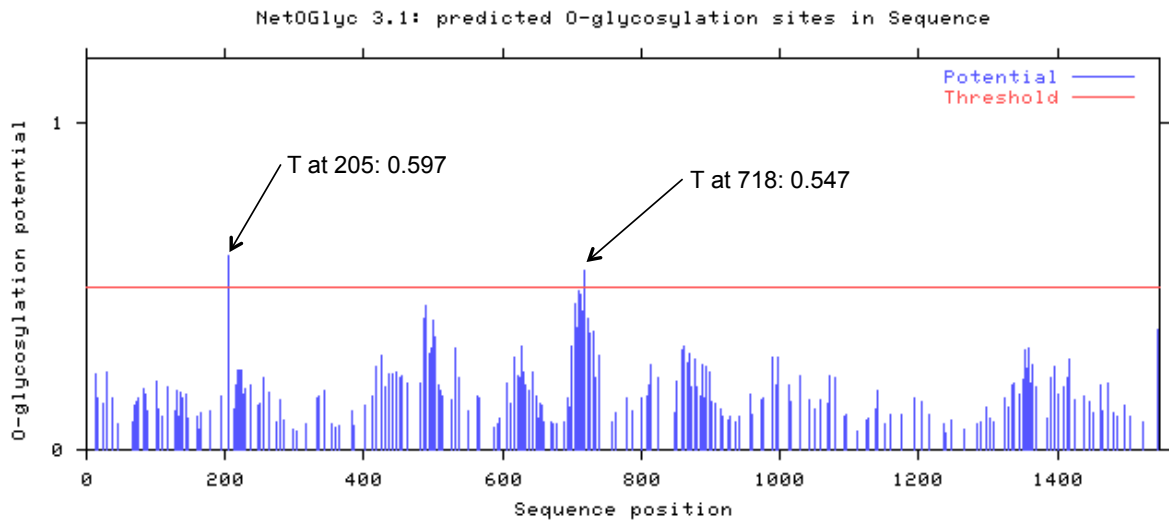


Figure 75 - Graphical output of the potential *O*-glycosylation sites on *Balanus amphitrite* SIPC from NetOGlyc 3.1 (Julenius et al., 2005). The blue line indicates the potential for the site and the red line shows the potential above which glycosylation is considered likely. The amino acid (T or S), position in the sequence and score (>0.5 is predicted to be glycosylated)

```
gff-version 2
source-version netCglyc-1.0b
Type Protein
```

seqname	source	feature	start	end	score	+/-	?
Sequence	netCglyc-1.0b	C-manno	124	124	0.304	.	.
Sequence	netCglyc-1.0b	C-manno	176	176	0.226	.	.
Sequence	netCglyc-1.0b	C-manno	188	188	0.198	.	.
Sequence	netCglyc-1.0b	C-manno	213	213	0.355	.	.
Sequence	netCglyc-1.0b	C-manno	286	286	0.286	.	.
Sequence	netCglyc-1.0b	C-manno	444	444	0.208	.	.
Sequence	netCglyc-1.0b	C-manno	612	612	0.281	.	.
Sequence	netCglyc-1.0b	C-manno	870	870	0.270	.	.
Sequence	netCglyc-1.0b	C-manno	1139	1139	0.232	.	.
Sequence	netCglyc-1.0b	C-manno	1168	1168	0.168	.	.
Sequence	netCglyc-1.0b	C-manno	1277	1277	0.155	.	.
Sequence	netCglyc-1.0b	C-manno	1321	1321	0.190	.	.

Figure 76 - Tabular output of the potential C-glycosylation sites on *Balanus amphitrite* SIPC from NetCGlyc 1.0 (Julenius, 2007). Scores above 0.5 are predicted to be glycosylated.

5.3.4 Mass spectrometry of proteins and N-glycans

Following the prediction of cleaving sites and treating the SIPC protein with Trypsin, Lys C and GluC, and Arg C, mass spectrometry using MALDI TOF/TOF was undertaken. In regard to cleavage sites around the N-glycosylation sites, ArgC was predicted to be the most useful as it cleaves between each of the glycosylation sites except the first two, which are very close together. In all of the MALDI TOF/TOF spectra, the only peaks present were those indicative of the presence of the matrix and no peptides. This was the case for all traces carried out on the digested protein, leaving these results inconclusive. This was also the case with the control samples run on the machine, (myosin, phosphorylase B and glutamic dehydrogenase). These known spectra also gave no peaks other than the matrix indicating instrumentation error rather than a sample issue.

5.4 Discussion

Despite the problems surrounding the addition of lectins to the SIPC during AFM, some progress has still been made in characterising the SIPC. The methyl-terminated glass showed globular proteins with a high adsorption and affinity of the SIPC to the surface. The network formed under these conditions was similar to that of the aggregated fibrillar cyprid footprint deposit structures shown in Phang et al. (2007) and Phang et al. (2009) as shown in Figure 64.

The amine-terminated glass showed less adsorption of the SIPC than the methyl-terminated glass but did show globular proteins. Previous research showed that cyprid footprints adsorbed more thickly to amine- than methyl-terminated glass but this was not the case here. However, Phang et al. (2009) carried out studies on *Semibalanus balanoides* footprints, thus there is likely some interspecies difference. It was unclear if the images produced showed a monolayer with globular peaks or a homogeneous layer with high regions. The mica surface required an extra incubation time of 4.5 hours to see adsorption and even at this point had slow and low-density adsorption. The proteins are elongated on the surface showing that certain domains of the protein have a strong affinity for the surface; however this should lead to more protein accumulating on the surface. Figure 65(b) shows the aggregated proteins of the native SIPC under TEM, this shows similar properties to the AFM findings, Figure 63(b), where globular groups of proteins were observed. Figure 67 shows a tentative image of how the SIPC could be orientated to expose the glycans. Although this is only the beginning of the process to understand the detailed protein structure of the SIPC, starting to visualise structure in relation to glycans provides a valuable starting point for increasing understanding of how the SIPC functions.

This discussion would not be complete without reference to the previous work on the protein structure of the SIPC by Dreanno et al. (2006c). In this paper, the SIPC was thought to contain 7 potential *N*-glycosylation sites, this has been shown again in Figure 74.

In addition the potential presence of *O*-glycans (Figure 75) and the absence of *C*-glycans (Figure 76) has also been demonstrated using prediction software. Dreanno et al. (2006c) also compared directly to an α_2 -macroglobulin, a group of large plasma proteins produced by the liver. The difference in immediate comparison is most likely due to the use of different protein databases. However, α_2 -macroglobulins are a subgroup of the thioester-containing protein family, thus both results agree that the SIPC is similar to TEPs. Ting and Snell (2003) similarly discussed a contact protein from the copepod *Tigriopus japonicus* which also bore a likeness to the α_2 -macroglobulin family. This contact protein has been implicated in mate recognition, similar to how barnacles use the SIPC to identify conspecifics.

The comparison of this sequence to a database by Dreanno et al. (2006c) highlighted the α_2 -macroglobulin family as a group of homologous proteins. This research has developed

this further by carrying out advanced database and software manipulation of the sequence to discover additional information about the protein. The combination of the DiANNA and DomPred software predicted 10 di-sulphide bonds and 8 domains within the SIPC. Although this would lead to more subunits than previously described, this could explain the three major subunits as well as the formation of smaller peptides during denaturing as shown in Figure 20. The secondary structure alignment (Appendix D) shows possible coils, strands and helices within the secondary structure of the SIPC. This in conjunction with future structural work may produce an accurate three-dimensional representation of the SIPC.

Unfortunately, as the mass spectrometry conducted during this research was inconclusive, it was difficult to discover some intricacies of the SIPC glycosylation sites. Using mass spectrometry, it was hoped to find which glycans were present at which glycosylation site, if the site was occupied at all as only two-thirds of potential sites are taken (Apweiler et al., 1999) and to also show which sites are on which subunit. However, as the amino acid sequence showed 7 potential glycosylation sites on the SIPC protein and the mannose ladder provides more than 7 mannose peaks; it is thought that the distribution of glycans on the protein is likely to be heterogeneous, i.e. there are different sugars in different sites on different protein molecules.

Despite laying the foundations for further study into the protein structure of the SIPC, this research has been limited. Due to the protein adopting a preferred orientation on the TEM grids under the sample conditions used, it was not possible to get a suitably homogeneous sample. Owing to the limitations in the quantity of the SIPC (both native and deglycosylated) available for analysis, only a small number of images (266) were taken. During a thorough assessment to create more accurate two or three-dimensional images, thousands of images would be analysed. The small amount of sample also limited the type of TEM employed for analysis, cryoelectron microscopy would be preferential. Confirming the crystal structure was also not possible for the same reasons; 40mg of native SIPC was required. This would require an impractical starting mass of around 7kg of raw material (the adult barnacles). However, if future research focussed on an abundant, locally available species such as *Semibalanus balanoides*, this becomes a realistic proposition.

A three-dimensional molecular model reconstruction of the SIPC through cryoelectron microscopy and crystallisation of the SIPC remains elusive. However, the study of deglycosylated SIPC by TEM and comparison of the amino acid sequence has taken the first steps to understanding the protein structure of *Balanus amphitrite* SIPC. Although the results presented are only initial analyses of the protein, this research presents the first view of the SIPC structure and provides a valuable starting point for increasing understanding of how the SIPC functions.

Chapter 6. Discussion

6.1 Introduction

This research set out to enhance the understanding of the gregarious mechanisms used by barnacles during settlement. This thesis has covered areas from basic barnacle biology to the financial consequences of hard fouling and the methods that have been employed to reduce them.

A series of preliminary experiments involving adult barnacles and the SIPC were carried out initially to provide background to the topic and barnacle species studied. The video tracking experiments showed the effect of an adult barnacle on cyprid exploratory behaviour. The adult barnacle caused cyprids to travel further and turn more when compared to the resin mimic or empty dish. Interesting results were obtained from the settlement assays associated with the dishes used for tracking experiments. The presence of an adult has distinct effects on the settlement pattern of cyprids, where the cyprid settled on or immediately next to the adult. The nitrocellulose spot assay showed significantly higher settlement on the SIPC when compared to another glycoprotein. These experiments highlighted the importance of the SIPC in barnacle gregariousness and ensured the following experiments were based on a solid foundation.

6.2 New findings in context

Referring back to the research rationale from Chapter 2.1, the themes and novelty of this research can be highlighted. The first research steps were carried out in Chapter 3.2.1-3.2.9 and focused on the purification and isolation of *B. amphitrite* SIPC. This allowed the SIPC-containing fractions to be visually detected by antibody immunoblotting. The established nature of this protocol ensured that the fractions collected and analysed for carbohydrate characterisation were definitely the SIPC.

The next steps towards testing the hypothesis set out to fully characterise the *N*-glycan moiety of the SIPC carbohydrates. *N*-glycans within the SIPC were deduced to be a high mannose ladder (M2 to M9) using JBM exoglycosidase digestions. This was in agreement with mannose binding lectin results published by Matsumura et al. (1998a). In addition, the

occurrence of α -1-6 core fucose monosaccharides were found using BKF digestions. This is similar to the results published by Matsubara et al. (2005) where high mannose chains with core fucosylations were found in *Megabalanus rosa* haemolymph.

Following the characterisation of the *N*-glycans as a high mannose ladder, experiments were carried out to assess the settlement-inducing efficacy of mannose in solution. These results involved both mannose and galactose and showed that the presence of mannose increased settlement more than galactose. The presence of galactose seemingly had no effect on the cyprids as the levels of settlement observed were comparable to those in artificial seawater. These results corroborate the findings of Khanderparker et al. (2002). In addition the SIPC was also diluted to observe the effect on settlement, as shown by Matsumura et al. (1998a). These results are in agreement with previous research as increasing the concentration only increases settlement. There did not appear to be a peak and decline where excessive SIPC caused a decline in settlement. Also in accordance with observations on the effect of time on settling cyprids, the amount of a cue required after 48 hours is less than that required at 24 hours due to the inductive effect of the newly settled cyprids providing an additional cue. This was in fact the case in all treatments as the positive feedback loop provided by settled cyprids on non-cueing surfaces creates a signal for others, masking the effect of the treatments being tested.

The final step in testing the hypothesis was to develop and test carbohydrate-functionalised polymers that mimic the SIPC settlement-inducing effect. This was carried out using surface-bound commercially-available polymers based on similar work by Johnson (2009). These surfaces were characterised using contact angle, ellipsometry and X-ray photoelectron spectroscopy. In addition, the biological activity of these surfaces was tested using bioassays. In this case the drop assay technique was employed. The contact angle data is more qualitative but provided an indication of the progression of surface modification. The contact angles change as expected with clean glass having a low angle, aminated increasing considerably, dropping for Gantrez[®], increasing again for the aminoethanol and decreasing for the carbohydrates. Ellipsometry provided a guide to the depth of layers of surface modification. This data was most useful for confirming the addition of Gantrez[®] to the surface as this led to the largest increase in depth. X-ray photoelectron spectroscopy supplied the most quantitative confirmation data by comparison. The wide scan survey

spectra showed the expected nitrogen, oxygen, carbon and silicon peaks as well as others. Auger peaks are commonly found on XPS spectra so the presence of these is not unexpected. There are unwanted and unexpected peaks on the wide scan survey, indicating the presence of fluorine and potassium. These are most likely from boron trifluoride diethyletherate and potassium bicarbonate, used during the modification process. There are also unidentified peaks, attributed to non-elemental peaks from the potassium bicarbonate. All of the high resolution spectra for the chosen elements; carbon, oxygen, nitrogen and silicon were as expected except carbon. This spectrum contained the peaks associated with the potassium carbonate contamination.

Following the chemical and physical assessments confirming the surface modification, the surfaces were subjected to bioassay techniques. The drop assay involving 0-day-old cyprids showed that there were differences between the different treatment surfaces. Settlement was high on the charged aminated and Gantrez[®] surfaces and OH terminated aminoethanol surface. These results were expected from previous observations on cyprid response to these surfaces. More importantly, it was shown that mannose-terminated surfaces displayed more settlement-inducing effect than the glucose and galactose surfaces. Due to the nature of the inductive feedback loop of settling cyprids, none of these results were significant due to the large standard errors and larval quality and reliability.

A mannose-terminated surface provided a stronger settlement cue than mannose in solution, but both were weaker than the native SIPC. There may be several reasons for this; the structure of native SIPC with the core protein and associated glycans is very flexible and allows the exposed carbohydrates to move considerably. An attempt at this flexibility was achieved using a linker in the surface modification. However, due to solubility issues only a short linker (aminoethanol) was used, thus reducing the flexibility of the structure from the original linker (aminohexanol). Obviously the carbohydrate functionalised polymers used in the SIPC mimic only form a much simplified imitation of the glycans present and may miss something fundamental which remains as yet unknown. This may be the role of the core fucoses. It was first considered that the monofucosylated glycans would not be readily displayed to the searching cyprids, due to the presence in such small proportions, and the fact that there are only single fucoses along with the internal position of the fucose on the core GlcNAcs. This may particularly be the case as there are between 2 and 9 mannoses to

which the cyprids would first make contact. However, there is certainly an aspect of the native SIPC not mimicked by the mannose functionalised Gantrez[®].

Adding to the knowledge of the protein structure would assist with the improvement of more accurate SIPC mimics, leading on to the final part of this research, which highlighted the importance of developing further understanding of the SIPC protein core. This approach used structural techniques to explore the core protein. The atomic force microscopy (AFM) techniques used on native SIPC showed similar network of aggregated proteins to that of the cyprid footprint protein when deposited on hydrophobic surfaces. Transmission electron microscopy produced results consistent with the AFM where the SIPC was native and to remove the aggregating tendencies the SIPC was deglycosylated. The class averages formed from the individual SIPC proteins give a suggestion of what the SIPC protein molecule looks like in two-dimensions.

Comparing amino acids using the online protein data base added to the work of Dreanno et al. (2006c). This previous research confirmed the similarity to $\alpha 2$ macroglobulins, part of the thioester containing protein family. This raised the parallels with the self/non-self recognition complement-like proteins such as the mate recognition contact protein found in *Tigriopus japonicus* (Ting and Snell, 2003). Research during this project used other online sequence manipulation tools to predict further structural components of the SIPC. This led to the prediction of 10 potential disulphide bonds and around 8 possible subunits (see Chapter 5.3.3). This is contrary to the three subunits and consequently two disulphide bonds, which had previously been observed (see Figure 12). However, the three main subunits may be present as shown in the SDS-PAGE gels but there may be other smaller peptides that are formed when stronger bonds break. An example of the possible presence of these smaller peptides is shown in Figure 21.

The original nature of this research extends initially to the species studied, with the characterisation of the SIPC glycans using established protocol. However the production of the SIPC mimics using surface bound carbohydrate functionalised polymers through the methods developed is entirely novel.

6.3 Future research

As with many research projects, this study has uncovered many more questions and possibilities for future work than it has answered. Further studies and the potential approaches these could take are outlined below.

The focus of the research presented in this thesis was to characterize the carbohydrate component of the barnacle SIPC. The approach focused upon the use of PNGaseF for the release of *N*-Glycans due to its ease of use accompanied by the fact that the digestion is performed on the glycoprotein level, which facilitates further proteomic, or protein characterization as required. A limitation of PNGaseF is that it only releases mammalian type *N*-glycans; those either without or those containing an alpha 1-6 linked fucose residue on the reducing terminal GlcNAc residue. As barnacles have more sequence homology with insects, this can form the basis of future work wherein the use of other exoglycosidases such as PNGaseA, that releases *N*-linked glycans either without or containing an alpha 1-3 or 1-6 linked fucose residue on the reducing terminal GlcNAc. PNGaseA digestion is performed on the glycopeptide level, which limits further protein structural analysis. For this reason alone, it was not investigated in the current study.

The presence of *O*-glycosylation and its role in settlement and adhesion is also worthy of investigation. *O*-glycans play a crucial role in the formation of mucinous gels in mammalian systems that provide surfaces capable of specific functions, similar to the role of the SIPC. As demonstrated by the *N*-glycosylation analysis performed here which revealed the presence of oligomannose glycans in agreement with previous hypothesis, the role of *O*-glycans on SIPC is also a focus for future work as *O*-glycans are predicted to be present. Chemical methods are required for *O*-glycan release, which also result in the degradation of the polypeptide backbone limiting any possible protein structural characterization. Also *O*-glycans are potentially present in a much lower carbohydrate to protein ratio than their *N*-link counterparts significantly more SIPC would be required.

As the generation of a crystal structure for SIPC remains elusive, proteomics technologies using a bottom-up approach focusing on characterization of the peptides and glycopeptides present in the SIPC accompanied by a high resolution top-down intact proteomic analysis of the SIPC would be beneficial. Site specific glycosylation analysis would add a further degree of localized structural information (Bones et al., 2011). Such information would

allow for the confirmation of the amino acid composition and allow for the identification of post translational modifications such as both *N*- and *O*-glycosylation and disulphide bond formation based upon the experimental conditions chosen (i.e. reducing or non reducing conditions prior to digestion in the bottom-up protease approach). Advances in proteomics technologies including new methods such as intact protein complex mass spectrometry (Taverner et al., 2008) or hydrogen-deuterium exchange mass spectrometry (Engen, 2009) could further our understanding of the molecular confirmation of the SIPC in the absence of a crystal structure.

It has been commented that mannose is ubiquitous in the environment and consequently why would mannose cue settlement. This research has produced supporting evidence with regard to the efficacy of mannose as a cue. This was in the form of settlement experiments using carbohydrates in solution and bound to a surface. However, although mannose did increase settlement, native SIPC appears more effective. This may be due to the molecular shape or display of the carbohydrates. The broader potential of aquatic glycan signalling has been covered in Chapter 3.1 but the ability of marine organisms to recognise specific sugars is of wide-spread importance. The direct relevance to this research is the use of lectins to recognise specific sugars. Barnacles may use lectins to recognise conspecifics as current research by Gregoris et al. (2011) showed that both cyprids and adult *B. amphitrite* produce a mannose receptor, which is 33% identical to a mannose binding lectin found in *Megabalanus rosa*. However, this lectin mechanism is also widely used for recognition, prevention and reducing invasion of pathogens through the recognition of sugar components in bacterial cell walls. This work was highlighted through characterisation of haemolymph lectins from the white shrimp *Litopenaeus setiferus* (Alpuche et al., 2005). The marine sponge, *Halichondria okadai*, produces three lectins that potentially protect from infection (Kawsar et al., 2008). Lectins may also interact with beneficial microorganisms to form part of a symbiotic relationship (Jimbo et al., 2000). Similarly, plant-pathogen interactions have been studied using the red algae, *Chondrus crispus*, and green algal endophyte, *Acrochaete operculata*, where certain oligosaccharides appear to inhibit pathogens (Bouarab et al., 2001).

In regard to the surface modification and synthetic chemistry, it was noted following XPS analysis of the surfaces that boron and fluorine, from boron trifluoride diethyl etherate and

potassium carbonate respectively, were present on test surfaces. By modifying the washing procedures to include multiple washes and additional solvents, it should be possible to remove the incidence of these compounds on the surface. In addition to the tests used to confirm the surface modification, (ellipsometry, contact angle and XPS), it would be interesting to use lectins on the modified surfaces. Lectins can be labelled with fluorescent stains and detected under ultraviolet conditions using methodology as demonstrated by Końska et al., (2003). This technique would only work on the final deprotected carbohydrate surface as it involves binding UV labelled lectins to the carbohydrates to show homogeneity of surface coverage and quantity of carbohydrates present.

The final part of this research was to begin to determine the protein structure of the SIPC. With previous research extending to the amino acid sequence, this research uncovered a two-dimensional structure of the SIPC protein molecule. Ideally, to fully appreciate the SIPC structure and the display of glycans on the surface a three-dimensional reconstruction of the crystal structure would be achieved. This requires more SIPC for TEM analysis to give an increased number of images leading to better class averages. This extra material could also be used for cryoelectron microscopy and crystallisation. Following the progress reported here, further funding is being sought to complete the analysis of the SIPC protein structure and provide a three-dimensional reconstruction of the molecule. To achieve this three-dimensional structure, large amounts of homogeneous deglycosylated protein would be required. However, a higher resolution cryoelectron microscopy structure would give a clearer suggestion of the protein three-dimensional envelope. In addition, a full X-ray structure would give a superior idea of the domains of the protein and how it is processed. This may also shed light on why the SIPC does not contain the thioester bond that its homologue (TEP1r) has.

It may also be possible to undertake heterologous expression of the protein in insect cells or some system that is likely to give the expressed protein in a native state, in a similar methodology to the production of TEP1r used by Baxter et al. (2007).

Another slightly different approach than simply looking for the three-dimensional structure of the SIPC, would be to find the receptor for the SIPC protein. As it is hypothesised that the SIPC is a platform for the presentation of specific glycans for recognition as a

settlement cue, this direction of assessing the structure of the SIPC could provide exciting developments.

There are several other areas of focus that have arisen from this research. The taxonomic affinity of barnacle species is the starting point for research focusing on a species such as *B. amphitrite*. The SIPC of other species may act as allospecific cues and thus analysis of these would provide additional insight (Clare, 2011). It may be that this gross genus reactivity gives evolutionary advantage perhaps providing settlement cues to the same habitat, ensuring survival of the genus as a whole. This cross reactivity invites further glycan analysis of the SIPC of other barnacle species to confirm variations. This may also highlight the significance of the core fucose in the SIPC as a possible means for distinguishing species at the time of settlement.

The cyprid footprint has often been considered analogous to the SIPC and consequently carrying out the same glycan analysis would confirm this. However, currently the study of the footprints of *B. amphitrite* is impractical for several reasons. The cyprid footprints of *B. amphitrite* are around 50% smaller than other studied barnacle species and are rarely seen on glass substrata (Aldred, 2007) thus collection only yields small amounts of protein. This has proved a problem during previous research by Phang et al. (2007). Working on a purely speculative basis, there are advantages to both including and excluding the SIPC from cyprid footprints. The main advantage to having SIPC as a footprint protein is the attraction of conspecific juveniles to a substratum where others have explored and successfully settled. This ability to identify that conspecific cyprids have searched the substratum previously is a valuable source of location information for the searching cyprid. However there could also be an advantage in not having SIPC in the footprints. This could be the reduction of overcrowding in a suitable environment, as the settlement of newer barnacles on established populations can reduce the ability to feed and reproduce effectively. It would also lead to effective separation of different communities of the same species and lead to effective competition between species. Another area for potential development is the debate over the disputed presence of the water borne cue. Elbourne and Clare (2010) have recently published some evidence of this controversial settlement pheromone. Even these results were partly contradictory with seawater standards showing results similar to that of the

adult conditioned water. This data highlights the difficulty in determining larval behavioural responses in settlement assays.

Another strategy to further understanding of the mechanism of the SIPC in gregariousness is to approach the problem from the cyprid. Whereas the SIPC is the ‘key’ rather than the ‘lock’, further research into the cyprid foot receptors to develop a molecule that blocks the receptor but does not trigger settlement would be a promising direction for future research.

Further research into behaviour on the modified surfaces under video tracking would have been an interesting conclusion to this work. However there are several reasons why this was not possible. With current equipment it is impossible to observe if exploring cyprids are touching the surface. Consequently, the video tracking method is only really reliable for in-solution work. In addition, there is no protocol optimised for using slides as tracking cannot be carried out using water droplets. Polystyrene dishes must be used and to functionalise these, the chemical protocol would have to change to the point that a comparison would not be possible. A three-dimensional tracking system using digital in-line holography has been developed by Heydt et al. (2007) for tracking *Ulva linza* zoospores. There has been some progress in developing a different approach to the three-dimensional tracking method at Newcastle University. This method is still in early development and trial stages, consequently the capabilities of the system are yet undefined, however the three-dimensional tracking of cyprids using this novel method may mitigate some of the issues mentioned.

The underlying rationale behind this project was the reduction of biofouling organisms on submerged structures. The relevance of this research to the wider field of antifouling knowledge is mainly the addition of new information regarding the glycoprotein structure of the SIPC. It may indeed be possible in the future to develop and produce custom surfaces to reduce fouling by certain target species. Although this research has successfully confirmed the hypothesis laid out in Chapter 2.1, barnacles are only one part of the biofouling problem. One of the greater economic impacts of hull biofouling is the introduction of invasive alien species into new geographical areas. It may be possible using vectors and predicted species to forecast future fouling organisms. Research similar to that of this project could be carried out so as to prophylactically include antifoulants for forecasted organisms, as well as known species, to prevent the spread of organisms.

However, as vessels are not usually confined to one geographic region, the number of targeted antifoulants would be vast. With the pressure to reduce biocides in coatings following the introduction of the Biocidal Products Directive (98/8/EC), the future of antifouling technology lies with the development of non-toxic coatings targeting heavy fouling organisms using knowledge about their adhesives and reproductive cycle.

In contrast, this research into the components and structure of *B. amphitrite* SIPC may provide a new avenue of development for the aquaculture industry. Certain larger species of barnacles such as *Austromegabalanus psittacus* are important food sources in Chile (Clare, 2011). If it became possible to closely manipulate larval settlement of such species through the use of an SIPC like mimic, the culture of such lucrative species would be economically significant.

6.4 Final Thoughts

The hypothesis being tested throughout this was that cyprids settle more in mannose solution because the SIPC contains mannose. This research has shown that not only does the SIPC molecule definitely contain mannose oligosaccharides, but also mannose increases settlement when used in solution and when bound to a surface when compared to other carbohydrates.

This research has provided the *N*-glycan characterisation of *B. amphitrite* SIPC and has gone some way to finding a structure of the SIPC protein. There is the possible avenue of *O*-glycans that may be present; two *O*-linked glycans are predicted (see Chapter 5.3.3). The preparation of an SIPC glycan mimic has shown the possibility of producing a ‘sacrificial anode’ of highly inducing surface for use to reduce fouling on the rest of a hull. Although, turning this into a working product would require considerably more testing and the additional research into the remaining glycan moiety of the SIPC as mentioned in Chapter 6.3. The prospect for an antifouling coating that is based on an antagonist to the SIPC is still a long way off and there are likely to be problems with the physical application of a coating with such specific surface chemistry.

Consequently, the implication of this research is currently purely academic, as it adds to the current knowledge of barnacle gregarious settlement mechanisms. It was hoped that an antagonist to the SIPC could be found following the characterisation of the cue. However,

due to the variables involved, currently this has not been possible. Nevertheless, the key outcome from this research is improved knowledge of the SIPC and increased understanding of the mechanisms behind gregarious settlement in barnacle species.

References

- Aldred, N. (2007) *The adhesion and adhesives of barnacle cyprids (Balanus amphitrite; Semibalanus balanoides) and mussels (Mytilus edulis)*. PhD thesis. Newcastle University.
- Aldred, N. and Clare, A. S. (2008) 'The adhesive strategies of cyprids and development of barnacle-resistant marine coatings', *Biofouling*, 24, (5), pp. 351-363.
- Aldred, N. and Clare, A. S. (2009) 'Mechanisms and principles underlying temporary adhesion, surface exploration and settlement site selection by barnacle cyprids: a short review', *Functional Surfaces in Biology*, Part 1, pp. 43-65.
- Aldred, N., Guozhu, L., Gao, Y., Clare, A. S. and Shaoyi, J. (2010) 'Modulation of barnacle (*Balanus amphitrite* Darwin) cyprid settlement behavior by sulfobetaine and carboxybetaine methacrylate polymer coatings', *Biofouling*, 26, (6), pp. 673-683.
- Aldred, N., Phang, I. Y., Conlan, S. L., Clare, A. S. and Vancso, G. J. (2008) 'The effects of a serine protease, Alcalase®, on the adhesives of barnacle cyprids (*Balanus amphitrite*)', *Biofouling*, 24, (2), pp. 97-107.
- Almeida, E., Diamantino, T. C. and Sousa, O. d. (2007) 'Marine paints: The particular case of antifouling paints', *Progress in Organic Coatings*, 59, pp. 2-20.
- Alpuche, J., Pereyra, A., Agundis, C., Rosas, C., Pascual, C., Slomianny, M.-C., Vázquez, L. and Zenteno, E. (2005) 'Purification and characterization of a lectin from the white shrimp *Litopenaeus setiferus* (Crustacea decapoda) hemolymph', *Biochimica et Biophysica Acta*, 1724, pp. 86-93.
- Ambrosi, M., Cameron, N. R. and Davis, B. G. (2005) 'Lectins: tools for the molecular understanding of the glycode', *Organic & Biomolecular Chemistry*, 3, pp. 1593-1608.
- Anderson, C., Atlar, M., Callow, M., Candries, M., Milne, A. and Townsin, R. L. (2003) 'The development of foul-release coatings for seagoing vessels', *Proceedings of the Institute of Marine Engineering, Science and Technology, Part B, Journal of Marine Design and Operations*, 4, pp. 11-23.
- Anderson, D. T. (1994) *Barnacles: Structure, function, development and evolution*. Chapman & Hall.

- Anderson, K. and Waite, J. (2002) 'Biochemical characterization of a byssal protein from *Dreissena bugensis* (Andrusov).' *Biofouling*, 18, pp. 37-45.
- Apweiler, R., Hermjakob, H. and Sharon, N. (1999) 'On the frequency of protein glycosylation, as deduced from analysis of the SWISS-PROT database.' *Biochimica et Biophysica Acta*, 1473, (1), pp. 4-8.
- Arbos, P., Wirth, M., Arangoa, M. A., Gabor, F. and Irache, J. M. (2002) 'Gantrez[®] AN as a new polymer for the preparation of ligand-nanoparticle conjugates', *Journal of Controlled Release*, 83, pp. 321-330.
- Armstrong, E., Boyd, K. G. and Burgess, J. G. (2000a) 'Prevention of marine biofouling using natural compounds from marine organisms', *Biotechnology Annual Review*, 6, pp. 221-230.
- Armstrong, E., Boyd, K. G., Piscane, A., Peppiatt, C. J. and Burgess, J. G. (2000b) 'Marine Microbial Natural Products in Antifouling Coatings', *Biofouling*, 16, (2-4), pp. 215-224.
- Bahamondes-Rojas, I. and Dherbomez, M. (1990) 'Purification partielle de substances glycoconjuguées capables d'induire le métamorphose des larves compétentes d'*Eubbranchus doriae* (Trinchèse, 1879), mollusque nudibranche', *Journal of Experimental Marine Biology and Ecology*, 144, pp. 17-27.
- Barnes, R. S. K., Calow, P., Olive, P. J. W., Golding, D. W. and Spicer, J. I. (2001) *The Invertebrates: A Synthesis*. Blackwell Science, Oxford.
- Barnett, B. E. and Crisp, D. J. (1979) 'Laboratory studies of gregarious settlement in *Balanus balanoides* and *Elminius modestus* in relation to competition between these species', *Journal of the Marine Biological Association of the UK*, 59, pp. 581-590.
- Barnett, B. E., Edwards, S. C. and Crisp, D. J. (1979) 'A field study of settlement behaviour in *Balanus balanoides* and *Elminius modestus* (Cirripedia:Crustacea) in relation to competition between them', *Journal of the Marine Biological Association of the UK*, 59, pp. 575-580.
- Bavington, C., Lever, R., Mulloy, B., Grundy, M., CP, P. and NV, R. (2004) 'Anti-adhesive glycoproteins in echinoderm mucus secretions', *Comparative Biochemistry and Physiology - Part B*, 139, pp. 607-617.
- Baxter, R. H. G., Chang, C.-I., Chelliah, Y., Blandin, S. p., Levashina, E. A. and Deisenhofer, J. (2007) 'Structural basis for conserved complement factor-like function

- in the antimalarial protein TEPI', *Proceedings of the National Academy of Sciences*, 104, (28), pp. 11615–11620.
- Beigbeder, A., Degee, P., Conlan, S. L., Mutton, R. J., Clare, A. S., Pettitt, M. E., Callow, M., Callow, J. A. and Dubois, P. (2008) 'Preparation and characterisation of silicone-based coatings filled with carbon nanotubes and natural sepiolite and their application as marine fouling-release coatings', *Biofouling*, 24, (4), pp. 291-302.
- Berry, F. and Breithaupt, T. (2008) 'Development of behavioural and physiological assays to assess discrimination of male and female odours in crayfish, *Pacifastacus leniusculus*', *Behaviour*, 145, pp. 1427-1446.
- Bertozzi, C. R. and Kiessling, L. L. (2001) 'Chemical Glycobiology', *Science*, 291, pp. 2357-2364.
- Bishop, M. W. H. (1950) 'Distribution of *Balanus amphitrite* Darwin var. *denticulata* Broch', *Nature*, 165, pp. 409-410.
- Bones, J., McLoughlin, N., Hilliard, M., Wynne, K., Kargeran, B. L. and Rudd, P. M. (2011) '2D-LC Analysis of BRP 3 Erythropoietin N-Glycosylation using Anion Exchange Fractionation and Hydrophilic Interaction UPLC Reveals Long Poly-N-Acetyl Lactosamine Extensions', *Analytical Chemistry*, In press.
- Boone, E. J., Boettcher, A. A., Sherman, T. D. and O'Brien, J. J. (2003) 'Characterisation of settlement cues used by the rhizocephalan barnacle *Loxothylacus texanus*', *Marine Ecology Progress Series*, 252, pp. 187-197.
- Bouarab, K., Potin, P., Weinberger, F., Correa, J. and Kloareg, B. (2001) 'The *Chondrus crispus*-*Acrochaete operculata* host-pathogen association, a novel model in glycobiology and applied phycopathology', *Journal of Applied Phycology*, 13, pp. 185–193.
- Bourget, E. (1987) 'Barnacle shells: composition, structure, and growth', in Southward, A. J.(ed), *Barnacle Biology - Crustacean Issues 5*. A. A. Balkema: Rotterdam, pp. 267–285.
- Brogdon, R. (2010) *M.Chem Report*. Department of Chemistry: Durham University
- Brooks, S. A., Dwek, M. V. and Schumacher, U. (2002) *Functional & Molecular Glycobiology*. BIOS Scientific Publishers Limited: Oxford.

- Burgess, J. G., Boyd, K. G., Armstrong, E., Jiang, Z., Yan, L., Berggren, M., May, U., Pisacane, T., Granmo, Å. and Adams, D. R. (2003) 'The development of a marine natural product-based antifouling paint', *Biofouling*, 19, pp. 197-205.
- Calarese, D. A., Scanlan, C. N., Zwick, M. B., Deeckongkit, S., Mimura, Y., Kunert, R., Zhu, P., Wormald, M. R., Stanfield, R. L., Roux, K. H., Kelly, J. W., Rudd, P. M., Dwek, R. A., Katinger, H., Burton, D. R. and Wilson, I. A. (2003) 'Antibody Domain Exchange Is an Immunological Solution to Carbohydrate Cluster Recognition', *Science*, 300, pp. 2065-2071.
- Caldwell, G. S. and Pagett, H. E. (2010) 'Marine glycobiology: current status and future perspectives', *Marine Biotechnology*, 12, pp. 241-252.
- Campbell, M. P., Royle, L., Radcliffe, C. M., Dwek, R. and Rudd, P. M. (2008) 'GlycoBase and autoGU: tools for HPLC-based glycan analysis', *Bioinformatics*, 24, pp. 1214-1216.
- Carmona, M. J. and Snell, T. W. (1995) 'Glycoproteins in daphnids: Potential signals for mating?' *Archiv für Hydrobiologie*, 134, (3), pp. 273-279.
- Central Directorate of Environmental Protection. (1986) *Organotin in antifouling paints: environmental considerations*. London: Her Majesty's Stationary Office
- Christie, A. O. and Dalley, R. (1987) 'Barnacle fouling and its prevention', in Southward, A. J.(ed), *Barnacle Biology - Crustacean Issues 5*. A. A. Balkema: Rotterdam.
- Clare, A. S. (2011) 'Towards a characterization of the chemical cue to barnacle gregariousness ', in Breithaupt, T. and Thiel, M.(eds) *Chemical Communication in Crustaceans*. Springer: New York, pp. 431-450.
- Clare, A. S., Freet, R. K. and McClary, M., Jr. (1994) 'On the antennular secretion of the cyprid of *Balanus amphitrite*, and its role as a settlement pheromone', *Journal of the Marine Biological Association of the UK*, 74, pp. 243-250.
- Clare, A. S. and Høeg, J. T. (2008) '*Balanus amphitrite* or *Amphibalanus amphitrite*? A note on barnacle nomenclature', *Biofouling*, 24, (1), pp. 55-57.
- Clare, A. S. and Matsumura, K. (2000) 'Nature and perception of barnacle settlement pheromones', *Biofouling*, 15, pp. 57-71.
- Clare, A. S., Rittchof, D., Gerhart, D. J. and Maki, J. S. (1992) 'Molecular approaches to nontoxic antifouling', *Invertebrate reproduction and fouling*, 22, pp. 67-76.

- Clare, A. S., Thomas, R. F. and Rittschof, D. (1995) 'Evidence for the involvement of cyclic AMP in the pheromonal modulation of barnacle settlement', *Journal of Experimental Biology*, 198, pp. 655-664.
- Corpet, F. (1988) 'Multiple sequence alignment with hierarchical clustering', *Nucleic Acids Research*, 16, (22), pp. 10881-10890.
- Crisp, D. J. (1955) 'The behaviour of barnacle cyprids in relation to water movement over a surface', *Journal of Experimental Biology*, 32, pp. 569-590.
- Crisp, D. J. (1960) 'Mobility of barnacles', *Nature*, 188, pp. 1208-1209.
- Crisp, D. J. (1965) 'Surface chemistry, a factor in the settlement of marine invertebrate larvae', *Botanica Gothoburgensia III*, 3, pp. 51-65.
- Crisp, D. J. (1976a) 'The role of the pelagic larva', in *Perspectives in Experimental Biology*. Pergamon Press: Oxford.
- Crisp, D. J. (1976b) 'Settlement responses in marine organisms', in Newell, R. C.(ed), *In adaptation to the environment: essays on the physiology of marine animals*. Butterworth, London, pp. 83-124.
- Crisp, D. J. (1979) 'Dispersal and re-aggregation in sessile marine invertebrates, particularly barnacles', in Larwood, G. and Rosen, B. R.(eds) *Biology and systematics of colonial organisms*. Academic Press, London, pp. 319-327.
- Crisp, D. J. (1985) 'Recruitment of barnacle larvae from the plankton', *Bulletin of Marine Science*, 37, (2), pp. 478-486.
- Crisp, D. J. (1990) 'Gregariousness and systematic affinity in some North Carolinian barnacles', *Bulletin of Marine Science*, 47, pp. 516-525.
- Crisp, D. J. and Meadows, P. S. (1962) 'The chemical basis of gregariousness on cirripedes', *Proceedings of the Royal Society of London, B*, 156, pp. 500-520.
- Crisp, D. J. and Meadows, P. S. (1963) 'Adsorbed layers: the stimulus to settlement in barnacles', *Proceedings of the Royal Society B*, 158, pp. 364-387.
- Crisp, D. J., Walker, G., Young, G. A. and Yule, A. B. (1985) 'Adhesion and substrate choice in mussels and barnacles', *Journal of Colloid and Interface Science*, 104, (1), pp. 40-50.
- da S. Maciel, J., Kosaka, P. M., de Paula, R. C. M., Feitosa, J. P. A. and Petri, D. F. S. (2007) 'Formation of cashew gum thin films onto silicon wafers or amino-terminated

- surfaces and the immobilisation of Concanavalin A on them', *Carbohydrate Polymers*, 69, pp. 522-529.
- de Nys, R., Guenther, J. and Uriz, M. J. (2010) 'Natural control of fouling', in Durr, S. and Thomason, J. C.(eds) *Biofouling*. Wiley Blackwell: Chichester, pp. 109-120.
- Dell, A. and Morris, H. R. (2001) 'Glycoprotein structure determination by mass spectrometry', *Science*, 291, pp. 2351-2356.
- Desai, D. V. and Anil, A. C. (2005) 'Recruitment of the barnacle *Balanus amphitrite* in a tropical estuary: implications of environmental perturbation, reproduction and larval ecology', *Journal of the Marine Biological Association of the UK*, 85, pp. 909-920.
- Dineen, J. F. and Hines, A. H. (1992) 'Interactive effects of salinity and adult extract upon the settlement of the estuarine barnacle *Balanus improvisus* (Darwin, 1854)', *Journal of Experimental Marine Biology and Ecology*, 156, pp. 239-252.
- Dineen, J. F. and Hines, A. H. (1994) 'Larval settlement of the polyhaline barnacle *Balanus eburneus* (Gould): cue interactions and comparisons with two estuarine congeners', *Journal of Experimental Marine Biology and Ecology*, 179, pp. 223-234.
- Dingmann, B. J. and Snell, T. W. (1999) 'Oligosaccharide structure of a mate recognition pheromone: Comparison of three closely related rotifer species', *American Zoologist*, 39, (5 Special Issue), pp. 31A - Abstract 178.
- Dobretsov, S., Dahms, H.-U. and Qian, P.-Y. (2006) 'Inhibition of biofouling by marine microorganisms and their metabolites', *Biofouling*, 22, (1), pp. 43-54.
- Donati, I., Gamini, A., Vetere, A., Campa, C. and Paoletti, S. (2002) 'Synthesis, characterisation, and preliminary biological study of glycoconjugates of poly(styrene-co-maleic acid)', *Biomacromolecules*, 3, pp. 805-812.
- Doniach, S. and Sunjic, M. (1970) 'Many-electron singularity in X-ray photoemission and X-ray line spectra from metals ', *Journal of Physics C*, 3, (285-291).
- Dreanno, C., Kirby, R. R. and Clare, A. S. (2006a) 'Locating the barnacle settlement pheromone: spatial and ontogenetic expression of the settlement-inducing protein complex of *Balanus amphitrite*', *Proceedings of the Royal Society B*, 273, pp. 2721-2728.
- Dreanno, C., Kirby, R. R. and Clare, A. S. (2006b) 'Smelly feet are not always a bad thing: the relationship between cyprid footprint protein and the barnacle settlement pheromone', *Biology Letters*, 2, pp. 423 - 425.

- Dreanno, C., Kirby, R. R. and Clare, A. S. (2007) 'Involvement of the barnacle settlement-inducing protein complex (SIPC) in species recognition at settlement', *Journal of Experimental Marine Biology and Ecology*, 351, pp. 276-282.
- Dreanno, C., Matsumura, K., Dohmae, N., Takio, K., Hirota, H., Kirby, R. R. and Clare, A. S. (2006c) 'An α 2-macroglobulin-like protein is the cue to gregarious settlement of the barnacle *Balanus amphitrite*', *Proceedings of the National Academy of Sciences of the United States*, 103, (39), pp. 14396-14401.
- Dube, P., Orlova, E. V., Zemlin, F. and Van Heel, M. (1995) 'Three-dimensional structure of keyhole limpet hemocyanin by cryoelectron microscopy and angular reconstruction', *Journal of Structural Biology*, 115, pp. 226-232.
- Ekblad, T., Bergstrom, G., Ederth, T., Conlan, S. L., Mutton, R. J., Clare, A. S., Wang, S., Liu, Y., Zhao, Q., D'Souza, F., Donnelly, G. T., Willemsen, P. R., Pettitt, M. E., Callow, M., Callow, J. A. and Liedberg, B. (2008) 'Poly(ethylene glycol)-containing hydrogel surfaces for antifouling applications in marine and freshwater environments', *Biomacromolecules*, 9, pp. 2775-2783.
- Elbourne, P. D. (2008) 'Interaction of conspecific cues in *Balanus amphitrite* Darwin (Cirripedia) settlement assays: Continued argument for the single-larva assay', *Biofouling*, 24, (2), pp. 87-96.
- Elbourne, P. D. and Clare, A. S. (2010) 'Ecological relevance of a conspecific, waterborne settlement cue in *Balanus amphitrite* (Cirripedia)', *Journal of Experimental Marine Biology and Ecology*, 392, (1), pp. 99-106.
- Elkin, C. and Marshall, D. J. (2007) 'Desperate larvae: influence of deferred costs and habitat requirements on habitat selection', *Marine Ecology Progress Series*, 335, pp. 143-153.
- Emlet, R. B. and Sadro, S. S. (2006) 'Linking stages of life history: How larval quality translates into juvenile performance for an intertidal barnacle (*Balanus glandula*)', *Integrated and Comparative Biology*, 46, (3), pp. 334-346.
- Engen, J. R. (2009) 'Analysis of Protein Conformation and Dynamics by Hydrogen/Deuterium Exchange MS', *Analytical Chemistry*, 81, (19), pp. 7870-7875.
- Eno, N. C. and Clark, R. A. (1997) *Non-native marine species in British waters: a review and directory*. Joint Nature Conservation Committee

- Evenson, S. A., Fail, C. A. and Badyal, J. P. S. (2000) 'Surface Esterification of Poly(Ethylene-*alt*-Maleic Anhydride) Copolymer', *Journal of Physical Chemistry B*, 104, pp. 10608-10611.
- Fernando, S. A. (1999) 'Reproductive biology of tropical barnacles', in Thompson, M.-F. and Nagabhushanam, R.(eds) *Barnacles: The Biofoulers*. Regency Publications: New Delhi, pp. 406.
- Ferrari, K. and Targett, N. (2003) 'Chemical attractants in horseshoe crab, *Limulus polyphemus*, eggs: The potential for an artificial bait ', *Journal of Chemical Ecology*, 29, pp. 477-496.
- Ferre, F. and Clote, P. (2005) 'DiANNA: a web server for disulfide connectivity prediction', *Nucleic Acids Research*, 33, (Web Server Issue), pp. W230-W232.
- Finelli, C. M. and Wetthey, D. S. (1999) 'Settlement in Balanomorph barnacles: the interaction of physics and settlement cues', in Thompson, M.-F. and Nagabhushanam, R.(eds) *Barnacles: The Biofoulers*. Regency Publications: New Delhi, pp. 406.
- Fontaine, A. (1964) 'The integumentary mucous secretions of the ophiuroid *Ophiocomina nigra*.' *Journal of the Marine Biological Association of the UK*, 44, pp. 145-162.
- Foster, B. A. (1987) 'Barnacle ecology and adaptation', in Southward, A. J.(ed), *Barnacle Biology - Crustacean Issues 5*. A. A. Balkema: Rotterdam.
- Freudenberg, U., Zschoche, S., Simon, F., Janke, A., Schmidt, K., Behrens, S. H., Auweter, H. and Werner, C. (2005) 'Covalent Immobilization of Cellulose Layers onto Maleic Anhydride Copolymer Thin Films', *Biomacromolecules*, 6, pp. 1628-1634.
- Fusetani, N. and Clare, A. S. (eds.) (2006) *Marine Molecular Biotechnology - Antifouling Compounds*. Springer.
- Gabbott, P. A. and Larman, V. N. (1987) 'The chemical basis of gregariousness in cirripedes: A review (1953-1984)', in Southward, A. J.(ed), *Barnacle Biology - Crustacean Issues 5*. A. A. Balkema: Rotterdam, pp. 377-388.
- Galgali, P., Agashe, M. and Varma, A. J. (2007) 'Sugar-linked biodegradable polymers: Regio-specific ester bonds of glucose hydroxyls in their reaction with maleic anhydride functionalised polystyrene and elucidation of the polymer structures formed', *Carbohydrate Polymers*, 67, pp. 576-585.

- Gardella, J. A., Ferguson, S. A. and Chin, R. L. (1986) ' $\pi^* \leftarrow \pi$ Shakeup satellites for the analysis of structure and bonding in aromatic polymers by X-ray photoelectron spectroscopy', *Applied Spectroscopy*, 40, (2), pp. 224-232.
- Gebauer, W., Harris, J. R. and Markl, J. (2002) 'Topology of the 10 subunits within the Decamer of KLH, the hemocyanin of the marine gastropod *Megathura crenulata*', *Journal of Structural Biology*, 139, pp. 153-159.
- Geyer, H. and Geyer, R. (2006) 'Strategies for analysis of glycoprotein glycosylation', *Biochimica et Biophysica Acta*, 1764, pp. 1853-1869.
- Giúdice, C. A. (1999) 'Bioactivity of antifouling paints', in Thompson, M.-F. and Nagabhushanam, R.(eds) *Barnacles: The Biofoulers*. Regency Publications: New Delhi, pp. 406.
- Gottlieb, H. E., Kotlyar, V. and Nudelman, A. (1997) 'NMR chemical shifts of common laboratory solvents as trace impurities', *Journal of Organic Chemistry*, 62, pp. 7512-7515.
- Gouet, P., Courcelle, E., Stuart, D. I. and Metoz, F. (1999) 'ESPrict: multiple sequence alignments in PostScript', *Bioinformatics*, 15, pp. 305-308.
- Gregoris, T. B. D., Rupp, O., Klages, S., Knaust, F., Bekel, T., Kube, M., Burgess, J. G., Arnone, M. I., Goesmann, A., Reinhardt, R. and Clare, A. S. (2011) 'Deep sequencing of naupliar-, cyprid- and adult-specific normalised Expressed Sequence Tag (EST) libraries of the acorn barnacle *Balanus amphitrite*', *Biofouling*, 27, (4), pp. 367-374.
- Grombe, R., Gouzy, M.-F., Nitschke, M., Komber, H. and Werner, C. (2006) 'Preparation and characterisation of glycosylated maleic anhydride copolymer thin films', *Colloids and Surfaces A: Physiochemical and Engineering Aspects*, 284-285, pp. 295-300.
- Gupta, R., Jung, E. and Brunak, S. (2004) 'Prediction of N-glycosylation sites in human proteins', *In preparation*.
- Harder, T. N., Thiagarajan, V. and Qian, P.-Y. (2001) 'Effect of cyprid age on the settlement of *Balanus amphitrite* Darwin in response to natural biofilms', *Biofouling*, 17, (3), pp. 211-219.
- Harris, J. R., Bhella, D. and Adrian, M. (2006) 'Recent developments in negative staining for transmission electron microscopy', *Microscopy and Analysis*, 20, (3), pp. 17-21.

- Harris, J. R., Meissner, U., Gebauer, W. and Markl, J. (2004) '3D reconstruction of the hemocyanin subunit dimer from the chiton *Acanthochiton fascicularis*', *Micron*, 35, pp. 23-26.
- Harris, R. and Horne, R. (1991) 'Negative Staining', in Harris, J. R.(ed), *Electron Microscopy in Biology: A Practical Approach*. Oxford University Press: Oxford, UK, pp. 328.
- Harvey, D. J., Merry, A. H., Royle, L., Campbell, M. P., Dwek, R. A. and Rudd, P. M. (2009) 'Proposal for a standard system for drawing structural diagrams of N- and O-linked carbohydrates and related compounds', *Proteomics*, 9, pp. 3796-3801.
- Hazelhurst, R. (2009) *M.Chem Report*. Department of Chemistry: Durham University
- Hellio, C., Simon-Colin, C., Clare, A. S. and Deslandes, E. (2004) 'Isethionic Acid and Floridoside Isolated from the Red Alga, *Grateloupia turuturu*, Inhibit Settlement of *Balanus amphitrite* Cyprid Larvae', *Biofouling*, 20, (3), pp. 139-145.
- Heydt, M., Rosenhahn, A., Grunze, M., Pettitt, M. E., Callow, M. and Callow, J. A. (2007) 'Digital in-line holography as a three-dimensional tool to study motile marine organisms during their exploration of surfaces', *Journal of Adhesion*, 83, pp. 417-430.
- Hills, J. M. and Thomason, J. C. (1996) 'A multi-scale analysis of settlement density and pattern dynamics of the barnacle *Semibalanus balanoides*', *Marine Ecology Progress Series*, 138, pp. 103-115.
- Holm, E. R., Cannon, G., Roberts, D., Schmidt, A. R., Sutherland, J. P. and Rittschof, D. (1997) 'The influence of initial surface chemistry on development of the fouling community at Beaufort, North Carolina', *Journal of Experimental Marine Biology and Ecology*, 215, pp. 189-203.
- Hui, E. and Moyse, J. (1982) 'Settlement of *Elminius modestus* cyprids in contact with adult barnacles in the field', *Journal of the Marine Biological Association of the UK*, 62, pp. 477-482.
- Hui, E. and Moyse, J. (1987) 'Settlement patterns and competition for space', in Southward, A. J.(ed), *Barnacle Biology - Crustacean Issues 5*. A. A. Balkema: Rotterdam.
- Humbertdavid, N. and Garrone, R. (1993) 'A 6-armed, tenascin-like protein extracted from the Porifera *Oscarella tuberculata* (Homosclerophrida)', *European Journal of Biochemistry*, 216, pp. 255-260.

- Jarrett, J. N. and Pechenik, J. A. (1997) 'Temporal variation in cyprid quality and juvenile growth capacity for an intertidal barnacle', *Ecology*, 78, (4), pp. 1262-1265.
- Jenkins, S. R. and Martins, G. M. (2010) 'Succession on hard strata', in Durr, S. and Thomason, J. C.(eds) *Biofouling*. Wiley Blackwell: Chichester, pp. 60-72.
- Jerome, R., Teyssie, P., Pireaux, J. and Verbist, J. (1986) 'Surface analysis of polymers end-capped with metal carboxylates using X-ray photoelectron spectroscopy', *Applied Surface Science*, 27, (93-105).
- Jimbo, M., Yanohara, T., Kioke, K., Kioke, K., Sakai, R., Muramoto, K. and Kamiya, H. (2000) 'The D-galactose-binding lectin of the octocoral *Sinularia lochmodes*: characterization and possible relationship to the symbiotic dinoflagellates', *Comparative Biochemistry and Physiology B*, 125, pp. 227-236.
- Johnson, D. (2008) *Report: XPS analysis of four coated silicon substrates*. University of Nottingham
- Johnson, D. W. (2009) *New applications for poly(ethylene-alt-maleic anhydride)*. PhD thesis. Durham University.
- Johnson, K. M. and Sieburth, J. M. (1977) 'Dissolved carbohydrates in seawater. I, a precise spectrophotometric analysis for monosaccharides', *Marine Chemistry*, 5, pp. 1-13.
- Jouuchi, T., Satuito, C. G. and Kitamura, H. (2007) 'Sugar compound products of the periphytic diatom *Navicula ramosissima* induce larval settlement in the barnacle, *Amphibalanus amphitrite*', *Marine Biology*, 152, pp. 1065-1076.
- Julenius, K. (2007) 'NetCGlyc 1.0: Prediction of mammalian C-mannosylation sites', *Glycobiology*, 17, pp. 868-876.
- Julenius, K., Mølgaard, A., Gupta, R. and Brunak, S. (2005) 'Prediction, conservation analysis and structural characterization of mammalian mucin-type O-glycosylation sites', *Glycobiology*, 15, pp. 153-164.
- Kaji, H., Saito, H., Yamauchi, Y., Shinkawa, T., Taoka, M., Hirabayashi, J., Kasai, K.-i., Takahasi, N. and Isobe, T. (2003) 'Lectin affinity capture, isotope-coded tagging and mass spectrometry to identify N-linked glycoproteins', *Nature Biotechnology*, 21, (6), pp. 667-672.
- Kato-Yoshinaga, Y., Nagano, M., Mori, S., Clare, A. S., Fusetani, N. and Matsumura, K. (2000) 'Species specificity of barnacle settlement-inducing proteins', *Comparative Biochemistry and Physiology Part A*, 125, pp. 511-516.

- Kawabata, S.-i. and Tsuda, R. (2002) 'Molecular basis of non-self recognition by the horseshoe crab tachylectins', *Biochimica et Biophysica Acta*, 1572, pp. 414-421.
- Kawsar, S. M. A., Fujii, Y., Matsumoto, R., Ichikawa, T., Tateno, H., Hirabayashi, J., Yasumitsu, H., Dogasaki, C., Hosono, M., Nitta, K., Hamako, J., Matsui, T. and Ozeki, Y. (2008) 'Isolation, purification, characterisation and glycan-binding profile of a D-galactoside specific lectin from the marine sponge, *Halichondria okadai*', *Comparative Biochemistry and Physiology B*, 150, pp. 349–357.
- Kelly, L. S. and Snell, T. W. (1998) 'Role of surface glycoproteins in mate-guarding of the marine harpacticoid *Tigriopus japonicus*', *Marine Biology*, 130, pp. 605-612.
- Khalaila, I., Pater-Katalinic, J., Tsang, C., Radcliffe, C. M., Afalo, E. D., Harvey, D. J., Dwek, R. A., Rudd, P. M. and Sagi, A. (2004) 'Structural characterisation of the N-glycan moiety and site of glycosylation in vitellogenin from the decapod crustacean *Cherax quadricarinatus*', *Glycobiology*, 14, (9), pp. 767-774.
- Khandeparker, L., Anil, A. C. and Raghukumar, S. (2002) 'Exploration and metamorphosis in *Balanus amphitrite* Darwin (Cirripedia; Thoracica) cyprids: significance of sugars and adult extract', *Journal of Experimental Marine Biology and Ecology*, 281, pp. 77-88.
- Khandeparker, L., Desai, D. V. and Shirayama, Y. (2005) 'Larval development and post-settlement metamorphosis of the barnacle *Balanus albicostatus* Pilsbry and the serpulid polychaete *Pomatoleios kraussii* Baird: Impact of a commonly used antifouling biocide, Irgarol 1051', *Biofouling*, 21, (3/4), pp. 169-180.
- Kirby, M. R. (2006) *Barnacle settlement behaviour in response to con- and allo-specific cues*. PhD thesis. Newcastle University.
- Kirchman, D., Graham, S., Reish, D. and Mitchell, R. (1982) 'Bacteria induce settlement and metamorphosis of *Janua (Dexiospira) brasiliensis* Grube (Polychaeta: Spirorbidae)', *Journal of Experimental Marine Biology and Ecology*, 56, pp. 153-153.
- Kitano, H., Anraku, Y. and Shinohara, H. (2006) 'Sensing Capabilities of Colloidal Gold Monolayer Modified with a Phenylboronic Acid-Carrying Polymer Brush', *Biomacromolecules*, 7, pp. 1065-1071.
- Knight-Jones, E. W. (1953) 'Laboratory experiments on gregariousness during setting in *Balanus balanoides* and other barnacles', *Journal of Experimental Biology*, 30, pp. 584-599.

- Knight-Jones, E. W. (1955) 'The gregarious setting reaction of barnacles as a measure of systematic affinity', *Nature*, 175, pp. 266.
- Knight-Jones, E. W. and Crisp, D. J. (1953) 'Gregariousness in barnacles in relation to the fouling of ships and to anti-fouling research', *Nature*, 171, pp. 1109-1110.
- Knight-Jones, E. W. and Stephenson, J. P. (1950) 'Gregariousness during settlement in the barnacle *Elminius modestus* Darwin', *Journal of the Marine Biological Association of the UK*, 29, pp. 281-297.
- Końska, G., Zamorska, L., Pituch-Noworolska, A., Szmciarz, M. and Guillot, J. (2003) 'Application of fluorescein-labelled lectins with different glycan-binding specificities to the studies of cellular glycoconjugates in human full-term placenta', *Folia Histochemica et Cytobiologica*, 41, (3), pp. 155-160.
- Kornfeld, K., Reitman, M. L. and Kornfeld, R. (1981) 'The Carbohydrate-binding Specificity of Pea and Lentil Lectins', *Journal of Biological Chemistry*, 256, (13), pp. 6633-6640.
- Krug, P. J. and Manzi, A. E. (1999) 'Waterborne and surface-associated carbohydrates as settlement cues for larvae of the specialist marine herbivore *Alderia modesta*', *The Biological Bulletin*, 197, pp. 94-103.
- Lagersson, N. C. and Høeg, J. T. (2002) 'Settlement behaviour and antennular biomechanics in cypris larvae of *Balanus amphitrite* (Crustacea:Thecostraca:Cirripedia)', *Marine Biology*, 141, pp. 513-526.
- Larman, V. N., Gabbot, P. A. and East, J. (1982) 'Physico-chemical properties of the settlement factor proteins from the barnacle *Balanus balanoides*', *Comparative Biochemistry and Physiology*, 72B, pp. 329-338.
- Lau, S. C. K., Thiagarajan, V. and Qian, P.-Y. (2003) 'The bioactivity of bacterial isolates in Hong Kong waters for the inhibition of barnacle (*Balanus amphitrite* Darwin) settlement', *Journal of Experimental Marine Biology and Ecology*, 282, pp. 43-60.
- Lee, H., Dellatore, S. M., Miller, W. M. and Messersmith, P. B. (2007) 'Mussel-inspired surface chemistry for multifunctional coatings', *Science*, 318, pp. 426-430.
- Lee, H., Scherer, N. F. and Messersmith, P. B. (2006) 'Single-molecule mechanics of mussel adhesion', *Proceedings of the National Academy of Sciences of the United States*, 103, (35), pp. 12999-13003.

- Liu, Y., Bruening, M. L., Bergbreiter, D. E. and Crooks, R. M. (1997) 'Multilayer dendrimer-polyanhydride composite films on glass, silicon and gold wafers', *Angewandte Chemie International Edition*, 36, pp. 2114-2116.
- Lonsdale, D. J., Frey, M. A. and Snell, T. W. (1998) 'The role of chemical signals in copepod reproduction', *Journal of Marine Systems*, 15, pp. 1-12.
- Lonsdale, D. J., Snell, T. W. and Frey, M. A. (1996) 'Lectin binding to surface glycoproteins on *Coullana* spp. (Copepoda:Harpacticoida) can inhibit mate guarding', *Marine and Freshwater Behaviour and Physiology*, 27, (2-3), pp. 153-162.
- Lunn, I. (1974) *Antifouling - A brief introduction to the origins and developments of the marine antifouling industry*. BCA Publications: Oxford.
- Magnadóttir, B., Crispin, M., Royle, L., Colominas, C., Harvey, D. J., Dwek, R. A. and Rudd, P. M. (2002) 'The carbohydrate moiety of serum IgM from Atlantic cod (*Gadus morhua* L.)', *Fish and Shellfish Immunology*, 12, pp. 209-227.
- Magnadóttir, B., Gudmundsdóttir, S. and Gudmundsdóttir, B. (1997) 'The carbohydrate moiety of IgM from salmon (*Salmo salar* L.)', *Comparative Biochemistry and Physiology - Part B*, 116, pp. 423-430.
- Marabotti, I., Morelli, A., Orsini, L. M., Martinelli, E., Galli, G., Chiellini, E., Lien, E. M., Pettitt, M. E., Callow, M. E., Callow, J. A., Conlan, S. L., Mutton, R. J., Clare, A. S., Kocijan, A., Donik, C. and Jenko, M. (2009) 'Fluorinated/siloxane copolymer blends for fouling releasing: chemical characterisation and biological evaluation with algae and barnacles', *Biofouling*, 25, (6), pp. 481-493.
- Marechal, J.-P., Hellio, C., Sebire, M. and Clare, A. S. (2004) 'Settlement behaviour of marine invertebrate larvae measured by EthoVision 3.0', *Biofouling*, 20, (4/5), pp. 211-217.
- Marsden, R. L., McGuffin, L. J. and Jones, D. T. (2002) 'Rapid protein domain assignment from amino acid sequence using predicted secondary structure', *Protein Science*, 11, (12), pp. 2814-2824.
- Mary, A., Sr. and Mary, V., Sr. (1999) 'Barnacle antifouling natural products from marine biota', in Thompson, M.-F. and Nagabhushanam, R.(eds) *Barnacles: The Biofoulers*. Regency Publications: New Delhi, pp. 406.
- Matsubara, H., Kabuto, S., Nakahara, N., Ogawa, T., Muramoto, K., Jimbo, M. and Kamiya, H. (2005) 'Structure and possible function of N-glycans of an invertebrate C-

- type lectin from the acorn barnacle *Megabalanus rosa*', *Fisheries Science*, 71, pp. 931-940.
- Matsumura, K. (2006) *Identification of fouling species in barnacle larvae by DNA analysis*. Tokyo, Japan: Central Research Institute of Electric Power Industry
- Matsumura, K., Hills, J. M., Thomason, P. O., Thomason, J. C. and Clare, A. S. (2000) 'Discrimination at settlement in barnacles: laboratory and field experiments on settlement behaviour in response to settlement-inducing protein complexes', *Biofouling*, 16, (2-4), pp. 181-190.
- Matsumura, K., Mori, S., Nagano, M. and Fusetani, N. (1998a) 'Lentil lectin inhibits adult extract-induced settlement on the barnacle, *Balanus amphitrite*', *Journal of Experimental Biology*, 280, pp. 213-219.
- Matsumura, K., Nagano, M. and Fusetani, N. (1998b) 'Purification of a larval settlement-inducing protein complex (SIPC) of the barnacle, *Balanus amphitrite*', *Journal of Experimental Biology*, 281, pp. 12-20.
- Matsumura, K., Nagano, M., Kato-Yoshinaga, Y., Yamazaki, M., Clare, A. S. and Fusetani, N. (1998c) 'Immunological studies on the settlement-inducing protein complex (SIPC) of the barnacle *Balanus amphitrite* and its possible involvement in larva-larva interactions', *Proceedings of the Royal Society of London, B*, 265, pp. 1825-1830.
- McKenzie, J. and Grigovala, I. (1996) 'The echinoderm surface and its role in preventing antifouling', *Biofouling*, 10, pp. 261-272.
- Meikle, P., Richards, G. and Yellowlees, D. (1987) 'Structural determination of the oligosaccharide side chains from a glycoprotein isolated from the mucus of the coral *Acropora formosa*', *Journal of Biological Chemistry*, 262, pp. 16941-16947.
- Meissner, U., Dube, P., Harris, J. R., Stark, H. and Markl, J. (2000) 'Structure of a Molluscan Hemocyanin Dodecamer (HtH1 from *Haliotis tuberculata*) at 12Å Resolution by Cryoelectron Microscopy', *Journal of Molecular Biology*, 298, pp. 21-34.
- Meissner, U., Stohr, M., Kusche, K., Burmester, T., Stark, H., Harris, J. R. and Orlova, E. V. (2003) 'Quaternary structure of the European spiny lobster (*Palinurus elephas*) 1 x 6-mer Hemocyanin from cryoEM and amino acid sequence data', *Journal of Molecular Biology*, 325, pp. 99-109.

- Miron, G., Walters, L., Tremblay, R. and Bourget, E. (2000) 'Physiological condition and barnacle behaviour: a preliminary look at the relationship between TAG/DNA ratio and larval substratum exploration in *Balanus amphitrite*', *Marine Ecology Progress Series*, 198, pp. 303-310.
- Morse, A. N. C. and Morse, D. E. (1984) 'Recruitment and metamorphosis of *Haliotis* larvae induced by molecules uniquely available at the surfaces of crustose red algae', *Journal of Experimental Marine Biology and Ecology*, 75, pp. 191-215.
- Mostaert, A. S., Higgins, M. J., Fukuma, T., Rindi, F. and Jarvis, S. P. (2006) 'Nanoscale Mechanical Characterisation of Amyloid Fibrils Discovered in a Natural Adhesive', *Journal of Biological Physics*, 32, (5), pp. 393-401.
- Murray, M. D. and Darvell, B. W. (1990) 'A protocol for contact angle measurement', *Journal of Physics D: Applied Physics*, 23, pp. 1150-1155.
- Nair, N. U. (1999) 'Innovative protective technology against barnacle fouling', in Thompson, M.-F. and Nagabhushanam, R.(eds) *Barnacles: The Biofoulers*. Regency Publications: New Delhi, pp. 406.
- Neal, A. L. and Yule, A. B. (1994) 'The tenacity of *Elminius modestus* and *Balanus perforatus* cyprids to bacterial films grown under different shear regimes', *Journal of the Marine Biological Association of the UK*, 74, pp. 251-257.
- Nizet, V. and Esko, J. D. (1999) 'Bacterial and Viral Infections', in Varki, A., Cummings, R. D., Esko, J. D., Freeze, H. H., Stanley, P., Bertozzi, C. R., Hart, G. W. and Etzler, M. E.(eds) *Essentials of Glycobiology*. Cold Spring Harbour Laboratory Press: Cold Spring Harbour, NY.
- Noldus, L. P. J. J., Spink, A. J. and Teglenbosch, R. A. J. (2001) 'EthoVision: A versatile video tracking system for automation of behavioral experiments', *Behavior Research Methods, Instruments, & Computers*, 33, (3), pp. 398-414.
- Nott, J. A. (1969) 'Settlement of barnacle larvae: surface structure of the antennular attachment disc by scanning electron microscopy', *Marine Biology*, 2, pp. 248-251.
- Nott, J. A. and Foster, B. A. (1969) 'On the structure of the antennular attachment organ of the cypris larva of *Balanus balanoides* (L.)', *Philosophical Transactions of the Royal Society of London, Series B, Biological Sciences*, 256, pp. 115-134.

- Nussbaumer, A. D., Bright, M., Baranyi, C., JBeisser, C. J. and Ott, J. A. (2004) 'Attachment mechanism in a highly specific association between ectosymbiotic bacteria and marine nematodes', *Aquatic Microbial Ecology*, 34, pp. 239-246.
- Pagett, H. E., Abrahams, J. L., Bones, J., O'Donoghue, N., Marles-Wright, J., Lewis, R. J., Harris, R., Caldwell, G. S., Rudd, P. M. and Clare, A. S. (2012) 'Structural characterisation of the N-glycan moiety of the barnacle settlement-inducing protein complex (SIPC) ', *Journal of Experimental Biology*, 215, pp. 1192-1198.
- Pahler, S., Blumbach, B., Muller, I. and Muller, W. (1998) 'Putative multiadhesive protein from the marine sponge *Geodia cydonium*: cloning of the cDNA encoding a fibronectin-, an SRCR-, and a complement control protein module', *Journal of Experimental Zoology*, 282, pp. 332-343.
- Pechenik, J. A., Rittschof, D. and Schmidt, A. R. (1993) 'Influence of delayed metamorphosis on survival and growth of juvenile barnacles *Balanus amphitrite*', *Marine Biology*, 115, (2), pp. 287-294.
- Pérez-Roa, R. E., Anderson, M. A., Rittschof, D., Orihuela, B., Wendt, D., Kowalke, G. L. and Noguera, D. R. (2008) 'Inhibition of barnacle (*Amphibalanus amphitrite*) cyprid settlement by means of localized, pulsed electric fields', *Biofouling*, 24, (3), pp. 177-184.
- Petrone, L., Di Fino, A., Aldred, N., Sukkaew, P., Ederth, T., Clare, A. S. and Liedberg, B. (2011) 'Effects of surface charge and Gibbs surface energy on the settlement behaviour of barnacle cyprids (*Balanus amphitrite*)', *Biofouling*, 27, (9), pp. 1043-1055.
- Pettitt, M. E., Henry, S. L., Callow, M., Callow, J. A. and Clare, A. S. (2004) 'Activity of commercially enzymes on settlement and adhesion of cypris larvae of the barnacle *Balanus amphitrite*, spores of the green alga *Ulva linza*, and the diatom *Navicula perminuta*', *Biofouling*, 20, (6), pp. 299-311.
- Phang, I. Y., Aldred, N., Clare, A. S., Callow, J. A. and Vancso, G. J. (2006) 'An in situ study of the nanomechanical properties of barnacle (*Balanus amphitrite*) cyprid cement using atomic force microscopy (AFM)', *Biofouling*, 22, (4), pp. 245-250.
- Phang, I. Y., Aldred, N., Clare, A. S. and Vancso, G. J. (2007) 'Towards a nanochemical basis for temporary adhesion in barnacle cyprids (*Semibalanus balanoides*)', *Journal of the Royal Society Interface*, 5, (21), pp. 397-401.

- Phang, I. Y., Aldred, N., Ling, X. Y., Tomczak, N., Huskens, J., Clare, A. S. and Vancso, G. J. (2009) 'Chemistry-Specific Interfacial Forces Between Barnacle (*Semibalanus balanoides*) Cyprid Footprint Proteins and Chemically Functionalised AFM Tips', *Journal of Adhesion*, 85, (9), pp. 616-630.
- Pitombo, F. B. (2004) 'Phylogenetic analysis of the Balanidae (Cirripedia, Balanomorph)', *Zoologica scripta*, 33, (3), pp. 261-276.
- Pompe, T., Zschoche, S., Herold, N., Salchert, K., Gouzy, M.-F., Sperling, C. and Werner, C. (2003) 'Maleic Anhydride Copolymers - A Versatile Platform for Molecular Biosurface Engineering', *Biomacromolecules*, 4, pp. 1072-1079.
- Prendergast, G. S., Zurn, C. M., Bers, A. V., Head, R. M., Hansson, L. J. and Thomason, J. C. (2008) 'Field-based video observations of wild barnacle cyprid behaviour in response to textural and chemical settlement cues', *Biofouling*, 24, (6), pp. 449-459.
- Prendergast, G. S., Zurn, C. M., Bers, A. V., Head, R. M., Hansson, L. J. and Thomason, J. C. (2009) 'The relative magnitude of the effects of biological and physical settlement cues for cypris larvae of the acorn barnacle, *Semibalanus balanoides* L.' *Biofouling*, 25, (1), pp. 35-44.
- Rico-Martinez, R., Dingmann, B. and Snell, T. W. (1996) 'Surface glycoproteins potentially involved in mate recognition in nine freshwater rotifer species', *Archiv für Hydrobiologie*, 138, pp. 1-10.
- Rittschof, D. (2000) 'Natural Product Antifoulants: One Perspective on the Challenges Related to Coatings Development', *Biofouling*, 15, (1-3), pp. 119-127.
- Rittschof, D., Branscom, E. S. and Costlow, J. D. (1984) 'Settlement and behavior in relation to flow and surface in larval barnacles, *Balanus amphitrite* Darwin', *Journal of Experimental Marine Biology and Ecology*, 82, pp. 131-146.
- Rittschof, D., Clare, A. S., J, G. D., Mary, A., Sr. and Bonaventura, J. (1992) 'Barnacle in vitro assays for biologically active substances: Toxicity and Settlement inhibition assays using mass cultured *Balanus amphitrite* Darwin ', *Biofouling*, 6, (2), pp. 115-122.
- Rittschof, D., Hooper, I. R. and Costlow, J. D. (1986) 'Barnacle settlement inhibitors from sea pansies, *Rennia reniformis*', *Bulletin of Marine Science*, 39, (2), pp. 376-382.
- Rousselot, M., Jaenicke, E., Lamkemeyer, T., Harris, J. R. and Pirow, R. (2006) 'Native and subunit molecular mass and quaternary structure of the hemoglobin from the

- primitive branchiopod crustacean *Triops cancriformis*', *Federation of the Societies of Biochemistry and Molecular Biology Journal*, 273, pp. 4055-4071.
- Royle, L., Radcliffe, C. M., Dwek, R. A. and Rudd, P. M. (2006) 'Detailed structural analysis of N-glycans released from glycoproteins in SDS-PAGE gel bands using HPLC combined with exoglycosidase array digestions', in Brockhausen-Schutzbach, I.(ed), *Glycobiology Protocols*. Vol. 347 Humana Press Inc: Totowa, NJ, pp. 125-143.
- Rudd, P. M., Colominas, C., Royle, L., Murphy, N., Hart, E., Merry, A. H., Hebestreit, H. F. and Dwek, R. A. (2001) 'A high-performance liquid chromatography based strategy for rapid, sensitive sequencing of N-linked oligosaccharide modifications to proteins in sodium dodecyl sulphate polyacrylamide electrophoresis gel bands', *Proteomics*, 1, pp. 285-294.
- Ruppert, E. E. and Barnes, R. D. (1994) *Invertebrate Zoology*. Saunders College Publishing, Fort Worth.
- Salman, H. H., Gamazo, C., Campanero, M. A. and Irache, J. M. (2006) 'Bioadhesive mannosylated nanoparticles for oral drug delivery', *Journal of Nanoscience and Nanotechnology*, 6, pp. 3203-3209.
- Satpathy, K. K., Venugopalan, V. P. and Nair, K. V. K. (1999) 'Barnacle fouling control technology in power plant cooling systems', in Thompson, M.-F. and Nagabhushanam, R.(eds) *Barnacles: The Biofoulers*. Regency Publications: New Delhi, pp. 406.
- Schultz, M. P. (2007) 'Effects of coating roughness and biofouling on ship resistance and powering', *Biofouling*, 23, (5), pp. 331-341.
- Schumacher, J. F., Aldred, N., Callow, M. E., Finlay, J. A., Callow, J. A., Clare, A. S. and Brennan, A. B. (2007) 'Species-specific engineered antifouling topographies; correlations between the settlement of algal zoospores and barnacle cyprids', *Biofouling*, pp. 1-11.
- Seah, M., Gilmore, I. and Beamson, G. (1998) 'XPS: Binding energy calibration of electron spectrometers 5 - a re-assessment of the reference energies', *Surface and Interface Analysis*, 26, pp. 642-649.
- Sears, P. and Wong, C.-H. (2001) 'Towards automated synthesis of oligosaccharides and glycoproteins', *Science*, 291, pp. 2344-2350.

- Selkirk, C. (2004) 'Ion Exchange Chromatography', in Cutler, P.(ed), *Methods in Molecular Biology: Protein Purification protocols*. Vol. 244 Humana Press: Totowa, New Jersey, pp. 125-131.
- Sharon, N. and Lis, H. (1989) *Lectins*. Chapman & Hall: London.
- Shimizu, K., Saikawa, W. and Fusetani, N. (1996) 'Identification and partial characterization of vitellin from the barnacle *Balanus amphitrite*', *Comparative Biochemistry and Physiology*, 115B, pp. 111–119.
- Shirley, D. (1972) 'High-Resolution X-Ray Photoemission Spectrum of the Valence Bands of Gold', *Physical Review B*, 5, pp. 4709-4714.
- Snell, T. and Carmona, M. (1994) 'Surface glycoproteins in copepods - potential signals for mate recognition', *Hydrobiologia*, 293, pp. 255-264.
- Snell, T. W. (2011) 'Contact chemoreception and its role in zooplankton mate recognition', in Breithaupt, T. and Thiel, M.(eds) *Chemical Communication in Crustaceans*. Springer: New York, pp. 451-466.
- Snell, T. W., Morris, P. D. and Cecchine, G. (1993) 'Localization of the mate-recognition pheromone in *Brachionus plicatilis* O.F Müller (Rotifera) by fluorescent labeling with lectins', *Journal of Experimental Marine Biology and Ecology*, 165, pp. 225-235.
- Spain, S. G., Albertin, L. and Cameron, N. R. (2006) 'Facile in situ preparation of biologically active multivalent glyconanoparticles', *Chemical Communications*, 40, pp. 4198-4200.
- Stelzer, C. P. and Snell, T. W. (2003) 'Induction of sexual reproduction in *Brachionus plicatilis* (Monogononta, Rotifera) by a density-dependant chemical cue', *Limnology and Oceanography*, 48, (2), pp. 939-943.
- Stouffer, J. M. and McCarthy, T. J. (1988) 'Polymer Monolayers Prepared by the Spontaneous Adsorption of Sulfur-Functionalized Polystyrene on Gold Surfaces', *Macromolecules*, 21, pp. 1204-1208.
- Su, R., Li, L., Chen, X., Han, J. and Han, S. (2009) 'Multivalent mannose-displaying nanoparticles constructed from poly{styrene-co-[(maleic anhydride)-alt-styrene]}', *Organic & Biomolecular Chemistry*, 7, pp. 2040-2045.
- Tan, B. H., Hussain, H., Chaw, K. C., Dickinson, G. H., Gudupati, C. S., Birch, W. R., Teo, S. L. M., He, C., Liu, Y. and Davis, T. P. (2010) 'Barnacle repellent nanostructured

- surfaces formed by the self-assembly of amphiphilic block copolymers', *Polymer Chemistry*, 1, pp. 276-279.
- Tang, G., Peng, L., Baldwin, P. R., Mann, D. S., Jiang, W., Rees, I. and Ludtke, S. J. (2007) 'EMAN2: An extensible image processing suite for electron microscopy', *Journal of Structural Biology*, 157, pp. 38-46.
- Tang, Y., Finlay, J. A., Kowalke, G. L., Meyer, A. E., Bright, F. V., Callow, M., Callow, J. A., Wendt, D. and Detty, M. R. (2005) 'Hybrid xerogel films as novel coatings for antifouling and fouling release', *Biofouling*, 21, (1), pp. 59-71.
- Taverner, T., Hernández, H., Sharon, M., Ruotolo, B. T., Matak-Vinkovi, D., Devos, D., Russell, R. B. and Robinson, C. V. (2008) 'Subunit Architecture of Intact Protein Complexes from Mass Spectrometry and Homology Modeling', *Accounts of Chemical Research*, 41, (5), pp. 617-627.
- Taylor, M. E. and Drickamer, K. (2003) *Introduction to Glycobiology*. Oxford University Press.
- Tegtmeyer, K. and Rittschof, D. (1989) 'Synthetic Peptide Analogs to Barnacle Settlement Pheromone', *Peptides*, 9, pp. 1403-1406.
- Thankappan, A., Fuller, J. R., Goodwin, U. B., Kearse, K. P. and McConnell, T. J. (2006) 'Characterisation of glycans on major histocompatibility complex class II molecules in channel catfish, *Ictalurus punctatus*', *Developmental and Comparative Immunology*, 30, pp. 772-782.
- Thiyagarajan, V. and Qian, P.-Y. (2008) 'Proteomic analysis of larvae during development, attachment, and metamorphosis in the fouling barnacle, *Balanus amphitrite*', *Proteomics*, 8, pp. 3164-3172.
- Ting, J. H., Kelly, L. S. and Snell, T. W. (2000) 'Identification of sex, age and species specific proteins on the surface of the harpacticoid copepod *Tigriopus japonicus*', *Marine Biology*, 137, pp. 31-37.
- Ting, J. H. and Snell, T. W. (2003) 'Purification and sequencing of a mate-recognition protein from the copepod *Tigriopus japonicus*', *Marine Biology*, 143, pp. 1-8.
- Toonen, R. and Pawlik, J. (1994) 'Foundations of gregariousness', *Nature*, 370, pp. 511-512.

- Tseneklidou-Stoeter, D., Gerwig, G., Kamerling, J. and Spindler, K. (1995) 'Characterisation of N-linked carbohydrate chains of the crayfish, *Astacus leptodactylus* hemocyanin', *Biological Chemistry Hoppe-Seyler*, 376, pp. 531-537.
- Ulman, A. (1996) 'Formation and structure of self-assembled monolayers', *Chemical Reviews*, 96, pp. 1533-1554.
- Uzawa, H., Ito, H., Izumi, M., Tokuhisa, H., Taguchi, K. and Minoura, N. (2005) 'Synthesis of polyanionic glycopolymers for the facile assembly of glycosyl arrays', *Tetrahedron*, 61, pp. 5895-5905.
- Varki, A. and Lowe, J. B. (1999) 'Biological Roles of Glycans', in Varki, A., Cummings, R. D., Esko, J. D., Freeze, H. H., Stanley, P., Bertozzi, C. R., Hart, G. W. and Etzler, M. E.(eds) *Essentials of Glycobiology*. Cold Spring Harbour Laboratory Press: Cold Spring Harbour, NY.
- Vogan, C. L., Maskrey, B. H., Taylor, G. W., Henry, S., Pace-Asciak, C. R., Clare, A. S. and Rowley, A. F. (2003) 'Hepoxilins and trioxilins in barnacles: an analysis of their potential roles in egg hatching and larval settlement processes', *Journal of Experimental Biology*, 206, pp. 3219-3226.
- Wahl, M. (1989) 'Marine epibiosis. I. Fouling and antifouling: some basic aspects', *Marine Ecology Progress Series*, 58, pp. 175-189.
- Walker, G. and Yule, A. B. (1984) 'The temporary adhesion of barnacle cyprids: effects of some differing surface characteristics', *Journal of the Marine Biological Association of the UK*, 64, pp. 429-439.
- Walker, G., Yule, A. B. and Nott, J. A. (1987) 'Structure and function in balanomorph larvae', in Southward, A. J.(ed), *Barnacle Biology - Crustacean Issues 5*. A. A. Balkema: Rotterdam.
- Wieringa, R. H. and Schouten, A. J. (1996) 'Oriented Thin Film Formation by Surface Graft Polymerization of γ -Methyl L-Glutamate N-Carboxyanhydride in the Melt', *Macromolecules*, 29, pp. 3032-3034.
- Yamamoto, H. (1999) 'Marine adhesive proteins', in Thompson, M.-F. and Nagabhushanam, R.(eds) *Barnacles: The Biofoulers*. Regency Publications: New Delhi, pp. 406.

- Yebra, D. M., Kiil, S. and Dam-Johnson, K. (2004) 'Antifouling technology - past, present and future steps towards efficient and environmentally friendly antifouling coatings', *Progress in Organic Coatings*, 50, pp. 75-104.
- Yeganeh, M., Coxon, P., Brieva, A., Dhanak, V., Siller, L. and Butenko, Y. (2007) 'Atomic hydrogen treatment of nanodiamond powder studied with photoemission spectroscopy', *Physical Review B*, 75, (15), pp. 155404-155411.
- Yen, J. and Lasley, R. (2010) 'Chemical communication between copepods: finding a mate in a fluid environment', in Breithaupt, T. and Thiel, M.(eds) *Chemical Communication in Crustaceans*. Springer: New York, pp. 177-198.
- Yin, C., Ying, L., Zhang, P.-C., Zhuo, R.-X., Kang, E.-T. and Leong, K. W. (2003) 'High density of immobilised galactose ligand enhances hepatocyte attachment and function', *Journal of Biomedical Materials Research Part A*, 67A, (4), pp. 1093-1104.
- Ying, L., Yin, C., Zhuo, R.-X., Leong, K. W., Mao, H. Q., Kang, E.-T. and Neoh, K. G. (2003) 'Immobilisation of galactose ligands on acrylic acid graft-copolymerised poly(ethylene terephthalate) film and its application to hepatocyte culture', *Biomacromolecules*, 4, pp. 157-165.
- Yule, A. B. and Crisp, D. J. (1983) 'Adhesion of cypris larvae of the barnacle, *Balanus balanoides*, to clean and arthropodin treated surfaces', *Journal of the Marine Biological Association of the UK*, 63, pp. 261-270.
- Yule, A. B. and Walker, G. (1985) 'Settlement of *Balanus balanoides*: the effect of cyprid antennular secretion', *Journal of the Marine Biological Association of the UK*, 65, pp. 707-712.
- Yule, A. B. and Walker, G. (1987) 'Adhesion in barnacles', in Southward, A. J.(ed), *Barnacle Biology - Crustacean Issues 5*. A. A. Balkema: Rotterdam.
- Zal, F., Küster, B., Green, B. N., Harvey, D. J. and Lallier, F. H. (1998) 'Partially glucose-capped oligosaccharides are found on the hemoglobins of the deep-sea tube worm *Riftia pachyptila*', *Glycobiology*, 8, (7), pp. 663-673
- Zhang, H., Li, X.-j., Martin, D. B. and Aebersold, R. (2003) 'Identification and quantification of N-linked glycoproteins using hydrazide chemistry, stable isotope labeling and mass spectrometry', *Nature Biotechnology*, 21, pp. 660-666.
- Zhou, Y., Bruening, M. L., Liu, Y., Crooks, R. M. and Bergbreiter, D. E. (1996) 'Synthesis of Hyperbranched, Hydrophilic Fluorinated

Surface Grafts', *Langmuir*, 12, pp. 5519-5521.

Zuber, C. and Roth, J. (2009) 'N-glycosylation', in Gabius, H.-J.(ed), *The Sugar Code: Fundamentals of Glycosciences*. Wiley-Blackwell: Weinheim.

Appendix A

SIPC Purification Buffer Recipes as used in Chapter 3.2. The number in [x] indicates the concentration of the solution and consequently if it must be diluted using dH₂O before use.

TrisBase (pH 7.5 Tris HCl 50mM) [10x]

157.6g Tris HCl
2 litres dH₂O
NaOH to buffer to pH 7.5

pH 6.8 TrisHCl 0.5M [1x]

7.88g TrisHCl
100ml dH₂O
Buffer to pH 6.8 with NaOH or HCl

Laemmli Buffer [5x]

6ml 0.5M TrisHCl pH 6.8
2g SDS stock
10ml 100% glycerol
0.01% w/v bromophenol blue
7ml dH₂O
2.5ml β-mercaptoethanol (added just before use)

Resolving gel [1x but makes 2 mini-gels]

9.6ml dH₂O
5ml acrylamide
5ml pH 8.8 TrisBase 1.5M
200μl SDS (10%)
100μl APS (10%)
8μl TEMED

pH 8.8 TrisBase 1.5M [1x]

18.17g TrisBase
100ml dH₂O
Buffer to pH 8.8 with NaOH or HCl

Antibody Buffer [1x]

500ml TBS
5g non-fat dried milk

Running Buffer [10x]

30.275g TrisBase
144.135g glycine
10g SDS
1litre dH₂O

TBS (10x)

31.52g TrisHCl
292g NaCl
1litre dH₂O

Transfer Buffer [5x]

30.275g TrisBase
144.125g glycine
250ml methanol
750ml dH₂O

TTBS (1x)

1litre TBS
0.5ml Tween20

Blocking Buffer [1x]

500ml TBS
15g non-fat dried milk

Staining Solution [1x]

10ml dH₂O
1 BCIP/NBT stain tablet

Stacking gel [1x but makes 2 mini-gels]

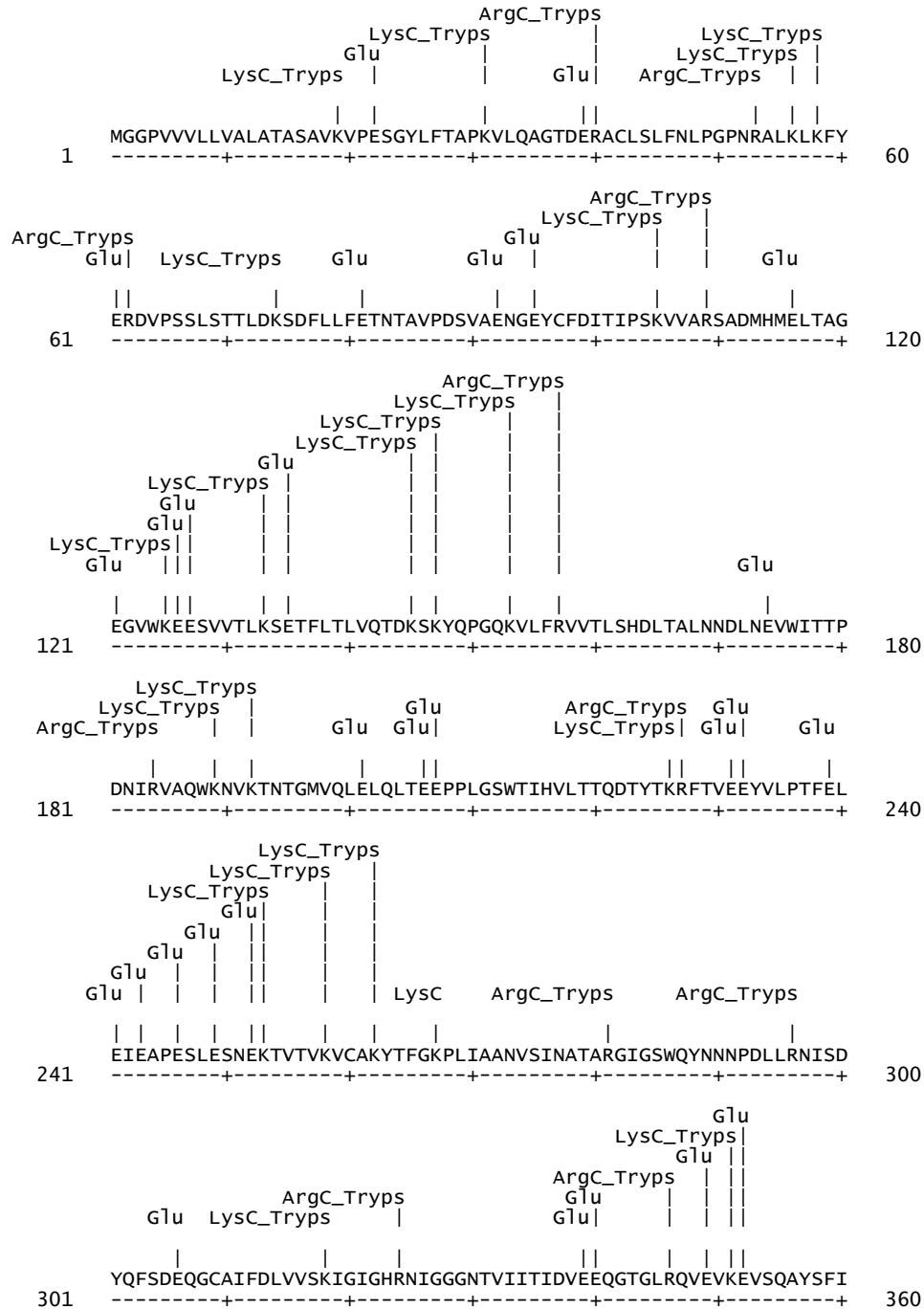
3.6ml dH₂O
800μl acrylamide
1.36ml pH 6.8 TrisHCl 0.5M
60μl SDS (10%)
164μl APS (10%)
6μl TEMED

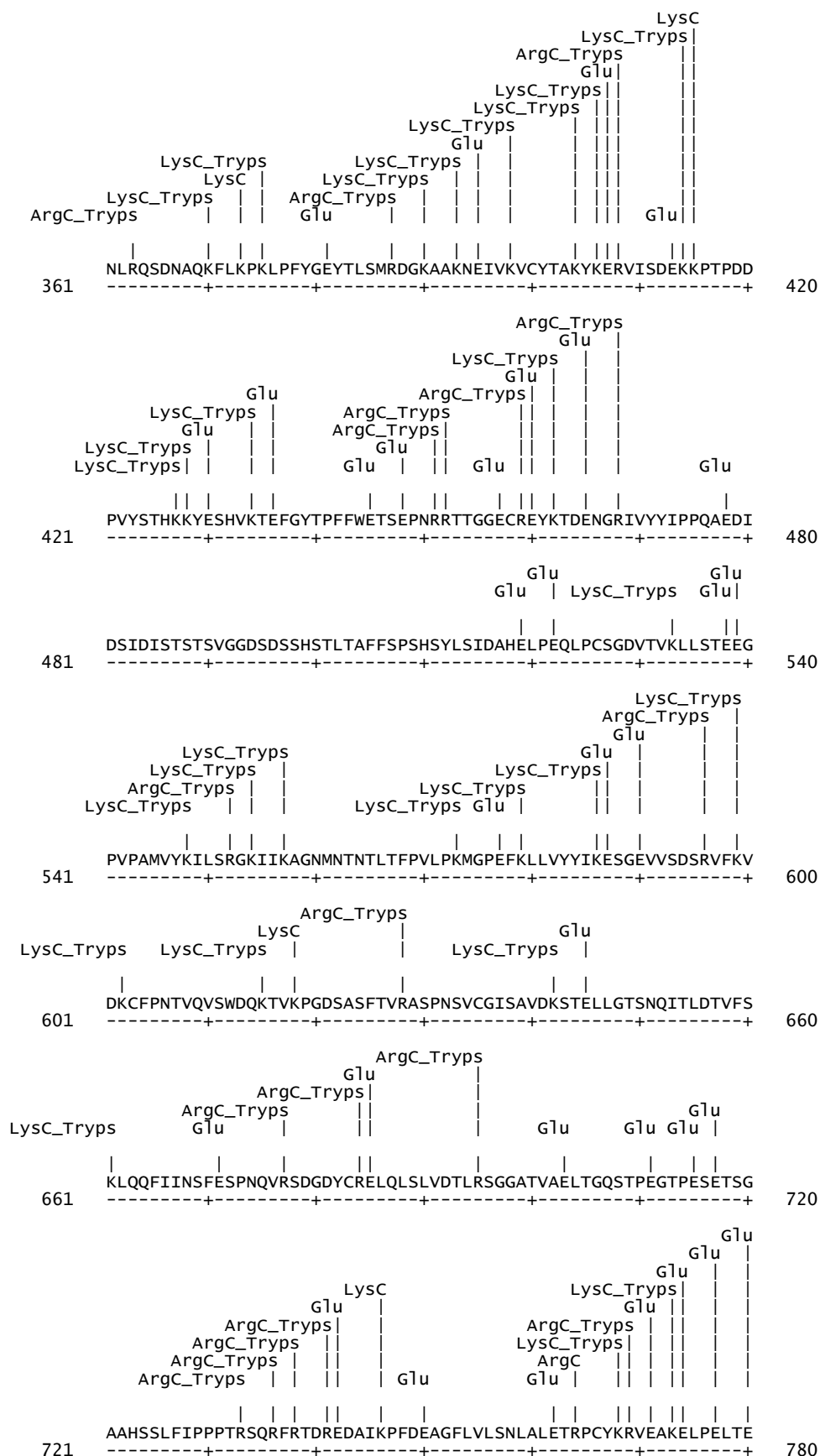
Coomassie Brilliant Blue Stain/Destain[1x]

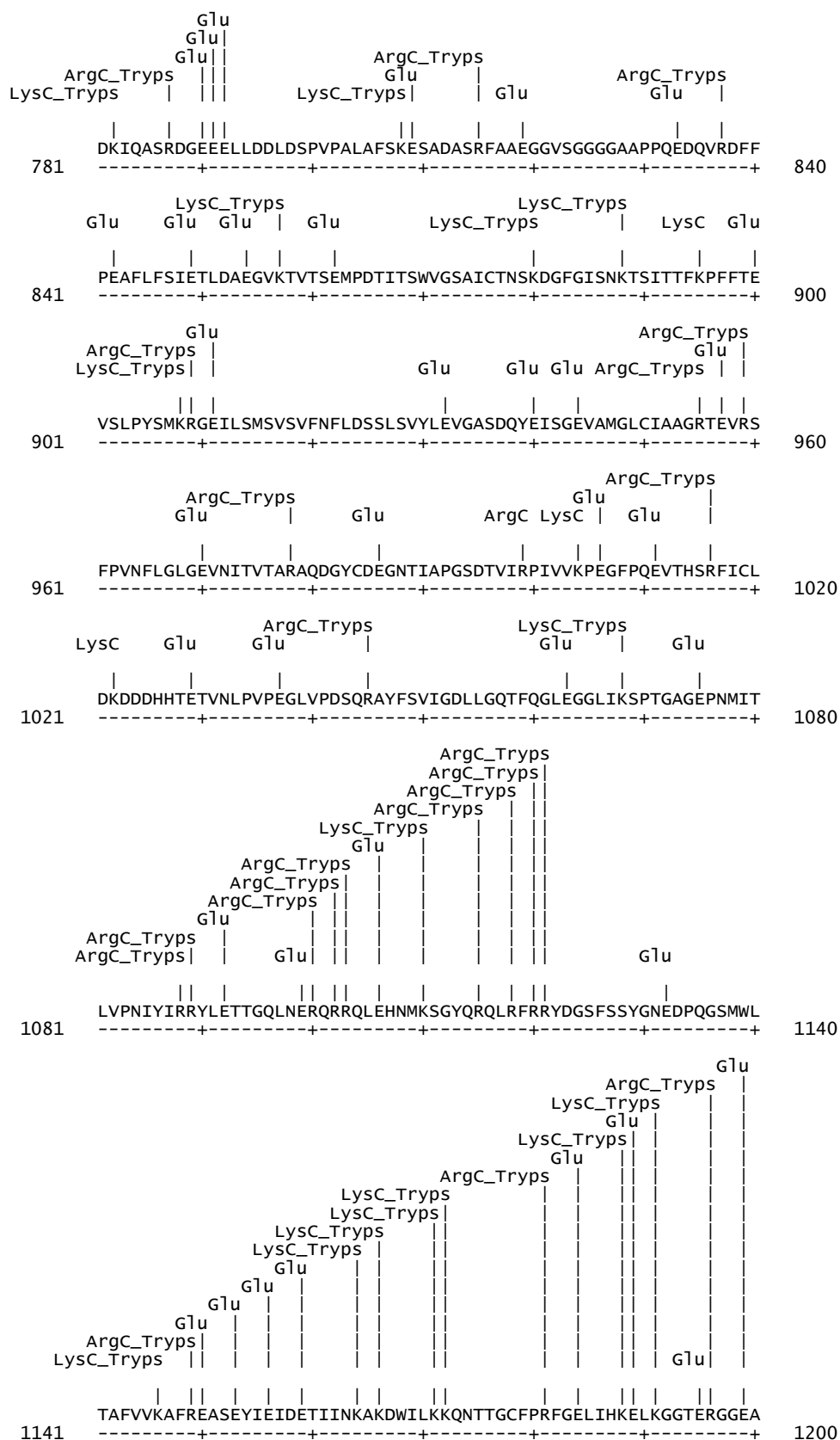
187.5ml glacial acetic acid
1250ml ethanol (95-100%)
1062.5ml dH₂O
2000ml of this forms the de-stain.
To the remaining 500ml, add 0.125g of CBB forming the stain.

Appendix B

SIPC enzyme cleavage sites as produced by <http://expasy.org/cgi-bin/peptidecutter/> for enzymatic cleavage by Arg-C, Glu-C, Lys-C and Trypsin as used in Chapter 5.2.3.







LysC_Tryps Glu LysC_Tryps Glu ArgC_Tryps
 1201 ALTA FV ML AL KDI AT T N E L A N G F A C L E D G L L P N K T L Y S E I L L A Y T Y L N M G Q D V K G E R L V 1260
 -----+-----+-----+-----+-----+-----+-----+-----+-----+-----+
 Glu
 ArgC_Tryps LysC_Tryps ArgC_Tryps ArgC_Tryps ArgC_Tryps ArgC_Tryps
 LysC_Tryps LysC_Tryps Glu Glu LysC_Tryps Glu
 1261 N K L M S K A K R E G D D I L Y W E G D R D S L F G G S R A V D V E M T A Y M A L S L M H I S G K G N M E E A A R A I R 1320
 -----+-----+-----+-----+-----+-----+-----+-----+-----+-----+
 ArgC_Tryps LysC_Tryps ArgC_Tryps ArgC_Tryps ArgC_Tryps
 ArgC_Tryps Glu Glu Glu Glu
 1321 W I N T Q R N S N G G F K S T Q D T I V A V E A L S E F A S R T F A S D L A T S V S V T A G G E T V Q R M V D G D N R L 1380
 -----+-----+-----+-----+-----+-----+-----+-----+-----+-----+
 LysC_Tryps ArgC_Tryps ArgC_Tryps ArgC_Tryps ArgC_Tryps
 Glu Glu Glu Glu Glu
 1381 L Y Q E S K V P D L T L P G T M N F D V S P P G C V V Y Q S I F R F S S T L E V P D P A F S L G V A A K K R G R T G Y E 1440
 -----+-----+-----+-----+-----+-----+-----+-----+-----+-----+
 LysC_Tryps LysC_Tryps ArgC_Tryps ArgC_Tryps ArgC_Tryps ArgC_Tryps
 Glu Glu Glu Glu Glu Glu
 1441 L E V C T S F L R N S G A V D R A I L E T E L P S G Y V A V D S T L R D L R R G S A V R S Y E I K E G K V I F T L Q G V 1500
 -----+-----+-----+-----+-----+-----+-----+-----+-----+-----+
 ArgC_Tryps LysC_Tryps LysC_Tryps LysC_Tryps LysC_Tryps LysC_Tryps
 ArgC_Tryps Glu Glu Glu Glu Glu
 1501 A E D K T C L E F R I I Q E N E V E Q L K P S I V K V H D F Y R P E E R N I Q E Y E L T P A A 1547
 -----+-----+-----+-----+-----+-----+-----+-----+-----+-----+

Appendix C

Disulphide Connectivity Prediction for *Balanus amphitrite* SIPC as used in Chapter 5.3.3

Appendix C. Table 1 - Disulphide bond scores: the score for each pair of cysteines, ranging from 0 to 1 (scores greater than 0.5 are highlighted).

Cysteine sequence position	Distance	Bond	Score
42 - 97	55	TDERACLSLFN-ENGEYCFDITI	0.01967
42 - 260	218	TDERACLSLFN-VTVKVCACYTF	0.01069
42 - 309	267	TDERACLSLFN-SDEQGCAIFDL	0.02408
42 - 400	358	TDERACLSLFN-EIVKVCYTAKY	0.01068
42 - 458	416	TDERACLSLFN-TTGGECEYKT	0.01042
42 - 526	484	TDERACLSLFN-PEQLPCSGDVT	0.0165
42 - 603	561	TDERACLSLFN-FKVDKCFPNTV	0.01056
42 - 635	593	TDERACLSLFN-SPNSVCGISAV	0.01529
42 - 683	641	TDERACLSLFN-SDGDYCRELQL	0.05521
42 - 766	724	TDERACLSLFN-LETRPCYKRVE	0.01045
42 - 876	834	TDERACLSLFN-VGSAICTNSKD	0.02586
42 - 950	908	TDERACLSLFN-VAMGLCIAAGR	0.01078
42 - 984	942	TDERACLSLFN-AQDGYCDEGNT	0.01905
42 - 1019	977	TDERACLSLFN-HSRFICLDKDD	0.01082
42 - 1178	1136	TDERACLSLFN-QNTTGCFPRFG	0.0152
42 - 1225	1183	TDERACLSLFN-ANGFACLEDGL	0.0105
42 - 1405	1363	TDERACLSLFN-VSPPGCVVYQS	0.01059
42 - 1444	1402	TDERACLSLFN-YELVCTSFLR	0.01041
42 - 1506	1464	TDERACLSLFN-AEDKTCLEFRI	0.01045
97 - 260	163	ENGEYCFDITI-VTVKVCACYTF	0.01114
97 - 309	212	ENGEYCFDITI-SDEQGCAIFDL	0.0128
97 - 400	303	ENGEYCFDITI-EIVKVCYTAKY	0.01277
97 - 458	361	ENGEYCFDITI-TTGGECEYKT	0.01053
97 - 526	429	ENGEYCFDITI-PEQLPCSGDVT	0.01081
97 - 603	506	ENGEYCFDITI-FKVDKCFPNTV	0.01039
97 - 635	538	ENGEYCFDITI-SPNSVCGISAV	0.0105
97 - 683	586	ENGEYCFDITI-SDGDYCRELQL	0.01369
97 - 766	669	ENGEYCFDITI-LETRPCYKRVE	0.01049
97 - 876	779	ENGEYCFDITI-VGSAICTNSKD	0.11093
97 - 950	853	ENGEYCFDITI-VAMGLCIAAGR	0.02428
97 - 984	887	ENGEYCFDITI-AQDGYCDEGNT	0.01182
97 - 1019	922	ENGEYCFDITI-HSRFICLDKDD	0.02564
97 - 1178	1081	ENGEYCFDITI-QNTTGCFPRFG	0.01064
97 - 1225	1128	ENGEYCFDITI-ANGFACLEDGL	0.01038
97 - 1405	1308	ENGEYCFDITI-VSPPGCVVYQS	0.01037
97 - 1444	1347	ENGEYCFDITI-YELVCTSFLR	0.01088
97 - 1506	1409	ENGEYCFDITI-AEDKTCLEFRI	0.01044
260 - 309	49	VTVKVCACYTF-SDEQGCAIFDL	0.01197
260 - 400	140	VTVKVCACYTF-EIVKVCYTAKY	0.01037
260 - 458	198	VTVKVCACYTF-TTGGECEYKT	0.01058
260 - 526	266	VTVKVCACYTF-PEQLPCSGDVT	0.01454
260 - 603	343	VTVKVCACYTF-FKVDKCFPNTV	0.01043
260 - 635	375	VTVKVCACYTF-SPNSVCGISAV	0.21585
260 - 683	423	VTVKVCACYTF-SDGDYCRELQL	0.01103
260 - 766	506	VTVKVCACYTF-LETRPCYKRVE	0.01042
260 - 876	616	VTVKVCACYTF-VGSAICTNSKD	0.05399
260 - 950	690	VTVKVCACYTF-VAMGLCIAAGR	0.01791
260 - 984	724	VTVKVCACYTF-AQDGYCDEGNT	0.01044
260 - 1019	759	VTVKVCACYTF-HSRFICLDKDD	0.01039
260 - 1178	918	VTVKVCACYTF-QNTTGCFPRFG	0.01052
260 - 1225	965	VTVKVCACYTF-ANGFACLEDGL	0.01038
260 - 1405	1145	VTVKVCACYTF-VSPPGCVVYQS	0.01323
260 - 1444	1184	VTVKVCACYTF-YELVCTSFLR	0.01041
260 - 1506	1246	VTVKVCACYTF-AEDKTCLEFRI	0.0105
309 - 400	91	SDEQGCAIFDL-EIVKVCYTAKY	0.01042
309 - 458	149	SDEQGCAIFDL-TTGGECEYKT	0.01078
309 - 526	217	SDEQGCAIFDL-PEQLPCSGDVT	0.01228
309 - 603	294	SDEQGCAIFDL-FKVDKCFPNTV	0.01239
309 - 635	326	SDEQGCAIFDL-SPNSVCGISAV	0.02195
309 - 683	374	SDEQGCAIFDL-SDGDYCRELQL	0.01095
309 - 766	457	SDEQGCAIFDL-LETRPCYKRVE	0.01038
309 - 876	567	SDEQGCAIFDL-VGSAICTNSKD	0.01044
309 - 950	641	SDEQGCAIFDL-VAMGLCIAAGR	0.01037
309 - 984	675	SDEQGCAIFDL-AQDGYCDEGNT	0.02579
309 - 1019	710	SDEQGCAIFDL-HSRFICLDKDD	0.01039
309 - 1178	869	SDEQGCAIFDL-QNTTGCFPRFG	0.01067
309 - 1225	916	SDEQGCAIFDL-ANGFACLEDGL	0.01188
309 - 1405	1096	SDEQGCAIFDL-VSPPGCVVYQS	0.01098
309 - 1444	1135	SDEQGCAIFDL-YELVCTSFLR	0.01038
309 - 1506	1197	SDEQGCAIFDL-AEDKTCLEFRI	0.01041
400 - 458	58	EIVKVCYTAKY-TTGGECEYKT	0.01096
400 - 526	126	EIVKVCYTAKY-PEQLPCSGDVT	0.76449
400 - 603	203	EIVKVCYTAKY-FKVDKCFPNTV	0.01112
400 - 635	235	EIVKVCYTAKY-SPNSVCGISAV	0.68174

400 - 683	283	EIVKVCYTAKY-SDGDYCRELQL	0.01669
400 - 766	366	EIVKVCYTAKY-LETRPCYKRVE	0.01041
400 - 876	476	EIVKVCYTAKY-VGSAICTNSKD	0.01121
400 - 950	550	EIVKVCYTAKY-VAMGLCIAAGR	0.01055
400 - 984	584	EIVKVCYTAKY-AQDGYCDEGNT	0.17209
400 - 1019	619	EIVKVCYTAKY-HSRFICLDKDD	0.01073
400 - 1178	778	EIVKVCYTAKY-QNTTGCPRFG	0.01219
400 - 1225	825	EIVKVCYTAKY-ANGFACLEDGL	0.01041
400 - 1405	1005	EIVKVCYTAKY-VSPPGCVVYQS	0.72746
400 - 1444	1044	EIVKVCYTAKY-YELEVCTSFLR	0.01101
400 - 1506	1106	EIVKVCYTAKY-AEDKTCLEFRI	0.01119
458 - 526	68	TTGGECREYKT-PEQLPCSGDVT	0.01484
458 - 603	145	TTGGECREYKT-FKVDKCFPNTV	0.01255
458 - 635	177	TTGGECREYKT-SPNSVCGISAV	0.01039
458 - 683	225	TTGGECREYKT-SDGDYCRELQL	0.07907
458 - 766	308	TTGGECREYKT-LETRPCYKRVE	0.01041
458 - 876	418	TTGGECREYKT-VGSAICTNSKD	0.01113
458 - 950	492	TTGGECREYKT-VAMGLCIAAGR	0.01065
458 - 984	526	TTGGECREYKT-AQDGYCDEGNT	0.0183
458 - 1019	561	TTGGECREYKT-HSRFICLDKDD	0.0112
458 - 1178	720	TTGGECREYKT-QNTTGCPRFG	0.01662
458 - 1225	767	TTGGECREYKT-ANGFACLEDGL	0.01046
458 - 1405	947	TTGGECREYKT-VSPPGCVVYQS	0.01037
458 - 1444	986	TTGGECREYKT-YELEVCTSFLR	0.01039
458 - 1506	1048	TTGGECREYKT-AEDKTCLEFRI	0.0104
526 - 603	77	PEQLPCSGDVT-FKVDKCFPNTV	0.01186
526 - 635	109	PEQLPCSGDVT-SPNSVCGISAV	0.07615
526 - 683	157	PEQLPCSGDVT-SDGDYCRELQL	0.0114
526 - 766	240	PEQLPCSGDVT-LETRPCYKRVE	0.01037
526 - 876	350	PEQLPCSGDVT-VGSAICTNSKD	0.01051
526 - 950	424	PEQLPCSGDVT-VAMGLCIAAGR	0.01058
526 - 984	458	PEQLPCSGDVT-AQDGYCDEGNT	0.01058
526 - 1019	493	PEQLPCSGDVT-HSRFICLDKDD	0.01067
526 - 1178	652	PEQLPCSGDVT-QNTTGCPRFG	0.01051
526 - 1225	699	PEQLPCSGDVT-ANGFACLEDGL	0.01038
526 - 1405	879	PEQLPCSGDVT-VSPPGCVVYQS	0.01068
526 - 1444	918	PEQLPCSGDVT-YELEVCTSFLR	0.01037
526 - 1506	980	PEQLPCSGDVT-AEDKTCLEFRI	0.01045
603 - 635	32	FKVDKCFPNTV-SPNSVCGISAV	0.99751
603 - 683	80	FKVDKCFPNTV-SDGDYCRELQL	0.02227
603 - 766	163	FKVDKCFPNTV-LETRPCYKRVE	0.01047
603 - 876	273	FKVDKCFPNTV-VGSAICTNSKD	0.01057
603 - 950	347	FKVDKCFPNTV-VAMGLCIAAGR	0.01043
603 - 984	381	FKVDKCFPNTV-AQDGYCDEGNT	0.06243
603 - 1019	416	FKVDKCFPNTV-HSRFICLDKDD	0.79343
603 - 1178	575	FKVDKCFPNTV-QNTTGCPRFG	0.01312
603 - 1225	622	FKVDKCFPNTV-ANGFACLEDGL	0.01069
603 - 1405	802	FKVDKCFPNTV-VSPPGCVVYQS	0.99701
603 - 1444	841	FKVDKCFPNTV-YELEVCTSFLR	0.91933
603 - 1506	903	FKVDKCFPNTV-AEDKTCLEFRI	0.99621
635 - 683	48	SPNSVCGISAV-SDGDYCRELQL	0.05939
635 - 766	131	SPNSVCGISAV-LETRPCYKRVE	0.01094
635 - 876	241	SPNSVCGISAV-VGSAICTNSKD	0.01046
635 - 950	315	SPNSVCGISAV-VAMGLCIAAGR	0.01074
635 - 984	349	SPNSVCGISAV-AQDGYCDEGNT	0.54931
635 - 1019	384	SPNSVCGISAV-HSRFICLDKDD	0.01091
635 - 1178	543	SPNSVCGISAV-QNTTGCPRFG	0.01872
635 - 1225	590	SPNSVCGISAV-ANGFACLEDGL	0.97794
635 - 1405	770	SPNSVCGISAV-VSPPGCVVYQS	0.01042
635 - 1444	809	SPNSVCGISAV-YELEVCTSFLR	0.0104
635 - 1506	871	SPNSVCGISAV-AEDKTCLEFRI	0.01038
683 - 766	83	SDGDYCRELQL-LETRPCYKRVE	0.01045
683 - 876	193	SDGDYCRELQL-VGSAICTNSKD	0.01336
683 - 950	267	SDGDYCRELQL-VAMGLCIAAGR	0.01158
683 - 984	301	SDGDYCRELQL-AQDGYCDEGNT	0.02924
683 - 1019	336	SDGDYCRELQL-HSRFICLDKDD	0.01095
683 - 1178	495	SDGDYCRELQL-QNTTGCPRFG	0.0108
683 - 1225	542	SDGDYCRELQL-ANGFACLEDGL	0.01039
683 - 1405	722	SDGDYCRELQL-VSPPGCVVYQS	0.01242
683 - 1444	761	SDGDYCRELQL-YELEVCTSFLR	0.0104
683 - 1506	823	SDGDYCRELQL-AEDKTCLEFRI	0.01676
766 - 876	110	LETRPCYKRVE-VGSAICTNSKD	0.99683
766 - 950	184	LETRPCYKRVE-VAMGLCIAAGR	0.01712
766 - 984	218	LETRPCYKRVE-AQDGYCDEGNT	0.01171
766 - 1019	253	LETRPCYKRVE-HSRFICLDKDD	0.01134
766 - 1178	412	LETRPCYKRVE-QNTTGCPRFG	0.01063
766 - 1225	459	LETRPCYKRVE-ANGFACLEDGL	0.01057
766 - 1405	639	LETRPCYKRVE-VSPPGCVVYQS	0.01062
766 - 1444	678	LETRPCYKRVE-YELEVCTSFLR	0.01185
766 - 1506	740	LETRPCYKRVE-AEDKTCLEFRI	0.01388
876 - 950	74	VGSAICTNSKD-VAMGLCIAAGR	0.02022
876 - 984	108	VGSAICTNSKD-AQDGYCDEGNT	0.01131
876 - 1019	143	VGSAICTNSKD-HSRFICLDKDD	0.01047
876 - 1178	302	VGSAICTNSKD-QNTTGCPRFG	0.01051
876 - 1225	349	VGSAICTNSKD-ANGFACLEDGL	0.0104
876 - 1405	529	VGSAICTNSKD-VSPPGCVVYQS	0.01124
876 - 1444	568	VGSAICTNSKD-YELEVCTSFLR	0.01043
876 - 1506	630	VGSAICTNSKD-AEDKTCLEFRI	0.01057
950 - 984	34	VAMGLCIAAGR-AQDGYCDEGNT	0.01059
950 - 1019	69	VAMGLCIAAGR-HSRFICLDKDD	0.01081

950 - 1178	228	VAMGLCIAAGR-QNTTGCFFRFG	0.01038
950 - 1225	275	VAMGLCIAAGR-ANGFACLEDGL	0.01041
950 - 1405	455	VAMGLCIAAGR-VSPPGCVVYQS	0.01049
950 - 1444	494	VAMGLCIAAGR-YELEVCTSFLR	0.01059
950 - 1506	556	VAMGLCIAAGR-AEDKTCLEFRI	0.01097
984 - 1019	35	AQDGYCDEGNT-HSRFICLDKDD	0.01062
984 - 1178	194	AQDGYCDEGNT-QNTTGCFFRFG	0.01039
984 - 1225	241	AQDGYCDEGNT-ANGFACLEDGL	0.01037
984 - 1405	421	AQDGYCDEGNT-VSPPGCVVYQS	0.01037
984 - 1444	460	AQDGYCDEGNT-YELEVCTSFLR	0.01039
984 - 1506	522	AQDGYCDEGNT-AEDKTCLEFRI	0.01038
1019 - 1178	159	HSRFICLDKDD-QNTTGCFFRFG	0.01058
1019 - 1225	206	HSRFICLDKDD-ANGFACLEDGL	0.0104
1019 - 1405	386	HSRFICLDKDD-VSPPGCVVYQS	0.01055
1019 - 1444	425	HSRFICLDKDD-YELEVCTSFLR	0.01037
1019 - 1506	487	HSRFICLDKDD-AEDKTCLEFRI	0.01048
1178 - 1225	47	QNTTGCFFRFG-ANGFACLEDGL	0.0142
1178 - 1405	227	QNTTGCFFRFG-VSPPGCVVYQS	0.01092
1178 - 1444	266	QNTTGCFFRFG-YELEVCTSFLR	0.01061
1178 - 1506	328	QNTTGCFFRFG-AEDKTCLEFRI	0.0112
1225 - 1405	180	ANGFACLEDGL-VSPPGCVVYQS	0.01037
1225 - 1444	219	ANGFACLEDGL-YELEVCTSFLR	0.01054
1225 - 1506	281	ANGFACLEDGL-AEDKTCLEFRI	0.01045
1405 - 1444	39	VSPPGCVVYQS-YELEVCTSFLR	0.0104
1405 - 1506	101	VSPPGCVVYQS-AEDKTCLEFRI	0.01041
1444 - 1506	62	YELEVCTSFLR-AEDKTCLEFRI	0.01093

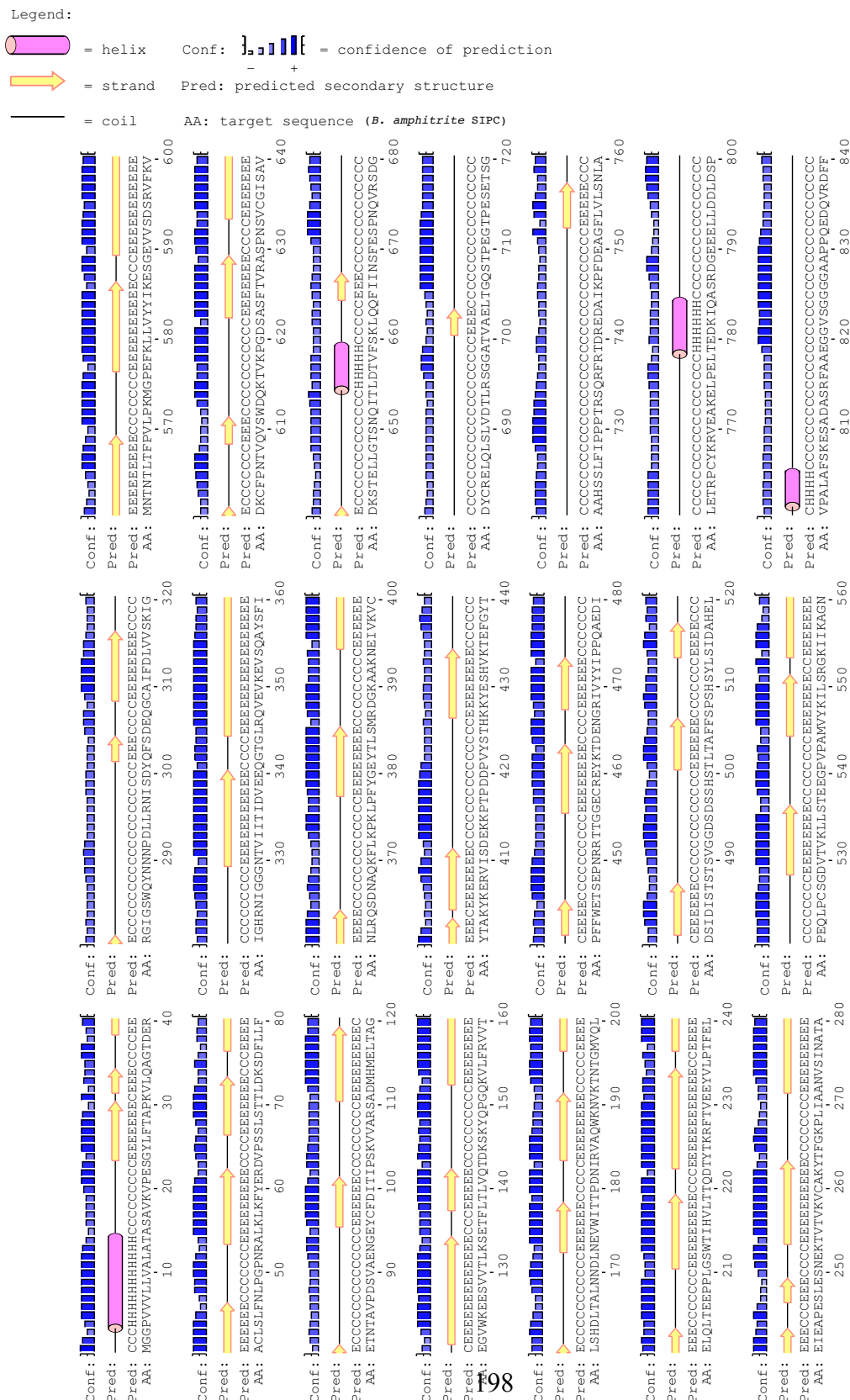
Appendix C. Table 2 - Predicted bonds, showing which cysteines have proposed connectivity

Cysteine Sequence Position	Bonds
42 - 1178	TDERACLSLFN - QNTTGCFFRFG
97 - 1019	ENGEYCFDITI - HSRFICLDKDD
260 - 950	VTVKVCAKYTF - VAMGLCIAAGR
309 - 984	SDEQGCAIFDL - AQDGYCDEGNT
400 - 526	EIVKVCYTAKY - PEQLPCSGDVT
458 - 683	TTGGECCREYKT - SDGDYCRELQL
603 - 1405	FKVDKCFPNTV - VSPPGCVVYQS
635 - 1225	SPNSVCGISAV - ANGFACLEDGL
766 - 876	LETNPCYKRVE - VGSAICTNSKD
1444 - 1506	YELEVCTSFLR - AEDKTCLEFRI

Predicted connectivity for sequence SIPC of length 1573 (cysteines in this sequence: 20)
1-16, 2-15, 3-13, 4-14, 5-7, 6-10, 8-18, 9-17, 11-12, 19-20

Appendix D

Secondary Structure Element Alignment for *Balanus amphitrite* SIPC from the DomPred protein domain predictor from Marsden et al. (2002).





Marine Glycobiology: Current Status and Future Perspectives

Gary S. Caldwell · Helen E. Pagett

Received: 31 July 2009 / Accepted: 19 January 2010
© Springer Science+Business Media, LLC 2010

Abstract Glycobiology, which is the study of the structure and function of carbohydrates and carbohydrate containing molecules, is fundamental to all biological systems. Progress in glycobiology has shed light on a range of complex biological processes associated with, for example, disease and immunology, molecular and cellular communication, and developmental biology. There is an established, if rather modest, tradition of glycobiology research in marine systems that has primarily focused on reproduction, biofouling, and chemical communication. The current status of marine glycobiology research is primarily descriptive with very limited progress on structural elucidation and the subsequent definition of precise functional roles beyond a small number of classical examples, e.g., induction of the acrosome reaction in echinoderms. However, with recent advances in analytical instrumentation, there is now the capacity to begin to characterize marine glycoconjugates, many of which will have potential biomedical and biotechnological applications. The analytical approach to glycoscience has developed to such an extent that it has acquired its own “-omics” identity. Glycomics is the quest to decipher the complex information conveyed by carbohydrate molecules—the carbohydrate code or glycode. Due to the paucity of structural information available, this article will highlight the fundamental importance of glycobiology for many biological processes in marine organisms and will draw upon the best defined systems. These systems therefore may prove genuine candidates for full carbohydrate characterization.

Keywords Carbohydrate · Cell recognition · Glycobiology · Glycomics · Glycoprotein · Lectin · Reproduction

Introduction

The term glycobiology, first coined in 1988 by Rademacher et al., incorporates a diverse array of molecules, collectively termed glycoconjugates which include saccharides, glycoproteins (macromolecules composed of protein and carbohydrate moieties), glycans (polysaccharide moiety of a glycoprotein), glycolipids (carbohydrate linked lipids), and proteoglycans (heavily glycosylated glycoproteins). The fundamental role of glycoconjugates in many biological processes is now widely recognized. There has been considerable effort dedicated to elucidating their relationships in mammalian systems; however, there has been comparatively little progress in marine systems. A number of important processes have been described in marine organisms, and there remains considerable scope to further develop marine glycobiology. The lack of structural elucidation has undoubtedly hindered the development of marine glycobiology.

Glycoconjugates seemingly are responsible for a remarkably diverse array of biological activities in marine organisms ranging from immunity (Smital et al. 2003), sperm–egg binding (Vacquier 1998), thrust generation in nonflagellar cyanobacteria (McCarren and Brahamsha 2005; McCarren et al. 2005), electroreception in sharks (Brown et al. 2002), and a multitude of cell–cell and cell–molecular recognition events. There is considerable interest in characterizing the glycan structures that mediate many of these processes as many will have potential medical and biotechnological applications. This brief review highlights areas within marine science that have a pronounced glycobiology component including reproductive biology, marine natural products,

G. S. Caldwell (✉) · H. E. Pagett
School of Marine Science and Technology,
Newcastle University, Ridley Building,
Claremont Road Newcastle upon Tyne NE1 7RU, England, UK
e-mail: gary.caldwell@ncl.ac.uk

pathobiology, and biofouling. However, in the majority of cases, structural detail of the glycan components is either poorly defined or entirely nonexistent. As such, this article is limited to describing biological processes without reference to molecular structures.

Prior to discussing the varied glycobiology-driven relationships in marine systems, it would be prudent to consider the role that lectins have played in their identification and elucidation. Lectins are ubiquitous recognition proteins of nonimmune origin that bind to carbohydrates. They perform many and varied biological functions including the regulation of cellular adhesion, recognition molecules in cell–cell and cell–molecule interactions, and are also known to have vital immune functions (Sharon and Lis 2004). Lectins have been isolated from a range of marine organisms including algae (Rogers and Hori 1993; Benevides et al. 1998, 2001), sponges (Bretting et al. 1981, Gundacker et al. 2001), mollusks (Bulgakov et al. 2004), and echinoderms (Hatakeyama et al. 1994). Lectins, as carbohydrate recognition tools, have proven extremely useful for the investigation of cell surface carbohydrates, particularly the isolation and characterization of glycoconjugates. Lectins have been employed extensively in marine biology with applications as disparate as identifying toxic dinoflagellates (Costas and Rodas 1994), determining copepod chemoreception sites (Snell and Carmona 1994; Kelly and Snell 1998), inhibiting settlement of barnacle cypris larvae (Matsumura et al. 1998a), and exploring biofilm spatial and chemical structure (Michael and Smith 1995; Wigglesworth-Cooksey and Cooksey 2005). Many of the marine glycobiology examples discussed below have only come to light due to the application and utility of lectins as versatile carbohydrate recognition molecules.

The Glycobiology of Reproduction

Reproduction is an evolutionary imperative and a fundamental feature of all known life. The diversity of reproductive strategies and the desire to better control the process makes reproductive science one of the most interesting, challenging, and socially contentious disciplines in modern-day science. Carbohydrates appear to be important functional groups in reproductive biology with variation in glycosylation products contributing toward reproductive functionality in male and female animals (Morris et al. 1996; Dell et al. 1999). For the purposes of this article, the relevance of glycobiology to gametes, fertilization, and embryogenesis will be discussed. Where marine examples could not be found parallels will be drawn from those biological systems that have thus far been described.

Gametogenesis is the production of sexual gametes by meiosis from gametocytes. Little is known regarding the

functions of glycoconjugates in gametogenesis in marine organisms; however, glycoconjugates have been investigated in other systems; for example, in mice, an *N*-glycan facilitates the adhesion of developing spermatogonia to testicular Sertoli cells (Fukuda and Akama 2003). In an insect model (*Drosophila melanogaster*), a surface associated mucin, hemomucin, is produced by follicle cells during the later stages of oogenesis and incorporated into the oocyte chorion. This process appears to be ecdysone regulated (Theopold et al. 2001).

Once gametes are formed and insemination is complete, the roles of glycoconjugates in the remaining stages of reproduction are much better characterized. The process of fertilization in animals involves a complex series of sequential and coordinated events culminating in the fusion of haploid male and female pronuclei to form the diploid zygote. Fertilization is orchestrated by a combination of cellular and molecular mechanisms of which glycoconjugates play a number of pivotal roles, including sperm–egg recognition, sperm–egg binding, and the block to polyspermy. The role of glycoconjugates in the fertilization process of deuterostomes (Chordata, Echinodermata, and Hemichordata) is relatively well defined compared with protostomes (Ecdysozoa, Lophotrochozoa, and Platyzoa). Glycoprotein interactions occur at both egg jelly and vitelline layers (Mengerink and Vacquier 2001) although both protein and carbohydrate moieties are required for sperm–egg binding.

Lectin-like proteins located on the surface of sperm bind to oligosaccharide containing glycoproteins (egg binding proteins) on the oocyte surface leading to the acrosomal reaction and sperm–egg binding. In sea urchins, the species-specific fucose sulfate polymer, bindin (1→3-linked α -L-fucopyranosyl units), mediates gamete binding and fusion (Vacquier and Moy 1997; Alves et al. 1998; Vacquier 1998). *Echinometra lucunter* utilises a homopolymer of a 3-linked α -L-galactan to induce the acrosome reaction whereas *Arbacia lixula* and *Lytechinus variegatus* contain linear sulfated α -L-fucans with regular tetrasaccharide repeating units (Alves et al. 1997; Vilela-Silva et al. 1999; Mourão 2007; Fig. 1). The three species coexist and crucially, the acrosome reaction in each case is conspecific, not heterospecific.

In the Asteroidea, the acrosome reaction inducing substance (ARIS) and the sulfated steroid saponin (co-ARIS) contain protein, carbohydrate, and sulfate moieties with a repeating pentasaccharide chain (Hoshi et al. 1991; Ushiyama et al. 1995) which bind with a high degree of species specificity. Glycosidases, enzymes that remove glucose molecules from glycosides, also play an important role in sperm–egg recognition and binding in ascidians (Hoshi et al. 1985; Baginski et al. 1999). As a protostome example, surface glycoproteins also mediate sperm–egg binding in

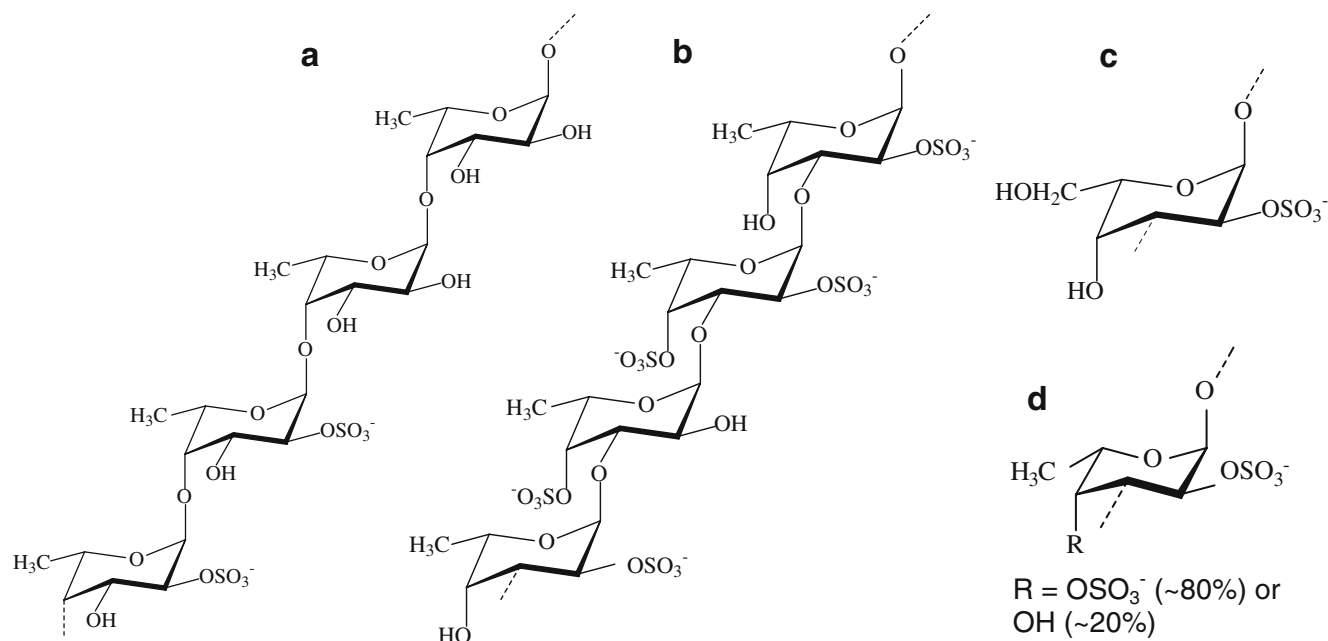


Fig. 1 Examples of sulfated polysaccharides from four sea urchin species: **a** *A. lixula*, **b** *L. variegatus*, **c** *E. lucunter*, and **d** *S. purpuratus* (from Mourão 2007)

Crustacea (Wikramanayake and Clark 1994). A large number of vertebrate sperm–egg binding examples exist; for example, in *Xenopus laevis*, the initial binding interaction is mediated by oligosaccharides attached to a pair of glycoproteins (gp64/gp69) derived from the egg jelly coat (Tian et al. 1997). Similarly, in their review of carbohydrate mediated events in mammalian fertilization, Tulsiani et al. (1997) describe glycoproteins located in the zona pellucida which are involved in sperm–egg binding. Evidence also exists for gender-specific glycosylation in human reproduction (Morris et al. 1996).

Once sperm–egg recognition and binding have occurred, the oocyte must react rapidly to prevent incidences of pathological polyspermy. Jelly coat responses have been documented in vertebrates, with egg surface oligosaccharides playing pivotal roles (Arranz-Plaza et al. 2002). In invertebrates, polyspermy is typically prevented by either elevation of the fertilization membrane or extrusion of a carbohydrate jelly layer which traps and immobilizes excess sperm. In ascidians, for example, sperm glycosidases and their respective egg vitelline coat glycosides are essential in the prevention of polyspermy (Lambert 1989).

Glycoconjugates have relevance for embryo implantation, tissue and cell specialization, and organogenesis (Armant et al. 1986; Karoumi et al. 1990; Sullivan et al. 1991; Wu et al. 1999; Carson 2002). Kari and Rottmann (1985) and Kabakoff and Lennarz (1990) describe changes within a glycoprotein complex present in the developing sea urchin embryo. As development proceeds, the composition of the complex changes to a major degree, although the relevance

of this is as yet unknown. However, it was observed that if glycoprotein synthesis was inhibited, spiculogenesis was blocked. It was hypothesized that the inhibited glycoproteins are functional in calcium deposition.

Glycosylation is important for folding, processing, and transport of protein into the yolk of developing oocytes and contributes a vital carbohydrate reservoir for embryogenesis. Vitellin is the major yolk protein in crustaceans and is the main protein component during oogenesis. In the blue lobster, *Cherax quadricarinatus*, vitellin is preceded by vitellogenin which itself consists of high mannose oligosaccharides, specifically Man₅GlcNAc₂ to Man₉GlcNAc₂ (Khalaila et al. 2004). These oligomannose moieties are similar to the carbohydrate components of hemocyanin from the freshwater crayfish, *Astacus leptodactylus* (Tseneklidou-Stoeter et al. 1995). A marine example of a similar oligomannose moiety is the glycosylated proteins found in the hemoglobins of *Riftia pachyptila*, the deep-sea tubeworm (Zal et al. 1998).

Biofouling

Biofouling is the accumulation of undesirable biological material on natural and manmade submerged structures and surfaces. The nature of biofouling can be subdivided into microfouling (primarily biofilms) and macrofouling (larger organisms such as barnacles, mussels, and seaweeds). The science of biofouling research is inextricably linked with the study of bioadhesion, larval settlement, and metamor-

phosis. Due to the ubiquitous distribution of carbohydrates and glycoconjugates and their broad bioactivities, it is unsurprising that glycoconjugates are an important factor in biological fouling.

Glycoconjugates have been implicated in the settlement and attachment processes of hard fouling organisms such as barnacles and mussels. Examples include the freshwater quagga mussel *Dreissena bugensis* which secretes an acidic monosaccharide glycoprotein containing *N*-acetylgalactosamine *O*-linked to a threonine residue. This glycoprotein, termed “foot protein 1” is a major constituent of the mussel’s byssus thread (Anderson and Waite 2002). A glycoprotein, once termed arthropodin due to its similarity to insect arthropodin, is now known as settlement-inducing protein complex (SIPC). This water-soluble cuticular glycoprotein contact pheromone (Crisp and Meadows 1963) plays a significant role in the settlement and gregariousness of barnacles. Searching cypris larvae use glycoproteins originating from the cuticle and shell of conspecifics as a settlement cue. The SIPC of *Balanus amphitrite* has an estimated molecular mass of 262 kDa and comprises of three major polypeptide subunits of 76, 88, and 98 kDa (Matsumura et al. 2000). These three specific sugar chains play an important role in the settlement of *B. amphitrite* larvae (Matsumura et al. 1998b), and it appears that each subunit induces larval settlement as effectively when isolated as when intact as SIPC (Matsumura et al. 1998c). Conspecific glycoprotein settlement has been shown to be inhibited in *B. amphitrite* by lentil lectin (Matsumura et al. 1998a). Cypris temporary adhesive also appears to be glycoprotein based (Clare and Matsumura 2000). Therefore, glycoproteins function as both settlement cues and bioadhesives in barnacles. Sponges produce the glycoprotein fibronectin as an adhesive from the basal lamina (Pahler et al. 1998). Another adhesive glycoprotein, tenascin, has also been described from a sponge (Humbertdavid and Garrone 1993).

Marine organisms are renowned for producing natural antifouling agents. Glycoproteins also appear to have a function in antifouling. Mucus secretions are a common mechanism utilized by marine animals to prevent fouling (McKenzie and Grigova 1996). The mucus can contain toxins and lytic compounds which act to deter settling organisms (Fontaine 1964). Meikle et al. (1987) determined the structure of oligosaccharide side chains from glycoproteins from a marine coral which may potentially have antifouling properties. Bavington et al. (2004) identified mucin-type glycoproteins produced by seastars and brittlestars which prevent fouling at the cellular level. Whereas the number of studies that have investigated the glycoprotein constituent of mucus in relation to antifouling is small, it is likely that other mucoid natural antifoulants will have a significant bioactive glycoprotein component.

A biofilm is a complex aggregation of microorganisms which excrete a protective and adhesive extracellular polymeric matrix. Biofilms are of particular interest in biofouling as many hard fouling organisms use biofilm surface compounds as settlement cues (Lam et al. 2005; Jin and Qian 2005). For organisms residing in biofilms space is often a limiting factor, thus creating an imperative for aggressive spatial competition. A staggering array of chemicals is produced by microbes in order to gain an advantage over competitors. Glycoconjugates are also an important functional group regulating ammensal competition in microbial biofilms. Glycoproteins and proteins play a key role in attachment of diatoms to surfaces (Cooksey and Wigglesworth-Cooksey 1995). Raphid diatoms produce proteoglycan-rich mucilage as an aid to motility and adhesion (Lind et al. 1997). The heterotrophic bacterium *Pseudoalteromonas* sp. releases lectins which reduce attachment and motility in diatom-dominated biofilms, presumably by binding to the proteoglycan mucilage. Continued exposure results in cell lysis (Wigglesworth-Cooksey and Cooksey 2005). An example of bacteria–bacteria interactions is a species of gliding bacteria of the genus *Cytophaga* that produces a glycoprotein which inhibits adhesion and motility in a related species; however, no such affect was observed in other gliding bacteria (Burchard and Sorongon 1998).

A surface coating of the marine bacteria *Pseudomonas* sp. excretes an exopolysaccharide that affects the attachment of *Ciona intestinalis* larvae to that surface. The eggs of *C. intestinalis* are nonbuoyant and covered in a sticky matrix. It has been found that both fertilized and unfertilized eggs, which had lost their natural slime matrix, settle at a significantly greater rate onto bacterial biofilms that produced slime. *C. intestinalis* larvae have two attachment mechanisms: active attachment by the adhesive organs and passive attachment caused by larvae becoming trapped in the bacterial excretion. The mechanism used seems to depend on the amount of exopolysaccharide present on the surface. It is thought that this attachment to surfaces possibly allows protection from predation. All larvae, whether trapped in the exopolysaccharide or attached to the surface, develop successfully into juveniles. From a biofouling perspective, this highlights the importance of bacterial exopolysaccharide biofilms for the formation of fouling communities (Szewzyk et al. 1991).

Infochemicals: Pheromones and Chemoattractants

An infochemical is a molecule that, when perceived by an organism, transmits information pertaining to biotic and abiotic factors including chemical communication between and within species. Included within this broad definition are

pheromones and chemoattractants. Pheromones transmit information only to conspecifics whereas chemoattractants transmit information to heterospecifics. The enormous structural diversity of glycoconjugates makes them ideal infochemical candidates. The following section will consider the role of glycoconjugates in marine chemical communication.

As discussed under biofouling, barnacles use a glycoprotein (SIPC) as a gregarious settlement pheromone (Clare and Matsumura 2000). There are similar instances of surface associated glycoproteins in other marine organisms (Dreanno et al. 2006), for example, contact chemoreception in mate recognition, mate guarding, and spermatophore transfer in the marine harpacticoid *Tigriopus japonicus* (Ting and Snell 2003). Protein receptors on the males' antennules detect the carbohydrate moieties of surface glycoproteins on females (Kelly and Snell 1998). Glycoproteins are also important for mate recognition in calanoid copepods (Snell and Carmona 1994). Another example is the contact mate recognition pheromone of the marine rotifer *Brachionus plicatilis* (RicoMartinez et al. 1996). Differences in glycoprotein structure probably have a primary role in maintaining *Brachionus* species boundaries (Kotani et al. 1997). The eggs of the horseshoe crab, *Limulus polyphemus*, are a popular and effective bait in eel and conch fisheries. Glycoproteins associated with the eggs act as potent chemoattractants (Ferrari and Targett 2003).

Glycoprotein Hormones

Glycoproteins also fulfill important hormonal functions. They are intrinsic, for example, to the human endocrine system as chorionic gonadotrophin, pituitary luteinizing hormone, follicle-stimulating hormone, and thyroid-stimulating hormone are all glycoproteins (Thotakura and Blithe 1995). The oligosaccharide moieties are major structural features that impact bioactivity. As a marine study, stanniocalcin is an interesting example to consider. Originally believed to be restricted to fish but now identified in mammals, stanniocalcin, also known as hypocalcin or teleocalcin, is a homodimeric glycoprotein. It is produced in fish by unique endocrine glands called the corpuscles of Stannius. In salmon (*Salmo salar*), stanniocalcin plays an integral role in calcium and phosphate homeostasis and functions to prevent hypercalcemia (Wagner et al. 1998).

Immunology, Pathogenesis, and Host–Parasite Interactions

Glycoproteins function extensively in the immune response of aquatic animals. Lacking an adaptive immune system,

invertebrates have developed other mechanisms to recognize pathogens. One of these mechanisms is the recognition of sugar components in bacterial cell walls and the induction of bacterial agglutination (Alpuche et al. 2005). As lectins recognize specific sugars, they are thought to function in cell recognition and regulation as well as preventing and limiting the invasion of pathogens. The purification of at least three lectins (HOL-I, HOL-II, and HOL-30) from the marine sponge, *Halichondria okadai* has raised questions as to the physiological role of lectins in sponges. The lectins may protect from infection or assist in regulating the internal environment (Kawsar et al. 2008) as well as possibly serving as part of a symbiotic relationship with beneficial microorganisms (Jimbo et al. 2000). Liao et al. (2003) found that lectins in the red algae, *Eucheuma serra* and *Galaxaura marginata*, expressed potent antibiotic activity against marine *Vibrio* bacteria. It is likely that the lectins were binding to glycoproteins located on the bacterial cell surface. Lectins from hemolymph of *Litopenaeus setiferus* (white shrimp) show binding specificity for *N*-acetylated sugars. EDTA treatment removes the lectins' agglutinating abilities by removing Ca^{2+} ; the addition of further Ca^{2+} restores the hemagglutinating properties (Alpuche et al. 2005). A novel lectin (referred to as PPL) from the mantle of the penguin wing oyster, *Pteria penguin*, defends against pathogens through lectin-carbohydrate binding specificity. PPL interacts with both Gram-positive and Gram-negative bacteria and inhibits growth in *Escherichia coli* (Naganuma et al. 2006).

The multixenobiotic resistance phenotype (MXR) is one of the primary immune capabilities in aquatic invertebrates (Epel 1998). The MXR system is mediated by permeability glycoproteins (P-gp) and has been extensively investigated in filter feeding mollusks (Smital et al. 2000, 2003; Eufemia et al. 2002). The P-gp molecule belongs to the ATP-dependent binding cassette of transmembrane glycoproteins.

Glycoproteins are important constituents in processes leading to pathogenesis and infection (Olofsson 1992). Similar patterns are observed in aquatic systems. Hyaluronic acid or hyaluronon, which is an anionic, nonsulfated glycosaminoglycan (Fig. 2a) is found in the extracellular matrix of vertebrate tissues and in the surface coating of certain *Streptococcus* and *Pasteurella* pathogens where it aids infectiousness. Interestingly, at least one virus directs its algal host to produce hyaluronic acid on the cell surface during early infection; however, the rationale behind this is unknown (DeAngelis 1999). A glycoprotein also appears to be a putative receptor responsible for the induction of zoospore encystment in the fungal pathogen *Pythium porphyrae* (Oomycota; Addepalli et al. 2002). The sea cucumber, *Stichopus badionotus* has fucosylated chondroitin sulfate as the major polysaccharide in the body wall. The polysaccharide core is chondroitin sulfate (Fig. 2b) contain-

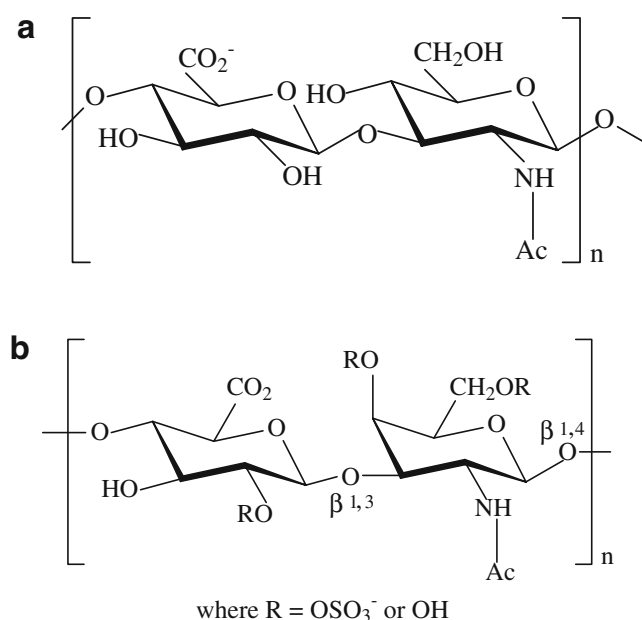


Fig. 2 **a** Hyaluronic acid is a straight chain polysaccharide consisting of alternating glucuronic acid and *N*-acetyl-glucosamine (from Toole 2000); **b** structure of chondroitin sulfate (from Calabro et al. 2000)

ing side chains of sulfated fucose units linked to glucuronic acid. This has a similar structure to hyaluronic acid, the difference being that chondroitin is sulfated. The relevance of these polysaccharides is not clear; however, the sulfated fucose branches make the polysaccharide resistant to certain enzymes thus preventing the digestion of the body wall by microorganisms. Interestingly, polysaccharides from marine invertebrates are much more highly sulfated than those found in mammalian tissues. One theory for this is that the interaction of components within the extracellular matrix of marine organisms occurs at higher salt concentrations, requiring polysaccharides with a higher charge density (Mourão 2007).

Glycoconjugates function in host–parasite recognition. A well-documented example would be schistosomiasis. Much of the immunity to the helminth parasite is directed against carbohydrate determinants in glycoproteins, glycolipids, and glycosaminoglycans from the adult worms and their eggs (Cummins and Nyame 1996). Glycoconjugates and carbohydrate-binding proteins from the parasites and their hosts also participate in egg adhesion and granuloma formation which is involved in disease pathology (Cummins and Nyame 1999). Glycoconjugates also function in aquatic parasitic infestations. Oligosaccharides are key in the complex *Chondrus crispus*–*Acrochaete operculata* pathosystem. The κ-carrageenan oligosaccharide inhibits pathogen virulence whereas λ-carrageenan promotes pathogenicity. This particular system has been proposed as a useful model to investigate recognition and transduction pathways of oligo-

saccharide elicitors in plant–pathogen interactions (Bouarab et al. 2001).

Carbohydrates are also involved in the infectivity of monogenean parasite such as *Gyrodactylus derjavini* which infects rainbow trout, *Oncorhynchus mykiss* (Buchmann 1998). A complement factor within the trout plasma binds in a lethal manner to carbohydrate-rich structures within the parasite so reducing the parasite burden. The Japanese flounder, *Paralichthys olivaceus*, recognizes antigens on the monogenean *Neobenedenia girellae*. The antigens appear to be located on the glycoprotein fraction of the ciliary integral membrane (Hatanaka et al. 2005). The Manila clam, *Ruditapes philippinarum*, produces a lectin which binds to carbohydrate sites on the protozoan parasite *Perkinsus* sp. and appears to function in an immune capacity (Bulgakov et al. 2004).

Serum immunoglobulins (IgM) are important for immune response in vertebrates, including fish. Atlantic cod, *Gadus morhua* IgM, is similar to mammalian as it contains complex, heterogenic *N*-linked glycans; however, it contains lower levels of oligomannose glycans than mammalian IgM (Magnadóttir et al. 2002). Work on salmon, *S. salar*, also highlights the importance of glycans for fish immunoglobulins (Magnadóttir et al. 1997).

Biomedical and Biotechnology Applications

There is considerable interest in developing and exploiting glycoconjugates and their related molecules, particularly glycosidases, for biomedical and industrial applications. Glycans and glycoconjugates are linked to a number of serious medical conditions such as malignancies, Creutzfeldt–Jakob disease, cystic fibrosis, and inflammatory disease (Axford 2001). Kren and Martinkova (2001) present a useful review of glycosides in pharmaceuticals highlighting the importance of the glycosidic residue for the biological activity of a number of compounds including antibiotics, steroids, and vitamins.

In marine organisms, the majority of research has focused on compounds derived from opisthobranch mollusks and sponges. Pachymatmin, a glycoprotein produced by the sponge *Pachymatisma johnstonii* exhibits antileishmanial activity (Le Pape et al. 2000) and is also strongly antineoplastic (Sangrajang et al. 2000). Bretting et al. (1981) identified lectins from 21 sponge species which reacted with human and animal erythrocytes. Sponge lectins were also identified by Kawagishi et al. (1994) and Gundacker et al. (2001). Another example is the polycyclic guanidine alkaloids Crambescidin 826 and Dehydrocrambine A which react with glycoprotein 120 on the HIV-1 virus to prevent membrane fusion (Chang et al. 2003). A number of compounds have been identified that inhibit or reverse

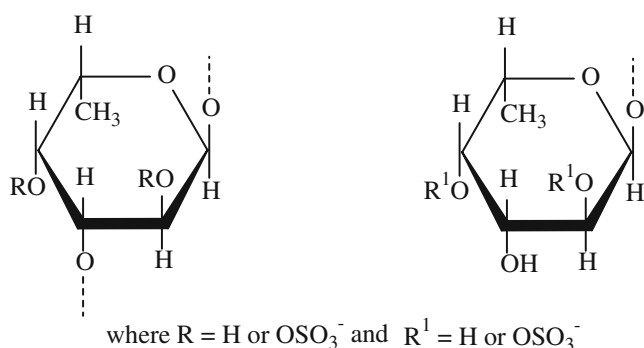


Fig. 3 The hypothetical structures of the two sulfated fucans isolated from the body wall of the sea cucumber, *S. japonicus* (from Kariya et al. 2004)

the MXR efflux pump, including Kendarimide A from *Haliclona* sp. (Aoki et al. 2004), Dictyostatin-1 from *Spongia* sp. (Isbrucker et al. 2003), and irciniasulfonic acid from *Ircinia* sp. (Kawakami et al. 2001).

Sea hares are marine opisthobranch mollusks that tend to store dietary derived toxins in their tissues as a predation deterrent. Glycoproteins isolated from *Aplysia kurodai*, *Aplysia juliana*, and *Dolabella auricularia* designated as aplysianins, julianins, and dolabellans, respectively, express pronounced antineoplastic and antimicrobial activities. The antineoplastic activity is via cytolysis whereas the antimicrobial activity is cytostatic (Yamazaki 1993). Aplysianin-A is a strongly antibacterial glycoprotein located in the albumen gland which inhibits growth of both Gram-positive and Gram-negative bacteria. Aplysianin-E is antineoplastic and antibacterial but also possesses fungicidal activity (Iijima et al. 1995). Dolabellin A, also located in the albumen gland, is antineoplastic, antibacterial, and fungicidal (Iijima et al. 1994). Its mode of action is not bactericidal but bacteriostatic (Kisugi et al. 1992). Another molluscan example is keyhole limpet hemocyanin derived from a circulating glycoprotein from *Megathura crenulata*, which is a novel immunostimulant in humans (McFadden et al. 2003).

Fucan sulfates from the sea cucumber, *Stichopus japonicus* (Fig. 3), are potent inhibitors of osteoclastogenesis in mice. The equilibrium that exists between the dynamic processes of osteoblast formation and osteoclast resorption is disturbed by the sulfated fucans leading to bone disorders such as rheumatoid arthritis and osteoporosis. Having found a trigger for resorption of bone tissue, steps are now being made toward developing an accelerant for bone formation (Kariya et al. 2004).

Chondroitin sulfate has been promoted as a potential “cosmeceutical” (Kim et al. 2008), in this case a dietary supplement for the possible improvement of osteoarthritis symptoms. Potential marine sources of chondroitin sulfate include giant squid, skate, and salmon cartilage. These

contain no other glycosaminoglycans, such as heparin, hyaluronic acid, keratan sulfate, or dermatan sulfate, making them particularly high quality sources. In particular, chondroitin sulfate obtained from giant squid (21.6%) and skate cartilage (12.48%) is of much higher purity than that from shark cartilage (9.71%; Im et al. 2008).

Sulfated homopolysaccharides and heteropolysaccharides isolated from a number of algae and cyanobacteria have demonstrated potent activity against retroviruses including human immunodeficiency virus and herpes simplex virus (Schaeffer and Krylov 2000). The polysaccharides inhibit the viral cytopathic effect and also prevent HIV-induced syncytium formation. An example from a marine vertebrate is elasmobranch cartilage which contains bioactive oligosaccharides that inhibit neurite outgrowth in murine models (Nadanaka et al. 1998).

Red and brown seaweeds along with marine angiosperms contain sulfated fucose or sulfated galactose. These sulfated groups are not found in terrestrial plants. The green seaweed, *Codium fragile*, contains linear mannans, pyruvated arabinogalactan sulfates, and hydroxyproline-rich glycoprotein epitopes (HRGP; Estevez et al. 2009). HRGPs are thought to be involved in aspects of growth and development such as cell–cell recognition, cell expansion, and cell proliferation as well as cell wall architecture (Seifert and Roberts 2007).

There is much interest from the nanotechnology sector in the potential connections between the biochemistry and micro-architecture of marine organisms such as diatoms (Neethirajan et al. 2009). Several glycoproteins with a high affinity for calcium have been identified from diatoms. There is strong evidence to suggest that these proteins have direct involvement, together with other cell wall proteins, in silica deposition (Kröger et al. 1994).

Besides cellulose, chitin is the most commonly occurring polysaccharide. Chitin occurs in three polymorphic forms,

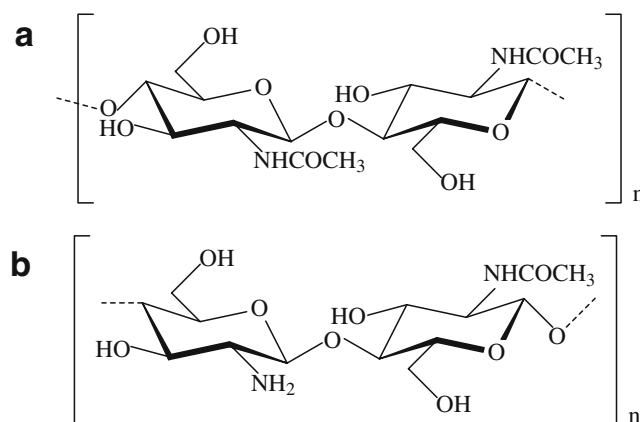


Fig. 4 **a** The structure of chitin (from Imai et al. 2003); **b** the structure of chitosan (from Al Sagheer et al. 2009), showing partial deacetylation from the chitin structure

α , β , and γ chitin. α chitin is the most common and is usually isolated from the exoskeletons of crustaceans and mollusks where it is the major structural element (Al Sagheer et al. 2009; Fig. 4). β chitin is less widespread and occurs in squid pens, pogonophoran tubes, and in the spines of some diatoms (Gaill et al. 1992). There is little known about γ chitin, which is found in fungi and yeast and is thought to be a combination of α and β chitins (Al Sagheer et al. 2009). Chitin is insoluble in most solvents due to its compact structure; thus, it is most useful when chemically modified. Chitin is normally industrially converted by deacetylation through alkaline hydrolysis and due to the presence of amino groups becomes soluble in certain media. Commercially produced chitosan (Fig. 4) has antimicrobial properties as well as increased biocompatibility and biodegradability (Abdou et al. 2008). The extent of the deacetylation of the chitin determines its physical, chemical, and biological properties. Consequently, chitin and chitosan have applications in numerous industries including cosmetics, agriculture, food, pharmaceutical, biomedical, paper, and wastewater (Bautista-Baños et al. 2006; Rashidova et al. 2004; Sashiwa and Aiba 2004).

Future Perspectives

The adoption of genetic model organisms has aided the advancement of bioscience to a remarkable degree. A number of the classical model organisms have been applied to glycobiology; *Caenorhabditis elegans*, *D. melanogaster*, and *Arabidopsis thaliana* in particular, with some degree of success (Altmann et al. 2001). Significant advancements are now being made in mammalian glycobiology combined with the application of genetic techniques (Lowe and Marth 2003). A number of prokaryote and eukaryote marine species have had their genomes sequenced. There exists tremendous potential for identifying glycobiology linked sequences from whole organism genome sequences. As the number of sequenced organisms continues to grow, so too do the opportunities to investigate comparative glycobiology. Bouarab et al. (2001) have already proposed the *C. crispus*–*A. operculata* association as a model system to investigate the glycobiology of marine plant host–pathogen relationships. Parallel model systems addressing broad themes of marine glycobiology should similarly be adopted, such as the sea urchin *Strongylocentrotus purpuratus* which is currently having its genome sequenced. Sea urchins have played a central role in understanding fundamental reproductive processes and would similarly provide a valuable model to further elucidate glycoconjugate roles in reproduction.

The “-omics” revolution has driven back the boundaries of genetic and biochemical knowledge and provided a

wealth of powerful investigative and analytical techniques for use in the medical and life sciences. The complementary disciplines of genomics, proteomics, and metabolomics represent the frontier of scientific discovery and have provided a phenomenal wealth of biotechnological and pharmacological opportunities for the improvement of quality of life. A fourth discipline has now emerged: glycomics—the search for the glycome, the collective identity of all carbohydrates in an organism. The information carried by sugar molecules, the glycode, potentially far exceeds that of oligopeptide genetic codes due to the vast structural diversity of carbohydrate chains. Consequently, this remarkable structural diversity presents considerable difficulties and has necessitated the development of high definition analytical methods (Kuno et al. 2005; Raman et al. 2005; Royle et al. 2008; Xia et al. 2005). Genome sequencing has provided us with a solid foundation for elucidating genetic and molecular functions within cells and organisms; the glycode will prove a much more challenging prospect but will create enormous opportunities for the marine biotechnology sector.

Acknowledgments This work was supported by a Natural Environment Research Council studentship to HEP.

References

- Abdou ES, Elkholy SS, Elsabee MZ, Mohamed E (2008) Improved antimicrobial activity of polypropylene and cotton nonwoven fabrics by surface treatment and modification with chitosan. *J Appl Polym Sci* 108:2290–2296
- Addepalli MK, Fujita Y, Kanai K (2002) A monoclonal antibody and the lectin wheat germ agglutinin induce zoospore encystment in *Pythium porphyrae*, a marine microbial pathogen. *Mycologia* 94:712–721
- Alpuche J, Pereyra A, Agundis C, Rosas C, Slomianny M-C, Vázquez L, Zenteno E (2005) Purification and characterisation of a lectin from the white shrimp *Litopenaeus setiferus* (Crustacea decapoda) hemolymph. *Biochim Biophys Acta-Gen Subjects* 1724:86–93
- Al Sagheer FA, Al-Sughayer MA, Muslim S, Elsabee MZ (2009) Extraction and characterization of chitin and chitosan from marine sources in Arabian Gulf. *Carbohydr Polym* 77:410–419
- Altmann F, Fabini G, Ahorn H, Wilson IBH (2001) Genetic model organisms in the study of N-glycans. *Biochimie* 83:703–712
- Alves AP, Mulloy B, Diniz JA, Mourao PAS (1997) Sulfated polysaccharides from the egg jelly layer are species-specific inducers of acrosomal reaction in sperms of sea urchins. *J Biol Chem* 272:6965–6971
- Alves AP, Mulloy B, Moy GW, Vacquier VD, Mourao PAS (1998) Females of the sea urchin *Strongylocentrotus purpuratus* differ in the structures of their egg jelly sulfated fucans. *Glycobiology* 8:939–946
- Anderson KE, Waite JH (2002) Biochemical characterization of a byssal protein from *Dreissena bugensis* (Andrusov). *Biofouling* 18:37–45
- Aoki S, Cao LW, Matsui K, Rachmat R, Akiyama S, Kobayashi M (2004) Kendarimide A, a novel peptide reversing P-glycoprotein-

- mediated multidrug resistance in tumor cells, from a marine sponge of *Haliclona* sp. *Tetrahedron* 60:7053–7059
- Armant DR, Kaplan HA, Lennarz WJ (1986) *N*-Linked glycoprotein biosynthesis in the developing mouse embryo. *Dev Biol* 113:228–237
- Arranz-Plaza E, Tracy AS, Siriwardena A, Pierce JM, Boons GJ (2002) High-avidity, low-affinity multivalent interactions and the block to polyspermy in *Xenopus laevis*. *J Am Chem Soc* 124:13035–13046
- Axford J (2001) The impact of glycobiology on medicine. *Trends Immunol* 22:237–239
- Baginski T, Hirohashi N, Hoshi M (1999) Sulfated *O*-linked glycans of the vitelline coat as ligands in gamete interaction in the ascidian, *Halocynthia roretzi*. *Dev Growth Differ* 41:357–364
- Bautista-Baños S, Hernández-Lauzardo AN, Velázquez-del Valle MG, Hernández-López M, Ait Barka E, Bosquez-Molina E, Wilson CL (2006) Chitosan as a potential natural compound to control pre and postharvest disease of horticultural commodities. *Crop Prot* 25:108–118
- Bavington CD, Lever R, Mulloy B, Grundy MM, Page CP, Richardson NV, McKenzie JD (2004) Anti-adhesive glycoproteins in echinoderm mucus secretions. *Comp Biochem Physiol B* 139:607–617
- Benevides NMB, Holanda ML, Melo FR, Freitas ALP, Sampaio AH (1998) Purification and partial characterisation of the lectin from the marine red alga *Enantiocladia duperreyi* (C. Agardh) Falkenberg. *Bot Mar* 41:521–525
- Benevides NMB, Holanda ML, Melo FR, Pereira MG, Monteiro ACO, Freitas ALP (2001) Purification and partial characterization of the lectin from the marine green alga *Caulerpa cupressoides* (Vahl) C. Agardh. *Bot Mar* 44:17–22
- Bouarab K, Potin P, Weinberger F, Correa J, Kloreg B (2001) The *Chondrus crispus*–*Acrochaete operculata* host–pathogen association, a novel model in glycobiology and applied phycopathology. *J Appl Phycol* 13:185–193
- Bretting H, Donadey C, Vacelet J, Jacobs G (1981) Investigations on the occurrence of lectins in marine sponges with special regard to some species of the family Axinellidae. *Comp Biochem Physiol B* 70:69–76
- Brown BR, Hutchison JC, Hughes ME, Kellogg DR, Murray RW (2002) Electrical characterization of gel collected from shark electrosensors. *Phys Rev E Stat Nonlin Soft Matter Phys* 65:061903
- Buchmann K (1998) Binding and lethal effect of complement from *Oncorhynchus mykiss* on *Gyrodactylus derjavini* (Platyhelminthes: Monogenea). *Dis Aquat Org* 32:195–200
- Bulgakov AA, Park KI, Choi KS, Lim HK, Cho M (2004) Purification and characterisation of a lectin isolated from the Manila clam *Ruditapes philippinarum* in Korea. *Fish Shellfish Immunol* 16:487–499
- Burchard RP, Sorongon ML (1998) A gliding bacterium strain inhibits adhesion and motility of another gliding bacterium strain in a marine biofilm. *Appl Environ Microbiol* 64:4079–4083
- Calabro A, Midura RJ, Hascall VC, Plaas A, Goodstone NJ, Rodén L (2000) Structure and biosynthesis of chondroitin sulfate and hyaluronan. In: Iozzo RV (ed) *Proteoglycans, structure, biology, and molecular interactions*. CRC, New York, pp 5–26
- Carson DD (2002) The glycobiology of implantation. *Front Biosci* 7:1535–1544
- Chang LC, Whittaker NF, Bewley CA (2003) Crambescidin 826 and dehydrocrambine A: new polycyclic guanidine alkaloids from the marine sponge *Monanchora* sp. that inhibit HIV-1 fusion. *J Nat Prod* 66:1490–1494
- Clare AS, Matsumura K (2000) Nature and perception of barnacle settlement pheromones. *Biofouling* 15:57–71
- Cooksey KE, Wigglesworth-Cooksey B (1995) Adhesion of bacteria and diatoms to surfaces in the sea—a review. *Aquat Microb Ecol* 9:87–96
- Costas E, Rodas VL (1994) Identification of marine dinoflagellates using fluorescent lectins. *J Phycol* 30:987–990
- Crisp DJ, Meadows PS (1963) Adsorbed layers: the stimulus to settlement in barnacles. *Proc R Soc Lond Ser B Biol Sci* 158:364–387
- Cummings RD, Nyame AK (1996) Glycobiology of schistosomiasis. *FASEB J* 10:838–848
- Cummings RD, Nyame AK (1999) Schistosome glycoconjugates. *Biochim Biophys Acta-Mol Basis Dis* 1455:363–374
- DeAngelis PL (1999) Hyaluronan synthases: fascinating glycosyltransferases from vertebrates, bacterial pathogens, and algal viruses. *Cell Mol Life Sci* 56:670–682
- Dell A, Morris HR, Easton RL, Patankar M, Clark GF (1999) The glycobiology of gametes and fertilisation. *Biochim Biophys Acta-Gen Subjects* 1473:196–205
- Dreanno C, Matsumura K, Dohmae N, Takio K, Hirota H, Kirby RR, Clare AS (2006) An α 2-macroglobulin-like protein is the cue to gregarious settlement of the barnacle *Balanus amphitrite*. *Proc Nat Acad Sci USA* 103:14396–14401
- Epel D (1998) Use of multidrug transporters as first lines of defence against toxins in aquatic organisms. *Comp Biochem Physiol* 120:23–28
- Estevez JM, Fernández PV, Kasulin L, Dupree P, Ciancia M (2009) Chemical and in situ characterisation of macromolecular components of the cell walls from the green seaweed *Codium fragile*. *Glycobiology* 19:212–228
- Eufemia N, Clerte S, Girshick S, Epel D (2002) Algal products as naturally occurring substrates for p-glycoprotein in *Mytilus californianus*. *Mar Biol* 140:343–353
- Ferrari KM, Targett NM (2003) Chemical attractants in horseshoe crab, *Limulus polyphemus*, eggs: the potential for an artificial bait. *J Chem Ecol* 29:477–496
- Fontaine AR (1964) The integumentary mucous secretions of the ophiuroid *Ophiocoma nigrum*. *J Mar Biol Assoc UK* 44:145–162
- Fukuda MN, Akama TO (2003) The in vivo role of α -mannosidase IIx and its role in processing of *N*-glycans in spermatogenesis. *Cell Mol Life Sci* 60:1351–1355
- Gaill F, Persson J, Sugiyama J, Vurong R, Chanzy H (1992) The chitin system in the tubes of deep sea hydrothermal vent worms. *J Struct Biol* 109:116–128
- Gundacker D, Leys SP, Schroder HC, Muller IM, Muller WEG (2001) Isolation and cloning of a C-type lectin from the hexactinellid sponge *Aphrocallistes vastus*: a putative aggregation factor. *Glycobiology* 11:21–29
- Hatakeyama T, Kohzaki H, Nagatomo H, Yamasaki N (1994) Purification and characterization of four Ca^{2+} dependent lectins from the marine invertebrate, *Cucumaria echinata*. *J Biochem* 116:209–214
- Hatanaka A, Umeda N, Yamashita S, Hirazawa N (2005) A small ciliary surface glycoprotein of the monogenean parasite *Neobenedenia girellae* acts as an agglutination/immobilization antigen and induces an immune response in the Japanese flounder *Paralichthys olivaceus*. *Parasitology* 131:591–600
- Hoshi M, Desantis R, Pinto MR, Cotelli F, Rosati F (1985) Sperm glycosidases as mediators of sperm–egg binding in the ascidians. *Zool Sci* 2:65–69
- Hoshi M, Okinaga T, Konati K, Araki T, Chiba K (1991) Acrosome reaction-inducing glycoconjugate in the jelly coat of starfish eggs. In: Baccetti B (ed) *Comparative spermatology 20 years after*. Raven, New York, pp 175–180
- Humbertdavid N, Garrone R (1993) A 6-armed, tenascin-like protein extracted from the Porifera *Oscarella tuberculata* (Homosclerophorida). *Eur J Biochem* 216:255–260

- Iijima R, Kisugi J, Yamazaki M (1994) Biopolymers from marine invertebrates. 14. Antifungal property of Dolabellin-A, a putative self-defense molecule of the sea hare, *Dolabella auricularia*. *Biol Pharm Bull* 17:1144–1146
- Iijima R, Kisugi J, Yamazaki M (1995) Antifungal activity of Aplysianin-E, a cytotoxic protein of sea hare (*Aplysia kurodai*) eggs. *Dev Comp Immunol* 19:13–19
- Im AR, Sim J-S, Park Y, Kim YS, Toshihiko T (2008) Isolation and characterization of chondroitin sulfate from marine organisms. *Glycobiology* 18:995–996
- Imai T, Watanabe T, Yui T, Sugiyama J (2003) The directionality of chitin biosynthesis: a revisit. *Biochem J* 374:755–760
- Isbrucker RA, Cummins J, Pomponi SA, Longley RE, Wright AE (2003) Tubulin polymerizing activity of dictyostatin-1, a polyketide of marine sponge origin. *Biochem Pharmacol* 66:75–82
- Jimbo M, Yanohara T, Kioke K, Kioke K, Sakai R, Muramoto K, Kamiya H (2000) The D-galactose-binding lectin of the octocoral *Sinularia lochmodes*: characterization and possible relationship to the symbiotic dinoflagellates. *Comp Biochem Physiol B* 125:227–236
- Jin T, Qian P (2005) Amino acid exposure modulates the bioactivity of biofilms for larval settlement of *Hydroides elegans* by altering bacterial community components. *Mar Ecol Prog Ser* 297:169–179
- Kabakoff B, Lennarz WJ (1990) Inhibition of glycoprotein processing blocks assembly of spicules during development of the sea urchin embryo. *J Cell Biol* 111:391–400
- Kari BE, Rottmann WL (1985) Analysis of changes in a yolk glycoprotein complex in the developing sea urchin embryo. *Dev Biol* 108:18–25
- Kariya Y, Mulloy B, Imai K, Tominaga A, Kaneko T, Asari A, Suzuki K, Masuda H, Kyogashima IT (2004) Isolation and partial characterisation of fucan sulfates from the body wall of sea cucumber *Stichopus japonicus* and their ability to inhibit osteoclastogenesis. *Carbohydr Res* 339:1339–1346
- Karoumi A, Croisille Y, Croisille F, Meiniel R, Belin MF, Meiniel A (1990) Glycoprotein synthesis in the subcommissural organ of the chick embryo. 2. An immunochemical study. *J Neural Transm* 80:203–212
- Kawagishi H, Yamawaki M, Isobe S, Usui T, Kimura A, Chiba S (1994) Two lectins from the marine sponge *Halichondria okadai*—an *N*-acetyl-sugar-specific lectin (Hol-I) and an *N*-acetyllactosamine-specific lectin (Hol-II). *J Biol Chem* 269:1375–1379
- Kawakami A, Miyamoto T, Higuchi R, Uchiumi T, Kuwano M, Van Soest RWM (2001) Structure of a novel multidrug resistance modulator, irciniasulfonic acid, isolated from a marine sponge, *Ircinia* sp. *Tetrahedron Lett* 42:3335–3337
- Kawsar SMA, Fujii Y, Matsumoto R, Ichikawa T, Tateno H, Hirabayashi J, Yasumitsu H, Dogasaki C, Hosono M, Nitta K, Hamako J, Matsui T, Ozeki Y (2008) Isolation, purification, characterisation and glycan-binding profile of a D-galactoside specific lectin from the marine sponge, *Halichondria okadai*. *Comp Biochem Physiol B* 150:349–357
- Kelly LS, Snell TW (1998) Role of surface glycoproteins in mate-guarding of the marine harpacticoid *Tigriopus japonicus*. *Mar Biol* 130:605–612
- Khalaila I, Peter-Katalinic J, Tsang C, Radcliffe CM, Aflalo ED, Harvey DJ, Dwek RA, Rudd PM, Sagi A (2004) Structural characterization of the *N*-glycan moiety and site of glycosylation in vitellogenin from the decapod crustacean *Cherax quadricarinatus*. *Glycobiology* 14:767–774
- Kim SK, Ravichandran YD, Khan SB, Kim YT (2008) Prospective of the cosmeceuticals derived from marine organisms. *Biotechnol Bioprocess Eng* 13:511–523
- Kisugi J, Ohye H, Kamiya H, Yamazaki M (1992) Biopolymers from marine invertebrates. 13. Characterization of an antibacterial protein, Dolabellin-A, from the albumin gland of the sea hare, *Dolabella auricularia*. *Chem Pharm Bull* 40:1537–1539
- Kotani T, Hagiwara A, Snell TW (1997) Genetic variation among marine *Brachionus* strains and function of mate recognition pheromone (MRP). *Hydrobiologia* 358:105–112
- Kren V, Martinkova L (2001) Glycosides in medicine: the role of glycosidic residue in biological activity. *Curr Med Chem* 8:1303–1328
- Kröger N, Bergsdorf C, Sumper M (1994) A new calcium-binding glycoprotein family constitutes a major diatom cell wall component. *EMBO J* 13:4676–4683
- Kuno A, Uchiyama N, Koseki-Kuno S, Ebe Y, Takashima S, Yamada M, Hirabayashi J (2005) Evanescent-field fluorescence-assisted lectin microarray: a new strategy for glycan profiling. *Nat Methods* 2:851–856
- Lam C, Harder T, Qian P (2005) Induction of larval settlement in the polychaete *Hydroides elegans* by extracellular polymers of benthic diatoms. *Mar Ecol Prog Ser* 286:145–154
- Lambert CC (1989) Ascidian eggs release glycosidase activity which aids in the block against polyspermy. *Development* 105:415–420
- Le Pape P, Zidane M, Abdala H, More MT (2000) A glycoprotein isolated from the sponge, *Pachymatisma johnstonii*, has anti-leishmanial activity. *Cell Biol Int* 24:51–56
- Liao WR, Lin JY, Shieh WY, Jeng WL, Huang R (2003) Antibiotic activity of lectins from marine algae against marine vibrios. *J Ind Microbiol Biotech* 30:433–439
- Lind JL, Heimann K, Miller EA, vanVliet C, Hoogenraad NJ, Wetherbee R (1997) Substratum adhesion and gliding in a diatom are mediated by extracellular proteoglycans. *Planta* 203:213–221
- Lowe JB, Marth JD (2003) A genetic approach to mammalian glycan function. *Ann Rev Biochem* 72:643–691
- Magnadóttir B, Gudmundsdóttir S, Gudmundsdóttir BK (1997) The carbohydrate moiety of IgM from salmon (*Salmo salar* L.). *Comp Biochem Physiol B* 116:423–430
- Magnadóttir B, Crispin M, Royle L, Colominas C, Harvey DJ, Dwek RA, Rudd PM (2002) The carbohydrate moiety of serum IgM from Atlantic cod (*Gadus morhua* L.). *Fish Shellfish Immunol* 12:209–227
- Matsumura K, Mori S, Nagano M, Fusetani N (1998a) Lentil lectin inhibits adult extract-induced settlement of the barnacle, *Balanus amphitrite*. *J Exp Zool* 280:213–219
- Matsumura K, Nagano M, Fusetani N (1998b) Purification of a larval settlement-inducing protein complex (SIPC) of the barnacle, *Balanus amphitrite*. *J Exp Biol* 281:12–20
- Matsumura K, Nagano M, Kato-Yoshinaga Y, Yamazaki M, Clare AS, Fusetani N (1998c) Immunological studies on the settlement-inducing protein complex (SIPC) of the barnacle *Balanus amphitrite* and its possible involvement in larva-larva interactions. *Proc R Soc Lond Ser B Biol Sci* 265:1825–1830
- Matsumura K, Hills JM, Thomason PO, Thomason JC, Clare AS (2000) Discrimination at settlement in barnacles: laboratory and field experiments on settlement behaviour in response to settlement-inducing protein complexes. *Biofouling* 16:181–190
- McCarren J, Brahamsha B (2005) Transposon mutagenesis in a marine *Synechococcus* strain: Isolation of swimming motility mutants. *J Bacteriol* 187:4457–4462
- McCarren J, Heuser J, Roth R, Yamada N, Martone M, Brahamsha B (2005) Inactivation of swmA results in the loss of an outer cell layer in a swimming *Synechococcus* strain. *J Bacteriol* 187:224–230
- McFadden DW, Riggs DR, Jackson BJ, Vona-Davis L (2003) Keyhole limpet hemocyanin, a novel immune stimulant with promising

- anticancer activity in Barrett's esophageal adenocarcinoma. *Amer J Surg* 186:552–555
- McKenzie JD, Grigovale IV (1996) The echinoderm surface and its role in preventing antifouling. *Biofouling* 10:261–272
- Meikle P, Richards GN, Yellowlees D (1987) Structural determination of the oligosaccharide side chains from a glycoprotein isolated from the mucus of the coral *Acropora formosa*. *J Biol Chem* 262:16941–16947
- Mengerink KJ, Vacquier VD (2001) Glycobiology of sperm–egg interactions in deuterostomes. *Glycobiology* 11:37–43
- Michael T, Smith CM (1995) Lectins probe molecular films in biofouling—characterization of early films on nonliving and living surfaces. *Mar Ecol Prog Ser* 119:229–236
- Morris HR, Dell A, Easton RL, Panico M, Koistinen R, Oehninger S, Patankar MS, Seppala M, Clark GF (1996) Gender-specific glycosylation of human glycodelin affects its contraceptive activity. *J Biol Chem* 271:32159–32167
- Mourão PAS (2007) A carbohydrate-based mechanism of species recognition in sea urchin fertilisation. *Braz J Med Biol Res* 40:5–17
- Nadanaka S, Clement A, Masayama K, Faissner A, Sugahara K (1998) Characteristic hexasaccharide sequences in octasaccharides derived from shark cartilage chondroitin sulfate D with a neurite outgrowth promoting activity. *J Biol Chem* 273:3296–3307
- Naganuma T, Ogawa T, Hirabayashi J, Kasai K, Kamiya H, Muramoto K (2006) Isolation, characterisation and molecular evolution of a novel pearl shell lectin from a marine bivalve, *Pteria penguin*. *Mol Divers* 10:607–618
- Neethirajan S, Gordon R, Wang L (2009) Potential of silica bodies (phytoliths) for nanotechnology. *Trends Biotechnol* 27:461–467
- Olofsson S (1992) Carbohydrates in herpesvirus infections. *Apmis* 100:84–95
- Pahler S, Blumbach B, Muller I, Muller WEG (1998) Putative multiadhesive protein from the marine sponge *Geodia cydonium*: cloning of the cDNA encoding a fibronectin-, an SRCR-, and a complement control protein module. *J Exp Zool* 282:332–343
- Rademacher T, Parekh R, Dwek R (1988) Glycobiology. *Ann Rev Biochem* 57:785–838
- Raman R, Raguram S, Venkataraman G, Paulson JC, Sasisekharan R (2005) Glycomics: an integrated systems approach to structure–function relationships of glycans. *Nat Methods* 2:817–824
- Rashidova SS, Milusheva RY, Voropaeva NL, Pulatova SR, Nikonovich GV, Ruban IN (2004) Isolation of chitin from a variety of raw materials, modification of the material, and interaction its derivatives with metal ions. *Chromatographia* 59:783–786
- RicoMartinez R, Dingmann B, Snell TW (1996) Surface glycoproteins potentially involved in mate recognition in nine freshwater rotifer species. *Archiv Für Hydrobiol* 138:1–10
- Rogers DJ, Hori K (1993) Marine algal lectins—new developments. *Hydrobiologia* 261:589–593
- Royle L, Campbell MP, Radcliff CM, White DM, Harvey DJ, Abrahams JL, Kim Y-G, Henry GW, Shadwick NA, Weinblatt ME, Lee DM, Rudd PM, Dwek RA (2008) HPLC-based analysis of serum N-glycans on a 96-well plate platform with dedicated database software. *Anal Biochem* 376:1–12
- Sangrajrang S, Zidane M, Berda P, More MT, Calvo F, Fellous A (2000) Different microtubule network alterations induced by pachymatismin, a new marine glycoprotein, on two prostatic cell lines. *Cancer Chemother, Pharmacol* 45:120–126
- Sashiwa H, Aiba S (2004) Chemistry modified chitin and chitosan as biomaterials. *Prog Polym Sci* 29:887–908
- Schaeffer DJ, Krylov VS (2000) Anti-HIV activity of extracts and compounds from algae and cyanobacteria. *Ecotoxicol Environ Saf* 45:208–227
- Seifert GJ, Robert K (2007) The biology of arabinogalactan proteins. *Ann Rev Plant Biol* 58:137–161
- Sharon N, Lis H (2004) History of lectins: from hemagglutinins to biological recognition molecules. *Glycobiology* 14:53–62
- Smital T, Sauerborn R, Pivcevic B, Krca S, Kurelec B (2000) Interspecies differences in P-glycoprotein mediated activity of multixenobiotic resistance mechanism in several marine and freshwater invertebrates. *Comp Biochem Physiol C* 126:175–186
- Smital T, Sauerborn R, Hackenberger BK (2003) Inducibility of the P-glycoprotein transport activity in the marine mussel *Mytilus galloprovincialis* and the freshwater mussel *Dreissena polymorpha*. *Aquat Toxicol* 65:443–465
- Snell TW, Carmona MJ (1994) Surface glycoproteins in copepods—potential signals for mate recognition. *Hydrobiologia* 293:255–264
- Sullivan CH, Hart JP, Kramer J (1991) The pattern of protein and glycoprotein synthesis in presumptive lens and nonlens ectoderm of the chicken embryo. *Roux Arch Dev Biol* 200:38–44
- Szewzyk U, Holmström C, Wrangstadh M, Samuelsson M-O, Maki JS, Kjelleberg S (1991) Relevance of the exopolysaccharide of marine *Pseudomonas* sp. strain S9 for the attachment of *Ciona intestinalis* larvae. *Mar Ecol Prog Ser* 75:259–265
- Theopold U, Dorian C, Schmidt O (2001) Changes in glycosylation during *Drosophila* development. The influence of ecdysone on hemomucin isoforms. *Insect Biochem Mol Biol* 31:189–197
- Thotakura NR, Blithe DL (1995) Glycoprotein hormones—glycobiology of gonadotropins, thyrotropin and free α -subunit. *Glycobiology* 5:3–10
- Tian JD, Gong H, Thomsen GH, Lennarz WJ (1997) Gamete interactions in *Xenopus laevis*: identification of sperm binding glycoproteins in the egg vitelline envelope. *J Cell Biol* 136:1099–1108
- Ting JH, Snell TW (2003) Purification and sequencing of a mate-recognition protein from the copepod *Tigriopus japonicus*. *Mar Biol* 143:1–8
- Toole BP (2000) Hyaluronan. In: Iozzo RV (ed) *Proteoglycans, structure, biology, and molecular interactions*. CRC, New York, pp 61–92
- Tseneklidou-Stoeter D, Gerwig GJ, Kamerling JP, Spindler KD (1995) Characterisation of N-linked carbohydrate chains of the crayfish. *Astacus leptodactylus* hemocyanin. *Biol Chem Hoppe-Seyler* 376:531–537
- Tulsiani DRP, YoshidaKomiya H, Araki Y (1997) Mammalian fertilization: a carbohydrate-mediated event. *Biol Reprod* 57:487–494
- Ushiyama A, Chiba K, Shima A, Hoshi M (1995) Estimation by radiation inactivation of the minimum functional size of acrosome-reaction-inducing substance (ARIS) in the starfish, *Asterias amurensis*. *Zygote* 3:351–355
- Vacquier VD (1998) Evolution of gamete recognition proteins. *Science* 281:1995–1998
- Vacquier VD, Moy GW (1997) The fucose sulfate polymer of egg jelly binds to sperm REJ and is the inducer of the sea urchin sperm acrosome reaction. *Dev Biol* 192:125–135
- Vilela-Silva A, Alves AP, Valente AP, Vacquier VD, Mourao PAS (1999) Structure of the sulfated α -L-fucan from the egg jelly coat of the sea urchin *Strongylocentrotus franciscanus*: patterns of preferential 2-O and 4-O-sulfation determine sperm cell recognition. *Glycobiology* 9:927–933
- Wagner GF, Jaworski EM, Haddad M (1998) Stanniocalcin in the seawater salmon: structure, function, and regulation. *Am J Physiol—Regul Integr Comp Physiol* 274:1177–1185
- Wigglesworth-Cooksey B, Cooksey KE (2005) Use of fluorophore-conjugated lectins to study cell–cell interactions in model marine biofilms. *Appl Environ Microbiol* 71:428–435
- Wikramanayake AH, Clark WH (1994) Two extracellular matrices from oocytes of the marine shrimp *Sicyonia ingentis* that independently mediate only primary or secondary sperm binding. *Dev Growth Differ* 36:89–101

- Wu SM, Arnold LL, Rone J, Trivadi M, Chan WY (1999) Effect of pregnancy-specific β 1-glycoprotein on the development of preimplantation embryo. *Proc Soc Exp Biol Med* 220:169–177
- Xia BY, Kowar ZS, Ju TZ, Alvarez RA, Sachdev GP, Cummings RD (2005) Versatile fluorescent derivatization of glycans for glycomic analysis. *Nat Methods* 2:845–850
- Yamazaki M (1993) Antitumor and antimicrobial glycoproteins from sea hares. *Comp Biochem Physiol C* 105:141–146
- Zal F, Küster B, Green BN, Harvey DJ, Lallier FH (1998) Partially glucose-capped oligosaccharides are found on the hemoglobins of the deep-sea tube worm *Riftia pachyptila*. *Glycobiology* 8:663–673

RESEARCH ARTICLE

Structural characterisation of the *N*-glycan moiety of the barnacle settlement-inducing protein complex (SIPC)

Helen E. Pagett¹, Jodie L. Abrahams², Jonathan Bones², Niaobh O'Donoghue², Jon Marles-Wright³, Richard J. Lewis³, J. Robin Harris³, Gary S. Caldwell¹, Pauline M. Rudd² and Anthony S. Clare^{1,*}

¹School of Marine Science and Technology, Newcastle University, Ridley Building, Claremont Road, Newcastle upon Tyne NE1 7RU, UK, ²National Institute for Bioprocessing Research and Training, Dublin–Oxford Glycobiology Laboratory, Conway Institute, University College Dublin, Belfield, Dublin 4, Ireland and ³Institute for Cell and Molecular Biosciences, Medical School, Newcastle University, Framlington Place, Newcastle upon Tyne NE2 4HH, UK

*Author for correspondence (a.s.clare@ncl.ac.uk)

Accepted 6 December 2011

SUMMARY

Many barnacle species are gregarious and their cypris larvae display a remarkable ability to explore surfaces before committing to permanent attachment. The chemical cue to gregarious settlement behaviour – the settlement-inducing protein complex (SIPC) – is an α_2 -macroglobulin-like glycoprotein. This cuticular protein may also be involved in cyprid reversible adhesion if its presence is confirmed in footprints of adhesive deposited during exploratory behaviour, which increase the attractiveness of surfaces and signal other cyprids to settle. The full-length open-reading frame of the SIPC gene encodes a protein of 1547 amino acids with seven potential *N*-glycosylation sites. In this study on *Balanus amphitrite*, glycan profiling of the SIPC via hydrophilic interaction liquid chromatography with fluorescence detection (HILIC-fluorescence) provided evidence of predominantly high mannose glycans (M2–9), with the occurrence of monofucosylated oligomannose glycans (F(6)M2–4) in lower proportions. The high mannose glycosylation found supports previous observations of an interaction with mannose-binding lectins and exogenous mannose increasing settlement in *B. amphitrite* cypris larvae. Transmission electron microscopy of the deglycosylated SIPC revealed a multi-lobed globular protein with a diameter of ~8 nm. Obtaining a complete structural characterisation of the SIPC remains a goal that has the potential to inspire solutions to the age-old problem of barnacle fouling.

Supplementary material available online at <http://jeb.biologists.org/cgi/content/full/215/7/1192/DC1>

Key words: *Balanus amphitrite*, biofouling, glycosylation, mannose, pheromone.

INTRODUCTION

The settlement-inducing protein complex (SIPC) is a contact pheromone that has been identified as the primary mediator of gregarious settlement in the barnacle *Balanus amphitrite*, though other chemical signals are involved (Clare, 2011). Barnacles are a key component of marine biofouling – the unwanted accumulation of biological material on man-made submerged surfaces. There are strong economic and environmental drivers to better understand the mechanisms involved in fouling and to devise effective antifouling technologies.

The barnacle life cycle involves sessile adult and mobile nauplius and cypris larval stages. The adults of most species studied cross-fertilise by pseudocopulation, requiring a compatible mate to be within reach of the penis. Gregarious settlement behaviour is an adaptive strategy to facilitate successful mating. The SIPC, which is implicated in both adult–larva and larva–larva interactions, is expressed throughout the barnacle life cycle (Matsumura et al., 1998c) and has been localised to the cuticle (Dreanno et al., 2006a).

The SIPC of *B. amphitrite* has a deglycosylated mass of ~170 kDa (predicted from the amino acid sequence) and an apparent native molecular mass of ~260 kDa (estimated from SDS-PAGE comparison with standards). The SIPC contains three major subunits of 76, 88 and 98 kDa (Matsumura et al., 1998b). These polypeptide chains play an important role in the settlement of *B. amphitrite* larvae

(Matsumura et al., 1998b). Each subunit, when assayed individually, induced cyprid settlement as effectively as the intact SIPC (Matsumura et al., 1998c). The gene sequence of the SIPC encodes a 1547 amino acid protein with seven potential *N*-glycosylation sites. There is significant homology to the highly *N*-glycosylated α_2 -macroglobulin (A2M) and insect thioester-containing proteins (TEP) (Dreanno et al., 2006). Cyprid temporary adhesive also appears to be glycoprotein based (Clare and Matsumura, 2000). Therefore, glycoproteins potentially function as both settlement cues and bioadhesives in barnacles.

Glycans on the cell surface play an important role in recognition both on cell surfaces and in solution (Ambrosi et al., 2005). There are other instances of surface-associated proteins playing similar roles to the SIPC in other marine organisms. The harpacticoid copepod *Tigriopus japonicus* secretes a protein with sequence similarities to A2M that has been shown to assist in mate recognition, mate guarding and spermatophore transfer through chemical contact (Ting and Snell, 2003). Similarly, a glycoprotein is involved in mate recognition in calanoid copepods (Snell and Carmona, 1994). Glycoproteins may also function as attractants for allospecifics; for example, eggs of the horseshoe crab, *Limulus polyphemus*, are used as bait in eel fisheries and it is thought that egg-derived glycoproteins act as chemo-attractants (Ferrari and Targett, 2003). In some marine organisms the settlement cue must come from live animals, such

as for the European flat oyster, *Ostrea edulis* (Crisp, 1965). There is also evidence for a settlement cue associated with oyster shell biofilm as bacterial films removed from oyster shells also caused changes in settlement activity (Tamburri et al., 1992). For barnacles, the cue appears to effect a settling response from living, dead or preserved animals (Crisp, 1965). Newly moulted or recently settled individuals strongly induce settlement activity (Crisp and Meadows, 1962), and it has been observed that even old cement bases on surfaces will attract cyprids (Knight-Jones, 1953).

To add to the understanding of glycans and their role in settlement, it is also important to understand the structure of the core protein of the SIPC. The general properties of barnacle settlement factors have been studied intensely for many years, focusing on bioassays and the reaction of proteins to varying physical conditions (Larman et al., 1982). Indeed, Yamamoto synthesised polypeptide models of *Balanus balanoides* (= *Semibalanus balanoides*) cement in the hope of developing compatible bioadhesives (Yamamoto, 1992). Here, we present a characterisation of the glycosylation pattern of the SIPC protein and initial structural characterisations using transmission electron microscopy (TEM).

An understanding of the mechanisms behind the gregarious settlement of organisms such as barnacles may highlight ways to interfere with unwanted fouling by these animals, e.g. through the development of antagonists. In an effort to further understand the contribution of the glycan moieties to the biological activity of the SIPC, the present study reports on the characterisation of the N-linked glycans present on this glycoprotein, in particular the potential presence of high mannose-type glycans, as mannose has previously been shown to affect settlement (Matsumura et al., 1998a).

MATERIALS AND METHODS

Purification of the SIPC

The striped acorn barnacle *Balanus amphitrite* (= *Amphibalanus amphitrite*) Darwin (Clare and Høeg, 2008) from North Carolina was maintained in an aquarium where individual broods of barnacles were kept in separate plastic tanks containing natural filtered (0.45 µm) seawater at 26°C, on a 12h:12h light:dark cycle. Tanks were aerated and the water changed daily. The adult broodstock were fed newly hatched *Artemia* sp. (*Artemia* International, Fairview, TX, USA) nauplii daily. Adults were cleaned thoroughly with water, briefly dried and frozen for extraction of the SIPC. The barnacles were roughly crushed for 30 min using a pestle and mortar; 150% volume of 50 mmol l⁻¹ Tris-HCl pH 7.5 was added during further crushing. The protein mixture was stirred for 2 h, then filtered through 200 µm paper to remove larger particles. The filtrate was centrifuged at 13,000 g for 30 min, retaining the supernatant, which was further filtered through glass fibre filter paper (Whatman No. 3, Whatman, Maidstone, Kent, UK). For every litre of filtered supernatant, 472 g of ammonium sulphate (NH₄)₂SO₄ was added slowly, and this was stirred overnight before centrifuging at 13,000 g for 30 min, retaining the pellet. The pellet was re-suspended in a small volume of 50 mmol l⁻¹ Tris-HCl pH 7.5, transferred to dialysis tubing (12,000 M_w cut-off) and dialysed in 3 l of 50 mmol l⁻¹ Tris-HCl pH 7.5 overnight, changing the buffer after 3 then 6 h. The content of the dialysis tubing was centrifuged for 3 h at 13,000 g, and the supernatant filtered using 0.2 µm cellulose acetate filter (Whatman) under vacuum. The filtrate constituted the total protein from the barnacles and total protein assays were carried out. The protein was diluted to 1:10, 1:50 and 1:100, and was compared with six dilutions from 0 to 1 mg ml⁻¹ of BSA (Sigma, Poole, Dorset, UK) at the same dye concentration (Total Protein Reagent, BioRad,

Hemel Hempstead, Herts, UK). The total protein obtained was purified by ion exchange chromatography for elution by charge using an EconoPump system and EconoSystem fraction collector (Bio-Rad). A 15 mm diameter, 100 cm column containing Q-Sepharose cation exchanger (Pharmacia Biotech, GE Healthcare, Little Chalfont, Bucks, UK) was equilibrated with 1 l of 50 mmol l⁻¹ Tris-HCl pH 7.5; 100 mg of crude extract was diluted in 30 ml of 50 mmol l⁻¹ Tris-HCl pH 7.5. Gradient buffers of 50 mmol l⁻¹ Tris-HCl pH 7.5 and 1 mol l⁻¹ NaCl were used to run a gradient at 1 ml min⁻¹. Fractions of 3 ml were collected on ice. Total protein assays were carried out on every second fraction of the unknown sample. The SIPC was eluted between 100 and 120 min when detected by SDS-PAGE with confirmatory immunoblotting using anti-rabbit IgG (Sigma) as previously outlined (Cutler, 2004). Following this, gel filtration for elution by size using the same system and the following setup was carried out. A 15 mm diameter, 100 cm long column containing Sephacryl S-200 size exclusion media (Pharmacia Biotech) was used with buffers consisting of a mixture of 2 mol l⁻¹ NaCl, 1.5 mol l⁻¹ Tris-HCl pH 7.5 and dH₂O. The column was run at 0.5 ml min⁻¹, collecting fractions of 3 ml on ice. Again, the SIPC was eluted at 25–37 min when detected by SDS-PAGE with confirmatory immunoblotting (Matsumura et al., 1998c).

N-glycan release and labelling

N-glycans were directly released from one-dimensional (1-D) SDS-PAGE gel bands or gel blocks as previously described (Royle et al., 2006). Briefly, the gel bands were excised and washed repeatedly with successive washes of 100% acetonitrile and 20 mmol l⁻¹ sodium bicarbonate buffer pH 7.0 while shaking on an orbital platform shaker (Heidolph, Schwabach, Germany) for 15 min. This ensured maximum recovery of glycans. After washing, glycans were liberated enzymatically with PNGase F (Prozyme, San Leandro, CA, USA) and 20 mmol l⁻¹ sodium bicarbonate buffer (pH 7.0) at 37°C overnight. PNGase F cleaves between the GlcNAc and asparagine residues of N-linked oligosaccharides. It does not cleave O-linked, C-linked or N-linked glycans containing α-1–3 core fucose. The released glycans were extracted from the gel pieces after digestion by successive washing and sonicating for 15 min at 37°C with water and finally with 100% acetonitrile. All extractions were combined and concentrated *via* vacuum centrifugation.

Once dry, the N-glycans were treated with 20 µl of 1% v/v formic acid for 40 min to convert the released glycosylamines back to reducing sugars before redrying. Glycans for HPLC analysis were then labelled with 5 µl of 2-aminobenzamide (2-AB) using the LudgerTag™ 2-AB kit (Ludger, Abingdon, Oxon, UK), vortexed for 10 min and incubated for 30 min at 65°C. Excess 2-AB was removed using solid-phase extraction by Whatman 3MM chromatography paper; 5 µl of the 2-AB-labelled sample was applied to the paper and allowed to dry, and 100% acetonitrile was used as the mobile phase. Labelled glycans were eluted by syringing dH₂O through the paper, in 4 × 500 µl aliquots of dH₂O, leaving the water in contact with the paper for 10 min in between water changes. All water was retained, combined and dried for analysis by HPLC (Royle et al., 2006).

HILIC-fluorescence glycan profiling

Dried samples were re-suspended with 20 µl dH₂O and 80 µl 100% acetonitrile. HILIC-fluorescence was performed using a Waters Alliance 2695 Separations Module with a Waters 2475 Multi Wavelength Fluorescence Detector (Waters Corporation, Millford, MA, USA). The detection wavelengths used were λ_{ex}=330 nm and

$\lambda_{\text{em}}=420\text{ nm}$. Separations were performed on a TSKgel Amide-80 $5\mu\text{m}$ ($250\times4.6\text{ mm}$) column. A 180 min gradient of 50 mmol l^{-1} ammonium formate pH 4.4 and 100% acetonitrile was used for glycan separation as previously described (Royle et al., 2006) (20% ammonium formate:80% acetonitrile to 80% ammonium formate:20% acetonitrile over 180 min). The system was calibrated by running an external standard of 2-AB-labelled dextran ladder ($5\mu\text{l}$ dextran, $15\mu\text{l}$ dH_2O and $80\mu\text{l}$ acetonitrile) (2-AB-glucose homopolymer, Ludger), which was used for annotation of the experimental data with glucose unit (GU) values using Empower GPC software. Throughout this research, carbohydrate structures and names are as per the nomenclature system outlined elsewhere (Harvey et al., 2009).

Structural assignments and exoglycosidase digestion

Aliquots of the labelled glycans were digested with the following exoglycosidase enzymes: bovine kidney α -fucosidase (BKF) and Jack-bean α -mannosidase (JBM; Prozyme) in $1\mu\text{l}$ of 50 mmol l^{-1} sodium acetate buffer pH 5.5, the required enzyme and dH_2O to make up to $10\mu\text{l}$, at 37°C for 16 h. Digested glycans were separated from enzyme by centrifugation through 10 kDa M_w cut-off enzyme filters (Millipore, Billerica, MA, USA) and then analysed by HILIC-fluorescence as outlined above. Structural assignments were made based on enzyme activity and incremental shifts in GU.

Sugars in solution

Following characterisation of the glycans on the SIPC, experiments were carried out using sugars in solution to investigate the efficacy of the dominant sugar, mannose, as a cue when in solution. One day old *B. amphitrite* cyprids were exposed to different concentrations of two sugars (methyl- α -mannopyranoside and methyl- β -galactopyranoside), 3-isobutyl-1-methylxanthine (IBMX) and the native SIPC for 24 h. An artificial seawater (ASW) control was also included. Settlement of 10 cyprids per well in a 24-well plate (Iwaki Cell Biology, Iwaki, Japan) was measured as the percentage of cyprids settled or metamorphosed compared with the total number present after 24 h. The following dilutions were used to produce 6 replicates of each dilution: for mannose, galactose and IBMX: 1 mmol l^{-1} , 0.1 mmol l^{-1} , 0.01 mmol l^{-1} , $1\mu\text{mol l}^{-1}$ and $0.1\mu\text{mol l}^{-1}$; and for the SIPC: 50 nmol l^{-1} , 25 nmol l^{-1} , 5 nmol l^{-1} , 2.5 nmol l^{-1} and 0.5 nmol l^{-1} . Because of the potential for the sugars to degrade during the freeze-thaw processes, these solutions were made up fresh for each experiment. Minitab probit analysis on the mannose and galactose data uses the concentrations and number settled to give a half-maximal effective concentration (EC_{50}) estimate for each replicate; these were then averaged to give the mean EC_{50} for each treatment. Galactose was chosen as a control as it has been used in comparative sugar experiments previously (Khandeparker et al., 2002). Although the glycans in the SIPC are

N-linked, when there is more than one glycan present, in the case of M2 to M9, they are O-linked to each other at the anomeric position. Consequently, using O-linked glycans was expected to produce a similar settlement effect.

Transmission electron microscopy

Native and deglycosylated samples of the SIPC were diluted to ~ 0.7 and 0.07 mg ml^{-1} with 50 mmol l^{-1} Tris-HCl pH 7.5. Samples were prepared for TEM by the 'single-droplet' parafilm procedure (Harris and Horne, 1991). Briefly, a copper grid (400-mesh) coated with carbon film was surface activated by glow discharge (Edwards Coating Unit) before the $10\mu\text{l}$ sample was loaded, then washed and stained with 2% uranyl acetate at pH 4.2–4.5. This heavy metal-containing cation forms a layer of negative stain, whereby the proteins are surrounded by the stain, which scatters electrons revealing the protein as white particles on a darker background. TEM was performed on a Philips CM100 transmission electron microscope with CCD camera, and digital images of areas of interest were taken at $130,000\times$ instrumental magnification. Protein concentration and sample conditions were optimised to generate grids with a homogeneous coverage of single particles before image processing. The glycosylated form of the SIPC protein aggregated under the conditions used for imaging; therefore, the protein was deglycosylated to produce optimal loading on EM grids for imaging. Deglycosylated SIPC in a 10% solution was chosen as the optimal dilution. Two-dimensional (2-D) image processing provided preliminary image averaging to give a qualitative assessment of the protein structure. 2-D processing involved selection of individual protein particles that were processed by multivariate analysis to determine the shape of the protein and define any surface projections.

To produce 2-D class averages, digital micrograph images were processed in e2boxer to select individual particles of interest and then EMAN2 (National Center for Macromolecular Imaging, <http://ncmi.bcm.edu/ncmi>) to extract the boxed particles and stack them. As particles lay at random orientations in the micrographs, to remove noise and create class averages, multivariate analysis was run on the 266 individual protein particle images, again using EMAN2, as described elsewhere (Tang et al., 2007).

RESULTS

HILIC-fluorescence profiling of enzymatically released N-glycans from the SIPC

N-Glycans released *via* overnight incubation with PNGaseF (N-glycosidase F) were labelled with 2-aminobenzamide and profiled using HILIC-fluorescence on an amide stationary phase as previously described (Royle et al., 2006). The resulting chromatographic data presented in Fig. 1 were annotated with GU values by comparison with a dextran hydrosylate ladder. Initial structural assignment of the glycans present in the chromatographic

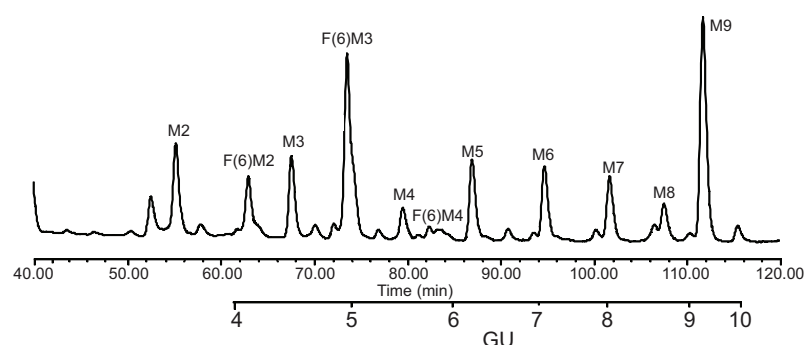


Fig. 1. Hydrophilic interaction liquid chromatography (HILIC)-fluorescence chromatogram of the glycans released from *Balanus amphitrite* native settlement-inducing protein complex (SIPC) in a gel block showing the oligomannose series M2–9 and the core fucosylated derivatives F(6)M2–4. GU, glucose units.

Table 1. Structure details of the glycans of *B. amphitrite* SIPC with glucose unit (GU) and percentage area from the HILIC-fluorescence data

Glycan	HPLC GU	% Area ^a
M2	3.57	6.7
F(6)M2	4.08	4.9
M3	4.42	5.2
F(6)M3	4.89	15
M4	5.43	2.1
F(6)M4	5.7	0.7
M5	6.19	5.3
M6D3	7.11	5.1
M7 or M7D1	8.06	4.4
M8	8.93	2.8
M9	9.61	15.5

^aThe amount of glycan present as a percentage of the total glycans measured by HPLC.
HILIC, hydrophilic interaction liquid chromatography.

peaks was performed by comparison of the experimental GU data with GlycoBase (Campbell et al., 2008). Table 1 lists the initial assignments for the glycans present in each peak, along with the relative proportions of each glycan present. From Table 1 the

experimental data suggest that high mannose-type glycans are the most prevalent glycans present in the native SIPC, forming a mannose ladder consisting of the oligomannose series M2–9. Monofucosylated oligomannose species [F(6)M2–4] were also found to be present, albeit in considerably lower quantities.

Exoglycosidase digestions of the *N*-glycan pool liberated from the SIPC were also performed in an attempt to refine the preliminary glycan structural assignments. The resulting HILIC-fluorescence traces of the *N*-glycan pool after exoglycosidase digestion are depicted in Fig. 2. Fig. 2A shows the oligomannose series M2–9 and core fucosylated oligomannose glycans F(6)M2–4 released from the native SIPC, while Fig. 2B shows the JBM digest of the glycans, wherein all peaks present were found to be trimmed back, yielding only M1 and F(6)M1. Fig. 2C is the resulting HILIC-fluorescence chromatogram following digestion with BKF, which shows the removal of the α 1–6-linked fucose residue of the reducing terminal *N*-acetylglucosamine (GlcNAc) residue in F(6)M2–4 to yield M2, M3 and M4, respectively. In addition, digestion of the F(6)M4 peak revealed a previously masked peak corresponding to a monoantennary glycan (A1). All other peaks associated with the oligomannose series M2–M9 were unaffected by the presence of α -fucosidase (BKF), indicating the absence of an α 1–6-linked fucose residue on their reducing terminal GlcNAc residue. Fig. 2D shows the gel blank.

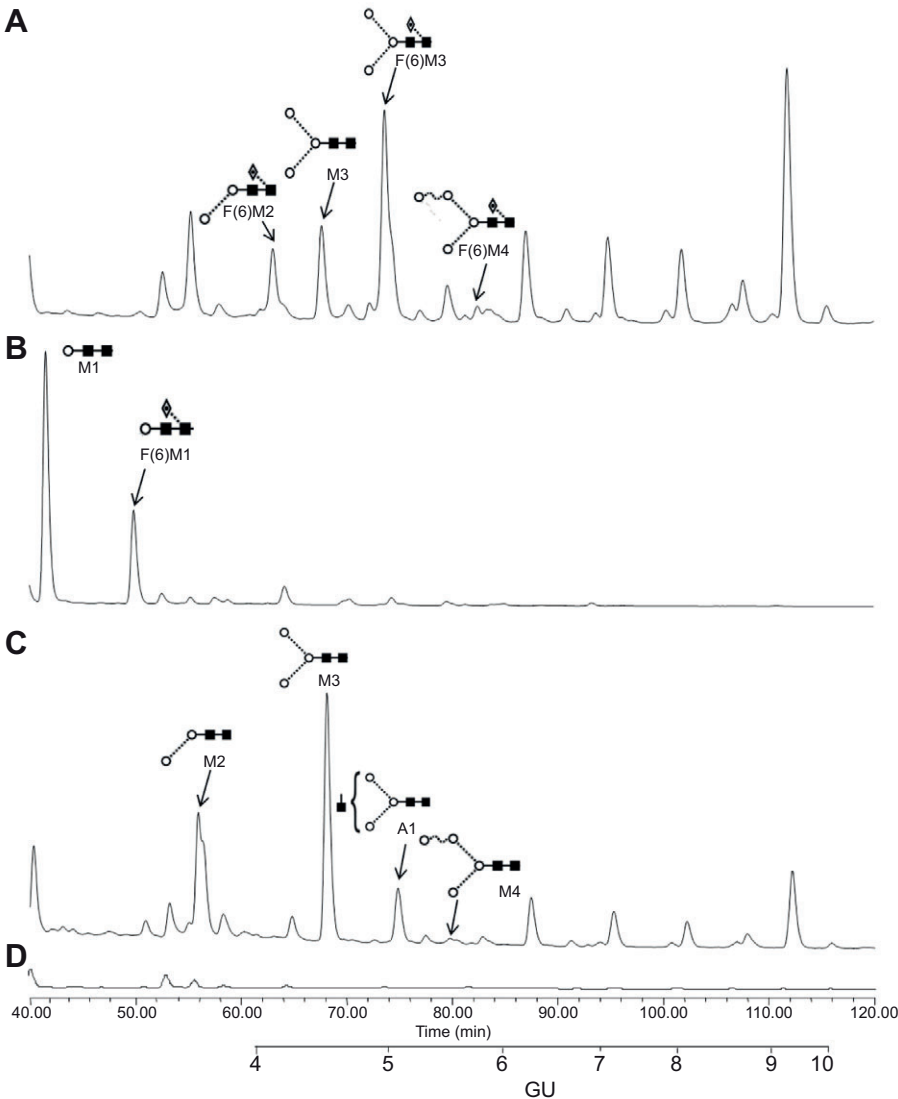


Fig. 2. (A) HILIC-fluorescence chromatogram of the glycans released from the native SIPC in a gel block showing the oligomannose series M2–9 with F(6)M2–4. (B) Chromatogram showing the Jack-bean α -mannosidase (JBM) digest of the glycans. (C) Chromatogram showing the bovine kidney α -fucosidase (BKF) digest of the glycans. (D) Chromatogram showing the gel blank. Molecular representations of the sugars are included. The individual monosaccharides are represented as described previously (Harvey et al., 2009).

Sugars in solution

The response of settling cyprids to different concentrations of sugars and other controls is shown in Fig. 3. Fig. 3A indicates that cyprids settle at a higher rate when exposed to exogenous mannose than to galactose. Cyprid settlement in 1 mmol l^{-1} mannose did not differ from that in the ASW control but was significantly different compared with settlement in 1 mmol l^{-1} , $1 \mu\text{mol l}^{-1}$ and $0.1 \mu\text{mol l}^{-1}$ galactose (data were not normal, Kolmogorov–Smirnov test statistic=0.121, $P<0.01$, equally variant; Levene's test statistic=0.37, $P=0.320$, significantly different; Kruskal–Wallis $H_{10}=26.37$, $P=0.003$). The SIPC elicited a similar maximum response to mannose (Fig. 3B); however, the concentrations involved were very different. To achieve around 40% settlement, 1 mmol l^{-1} of mannose was required, whereas only 25 nmol l^{-1} of the SIPC achieved this response. It is noticeable in Fig. 3 that in solutions that cue settlement (mannose and the SIPC), there was a decline in settlement with decreasing concentration. However, in the non-cueing case of galactose, settlement remained approximately constant at all concentrations. Fig. 3C is the exception to this, and as IBMX is known to be a strong inducer of cyprid settlement, the much higher levels of settlement were expected. However, it appears that at the highest concentrations, IBMX stops all settlement. These results corroborate previous findings (Clare et al., 1995) that concentrations of more than 0.1 mmol l^{-1} elicit very little or zero settlement. This was followed by a peak in settlement of around 70% at 0.01 mmol l^{-1} then a gradual decline with decreasing concentration to $0.1 \mu\text{mol l}^{-1}$.

From the settlement data, the EC_{50} for settlement was determined using Minitab probit analysis. After 24 h, galactose EC_{50} was $2.29 \pm 1 \text{ mmol l}^{-1}$, mannose EC_{50} was $1.548 \pm 0.23 \text{ mmol l}^{-1}$ and the SIPC EC_{50} was $102 \pm 40.1 \text{ nmol l}^{-1}$.

Transmission electron microscopy

Deglycosylated SIPC appeared homogeneous and globular by TEM imaging of negatively stained particles. 2-D class averages of the protein were calculated using multivariate statistical analysis. This revealed a multi-lobed view of the globular protein with a diameter of $\sim 8 \text{ nm}$; no obvious symmetry was present in the images. The nine class averages produced (representing slightly different molecular orientations) are shown in Fig. 4B. Because of the protein adopting a limited number of preferred orientations on the TEM grids under the sample conditions used and the limitations in the quantity of the SIPC available for analysis, it was not possible to carry out three-dimensional (3-D) reconstruction of the protein or attempt crystallisation. However, some attempts can be made to draw structural comparisons from sequence similarity searches of protein databanks carried out by Dreanno et al. (Dreanno et al., 2006). These identified proteins similar to the SIPC belonging to the $\alpha 2$ -macroglobulin family, and included complement-like factors such as the TEPIr protein (PDBid 2PN5) from the anti-parasite immune system of the mosquito *Anopheles gambiae* (Baxter et al., 2007). The amino acid sequence for the SIPC (supplementary material Fig. S1) along with ESPript sequence alignment (Gouet et al., 1999) for TEPIr and the SIPC (supplementary material Fig. S2) are shown in the supplementary data. The two sequences appear analogous and display 26% homology. However, the main difference is that the SIPC does not contain the GCGEQ signature sequence of the thioester bond. Fig. 5 shows a visualisation overlay of the mature SIPC protein (deglycosylated) onto the full structure of mature TEPIr macroglobulin, showing structural similarities. This structure potentially illustrates how the protein might display glycans for detection by cyprids.

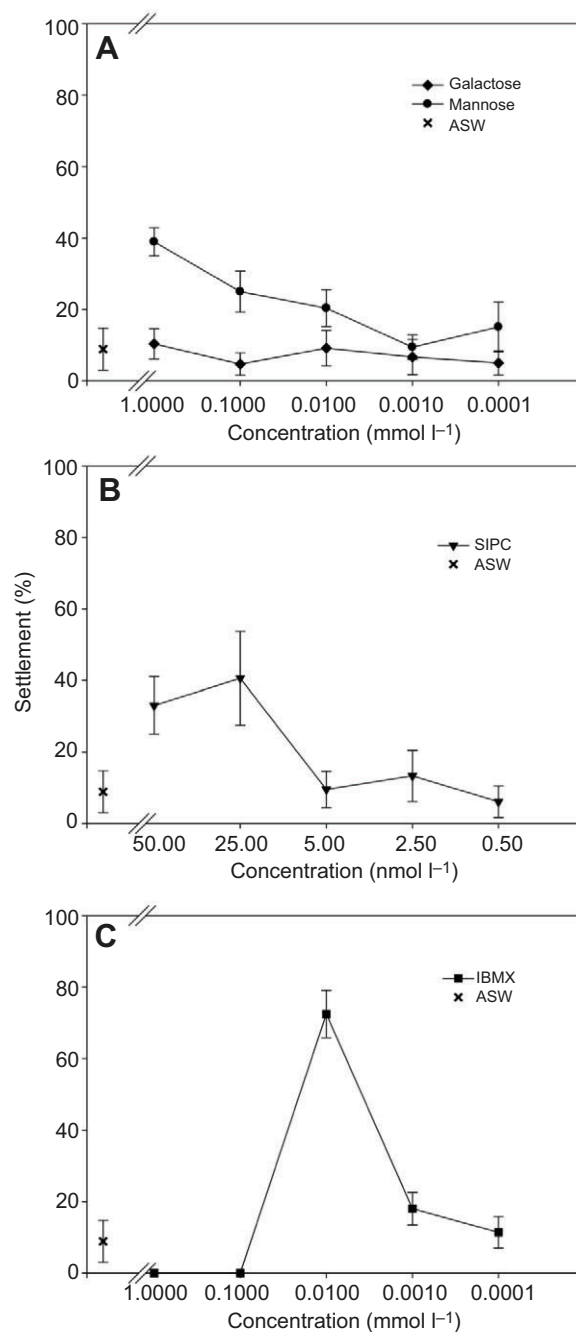


Fig. 3. Effect of exogenous sugars on the settlement of 1 day old *B. amphitrite* cyprids when compared with artificial sea water (ASW). (A) mannose and galactose at 24 h. (B) The SIPC at 24 h. (C) IBMX at 24 h. Note the different scales on the x-axes.

DISCUSSION

Cell surface oligosaccharides play an important role in recognition both on cell surfaces and in solution (Ambrosi et al., 2005; Caldwell and Pagett, 2010). The presence of the glycoprotein SIPC in barnacle cuticle is a key factor in the gregarious settlement of barnacles. The aim of this study was to characterise the glycosylation present on the SIPC to help reveal the role of the glycans in barnacle settlement. Through understanding the process, further progress can be made in reducing settlement. *N*-Linked glycans enzymatically liberated from the SIPC were found to be high mannose-type,

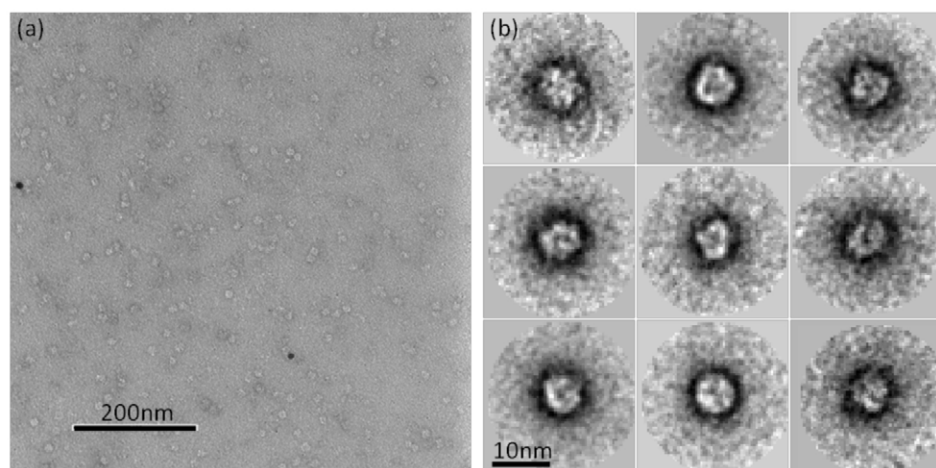


Fig. 4 (A) A representative transmission electron microscopy (TEM) image of deglycosylated *B. amphitrite* SIPC (0.07 mg ml^{-1}) using 2% w/v uranyl acetate stain on a carbon film. (B) The nine class averages, based on 266 protein particles of the deglycosylated SIPC.

ranging from M2 to M9. Previous studies have reported the presence of similar oligosaccharide structures on the proteins isolated from other aquatic organisms such as haemocyanin from the crayfish *Astacus leptodactylus* (Tseneklidou-Stoeter et al., 1995) and haemoglobins from the hydrothermal vent tube worm *Riftia pachyptila* (Zal et al., 1998).

The high mannose-type oligosaccharide structures identified on the SIPC expressed by *B. amphitrite* are in agreement with previous studies in which lectin inhibition experiments were performed. Both lentil lectin (LCA) and jack-bean lectin (ConA) were reported to inhibit settlement of *B. amphitrite*, with both lectins displaying affinity for mannose. The glucosamine- and galactose-binding lectins, wheat germ agglutinin (WGA) and peanut agglutinin (PNA), respectively, do not inhibit settlement (Matsumura et al., 1998a). Mannose in solution has also been shown to act as a settlement cue whereas galactose and glucose do not (Khandeparker et al., 2002). Dreanno and colleagues identified seven potential N-glycosylation sites in the amino acid sequence of the SIPC (Dreanno et al., 2006). Future work could use other exoglycosidases such as PNGaseA, which releases N-linked glycans with an α 1-3- or α 1-6-linked fucose residue on the reducing terminal GlcNAc. PNGaseA digestion is performed at the glycopeptide level, which limits further protein structural analysis. For this reason alone, it was not investigated in the current study.

Moreover, the present study found that the EC_{50} for mannose was less than that for galactose. The large standard errors seen with these EC_{50} values are common in bioassays where there is positive feedback from newly metamorphosed barnacles providing additional settlement cues to exploring cyprids. The SIPC induces consistently high settlement as it is the barnacles' natural settlement pheromone. However, this settlement is only approximately half of the maximal response to IBMX. This may be due to the SIPC forming the part of the cascade to initiate settlement, whereas IBMX may act further downstream, possibly by-passing this cascade and initiating settlement directly; a theory proposed previously (Clare et al., 1995). The efficacy of the SIPC was reduced with decreasing concentration. The pattern of results is very similar to those found by Matsumura and colleagues in both settled and metamorphosed cyprids (Matsumura et al., 1998a). Similarly, the same result was observed by Dreanno and colleagues investigating the settlement response of *B. amphitrite* cyprids to the SIPC but using the SIPC glycoprotein bound to nitrocellulose membrane (Dreanno et al., 2007).

Cyprid settlement in response to the control monosaccharide, exogenous galactose (Kruskall-Wallis $H_{10}=26.37$, $P=0.003$, where

only mannose was significantly different), was not significantly different to the ASW control at all concentrations tested. These assay results, taken together with the glycan analysis data, suggest that the mannose oligosaccharides of the SIPC contribute to the settlement-inducing activity of the glycoprotein pheromone.

The study of deglycosylated SIPC by TEM, taken in conjunction with existing protein sequence data (Dreanno et al., 2006) showing similarities to α_2 -macroglobulin-like proteins, represents the first steps to understanding the protein structure of *B. amphitrite* SIPC and relating structure to function. Ting and Snell similarly discussed a contact protein from the copepod *Tigriopus japonicus*, which also possesses a likeness to the α_2 -macroglobulin family (Ting and Snell, 2003). This contact protein has been implicated in mate recognition, similar to barnacles using the SIPC to identify conspecifics. A recently published conceptual model of copepod mate recognition may provide some insight into the mechanism of action of the SIPC. Snell proposed that male antennules contain receptors to female mate-recognition proteins (Snell, 2011). These proteins are secreted through ducts on the female exoskeleton and displayed but not tightly

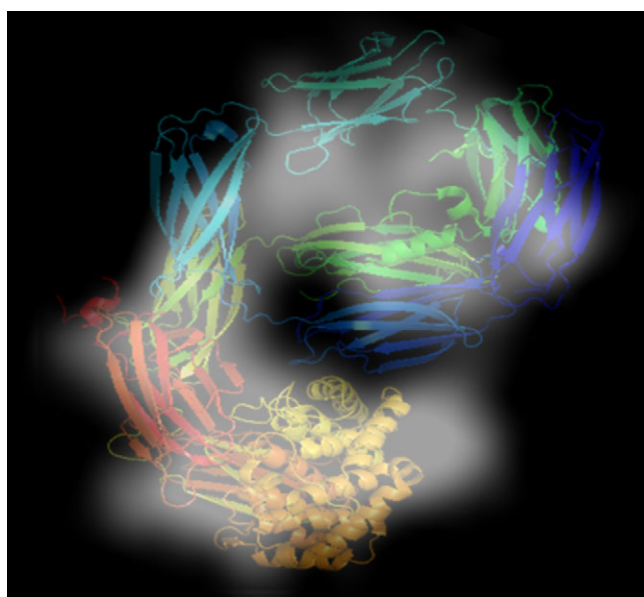


Fig. 5 Visual overlay of the structure of TEP1r (colour) and one of the SIPC class averages (white), indicating structural similarity.

bound to the surface. The proteins are thought to activate a response in the male though a protease-trapping mechanism, although the exact interaction is not yet known and it is not even clear that a 'lock and key' receptor-ligand interaction is required for signal detection (Franco et al., 2011). Although the TEM results presented in this paper are only initial analyses of the protein, this research presents the first view of the SIPC structure and provides a valuable starting point for increasing understanding of how the SIPC functions. The similarity of the SIPC to other proteins with a complement-like structure hints at the role of the protein in self/non-self recognition as the complement system functions as a defence mechanism in invertebrates, although this requires the presence of the thioester bond (Kawabata and Tsuda, 2002).

There is a considerable body of work on the protein structure of other aquatic organisms, using similar TEM protocols to that used here (Harris and Horne, 1991), mainly focusing on haemoglobins and haemocyanins. Studies on the branchiopod crustacean *Triops cancriformis* showed detailed information on the structure and function of the haemoglobin. TEM images revealed both circular shapes of 14 nm diameter and rectangular structures of 16 × 9 nm (Rousselot et al., 2006). Again focusing on haemocyanin, Meissner and colleagues presented the structure for the haemocyanin of the European spiny lobster *Palinurus elephas*, using a combination of cryoelectron microscopy and analysis of the amino acid sequence (Meissner et al., 2003). Comparison of the sequence with that of the American counterpart, *Panulirus interruptus*, showed more than 80% sequence homology.

The results gained through this research have provided some insight into the N-glycan moiety of *B. amphitrite* SIPC, indicating that mannose is present at high levels. The settlement assays suggest that mannose, as a terminal monosaccharide, may contribute to the settlement of cyprids. However, the true signal is likely to be a complex oligosaccharide. It is hoped that more advanced glycan analysis and additional assays using the deglycosylated protein would establish further examination of the SIPC glycans within the scope of this research. As cryoelectron microscopy and crystal structure determination of the SIPC to create a full 3-D molecular model remains elusive, the current knowledge will be built upon further with continued characterisation of the SIPC protein.

ACKNOWLEDGEMENTS

We thank Dr Nick Aldred, Sheelagh Conlan and Dr Rebecca Duke for help during the course of this research and Prof. Dan Rittschof (Duke University) for supplying barnacles.

FUNDING

This work was supported by a National Environment Research Council studentship [grant number NER/S/A/2007/14628] to H.E.P. and by EU FP6 GLYFDIS [grant reference no. 037661] to J.B.

REFERENCES

- Ambrosi, M., Cameron, N. R. and Davis, B. G. (2005). Lectins: tools for the molecular understanding of the glycode. *Org. Biomol. Chem.* **3**, 1593-1608.
- Baxter, R. H. G., Chang, C.-I., Chelliah, Y., Blandin, S., Levashina, E. A. and Delsenhofer, J. (2007). Structural basis for conserved complement factor-like function in the antimalarial protein TEPI. *Proc. Natl. Acad. Sci. USA* **104**, 11615-11620.
- Caldwell, G. S. and Pagett, H. E. (2010). Marine glycobiology: current status and future perspectives. *Mar. Biotechnol.* **12**, 241-252.
- Campbell, M. P., Royle, L., Radcliffe, C. M., Dwek, R. and Rudd, P. M. (2008). GlycoBase and autoGU: tools for HPLC-based glycan analysis. *Bioinformatics* **24**, 1214-1216.
- Clare, A. S. (2011). Toward a characterization of the chemical cue to barnacle gregariousness. In *Chemical Communication in Crustaceans* (ed. T. Breithaupt and M. Thiel), pp. 431-450. New York: Springer.
- Clare, A. S. and Hoeg, J. T. (2008). *Balanus amphitrite* or *Amphibalanus amphitrite*? A note on barnacle nomenclature. *Biofouling* **24**, 55-57.
- Clare, A. S. and Matsumura, K. (2000). Nature and perception of barnacle settlement pheromones. *Biofouling* **15**, 57-71.
- Clare, A. S., Thomas, R. F. and Rittschof, D. (1995). Evidence for the involvement of cyclic AMP in the pheromonal modulation of barnacle settlement. *J. Exp. Biol.* **198**, 655-664.
- Crisp, D. J. (1965). Surface chemistry, a factor in the settlement of marine invertebrate larvae. *Botanica Gothoburgensia* **III** **3**, 51-65.
- Crisp, D. J. and Meadows, P. S. (1962). The chemical basis of gregariousness on cirripedes. *Proc. R. Soc. Lond. B* **156**, 500-520.
- Cutler, P. (2004). *Protein Purification Protocols*. Clifton, NJ, USA: Humana Press.
- Dreanno, C., Matsumura, K., Dohmae, N., Takio, K., Hirota, H., Kirby, R. R. and Clare, A. S. (2006). An α 2-macroglobulin-like protein is the cue to gregarious settlement of the barnacle *Balanus amphitrite*. *Proc. Natl. Acad. Sci. USA* **103**, 14396-14401.
- Dreanno, C., Kirby, R. R. and Clare, A. S. (2007). Involvement of the barnacle settlement-inducing protein complex (SIPC) in species recognition at settlement. *J. Exp. Mar. Biol. Ecol.* **351**, 276-282.
- Ferrari, K. and Targett, N. (2003). Chemical attractants in horseshoe crab, *Limulus polyphemus*, eggs: the potential for an artificial bait. *J. Chem. Ecol.* **29**, 477-496.
- Franco, M. I., Turin, L., Mershin, A. and Skoulakis, E. M. C. (2011). Molecular vibration-sensing component in *Drosophila melanogaster* olfaction. *Proc. Natl. Acad. Sci. USA* **108**, 3797-3802.
- Gouet, P., Courcelle, E., Stuart, D. I. and Metz, F. (1999). ESPript: multiple sequence alignments in PostScript. *Bioinformatics* **15**, 305-308.
- Harris, R. and Horne, R. (1991). Negative Staining. In *Electron Microscopy in Biology: a Practical Approach* (ed. J. R. Harris), 328pp. Oxford, UK: Oxford University Press.
- Harvey, D. J., Merry, A. H., Royle, L., Campbell, M. P., Dwek, R. A. and Rudd, P. M. (2009). Proposal for a standard system for drawing structural diagrams of N- and O-linked carbohydrates and related compounds. *Proteomics* **9**, 3796-3801.
- Kawabata, S. and Tsuda, R. (2002). Molecular basis of non-self recognition by the horseshoe crab tachylectins. *Biochim. Biophys. Acta* **1572**, 414-421.
- Khandeparker, L., Anil, A. C. and Raghukumar, S. (2002). Exploration and metamorphosis in *Balanus amphitrite* Darwin (Cirripedia; Thoracica) cyprids: significance of sugars and adult extract. *J. Exp. Mar. Biol. Ecol.* **281**, 77-88.
- Knight-Jones, E. W. (1953). Laboratory experiments on gregariousness during setting in *Balanus balanoides* and other barnacles. *J. Exp. Biol.* **30**, 584-599.
- Larman, V. N., Gabbot, P. A. and East, J. (1982). Physico-chemical properties of the settlement factor proteins from the barnacle *Balanus balanoides*. *Comp. Biochem. Physiol.* **72B**, 329-338.
- Matsumura, K., Mori, S., Nagano, M. and Fusetani, N. (1998a). Lentil lectin inhibits adult extract-induced settlement on the barnacle, *Balanus amphitrite*. *J. Exp. Biol.* **280**, 213-219.
- Matsumura, K., Nagano, M. and Fusetani, N. (1998b). Purification of a larval settlement-inducing protein complex (SIPC) of the barnacle, *Balanus amphitrite*. *J. Exp. Biol.* **281**, 12-20.
- Matsumura, K., Nagano, M., Kato-Yoshinaga, Y., Yamazaki, M., Clare, A. S. and Fusetani, N. (1998c). Immunological studies on the settlement-inducing protein complex (SIPC) of the barnacle *Balanus amphitrite* and its possible involvement in larva-larva interactions. *Proc. R. Soc. Lond. B* **265**, 1825-1830.
- Meissner, U., Stohr, M., Kusche, K., Burmester, T., Stark, H., Harris, J. R. and Orlova, E. V. (2003). Quaternary structure of the European spiny lobster (*Palinurus elephas*) 1 × 6-mer hemocyanin from cryoEM and amino acid sequence data. *J. Mol. Biol.* **325**, 99-109.
- Rousselot, M., Jaenicke, E., Lamkemeyer, T., Harris, J. R. and Pirow, R. (2006). Native and subunit molecular mass and quaternary structure of the hemoglobin from the primitive branchiopod crustacean *Triops cancriformis*. *FEBS J.* **273**, 4055-4071.
- Royle, L., Radcliffe, C. M., Dwek, R. A. and Rudd, P. M. (2006). Detailed structural analysis of N-glycans released from glycoproteins in SDS-PAGE gel bands using HPLC combined with exoglycosidase array digestions. In *Glycobiology Protocols*, Vol. 347 (ed. I. Brockhausen-Schutzbach), pp. 125-143. Totowa, NJ: Humana Press Inc.
- Snell, T. and Carmona, M. (1994). Surface glycoproteins in copepods-potential signals for mate recognition. *Hydrobiologia* **293**, 255-264.
- Snell, T. W. (2011). Contact chemoreception and its role in zooplankton mate recognition. In *Chemical Communication in Crustaceans* (ed. T. Breithaupt and M. Thiel), pp. 451-466. New York: Springer.
- Tamburri, M. N., Zimmer-Faust, R. K. and Tamplin, M. L. (1992). Natural sources and properties of chemical inducers mediating settlement of oyster larvae: a re-examination. *Biol. Bull.* **183**, 327-338.
- Tang, G., Peng, L., Baldwin, P. R., Mann, D. S., Jiang, W., Rees, I. and Ludtke, S. J. (2007). EMAN2: an extensible image processing suite for electron microscopy. *J. Struct. Biol.* **157**, 38-46.
- Ting, J. H. and Snell, T. W. (2003). Purification and sequencing of a mate-recognition protein from the copepod *Tigriopus japonicus*. *Mar. Biol.* **143**, 1-8.
- Tseneklidou-Stoeter, D., Gerwig, G., Kamerling, J. and Spindler, K. (1995). Characterisation of N-linked carbohydrate chains of the crayfish, *Astacus leptodactylus* hemocyanin. *Biol. Chem. Hoppe-Seyler* **376**, 531-537.
- Yamamoto, H. and Nagai, A. (1992). Polypeptide models of the arthropodin protein of the barnacle *Balanus balanoides*. *Mar. Chem.* **37**, 131-143.
- Zal, F., Küster, B., Green, B. N., Harvey, D. J. and Lallier, F. H. (1998). Partially glucose-capped oligosaccharides are found on the hemoglobins of the deep-sea tube worm *Riftia pachyptila*. *Glycobiology* **8**, 663-673.